Middle Rio Grande
Rio Puerco Reach

Rio Puerco to San Acacia Diversion Dam

Hydraulic Modeling and Silvery Minnow Habitat Analysis 1918-2016

May 2019

Prepared for:
US Bureau of Reclamation

Prepared by:
Kristin LaForge
Chun-Yao Yang
Dr. Pierre Julien
Colorado State University
Engineering Research Center
Department of Civil Engineering
Fort Collins, Colorado 80523

Abstract

The Rio Puerco Reach spans about 11 miles of the Middle Rio Grande, from the confluence with the Rio Puerco to the San Acacia Diversion Dam, in central New Mexico. This reach report for the U.S. Bureau of Reclamation seeks better understanding of the morphodynamic processes of the reach and how this links to Rio Grande silvery minnow habitat quality. The reach was split into five subreaches (P1, P2, P3, P4 and P5) to facilitate the analysis of spatial and temporal trends in channel geometry, morphology and habitat quality.

The hydrology and hydraulics have been in flux over the past century. For instance, the mean annual discharge decreased since the 2000s. Also, suspended sediment discharge has been declining since the 1970s, resulting in channel degradation.

The GIS analysis of aerial photographs dating as far back as 1918 and HEC-RAS analyses showed geomorphic changes for each subreach. The current channel width is less than one-fifth of what it was in 1918. This pattern was consistent throughout the subreaches. There had also been a slight increase in sinuosity (P3 has the highest sinuosity), depth, velocity, and median grain size while the slope decreased from 1972-2012. Also, a geomorphic conceptual model based on Massong et al. (2010) and Klein et al. (2018a) was considered to help to understand the channel evolution.

In the Appendix of this report, a novel approach is proposed. It combines a 1-D HEC-RAS analysis in combination with visual observations from aerial photographs in GIS to assess habitat conditions for the endangered Rio Grande Silvery Minnow (RGSM). This initial step should be pursued and likely integrated into a comprehensive linkage report to tie hydraulic processes with RGSM habitat quality.

Table of Contents

List of Figures

List of Tables

1. Introduction

The Middle Rio Grande is in central New Mexico and spans about 170 miles from the Cochiti Dam to Elephant Butte Reservoir (Tetra Tech 2002). It has been heavily impacted over the past few centuries due to settlements along the river (Scurlock 1998). Levees, jetty jacks, and dams were put in place throughout the 1900s to control the flow and mitigate extreme floods and droughts. These measures caused the river to become narrower and more incised than its previous shallow braided planform (Larsen 2007). In response to these changes, there has been a shift towards more sustainable management of the river in the past few decades (Scurlock 1998; Tetra Tech 2014). Current maintenance goals include habitat improvements for species listed by the Endangered Species Act and support of channel sustainability while continuing to provide effective water delivery (U.S. Bureau of Reclamation 2012).

The purpose of this reach report is to evaluate the morpho-dynamic conditions on the MRG. It is part of a series of reports commissioned by the USBR to include morpho-dynamic reach reports (like this one), reports on the biological-habitat conditions for the RGSM, and process linkage reports. The process linkage reports will connect morpho-dynamic conditions with the required biological-habitat conditions. This report focuses on the physical habitat and it is a first step towards that larger goal. The specific objectives are to:

- Delineate the reach into meaningful subreaches;
- Summarize the flow and sediment discharge history;
- Analyze the geomorphologic drivers at a subreach level (sinuosity, width, braiding, bed elevation, bed material, volume change, and hydraulic parameters); and
- Examine a conceptual geomorphic model to help predict future river changes.

Many studies have been done to understand the geomorphology of the Rio Grande (Baird 2014; Bauer 2000; Berry and Lewis 1997; Bovee et al. 2008; Crawford et al. 1993; Easterling 2015; Happ 1948; Horner 2016; Klein et al. 2018a; Larsen 2007; Makar 2010; Massong 2010; MEI 2002; Posner 2017; Richard 2001; Swanson et al. 2010; Tetra Tech 2014; Varyu 2016). This report will build upon the recent work from Klein et al. (2018), "Isleta to San Acacia Geomorphic Analysis". Analysis from the Klein report (which processed data through 2013), has been extended through 2017 whenever possible. Klein's report also did not analyze trends on a subreach level, which is a specific objective and contribution of our report.

This report extends the analysis from the Klein et al. (2018a) report (which processed data through 2014), to include data through 2017 whenever possible. Klein's report also did not analyze trends on a subreach level, which is a specific objective and contribution of this report.

Since a fair amount of work had been previously completed by Klein et al. (2018), it was suggested by the Bureau of Reclamation that we extend our analysis beyond the original scope of work to start linking biological trends with morphologic ones (Ari Posner, email, May 29, 2018). Therefore, initial attempts were made by CSU to start linking silvery minnow habitat and hydraulic/morpho-dynamic conditions in the river.

The objectives for this additional work aim at:

- Developing a framework for the analysis of silvery minnow habitat based on morpho-dynamic characteristics (including visual information such as bars, vegetation and side channels… from aerial photos at different times and discharges); and
- Carrying out a complementary hydraulic analysis of flow depths and velocities with models like HEC-RAS at comparative discharges for the determination of suitable habitat conditions for the RGSM under different phases of their life cycle.

Since this effort has been presented in preliminary form and requires more discussion with the UNM team and with Reclamation, the results that we developed so far are hereby presented as a brief summary in Section 4 of this report with plenty of additional details in Appendices.

1.1. Site Description and Background

The Middle Rio Grande has historically been characterized by occasional large spring floods from snowmelt, with periods of droughts, sometimes lasting years. These floods often caused large scale shifts of the course of the river and rapid aggradation (Massong et al 2010). Floods, while sometimes resulting in loss of life or land along the Rio Grande, also provided benefits. The floods leached out salts and supplied rich alluvium to the farm land, and helped maintain aquatic ecosystems by connecting the main channel flow to the floodplains (Scurlock 1998). Starting in the 1900s, levees, dams and channelization techniques were used to control the river (Scurlock 1998). While these efforts enabled development of agriculture and large settlements along the MRG, they have also fundamentally changed the river, reducing peak flows and sediment supply, and altering channel geometry and vegetation (Posner 2017). This has created an environment with considerable ecological stress, as seen in the decline of species such as the Rio Grande Silvery Minnow (Mortensen et al 2019).

The Rio Puerco Reach of the Middle Rio Grande spans 10.8 miles from the confluence of Rio Puerco and Rio Grande (agg/deg line 1097) to San Acacia Diversion Dam (agg/deg line 1206) Figure 1. The tributaries that join the Middle Rio Grande in this reach include the Rio Puerco, Salas Arroyo, Arroyo los Alamo, Cañada Ancha and Rio Salado. The confluence of Salas Arroyo is 0.1 miles downstream the confluence of Rio Puerco. Arroyo los Alamo enter the Middle Rio Grande after running through a relatively straight and mildly sloped 3 miles (agg/deg 1126). These confluences are important features of the reach because they carry sediment and act as a local grade control (Easterling Consultants LLC 2015). The channel flows another 3 miles and enters a geologic constriction associated with the San Acacia basalt intrusion (Posner 2017). The river valley becomes narrower and the constriction causes river to bend west. The Rio Salado confluence is located at the end of the constriction. After the confluence, the river valley becomes wide and the river meanders and ends at the SADD (San Acacia Diversion Dam).

1.2. Subreach Delineation

To analyze hydraulic trends along the Puerco Reach, the reach was segmented into five subreaches. These subreaches were determined first by geomorphic characteristics such as confluences or bridges, and then where no such features were available, by cumulative plots of hydraulic variables including flow depth, velocity, slope and width. The location breaks of subreach are designated when there is noticeable change in slope in the cumulative plots. A discharge of 3000 cfs was selected for this analysis based on guidance from the USBR that this flow is contained within the main channel and does not require levee designations within HEC-RAS (Drew Baird, personal communication, June 19, 2018). The variables were obtained by using HEC-RAS with the geometry files provided by the USBR. The geometry files of 1992, 2002, and 2012 were used. **Error! Reference source not found.** shows the subreach definition that is used in this study. These subreaches are used in analyses throughout this report.

Subreaches are identified by aggradation/degradation lines (agg/deg line) which are "spaced approximately 500-feet apart and are used to estimate sedimentation and morphological changes in the river channel and floodplain for the entire MRG" (Posner 2017). The agg/deg line that fell closest to a change in slope of a cumulative plot or other feature was used to delineate a subreach (Figure 2).

Subreach P1 (Puerco-1) begins at the confluence with the Rio Puerco and continues to the confluence with Los Alamos Arroyo at agg/deg 1126. Subreach P2 continues from there to a narrow geologic control at agg/deg line 1151. Subreach P3 stops at the confluence with Rio Salado (agg/deg 1182), which flows in from the west. Subreach P4 stops at an alluvial fan downstream of Rio Salado at agg/deg line 1191. This is a location where the slope of the cumulative width changes. Subreach I5 continues until the San Acacia Diversion Dam (agg/deg 1206). See Appendix A for all cumulative mass plots used in making these determinations.

Table 1: Rio Puerco Reach subreach delineation.

Subreach Number	Agg-Deg Rangeline Numbers	Notable Geomorphic Controls and Comments
P1	1097-1126	Rio Puerco confluence (1097); Arroyo los Alamos (1126)
P2	1126-1151	Narrow Geologic Control (1151)
P3	1151-1182	Rio Salado (1182)
P4	1182-1191	Alluvial fan downstream of Rio Salado. Subreach where the width changes depending on the most recent Rio Salado high flow events (1191)
P5	1191-1206	San Acacia Diversion Dam (1206)

Figure 1: Map of Rio Puerco Reach.

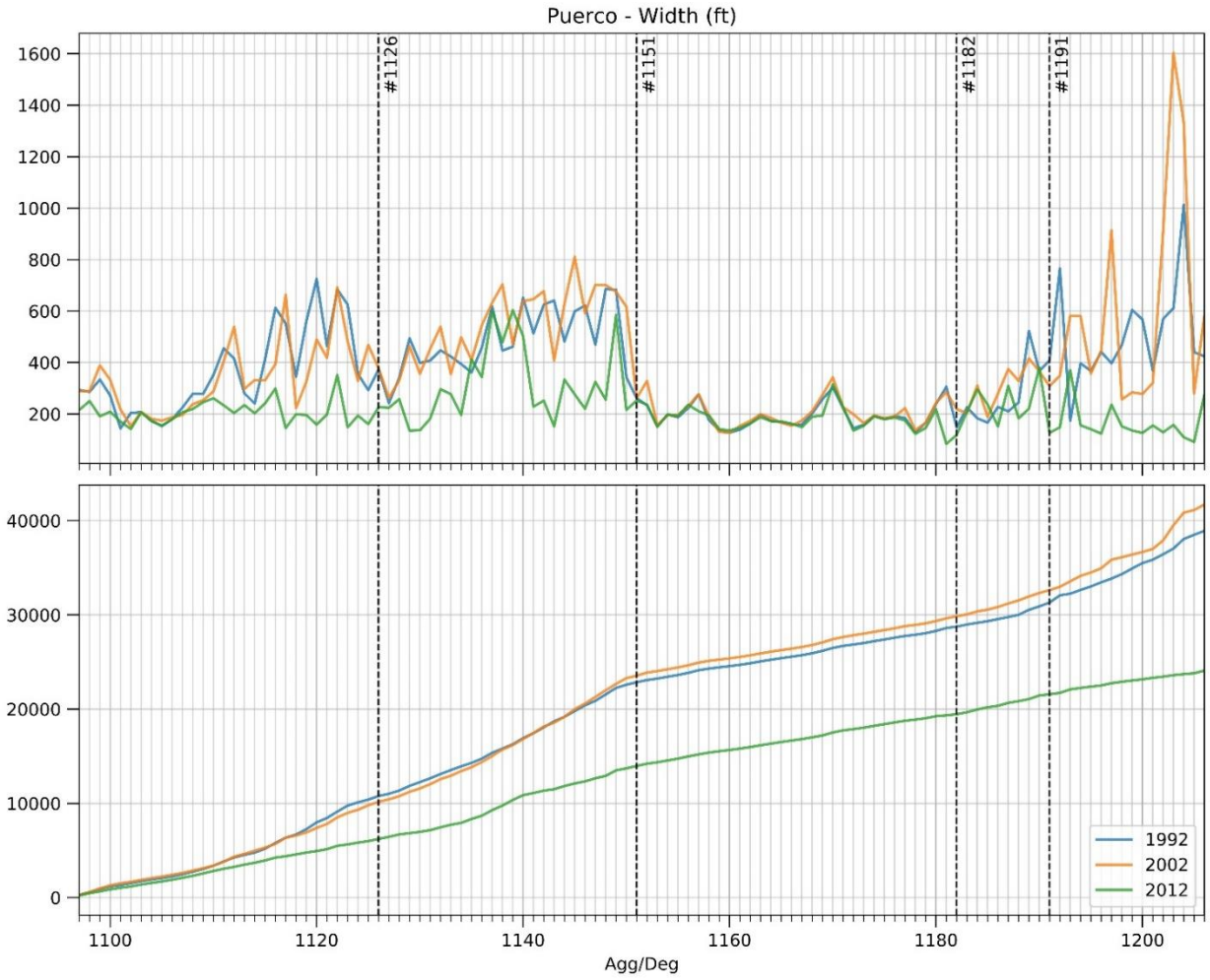

Figure 2: Width (up) and cumulative width (down) at agg/deg line 1098 to 1206

2. Precipitation, Flow and Sediment Discharge Analysis

2.1 Precipitation

Precipitation data is collected from areas in between Los Lunas and Sevilleta by the Bosque Ecosystem Monitoring Program from University of New Mexico (BEMP Data 2017). The locations of data collection are shown in Figure 3.

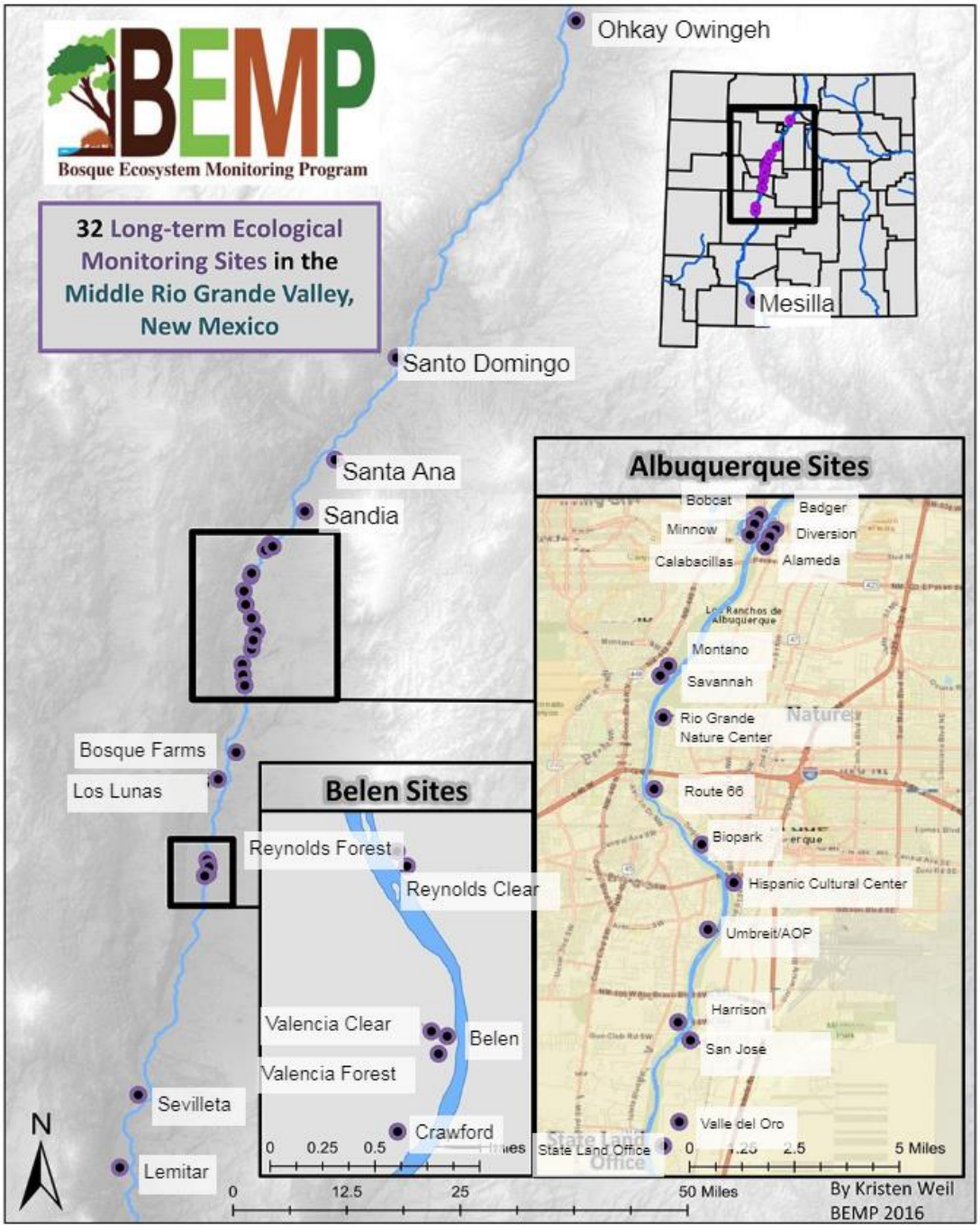

Figure 3: BEMP data collection sites (figure source: http://bemp.org/).

The Los Lunas site is just downstream of the start of the Isleta reach and the Sevilleta site is in the Sevilleta National Wildlife Refuge near the confluence of the Rio Puerco and the end of the Isleta reach. The average annual and monthly precipitation data accounts for both open and vegetated areas. The annual precipitation data between Los Lunas and Sevilleta are shown in Figure 4, with all station averages in Figure 5.

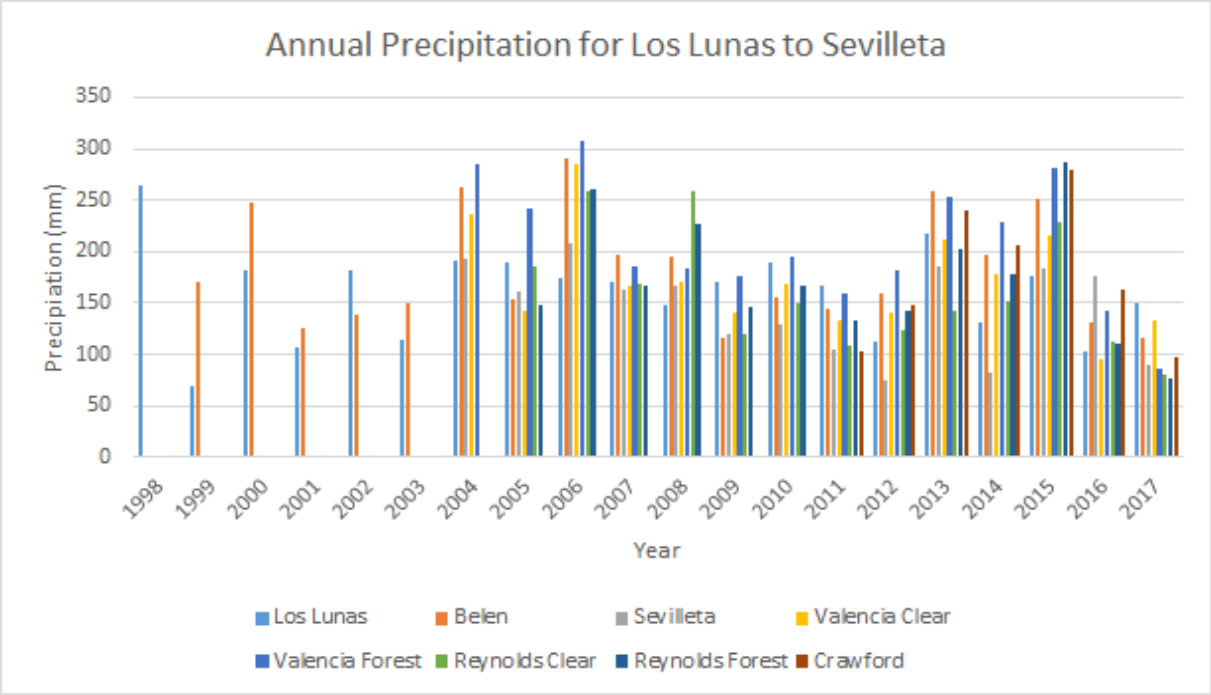

Figure 4: Average annual precipitation graph from 1998-2017

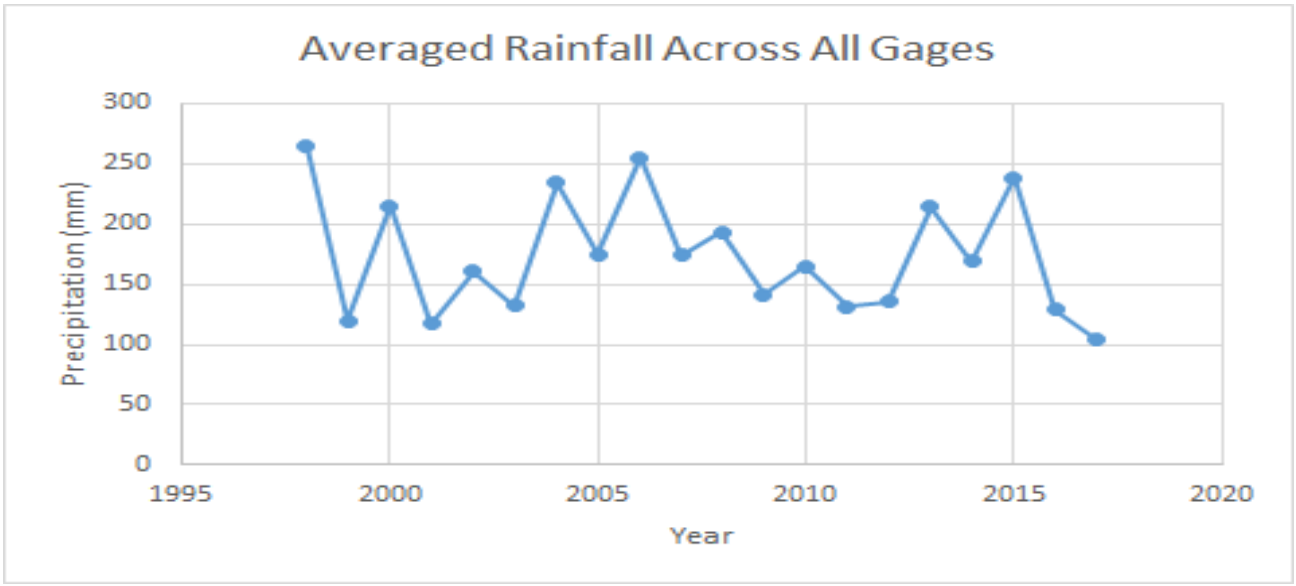

Figure 5: Averaged precipitation graph between Los Lunas to Sevilleta

Years 1998, 2006 and 2015 have peaks in precipitation. The driest years are around 2001 and 2011. Figure 6 shows monthly trends for the Los Lunas gage (the longest record).

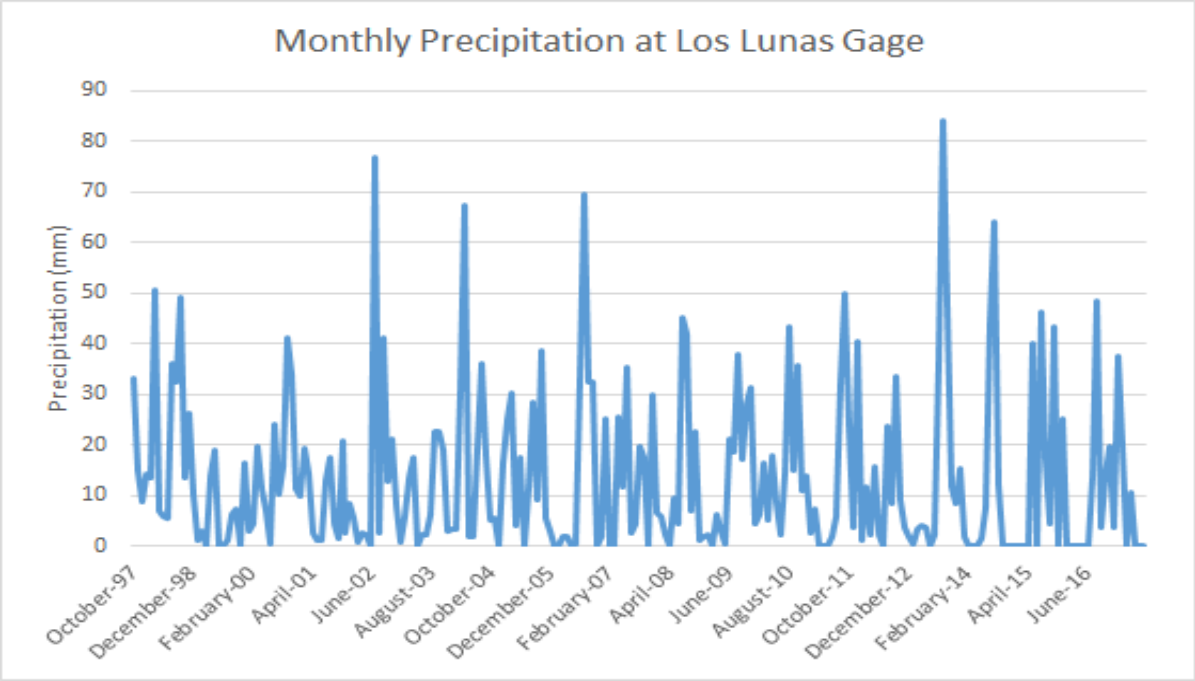

Figure 6: Monthly precipitation trends at the Los Lunas gage

The highest rainfall events tend to happen in late summer or early fall. Winter and early spring rain events still occur but are less common.

2.1. Flow Discharge

Available gages near the study reach are found in the USGS National Water Information System. Table 2 lists the gages that were analyzed in this report.

Table 2: List of USGS gages used in this study.

Station	Station #	Mean daily discharge	Suspended sediment
Rio Grande at Albuquerque	08330000	Oct 1989 - Current	Oct 1969 – Sep 2016
Rio Grande at Isleta Lakes Near Isleta	08330875	Oct 2002 - Current	
Rio Grande Near Bosque Farms	08331160	Oct 2007 - Current	
Rio Grande at State HWY 346 near Bosque	08331510	Oct 2006 - Current	
Rio Grande Floodway Near Bernardo	08332010	Oct 1990 - Current	Oct 1964 – Sep 2015
Rio Puerco near Bernardo	08353000	Sep 1939 - Current	Oct 1955 – Sep 2015
Rio Grande Floodway at San Acacia	08354900	Oct 1958 - Current	Oct 1959 – Sep 2016

The daily discharge of the Albuquerque (08330000), Bernardo (08332010) and San Acacia (08354900) are plotted in Figure 7 to 9. No data are available from July 2005 through September 2011 at the Bernardo gage. The plots show seasonal flow patterns: the high flow occurs in April through June, followed by low flow in July to October, and medium flow from November to March. The spring high flow is attributed to snow melt runoff. Spring flow has generally decreased since around 1980 through the Albuquerque gage (Figure 7). At the Bernardo gage, flows dramatically increased after 1985 and have declined since the mid-1990s (Figure 8). At the San Acacia gage, flows increased starting around 1980 and then also declined in the 1990s (Figure 9), following a similar pattern to that of the Bernardo gage. The Rio Puerco is unregulated and has large peak flows. Current peak flows are still lower than peak flows observed in the 1920s to the 1940s (MEI 2002 in Klein et al. 2018a). Similar trends can also be found in Figures 6 to 8 which are the 3D water magnitude plots of Rio Grande at Albuquerque, Bernardo, and San Acacia. At Albuquerque, Figure 8, the low flow periods after the 80's are not as severe as they were prior to Cochiti Dam.

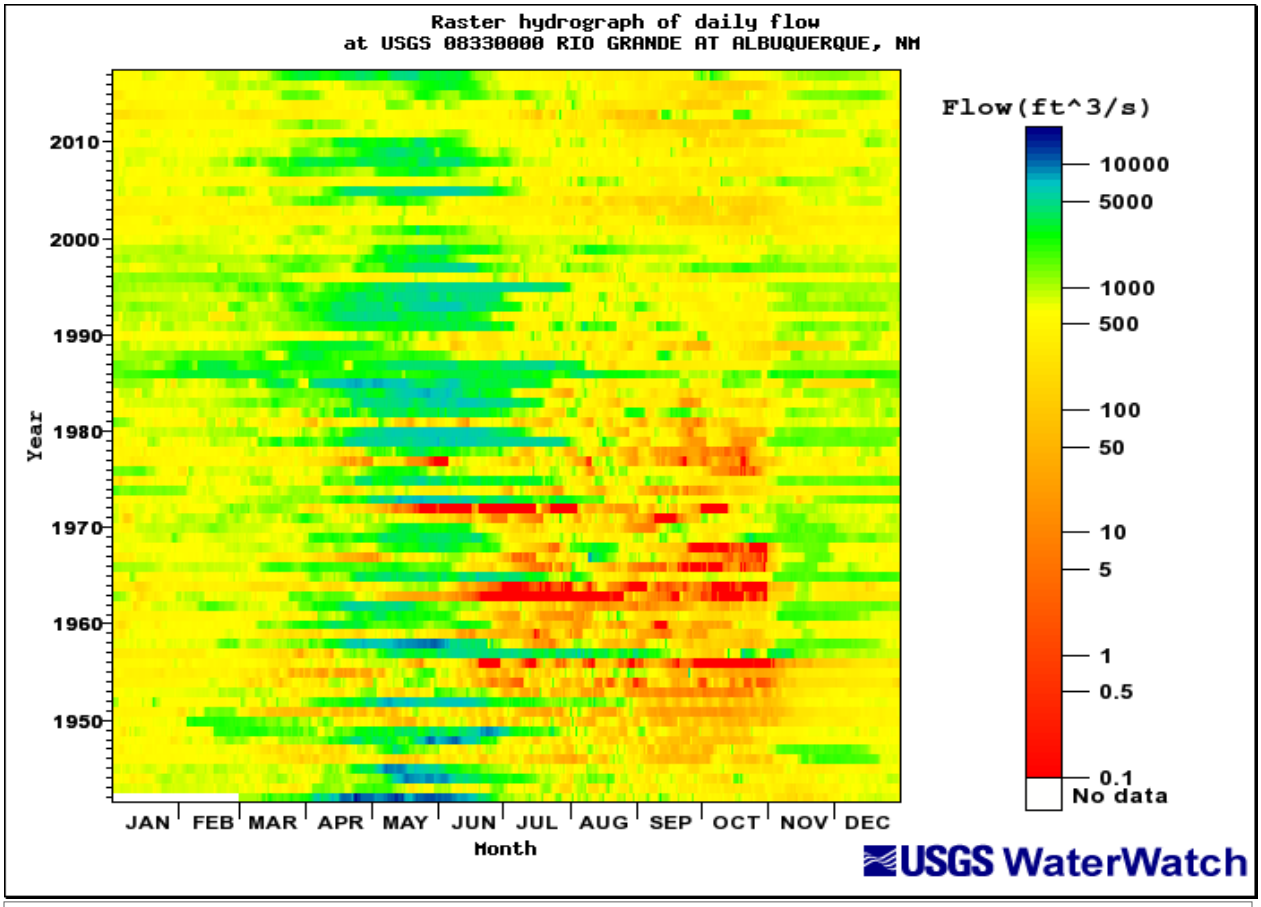

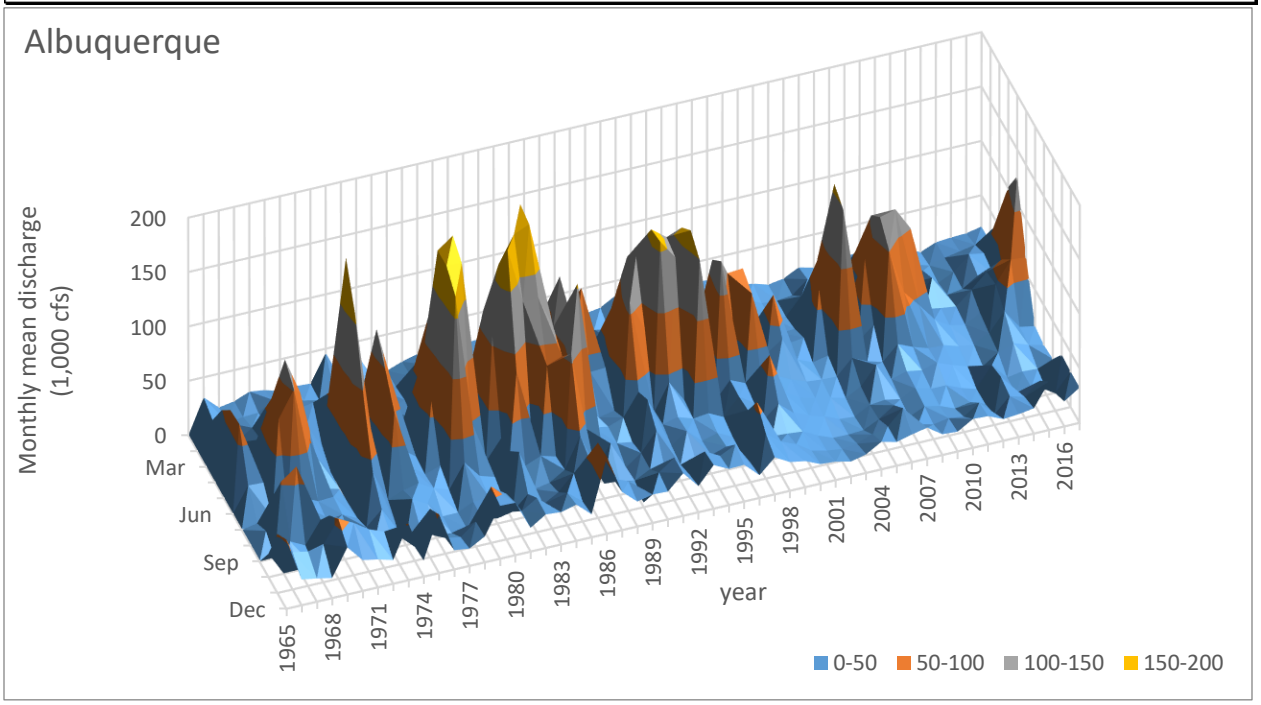

Figure 7: Raster hydrograph for the Rio Grande at Albuquerque (08330000): 1942 to 2017.

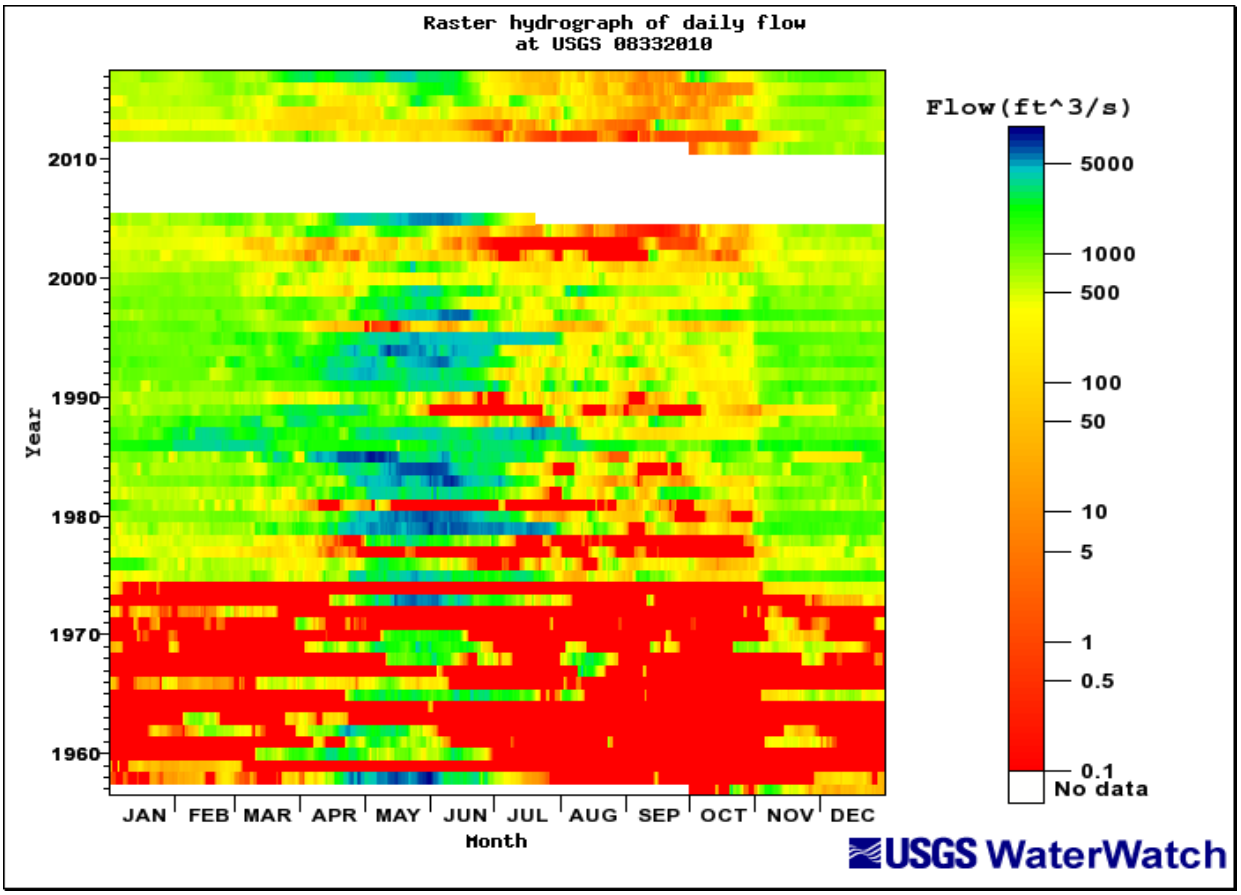

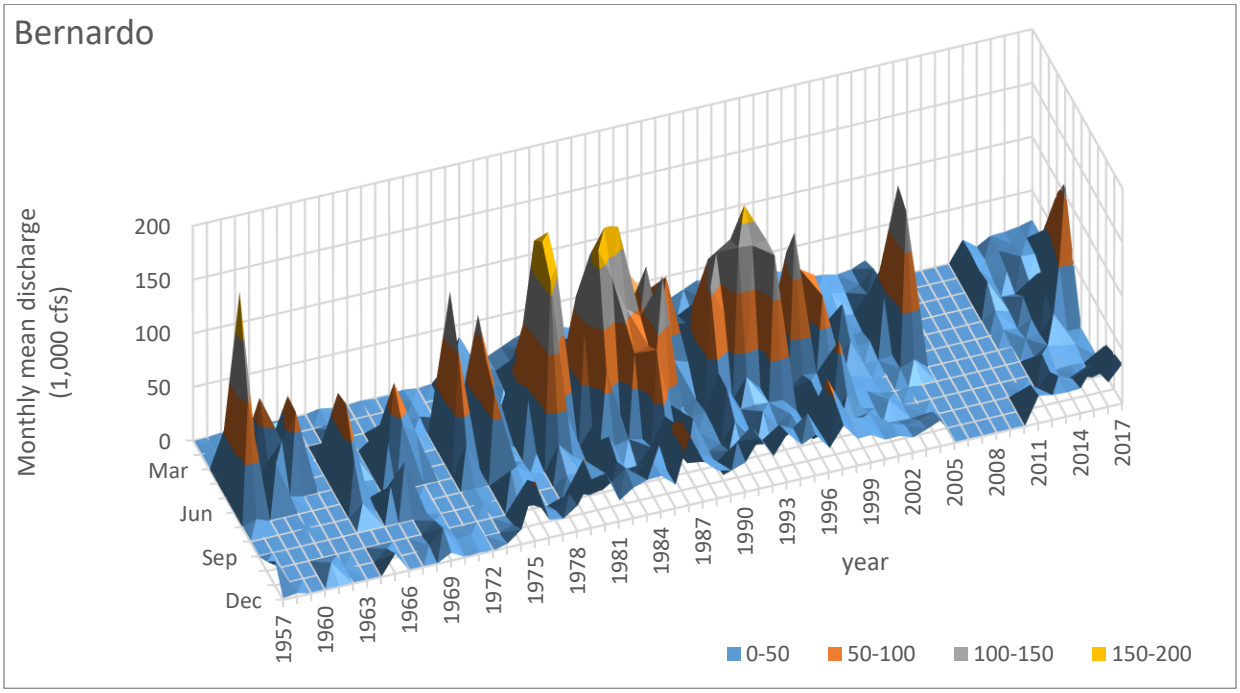

Figure 8: Raster hydrograph for the Rio Grande floodway near Bernardo (08332010): 1958 to 2017.

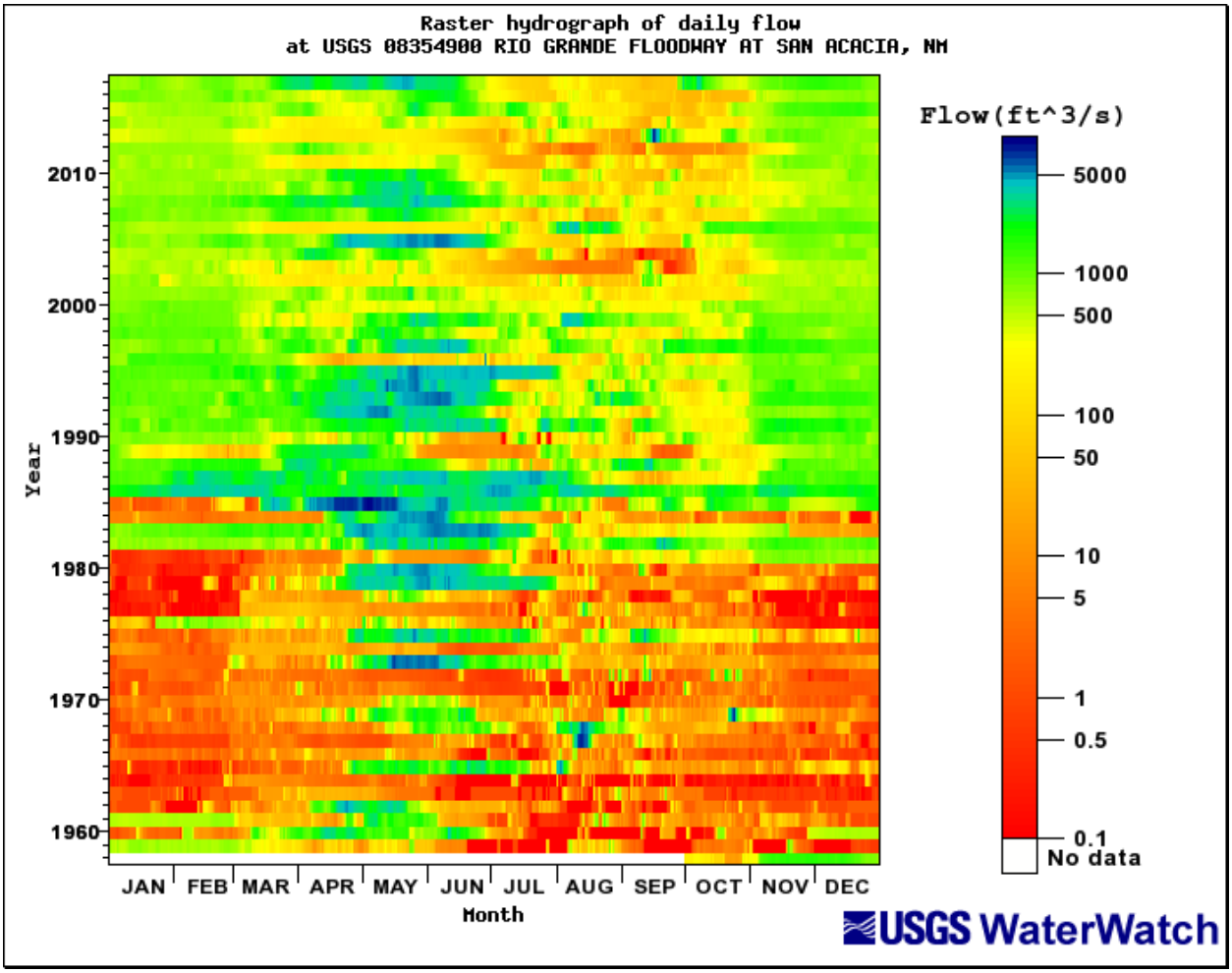

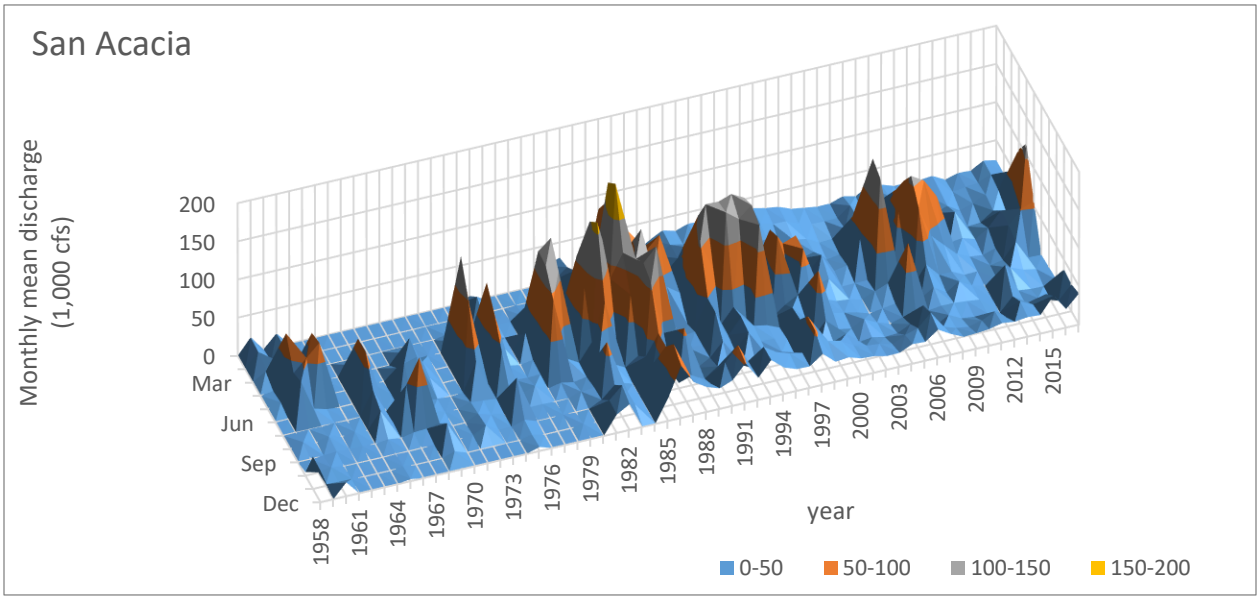

Figure 9: Raster hydrograph for the Rio Grande floodway at San Acacia (08354900): 1958 to 2017.

2.1.1. Cumulative Discharge Curves

Cumulative discharge curves are used to show changes in annual flow volume over time. The cumulative discharge is presented as a function of time in years. The slope of the line gives the mean annual discharge. Breaks in slope show changes in the flow volume. Figure 10 shows the flow mass curves of gages at Albuquerque, Isleta, Bosque Farms, Bosque, Bernardo, and San Acacia. The annual flow volume shows slight reduction in the downstream direction. The discharge mass curves are divided by the time periods 1942 to 1978, 1978 to 1980, 1980 to 1981, 1981 to 1987, 1987 to 1990, 1990 to 1995, 1995 to 2001, 2001 to 2004, 2004 to 2010, 2010 to 2014 and 2014 to 2017. The average discharge of each period is listed in Table 3. For the Albuquerque gage (08330000), the annual flow increases from 0.74 million acre-feet to 1.21 million acre-feet after 1978. A decrease in discharge between 1995 and 2010 and another decrease in discharge is found after 2010. Similar trends are found in the other stations as well.

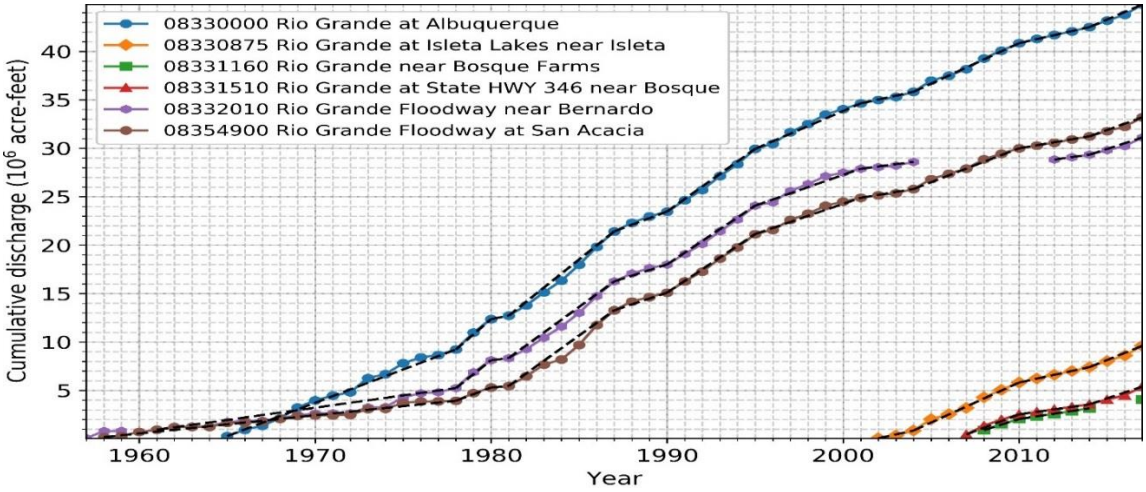

Figure 10: Cumulative discharge curves vs time.

Table 3: Average discharge at different time periods in million acre-feet.

Time	08330000	08330875	08331160	08331510	08332010	08354900
1958 - 1978	0.74				0.25	0.19
1978 - 1980	1.57				1.44	0.68
1980 - 1981	0.34				0.22	0.16
1981 - 1987	1.45				1.32	1.30
1987 - 1990	0.68				0.58	0.61
1990 - 1995	1.29				1.21	1.21
1995 - 2001	0.78				0.64	0.62
2001 - 2004	0.40	0.29			0.23	0.31
2004 - 2010	0.84	0.83	0.68	0.63		0.70
2010 - 2014	0.42	0.40	0.28	0.26	0.25	0.31
2014 - 2017	0.78	0.73	0.63	0.46	0.59	0.65

2.1.2. Recurrence Intervals

Using gages previously mentioned, recurrence intervals were calculated and presented in a report from the U.S. Bureau of Reclamation (USBR). The report from USBR, authored by Klein et al. (2018a) is closely related to this report, but the USBR geomorphic analysis is not broken up into subreaches, unlike this report. Therefore, the USBR report provides a great deal of background and summary of this reach, so is referenced frequently. summarizes flood frequencies in the Klein et al. (2018a) report.

Table 4: Return periods (Klein et al. 2018a).

Discharge (cfs)	2 Year	5 Year	10 Year	25 Year	50 Year	100 Year
Albuquerque (MEI (2002))	5,410	7,600	8,940	10,100	11,600	12,600
Albuquerque (Wright (2010))	4,000	6,200	7,500	9,000	10,000	10,000
Albuquerque, 1993-2013	3,370	5,280	6,550	8,100	9,230	10,300
Bernardo (Wright (2010))	4,900	7,700	9,300	11,200	12,500	12,700
Bernardo, 1993-2013	3,290	5,610	7,090	8,820	10,000	11,100
San Acacia (Wright (2010))	7,800	12,000	14,500	17,400	19,300	20,100
San Acacia (Harris, 2016)	4,410	6,380	7,570	8,920	9,820	10,600

The number of days exceeding certain flow values was also examined. Flow is available at the Albuquerque, Bernardo and San Acacia gages. The data is analyzed in water years. Figure 11 through Figure 13 show a reduction in peak flows, with flows above 6,000 cfs not seen after 2004 at any gages. Both the number of days where Q > 500 cfs and Q > 1,000 cfs show a general decrease at Albuquerque and San Acacia gages since 2000, perhaps with the exception of the Bernardo gage because the missing data make it difficult to see the trend.

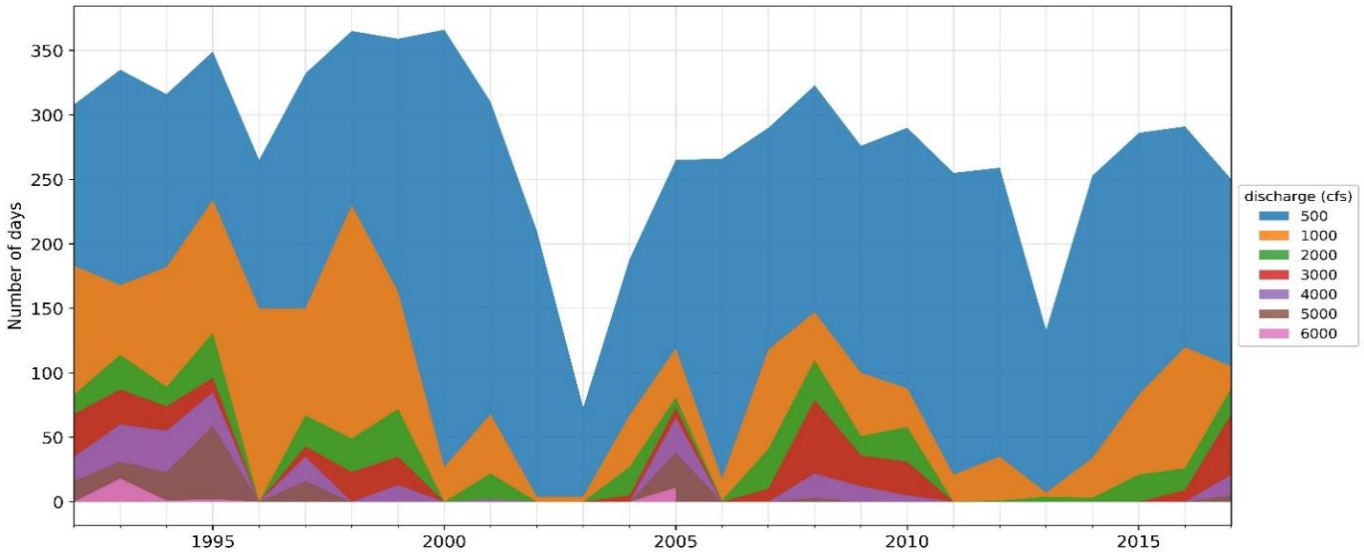

Figure 11: Graph of days exceeding flow values at Albuquerque (USGS Gage 08330000) (modified from Klein et al. 2018a).

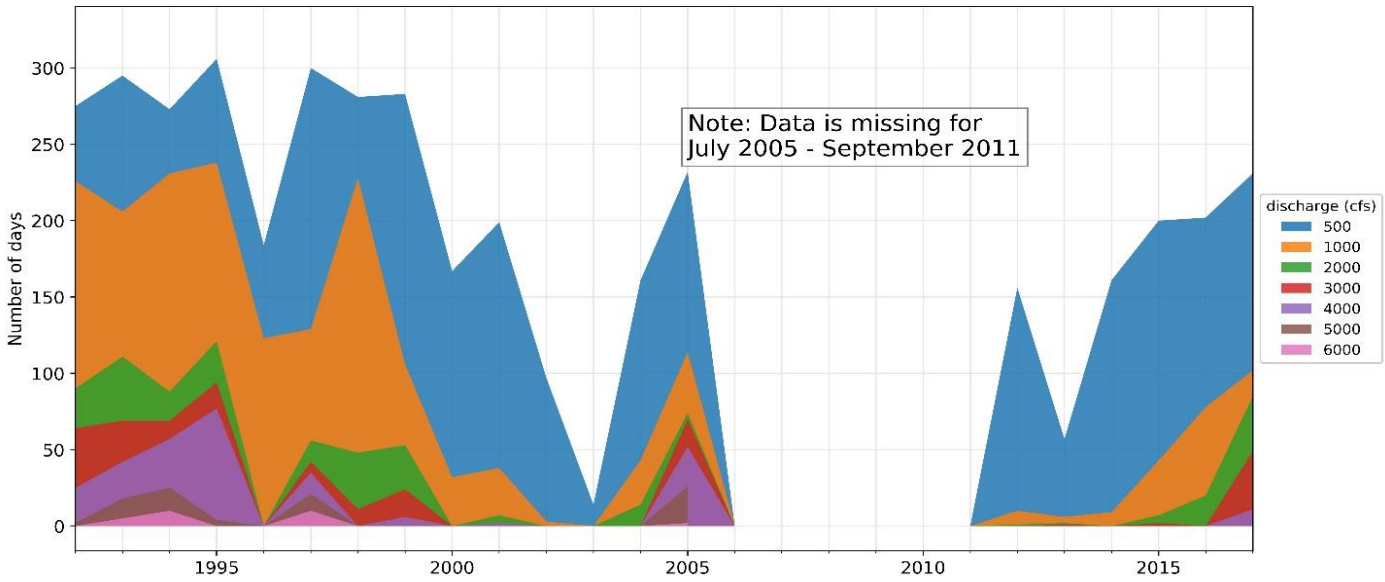

Figure 12: Graph of days exceeding flow values at Bernardo (USGS Gage 08332010) (modified from Klein et al. 2018a).

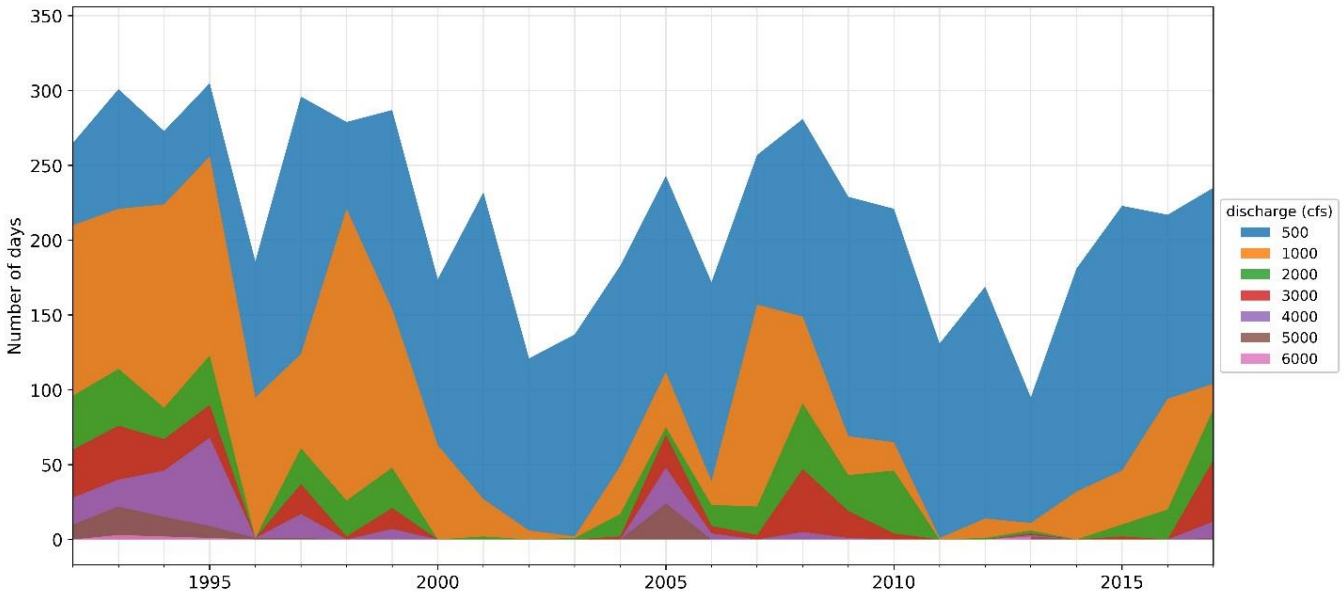

Figure 13: Graph of days exceeding flow values at San Acacia (USGS Gage 08354900) (modified from Klein et al. 2018a).

2.3. Suspended Sediment Load

2.3.1. Mass Curves

Single mass curves of cumulative suspended sediment flux (in millions of tons) are shown in Figure 14 through Figure 16. Breaks in slope show the changes in flux. Data comes from the USGS gages at the Albuquerque (08330000) gage and Bernardo (08332010) gage upstream of the Rio Puerco confluence. The Rio Puerco gage (USGS 0853000) is used for the Rio Puerco single mass curve. The data on the graph is based on annual sediment amounts.

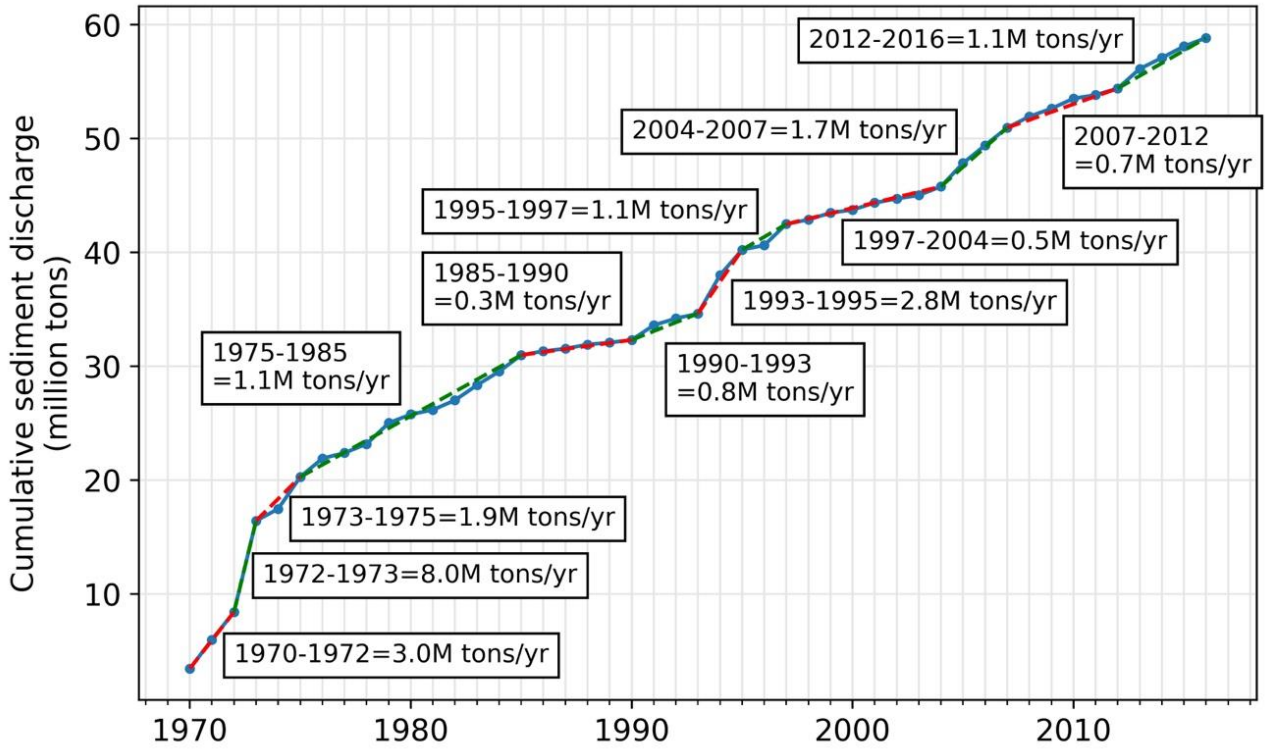

Figure 14: Single mass curve at Albuquerque (08330000) for suspended sediment (modified from Klein et al. 2018a).

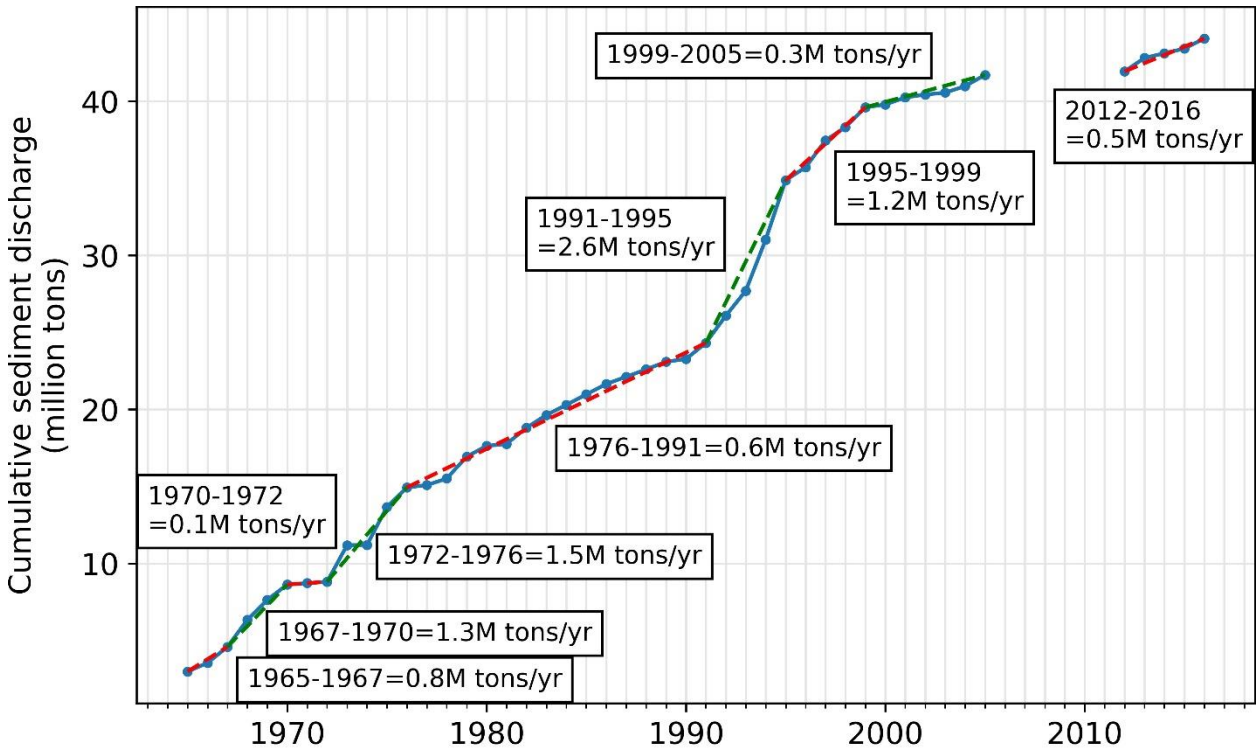

Figure 15: Single mass curve upstream at Bernardo (08332010) for suspended sediment (modified from Klein et al. 2018a).

Albuquerque experienced a larger decrease in sediment load after the mid -70's than the Bernardo gage, which can be attributed to the influence of Cochiti Dam. The sediment load at the Bernardo gage also was fairly high in the 90's, it also decreased to a fairly constant and sustained low suspended sediment load in the new millennium. The Bernardo and Albuquerque gage have alternated which transports more suspended sediment. For instance, the average suspended sediment load from 1991-93 was low at Albuquerque but high at Bernardo. Since 2000, the suspended sediment load at the Albuquerque gage appears to be larger than at Bernardo.

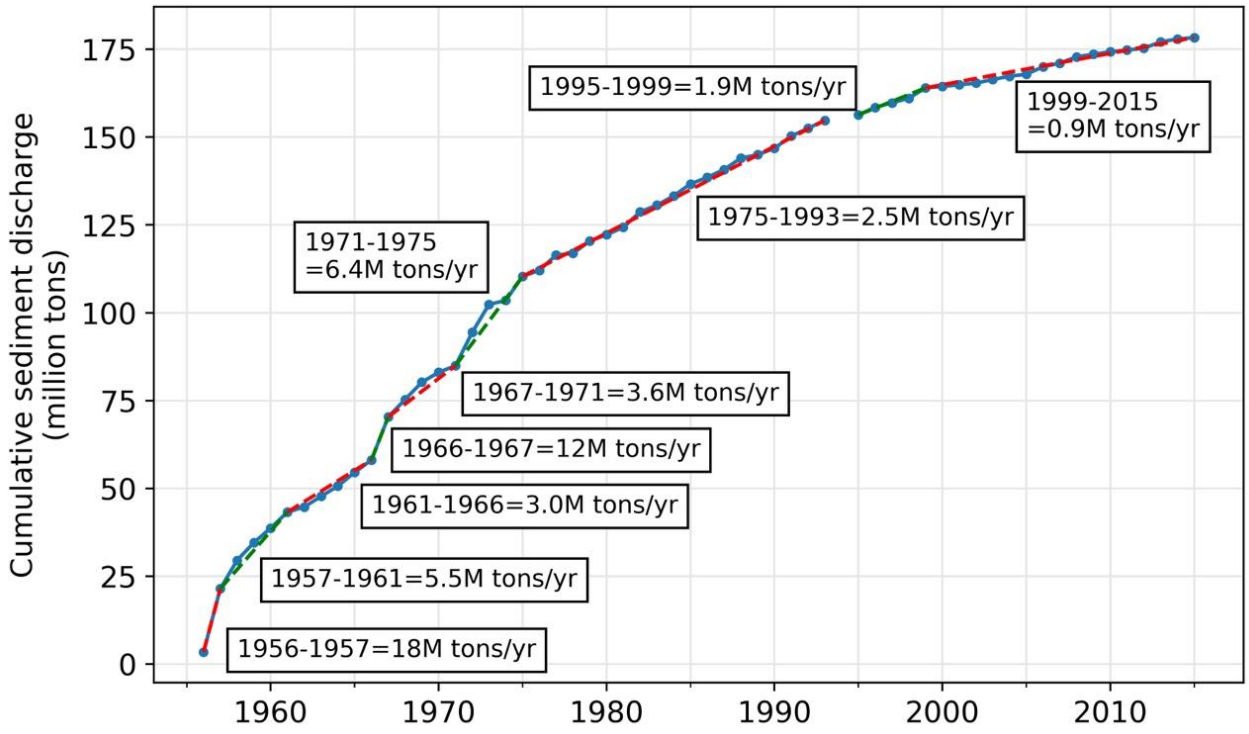

Figure 16: Single mass curve for suspended sediment on the Rio Puerco (08353000) (modified from Klein et al. 2018a).

The Rio Puerco's sediment discharge has gradually decreased since the 1970s. It contributed 70% of the annual suspended sediment volume recorded at the San Acacia gage from the late 1970s through the early 1980s. The contribution decreased to about 38% of the annual suspended sediment load (Klein et al. 2018a).

2.3.2. Double Mass Curves

Double mass curves are used to show how suspended sediment volumes pair with annual discharge volume. The slope of the double mass curves represents the mean sediment concentration. The double mass curves at Albuquerque and Bernardo are shown on Figures 17 and 18 respectively.

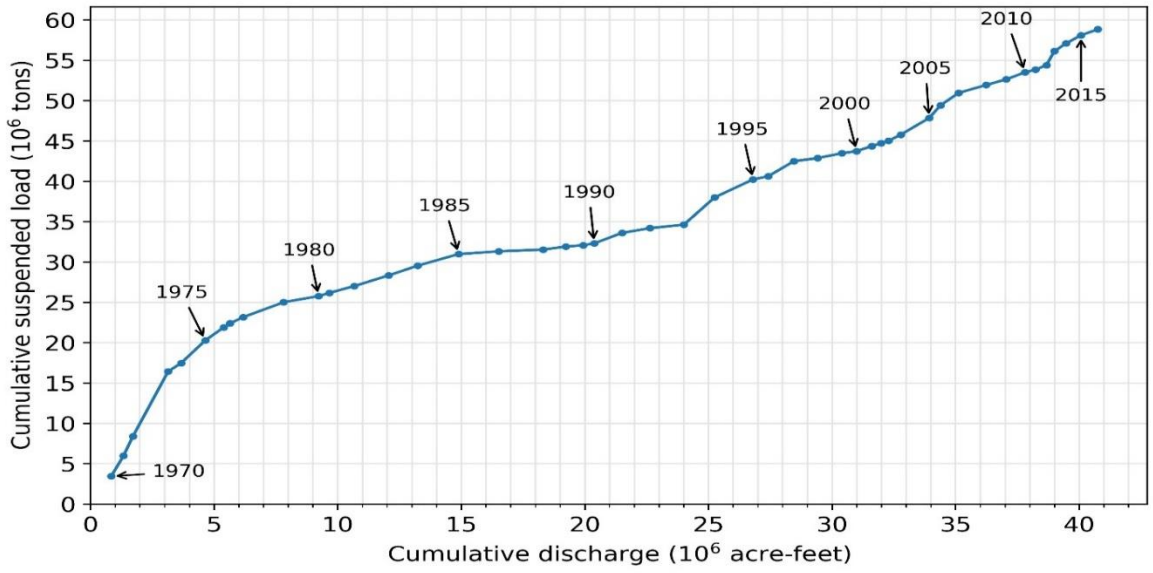

Figure 17: Double mass curve at Albuquerque gage (08330000) from 1970 to 2016.

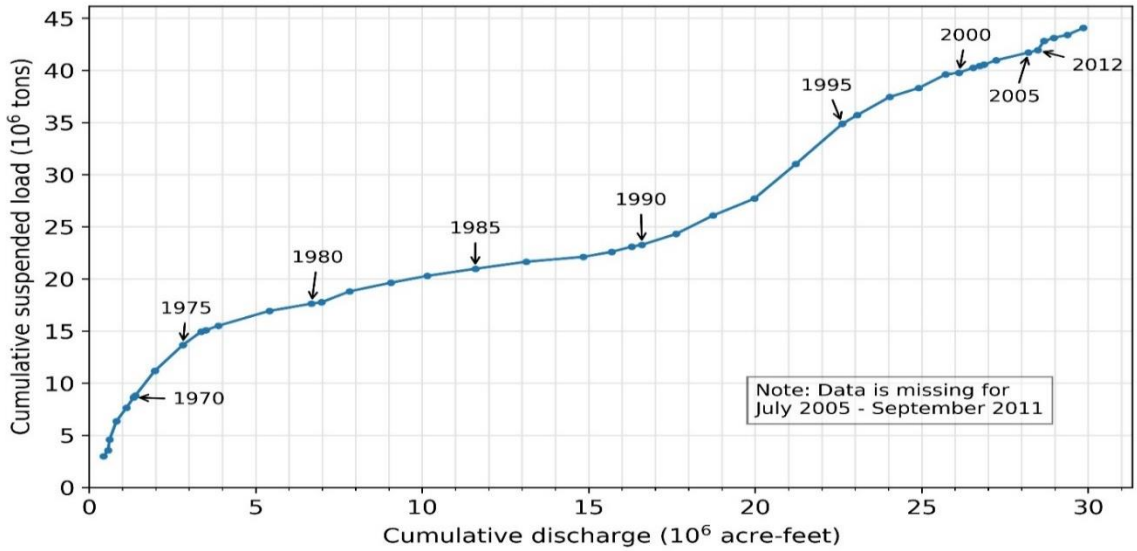

Figure 18: Double mass curve at Bernardo gage (08332010) from 1965 to 2016.

Overall, the mean annual suspended sediment concentration has decreased since the 1960s (Klein et al. 2018a). The highest concentration occurred prior to 1975 at Albuquerque gage (Figure 17). The Bernardo gage shows a similar trend to the Albuquerque gage, although the values are lower (Figure 18). Additionally, there is a more distinct increase in sediment concentration in the early 1990s at the Bernardo gage. From 1975 to 1993 the average sediment concentration was about 1,174 mg/l at Albuquerque and 1,270 mg/l at Bernardo. After 1993, the average suspended sediment concentration was 1,657 mg/l at Albuquerque and 1,864 mg/l at Bernardo.

2.4. Total Sediment Load

This section is divided into two parts: (1) BORAMEP analysis of the total sediment load from Klein et al. (2018a); and (2) Analysis of the total sediment load from SEMEP from Yang (2019).

2.4.1. BORAMEP

The total sediment load can be calculated from sediment concentration measurements and discharge using the Modified Einstein Procedure (MEP). The Bureau of Reclamation Automated Modified Einstein Procedure was developed by Holmquist-Johnson et al. (2009). The details of the calculations, methods and results on the Rio Grande were presented by Klein et al. (2018a). The total load was calculated using sediment data from the San Acacia gage downstream of the Diversion Dam (SADD). This is the only gage USBR used to calculate the total sediment load. The calculations using BORAMEP included the early 1990s through 2010.

Error! Reference source not found. Figure 19 shows the total sediment discharge against the flow discharge. At a given discharge, silt or sand bed channel has a higher total sediment discharge. The San Acacia gage shows that the predominant material being transported is sand. Silts and clays are transported less than sand, and gravel is less than 1% of the total load. According to Klein et al. (2018a), sand loads are 5 times greater during summer or fall monsoon rain events compared to spring snow-melt runoff periods up to 2,000 cfs. Gravels move primarily during spring snow-melt periods, whereas sand and smaller particles move during both spring and summer peak flow periods.

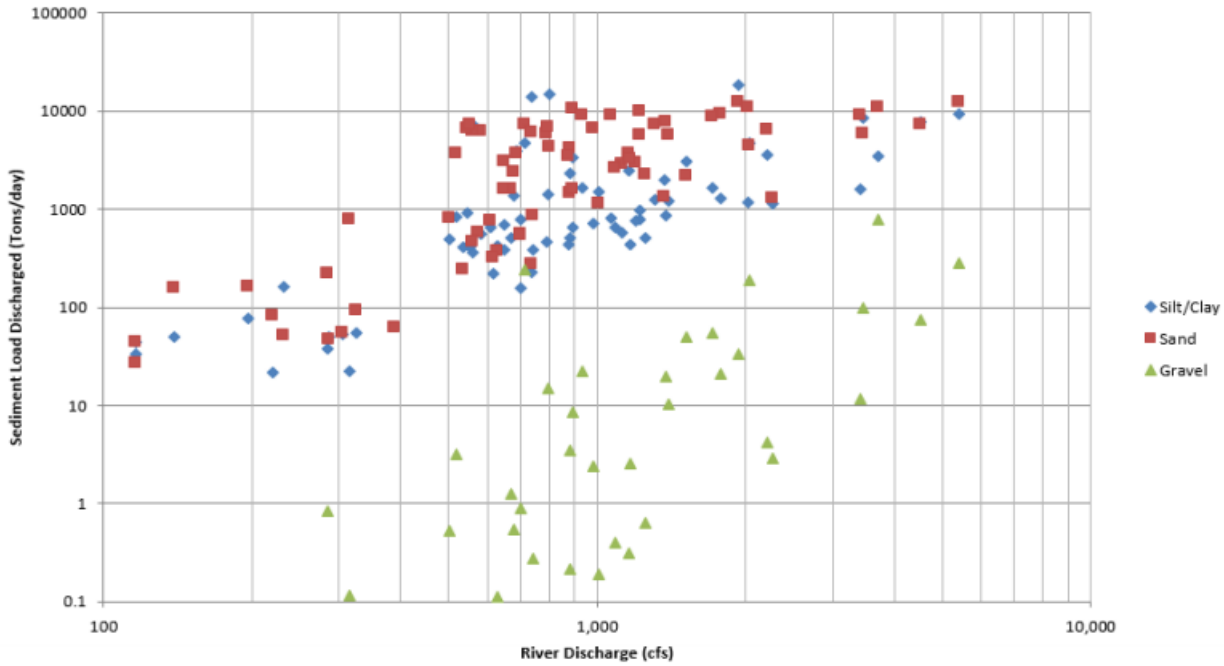

Figure 19: Graph of total load for gravels, sands and fines at the San Acacia gage from 1995-2010. Gravel data below 0.1 tons/day is omitted. (Klein et al. 2018a)

Figure 20 shows the percentage of sediment transport for gravels, sands and fines. Figure 21 gives the total sediment rating curve at San Acacia.

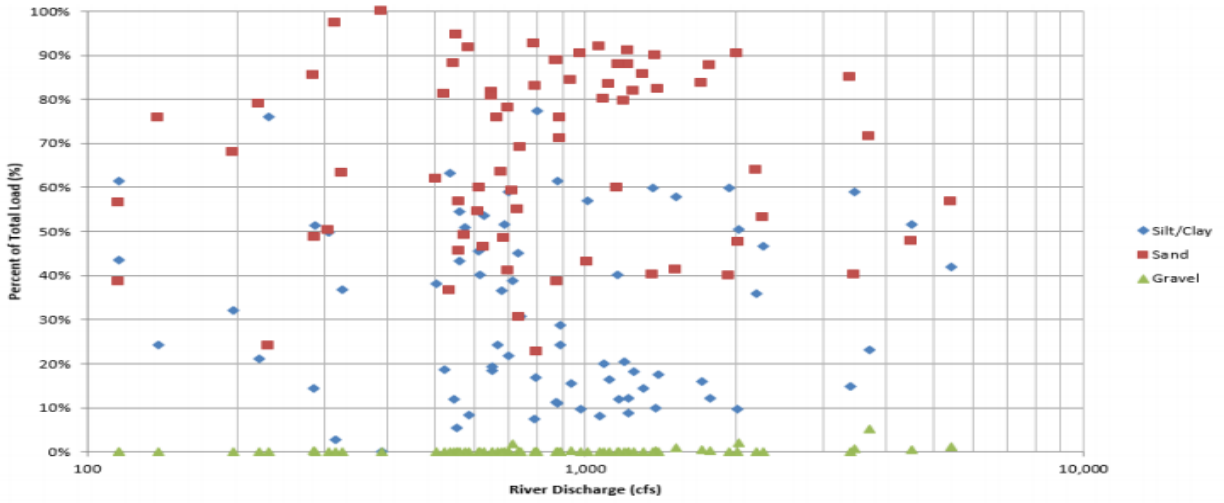

Figure 20: Percent of the total load in gravels, sands and fines as a function of discharge at San Acacia (Klein et al. 2018a)

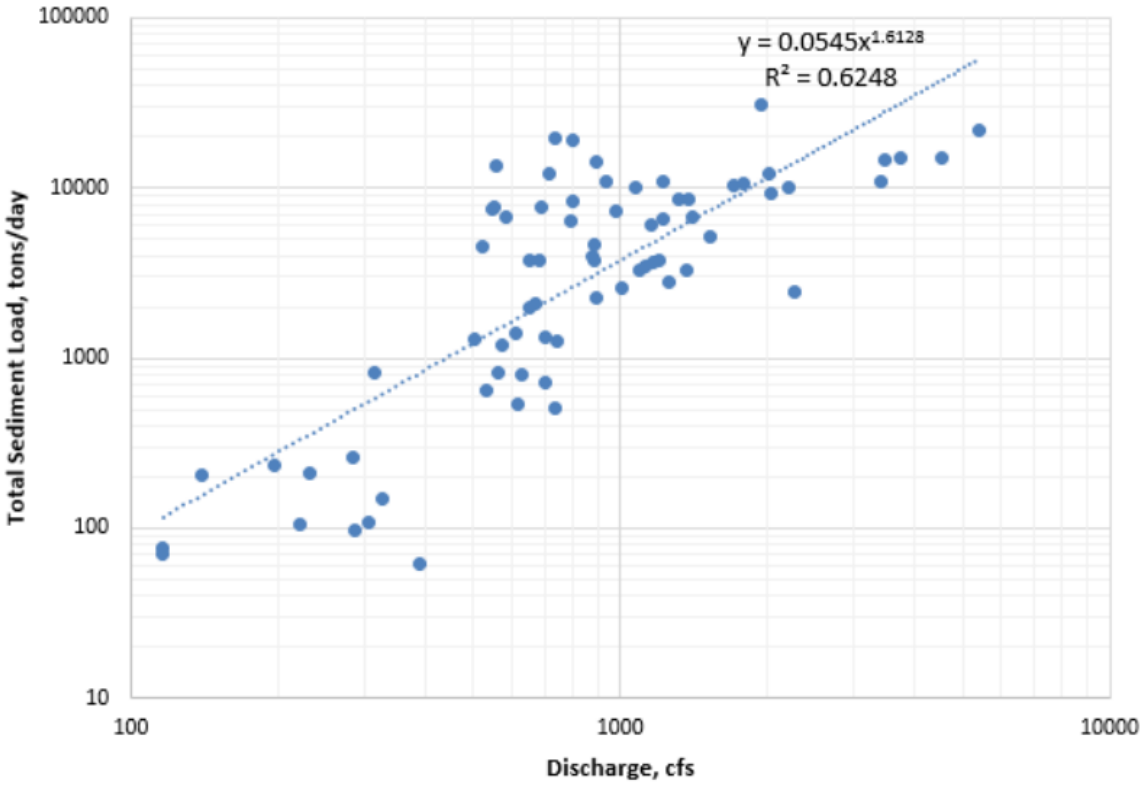

Figure 21: Total sediment load at San Acacia (Klein et al. 2018a)

2.4.2. SEMEP

The Series Expansion of Einstein Procedure (SEMEP) was also used in this study. The method was developed at CSU with the procedure detailed in Shah-Fairbank et al. (2011) as a function of shear velocity u_* and fall velocity ω. It was recently tested by Yang (2019) with applications on 35 rivers in South Korea. In this report, SEMEP is applied at three stations on the Rio Grande, at San Acacia gage 08354900, as well as Albuquerque and Bernardo at gages 08330000 and 08332010. The number of field samples calculated by the SEMEP are respectively 306, 211, and 173 samples at gages 08330000, 08332010, and 08354900. For these stations, the values of u_*/ω range from 1.5 to 37,600. According to Shah-Fairbank et al. (2011), SEMEP performs accurately when $u_*/\omega > 5$ so we expected good results from the applications on the Rio Grande.

It can be seen in Figure 22a that the SEMEP predictions and total sediment load measurements fall close to the 45 degree line of perfect agreement. Figure 22b also shows the prediction errors between SEMEP calculations and measurements as a function of u_*/ω. The mean absolute percentage error is 27% (Figure 22b). Figures 23 to 25 show the sediment rating curves for total sediment discharges at gages 08330000, 08332010, and 08354900.

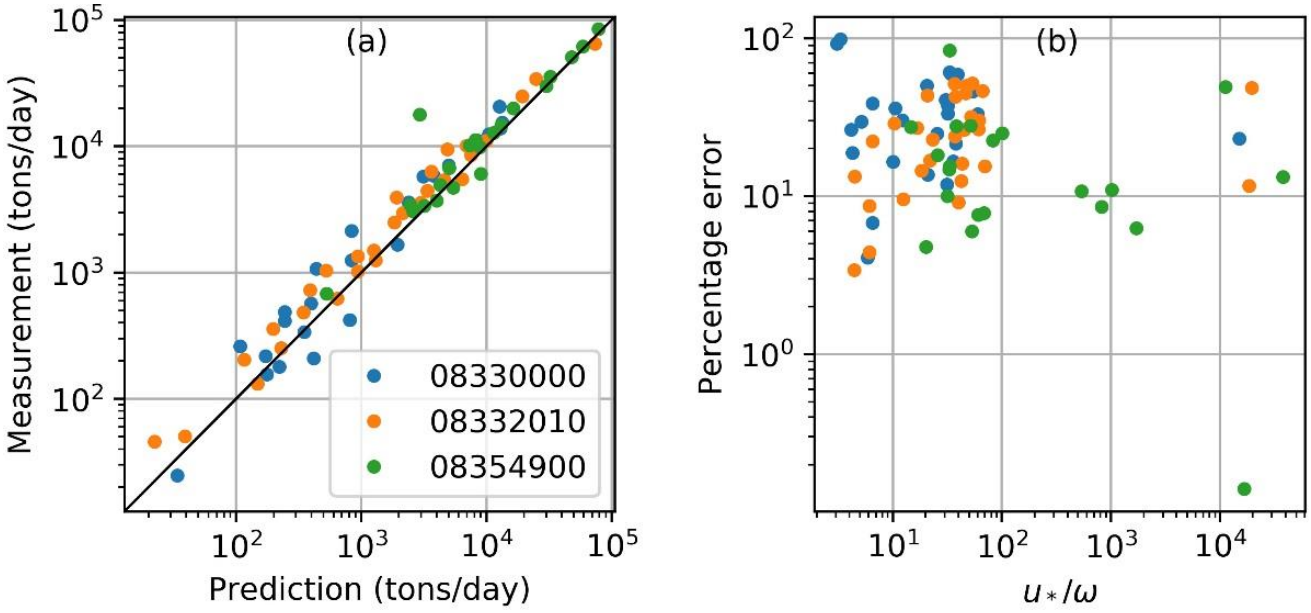

Figure 22: (a) Comparison between predicted and measured total sediment load, and (b) percentage error versus u_*/ω

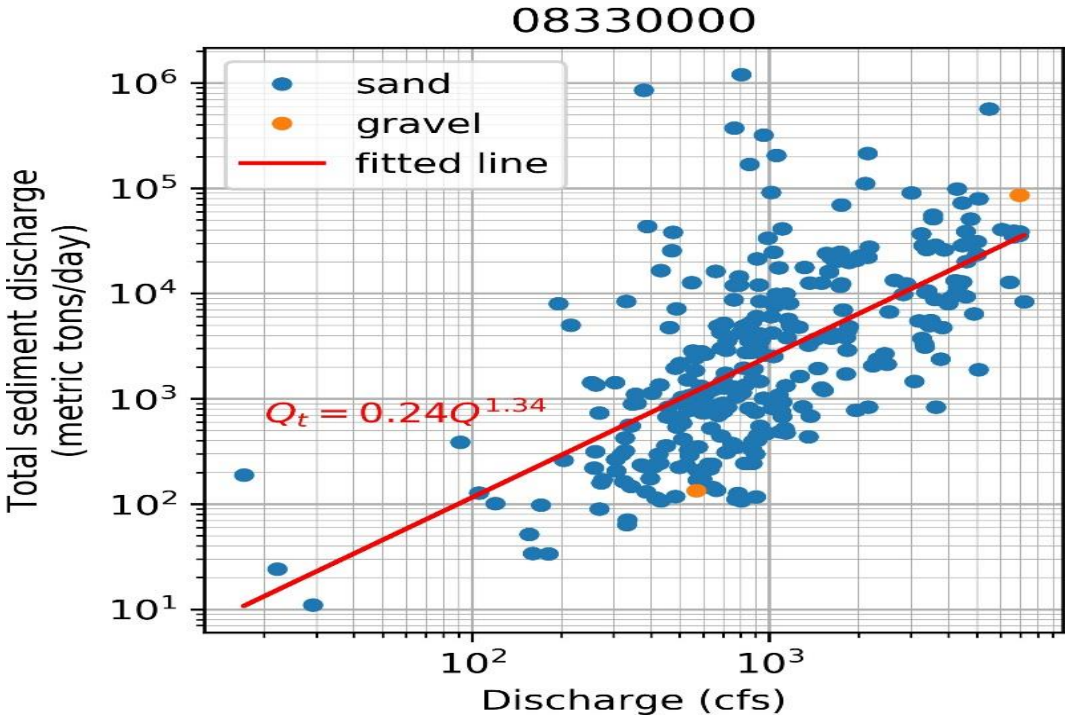

Figure 23: Total sediment rating curve at Rio Grande at Albuquerque (08330000)

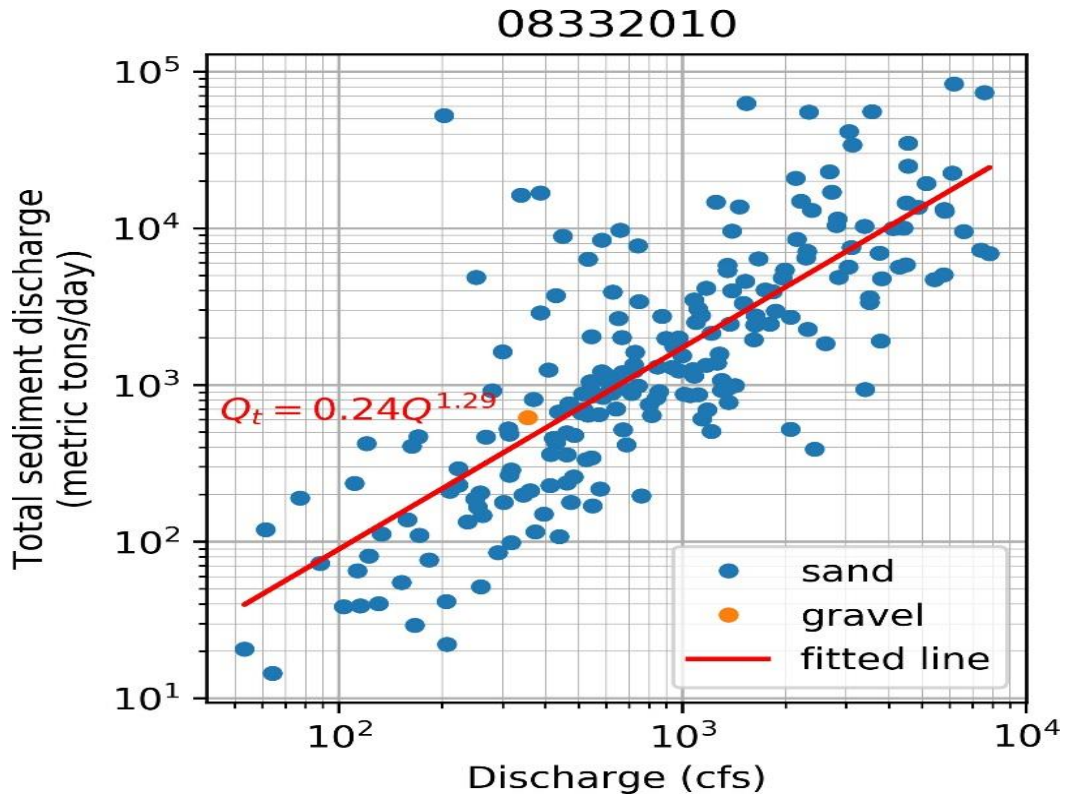

Figure 24: Total sediment rating curve at Rio Grande Floodway Near Bernardo (08332010)

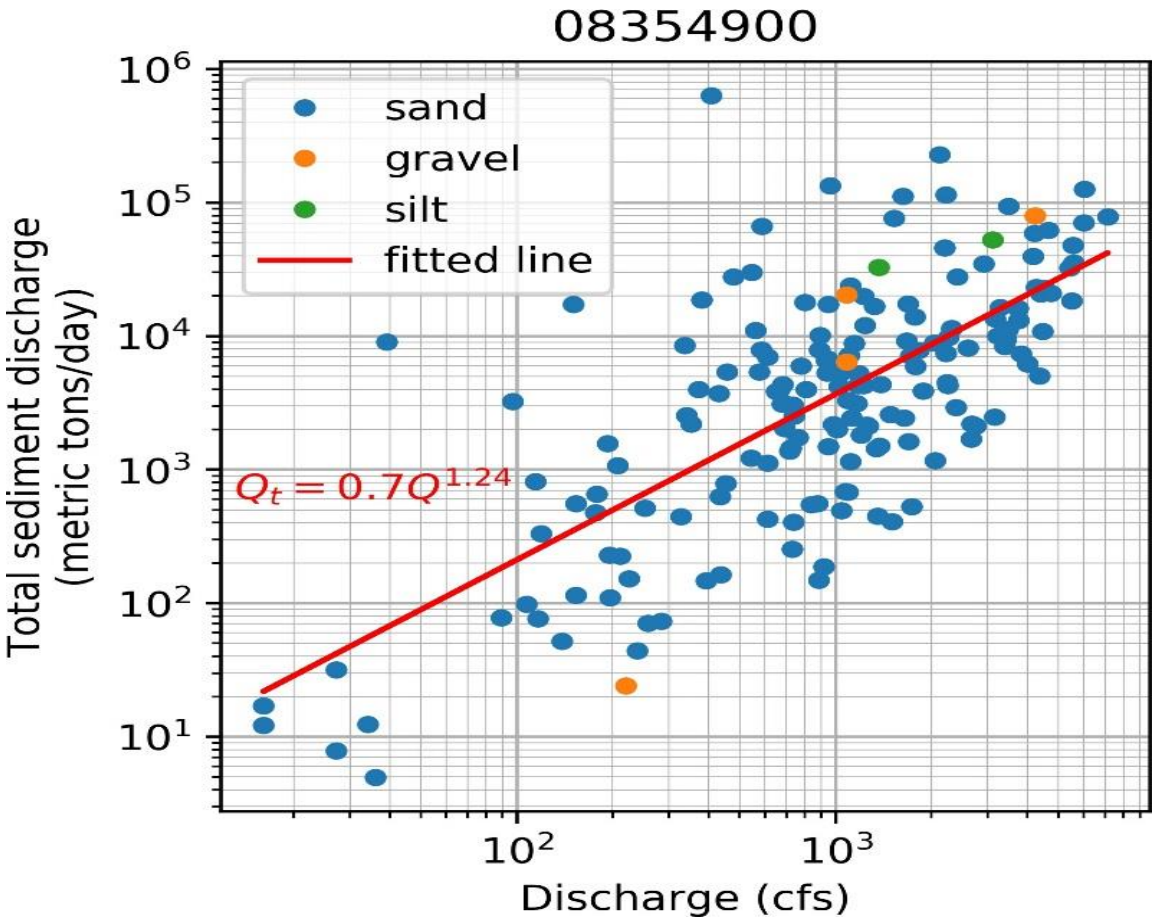

Figure 25: Total sediment rating curve at the Rio Grande Floodway at San Acacia (08354900)

The ratio of measured to total sediment discharge is a function of flow depth h, bed material d_s, and Rouse number Ro ($2.5/\text{Ro} = u_*/\omega$) according to SEMEP (Shah-Fairbank et al. 2011; Yang and Julien 2019). On the other hand, the ratio of suspended to total sediment discharge is a function of the ratio h/d_s of flow depth h to grain size d_s and Ro. The calculated ratio Q_m/Q_t of measured $Q_m$to total sediment discharge Q_t, and the ratio $Q_s/Q_t$of suspended Q_s to total sediment discharge Q_t are plotted with the analytical solutions in Figures 26 to 28 for the three different gaging stations. As expected, when the value of Ro is low (Ro < 0.3), the ratio Q_s/Q_t is close to 100% during floods when h/d_s > 100. These ratios are also in good agreement with the theory for both sands and gravels.

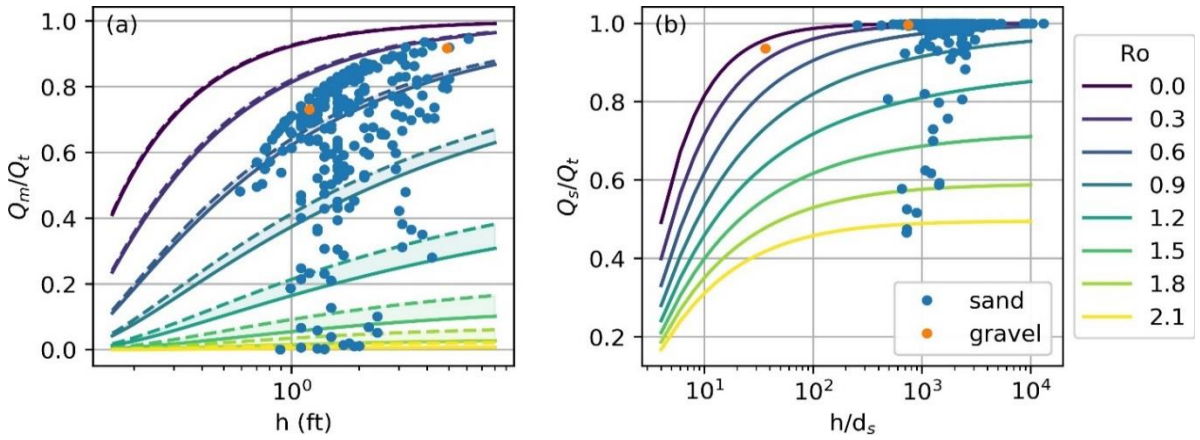

Figure 26: (a) the ratio of measured to total sediment discharge vs depth; and (b) the ratio of suspended to total sediment discharge vs h/ds at Albuquerque (08330000)

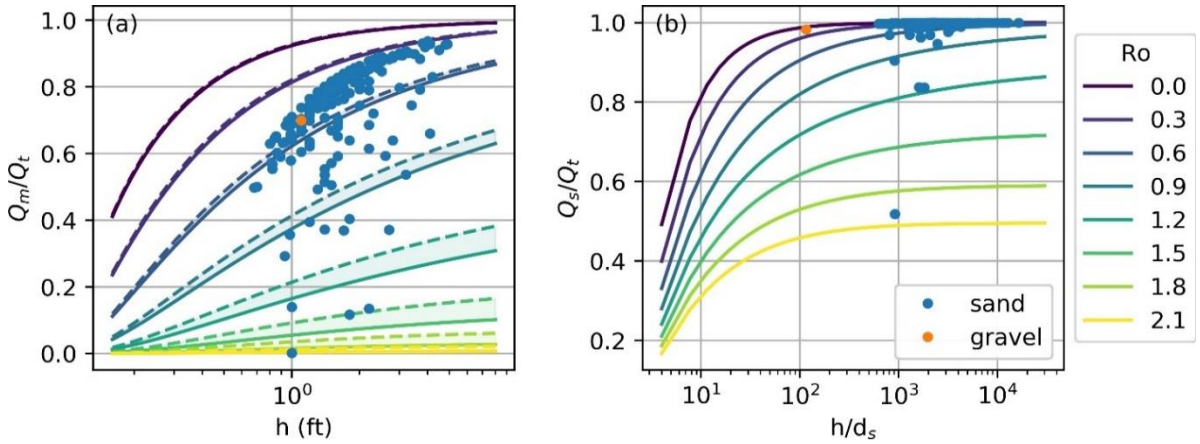

Figure 27: (a) the ratio of measured to total sediment discharge vs depth; and (b) the ratio of suspended to total sediment discharge vs h/ds at the Rio Grande Floodway Near Bernardo (08332010)

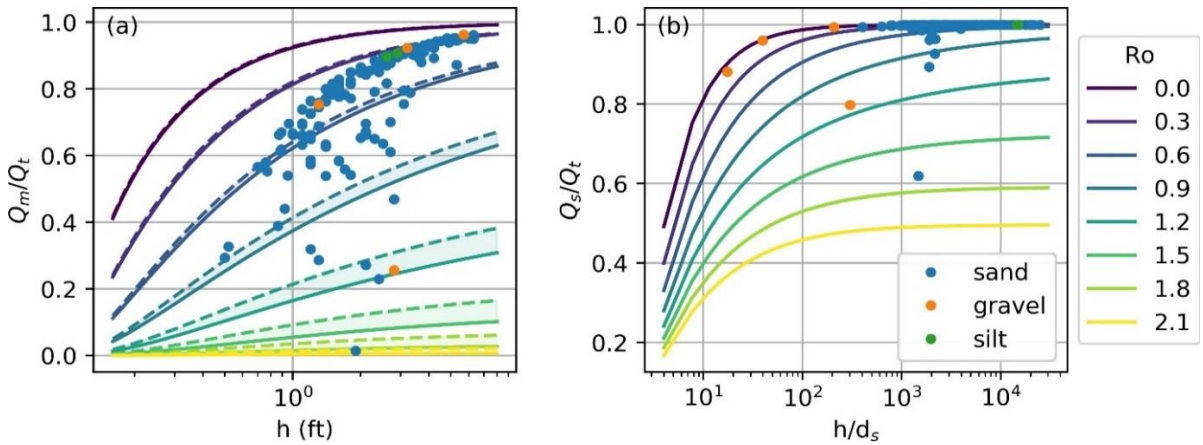

Figure 28: (a) the ratio of measured to total sediment discharge vs depth; and (b) the ratio of suspended to total sediment discharge vs h/ds at the Rio Grande Floodway at San Acacia (08354900)

3. Geomorphic and River Characteristics

Middle Rio Grande has been changing due to the dynamic of flow and sediment regimes, and the influence of human activities. In this section, the temporal changes in geomorphic attributes were analyzed. The analysis was conducted based on aerial photos, cross sectional surveys at agg/deg line and rangelines, and HEC-RAS simulations. The changes of the following parameters are present: sinuosity, active channel width, bed elevation, channel volume, and hydraulic variables.

3.1. Sinuosity

As shown in Figure 29, sinuosity has been increasing slightly over time for the Isleta to Rio Puerco reach since the 1990s. Data on the entire reach was compiled from various sources. Years 1935 through 2006 came from Makar (2010), who calculated sinuosity as the active channel centerline divided by valley length using historic aerial photographs. The following years came from Klein et al. (2018a), who calculated sinuosity using active channel centerlines generated by various Reclamation contractors or Google Earth imagery. There is a small spike in 1950, which then decreases and stays constant until about 1990. This is likely due to channelization efforts from the USBR in the 1950s and 1960s and ongoing river maintenance through that period (Makar 2010). From 1990 onwards, sinuosity increases through 2016. This may be due to the reduction in sediment supply following the Cochiti Dam construction and a change in management strategies by the USBR.

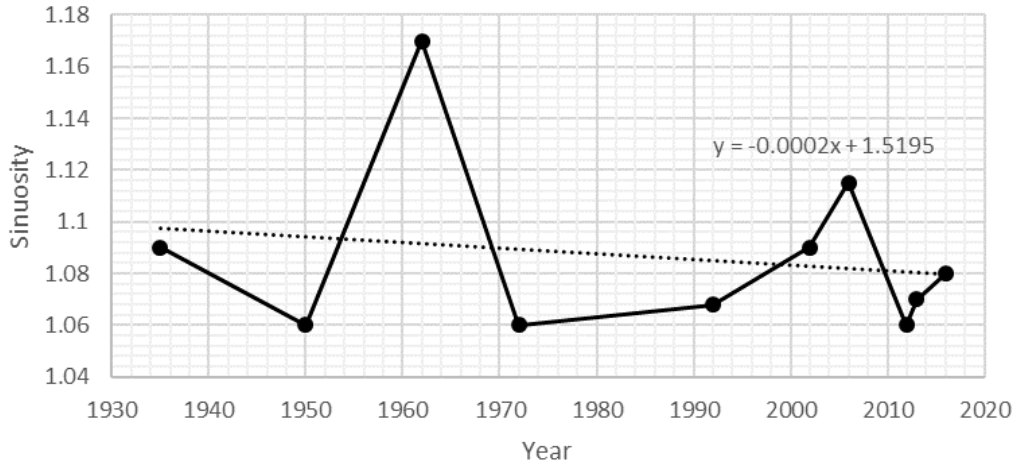

Figure 29. Trend of sinuosity from the Rio Puerco confluence to the San Acacia diversion dam. A negative slope of 0.0002 is observed. The data for this graph was extracted from a graph provided by USBR (Klein et al. 2018a).

Figure 30 show the sinuosity at each subreach. Sinuosity was calculated for each individual subreach using digitized channel centerlines provided by the USBR's GIS and Remote Sensing Group. Aerial photographs and accompanying digital shapefiles were provided for years 1918, 1935, 1949, 1962, 1972, 1985, 1992, 2001, 2002, 2006, 2008, 2012 and 2016. The centerlines were then split up by subreach and divided by the length of the subreach as shown in Figure 30.

Overall, the sinuosity is near one which indicates a very straight channel. Subreach P3 has the highest sinuosity, which locates at a geological constraint and turns the river from southward to westward. There is a large spike in 1962. There is an increase in sinuosity from the 1970's to the second peak, but then it drops greatly in 2012 and starts increasing again after that.

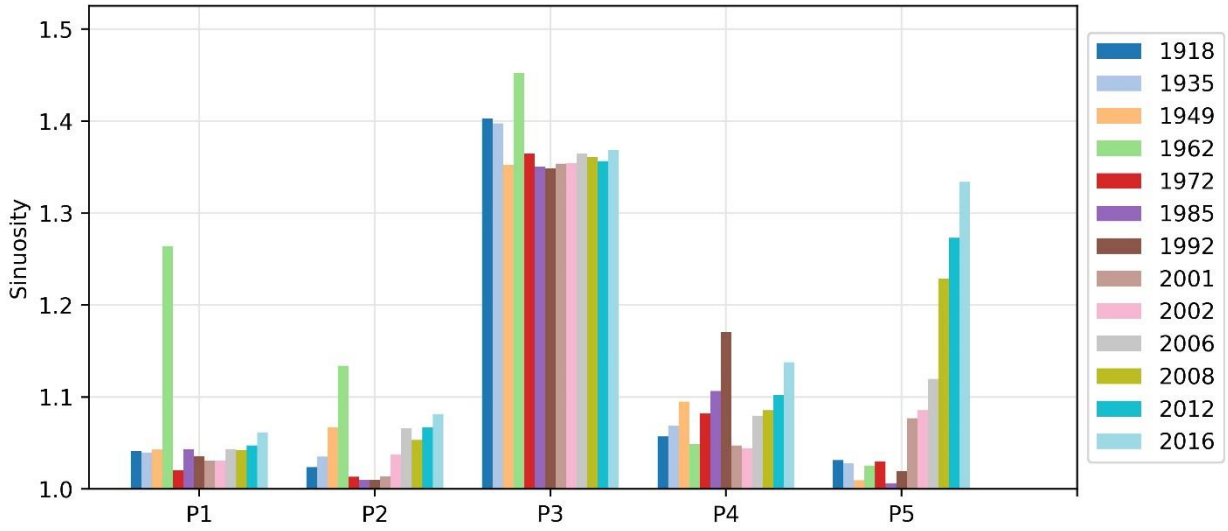

Figure 30: Sinuosity at subreach scale.

3.2. Channel Width

The width has generally decreased over time since 1918 in this reach due to infrastructure building, channelization, reduction in peak flows, upstream sediment reduction and vegetation encroachment (Culbertson and Dawdy 1964; Crawford et al. 1993; Berry and Lewis 1997; Bauer 2000; MEI 2002; Bauer and Hilldale 2006; Tashjian and Massong 2006; Parametrix 2008; Bauer 2009; Makar 2010; Makar and AuBuchon 2012; Baird 2014 in Klein et al. 2018a). This has made the widths more uniform as well (Crawford et al. 1993; Parametrix 2008; Makar and AuBuchon 2012 in Klein et al. 2018a).

Digitized data provided by the USBR's GIS and Remote Sensing Group from aerial photographs was used to analyze the active channel width at agg/deg cross-sectional lines. The active channel is defined as non-vegetated channel. Measurement of the active channel width was performed by clipping the agg/deg line coverage with the active channel polygon. The average width for each subreach is calculated by averaging the width of all agg/deg lines within the subreach (Figure 31).

For each subreach, the width has decreased since 1918 (except in P1). The decline in channel width from 1918 to 1962 is the most significant and the biggest decrease is found at subreach P5: 2300 feet over 44 years. There is also a major drop in P5 that occurred from 1935 to 1949. This suggests the width was greatly impacted by the construction of the diversion dam in 1934. P3 is relatively stable because of the geologic constriction. The widths across subreaches tend

to drop off dramatically after 1949 because channelization systems started around the 1950's (Easterling Consultants LLC 2015). The decrease in width between 1918 and 1985 is due to the vegetation encroachment on the right bank as seen in the aerial images. The channel and vegetation reach a balance after 1985. Subreach P4 changes back and forth between single-thread and double-thread so we can see the width goes up and down after 2001. The change might be due the fluctuation of sediment supply from Rio Salado since subreach P4 is located right downstream of the Rio Salado. A similar trend was observed on the Cochiti Reach by Richard (2001).

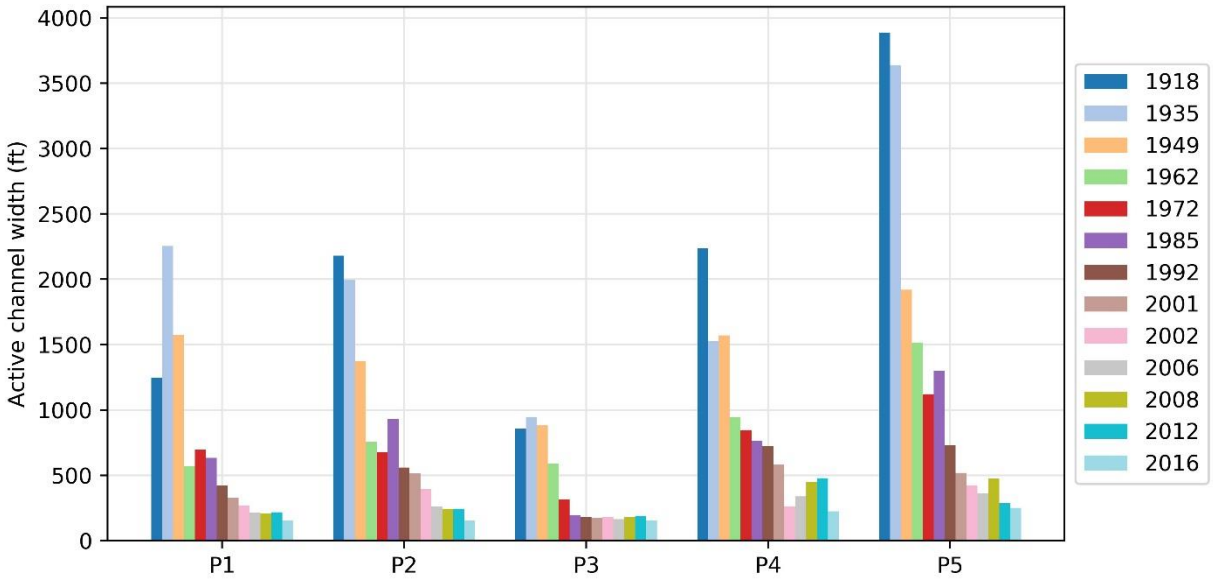

Figure 31: Reach averaged active channel width.

3.3. Low Flow Channels

At low flows, the number of channels at each agg/deg line is measured from digitized planforms from the aerial photographs provided by the USBR. The average number of channels is calculated for each subreach and presented in Figure 32.

From the aerial photographs, the Rio Puerco Reach was braided between 1935 to around 2005. After 2005 the channel developed anabranching. The number of channels is low for 1962, 1972, and 1982, because the digitized planforms for these years did not capture the bars or islands in the channel. 2002 and 2006 have some of the highest numbers of channels across all subreaches. Braiding has generally decreased from 2002-2012. In terms of subreaches, P2 and P4 tended to have the most channels throughout time.

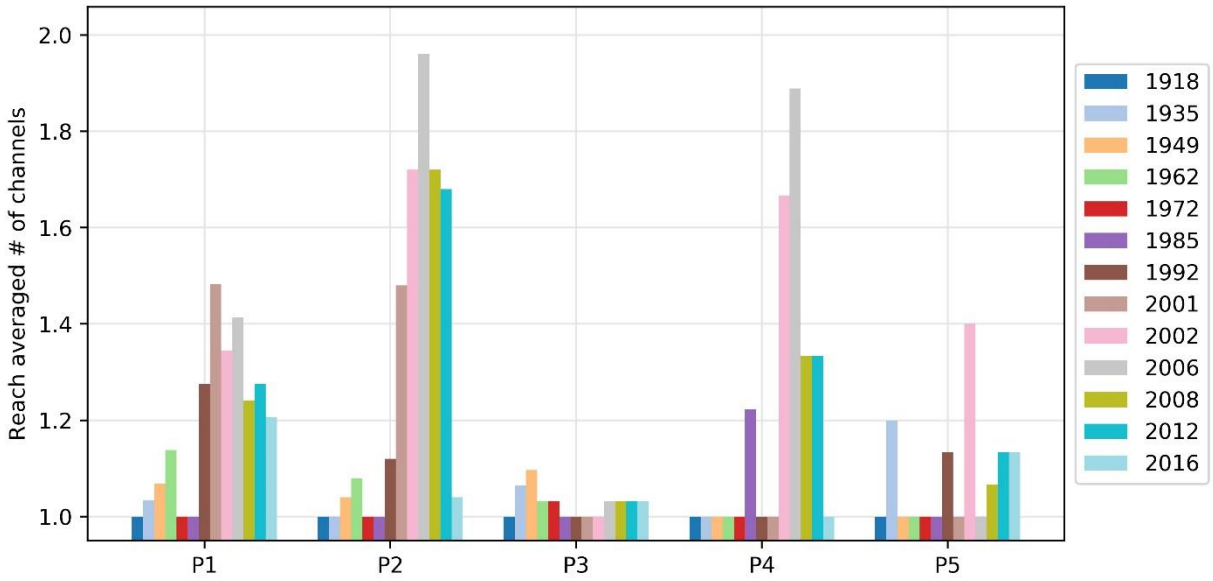

Figure 32: Average number of channels at each subreach.

3.4. Bed Elevation

The mean bed elevation is used to compare the change in long profile in this report. Cross-section geometry models along agg/deg lines were developed by the Bureau of Reclamation, Albuquerque Area Office. The geometry models are available for 1962, 1972, 1992, 2002 and 2012. For the models prior to 2012, the cross-section geometry is captured using photogrammetry techniques. The 2012 model is from LiDAR (Klein et al. 2018a). In addition, an underwater prism was developed (Varyu 2013). All the models were using the NAV88 vertical datum.

Figure 33 shows the long profiles of 1962, 1972, 1992, 2002, and 2012. Significant degradation between 1972 and 1992 is observed. Figure 34 shows the change in mean bed elevation for each subreach.

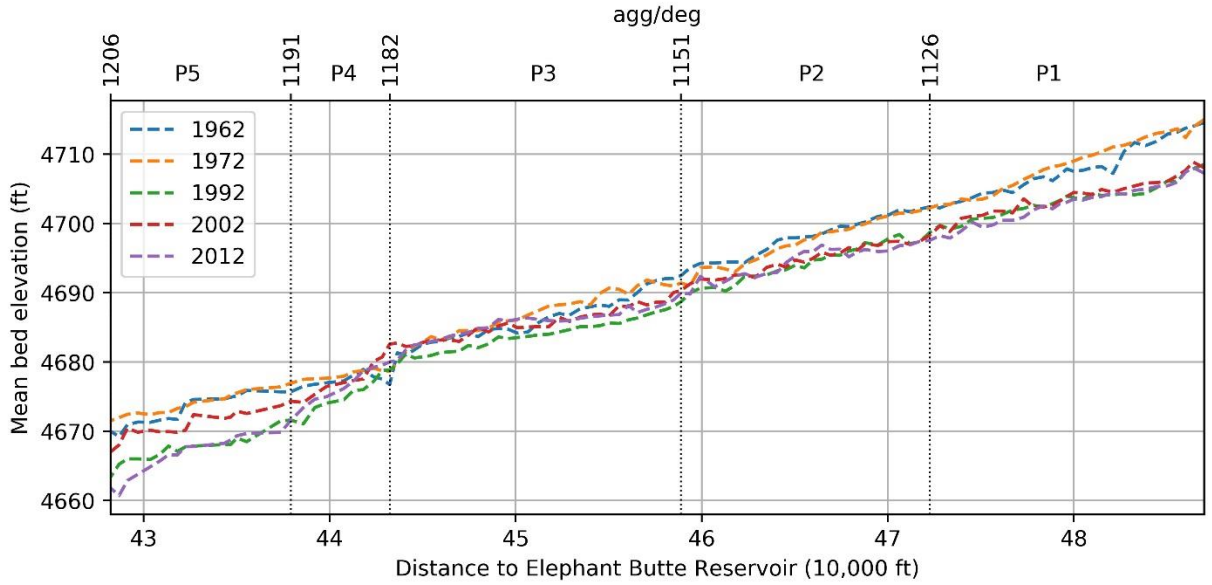

Figure 33: Long profiles for 1962, 1972, 1992, 2002, and 2012.

The long profiles degraded 5.2, 3.1, 3.0, 3.4, and 6.4 ft at P1, P2, P3, P4, and P5 respectively, from 1972 to 1992. Between 1992 and 2002, the bed elevation rose 0.4, 0.5, 1.8, 2.3, 3.5 ft at P1, P2, P3, P4 and P5 respectively. From 2002 to 2012, the river bed degraded. The amount of degradation ranged from 0.1 ft (P2) to 4.4 ft (P5).

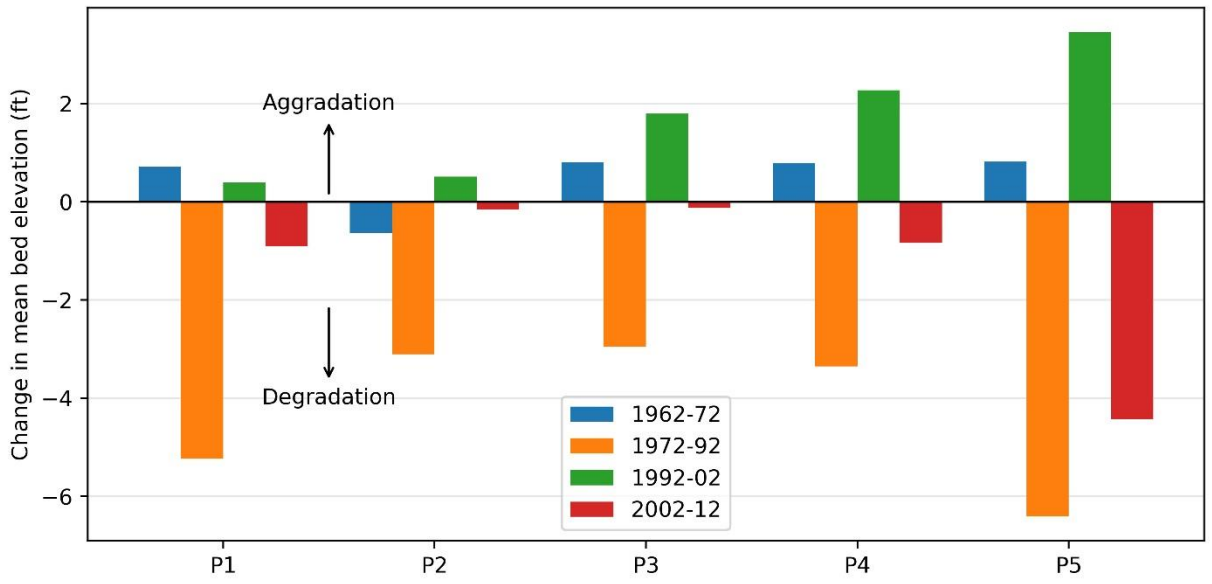

Figure 34: Change in bed elevation.

3.5. Volume Change

The change in main channel sediment volume for the time periods 1962 to 1972, 1972 to 1992, 1992 to 2002, and 2002 to 2012 is analyzed. This analysis follows a procedure by Varyu (2013) which provides an example of how to calculate the volume change. The extent of main channel is determined based on banklines. Banklines are given in the geometry models and are where the active channel intersects agg/deg lines. Due to the dynamic nature of the channel, banklines are likely to shift from year to year. The portion of the cross section within the outer-most right and outer-most left location of the banklines from two input datasets are defined as the main channel. The cross-section area between the banklines is then calculated for each of the two input datasets. Then the volume change is calculated as the difference in cross section area between two years multiplied by the length. The length is determined as half of distance of a cross section to its upstream cross section plus one-half the distance to the downstream cross section. Figure 35 presents the main channel volume change of each subreach. The change generally follows the trend in mean channel bed elevation.

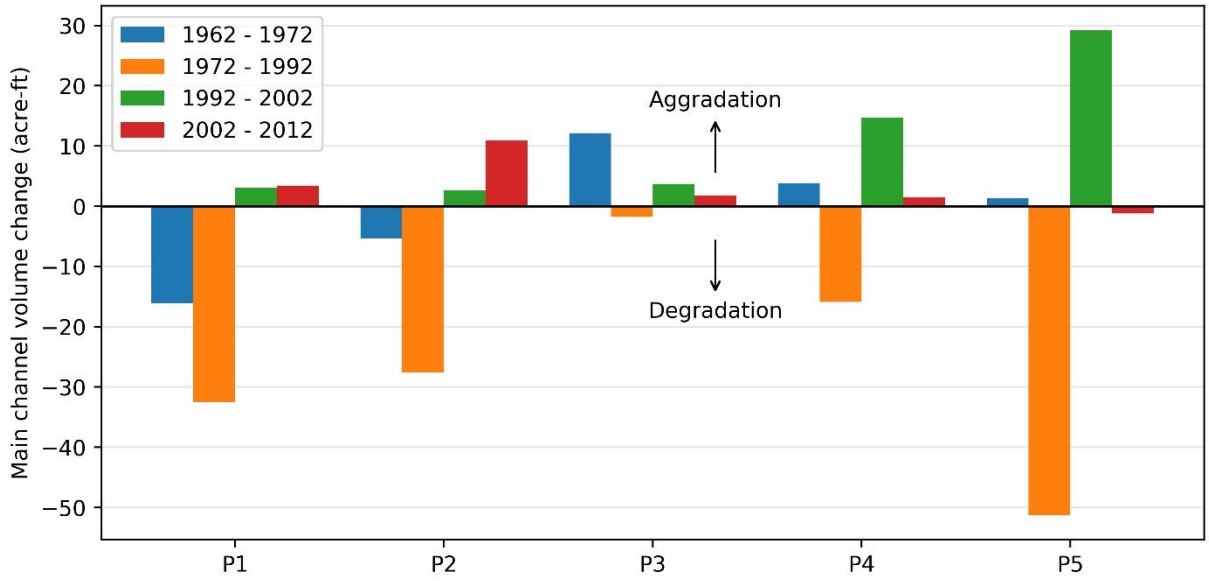

Figure 35: Change in main channel volume.

Notice that during 2002 to 2012, most of the reaches show aggradation based on volume change but degradation based on the elevation change. It reflects that the channel is narrowing and incising.

3.6. Bed Material

Bed material samples were collected at rangelines that differ from the agg/deg lines. These rangelines don't date back as far as the agg/deg lines and are also spaced out further. They are used in this analysis because bed material has been surveyed in these rangeline cross-sections. The sediment samples are grouped by decade and the statistical summary of the median grain size d_{50} is shown in Table 5. Overall, the grain size has increased over time. The typical grain size is medium sand (d_{50} ranges from 0.25 mm to 0.5 mm) at P1 and P2. The gravel found at P4 is likely coming from Rio Salado (Easterling Consultants LLC 2015).

Table 5: d_{50} grain size statistics from the bed material samples in Isleta reach.

	Subreach	Min	Max	Mean	# of samples	# in sand	# in gravel
1990s	P1	0.05	2	0.54	7	6	7
	P2						
	P3	0.24	0.36	0.32	21	21	0
	P4						
	P5	0.05	0.68	0.26	12	12	0
2000s	P1	0.35	0.37	0.35	4	4	0
	P2	0.14	0.35	0.3	7	7	0
	P3			0.32			
	P4	0.35	2.58	1.47	2	1	1
	P5	0.12	0.3	0.19	8	8	0
2010s	P1	0.34	0.35	0.34	2	2	0
	P2	0.36	0.38	0.37	2	2	0
	P3	0.35	0.41	0.38	2	2	0
	P4	13.08	13.08	13.08	1	0	1
	P5	0.56	7.21	1.26	10	9	1

3.7. Flow Depth, Velocity, Width, Wetted Perimeter and Slope

Flow depth, velocity, width, and wetted perimeter are obtained by using HEC-RAS 5.0.3 with a discharge of 3,000 cfs. A discharge of 3,000 cfs was selected because, anecdotally, it does not cause overbanking (Drew Baird, personal communication, June 19th, 2018). Available years of analysis with HEC-RAS include 1972, 1992, 2002, and 2012. The bed slope is calculated using both the cross-section from HEC-RAS and the channel length from the planform. The mean channel bed elevations at the beginning and the end of a subreach can be obtained from the HEC-RAS model. The difference of these two elevations divided the length of the subreach is the bed slope that is used here. The average value of each variable at subreach scale is plotted in Figure 36 and Figure 37. The change between ranges of years is summarized in Table 6.

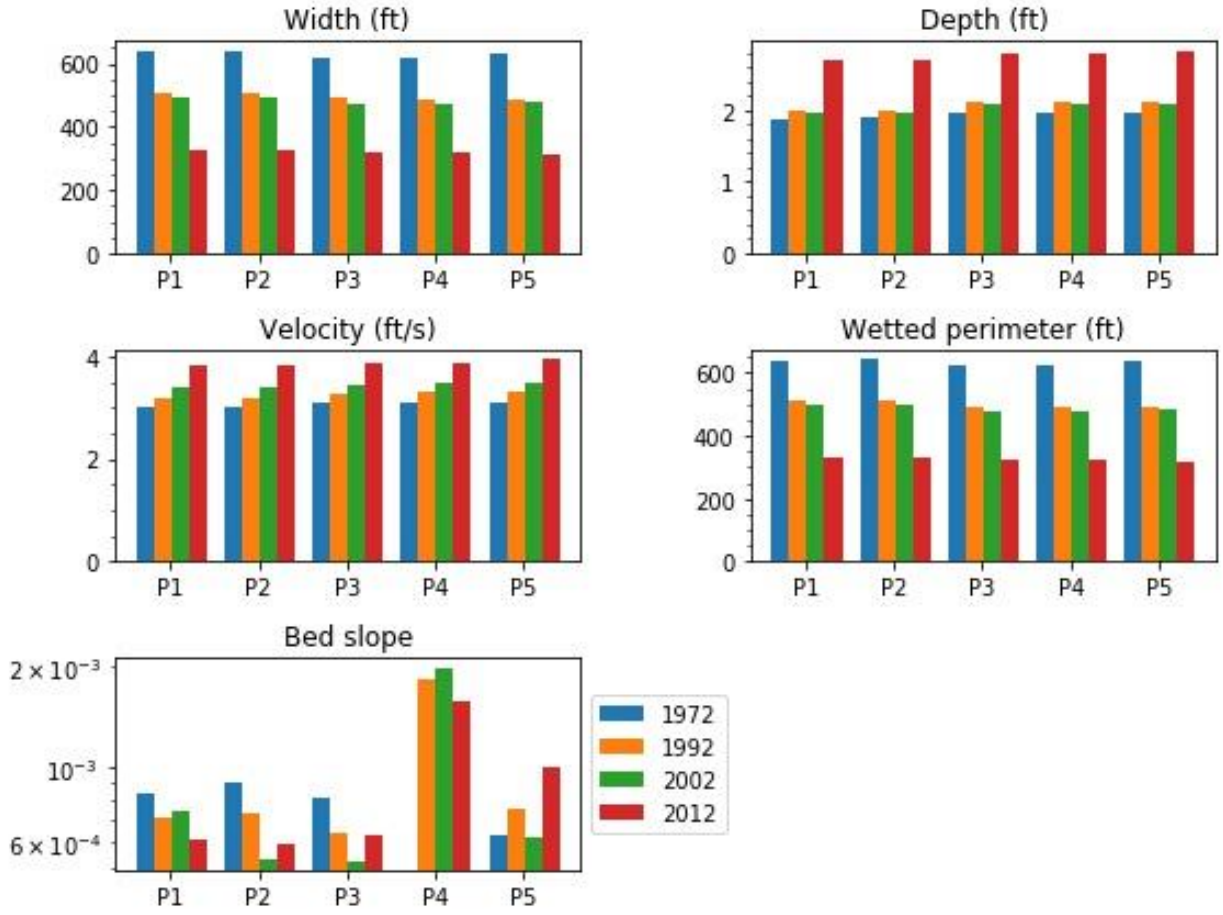

Figure 36: Width, depth, velocity, wetted perimeter, energy slope, and bed slope at each subreach for 1972, 1992, 2002, and 2012 at 3000 cfs.

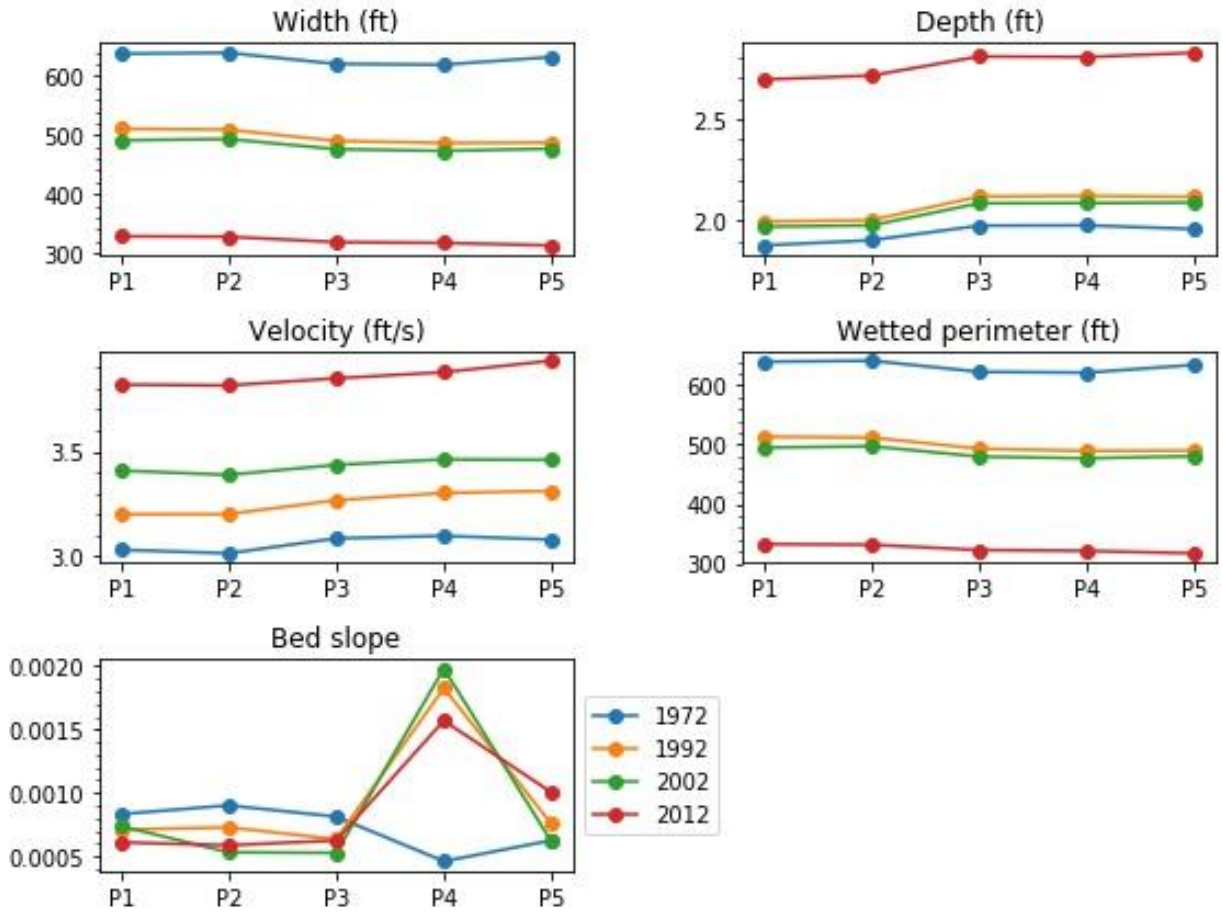

Figure 37: Width, depth, velocity, wetted perimeter, energy slope, and bed slope at each subreach for 1972, 1992, 2002, and 2012 at 3000 cfs.

A continuous decrease in width and increase in velocity was found. The widths and wetted perimeter have decreased about 300 ft since 1972. The average velocity increased from 3.0 ft/s to 3.8 ft/s. The flow depth increased between 1972 – 1992 and 2002 – 2012, while decreasing between 1992 and 2002. It appears that channel degradation causes the increase in depth and aggradation causes a decrease. The slope increased from 1972 – 1992 and decreased after 1992. Subreach P3 has the mildest slope. From 2002-2012 the slope decreases as shown in Figure 37. A braided channel is generally steeper than a single sinuous channel (Julien 2002), so it is expected that the channel becomes more sinuous like it does when the slope decreases from 2002-2012 as shown in Figure 37. During this time period, the channel also becomes less braided as seen in Figure 32 which supports the fact that it becomes more sinuous.

Table 6: Rio Puerco reach channel geometry temporal change summary (+: increase in parameter value; -: decrease in parameter value).

Reach	Year	Width	Bed slope	Depth	Velocity
P1	1972 - 92	-	-	+	+
	1992 - 02	-	+	-	+
	2002 - 12	-	-	+	+
P2	1972 - 92	-	-	+	+
	1992 - 02	-	-	-	+
	2002 - 12	-	+	+	+
P3	1972 - 92	-	-	+	+
	1992 - 02	-	-	-	+
	2002 - 12	-	+	+	+
P4	1972 - 92	-	+	+	+
	1992 - 02	-	+	-	+
	2002 - 12	-	-	+	+
P5	1972 - 92	-	+	+	+
	1992 - 02	-	-	-	+
	2002 - 12	-	+	+	+

3.8. Channel Response Models: Schumm's (1969) river metamorphosis

Schumm (1969) suggested the following dynamic responses of a channel to changes in water and sediment discharges.

$$Q_t^+ \sim W^+ h^- P^- L^+ S^+$$

$$Q^+ \sim W^+ h^+ L^+ S^-$$

$$Q^- Q_t^- \rightarrow W^- h^\pm F^- L^- S^\pm P^+$$

where Q is the flow discharge, Q_t is the percentage of the total sediment load transported as bedload, W is the channel top width, h is the flow depth, L is the meander wavelength, F is the width-depth ratio, S is the slope, and P is the sinuosity. The exponent, expressed as either a plus or minus, indicate whether the dimensions of the variables are increasing or decreasing.

Schumm's river metamorphosis model suggests qualitative changes in hydraulic geometry from a general decrease in water discharge and bed material load in Sections 2.2 and 2.3. Although some subreaches could not be evaluated by the model, overall the model suggests a response summarized in Table 7.

Table 7: Analysis of channel responses to water and sediment discharge based on the Schumm's model

Year	Subreach	W	h	S	F	P	Schumm's model
1972-1992	P1	-	+	-	-	+	$Q^- Q_t^-$
	P2	-	+	-	-	-	N/A
	P3	-	+	-	-	-	N/A
	P4	-	+	+	-	+	$Q^- Q_t^-$
	P5	-	+	+	-	-	N/A
1992-2002	P1	-	-	+	-	-	N/A
	P2	-	-	-	-	+	$Q^- Q_t^-$
	P3	-	-	-	-	+	$Q^- Q_t^-$
	P4	-	-	+	-	-	N/A
	P5	-	-	-	-	+	$Q^- Q_t^-$
2002-2012	P1	-	+	-	-	+	$Q^- Q_t^-$
	P2	-	+	-	-	+	$Q^- Q_t^-$
	P3	-	+	+	-	+	$Q^- Q_t^-$
	P4	-	+	-	-	+	$Q^- Q_t^-$
	P5	-	+	+	-	+	$Q^- Q_t^-$

3.9. Equilibrium Width Predictors

The downstream hydraulic geometry of rivers was derived by Julien and Wargadalam (1995):

$$h = 0.2Q^{\frac{2}{6m+5}} d_s^{\frac{6m}{6m+5}} S^{\frac{-1}{6m+5}}$$

$$W = 1.33Q^{\frac{4m+2}{6m+5}} d_s^{\frac{-4m}{6m+5}} S^{\frac{-1-2m}{6m+5}}$$

$$V = 3.76Q^{\frac{2m+1}{6m+5}} d_s^{\frac{-2m}{6m+5}} S^{\frac{2m+2}{6m+5}}$$

where $m = 1/\ln(12.2\, h/d_s)$, h is the flow depth, W is the channel width, V is the velocity, Q is the flow discharge, d_s is the median grain size, and *S* is the slope. A discharge of 3,000 cfs, same as the HEC-RAS analysis, is used in order to compare the results to field observation. The values of grain size and slope are obtained from previous sections. The mean d_{50} of 1990s is used for 1992, 2000s for 2002, and so forth. The measured and predicted width can be found in Table 8. The method of Julien and Wargadalam predicts a channel equilibrium width between 185 to 244 feet, which is narrower than the observed channel widths for all subreaches and all years. This corroborates the observed channel width decrease noted in Section 3.2.

Table 8: Input and Output for Julien and Wargadalam's equations

Year	Subreach	Q (cms)	d_s (mm)	Slope	Observed width (ft)	Predicted width (ft)
1992	P1	85	0.54	0.000709	510.4	228.8
	P2	85		0.000727	509.0	
	P3	85	0.32	0.000633	489.9	234.9
	P4	85		0.001827	486.4	
	P5	85	0.26	0.000754	487.0	227.0
2002	P1	85	0.35	0.000737	491.0	227.7
	P2	85	0.3	0.00053	493.3	243.5
	P3	85	0.32	0.000526	476.0	243.8
	P4	85	1.47	0.00198	473.1	184.7
	P5	85	0.19	0.000615	476.7	236.9
2012	P1	85	0.34	0.000609	328.7	236.6
	P2	85	0.37	0.000586	327.7	238.3
	P3	85	0.38	0.000624	318.7	235.3
	P4	85	13.08	0.00157	317.3	189.3
	P5	85	1.26	0.001003	313.1	212.1

3.10. Geomorphic Conceptual Model

Massong et al. (2010) developed a channel planform evolution model for the Rio Grande based on historic observations. The sequence of the planform evolution is outlined in Figure 38. Stage 1 describes a large channel with a high sediment load and frequent floods such that a wide, clear channel is maintained. As water levels fall, Stage 2 occurs and dunes from Stage 1 begin to stabilize into bars. In Stage 3, this stabilization is maintained by encroaching vegetation, regardless of flow levels. Only after the third stage does sediment transport become important in determining future stages. A lack of transport capacity leads to avulsion, as the channel aggrades and eventually the main flow shifts on to the now lower floodplain, progressing to the A (aggrading) stages. Excessive transport capacity leads to the M (migrating) stages. Bends occur where bed and bank material erode both laterally and vertically. Transition between the M stages and the A stages can occur, however, a reset to Stage 1 requires a large, prolonged flood event (Massong et al., 2010). The gold color represents sand bars, while green represents vegetated bars.

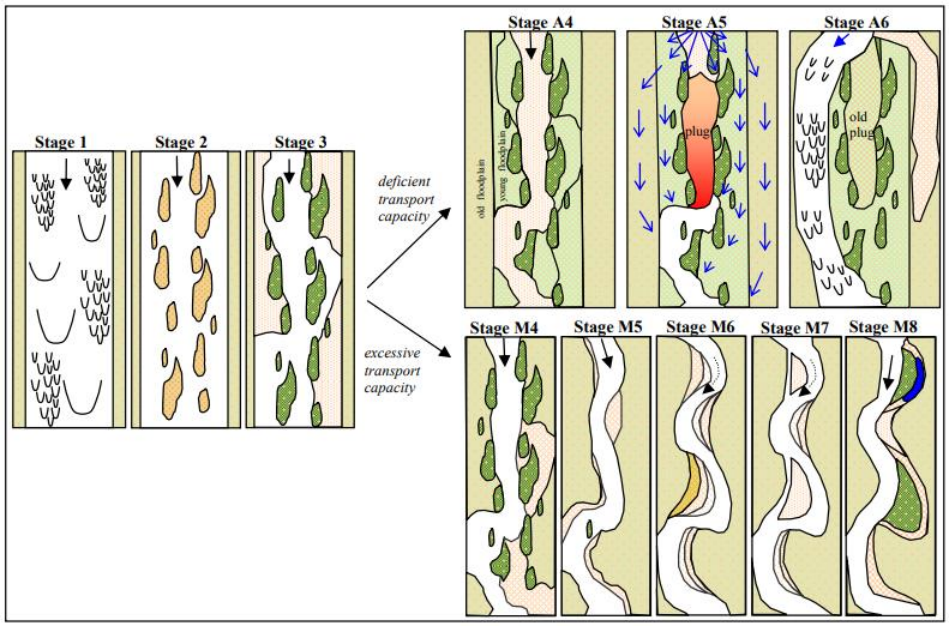

Figure 38: Planform evolution model from Massong et al. (2010). The river undergoes stages 1-3 first and then A4-A6 or M4-M8 depending on the transport capacity.

Stages M4-M8 are the most relevant to the Isleta Reach because it has an excessive transport capacity (Massong et al. 2010). The transition between Stage 1 and 2 occurred on much of the Middle Rio Grande from 1999-2004, during a long period of drought with minimal spring peak

flows. During this time, considerable vegetation encroachment was also seen. In 2005, high peak flows returned, but the bars were sufficiently stabilized to avoid a return to Stage 1. High water levels allowed vegetation to flourish, thus forming Stage 3 (Massong et al. 2010). The latest classification of the Isleta reach has been M5 and has undergone various stages since the early 1900s. USBR assigned planform stages to the Isleta reach over multiple years based on aerial photography in their report from 2018. Their results are shown in Table 9.

Table 9: Planform classification by stages for the Puerco reach (Klein et al. 2018a).

Years	Massong et al. (2010)
1918	1
1935	1
1949	1
1962	2
1972	3/2
1985	3
1992	3
2002	M4
2012	M5/M6
2016	M5/M6

Using these years of data and the classification from Massong et al. (2010), a conceptual model was considered. The intent is to understand how the river is changing and predict future planform of the river. The model is formed from a plan view and cross-sectional view of a typical cross-section and presented with the stages assigned by Klein et al. (2018a). The evolution of cross-section is evaluated by two randomly chosen agg/deg lines 1124 and 1190 and spans from 1962-2016. (Figure 38 to 44). The plan view was obtained using GIS, and the cross-section was from HEC-RAS.

The conceptual model only dates back to 1962 for a few reasons. Although there are seven year of available data, the analysis could only start with 1962. Determining which agg/deg cross-section was which before 1962 was difficult because the surveys were not consistent between the years. This may be due to the agg/deg lines being established in 1962 (Posner 2017).

The cross-sections at agg/deg line 1124 and 1190 from 2016 data was acquired from AutoCAD from rangeline LJ-10 and RP-1190, respectively. The rangeline data does not cover as much distance because the survey was not as extensive as the agg/deg surveys in previous years. A comparison of the results are shown in Figure 39 and 40. Over time the active channel has become narrower and more incised. This makes sense as the stages progress from 2-M5/M6 and become more of a narrow, single-threaded channel. The active channel width is based on planforms provided by USBR in GIS, and they may differ based on the flow when the

photograph was taken. For instance, 1992, 2002, and 2012 are all around 650 cfs. 1972 is around 5 cfs and 2016 is at 40 cfs. The flow in 1962 is also about 650 cfs (Swanson et al. 2010).

Figure 45 show the conceptual model with the cross-section and plan views.

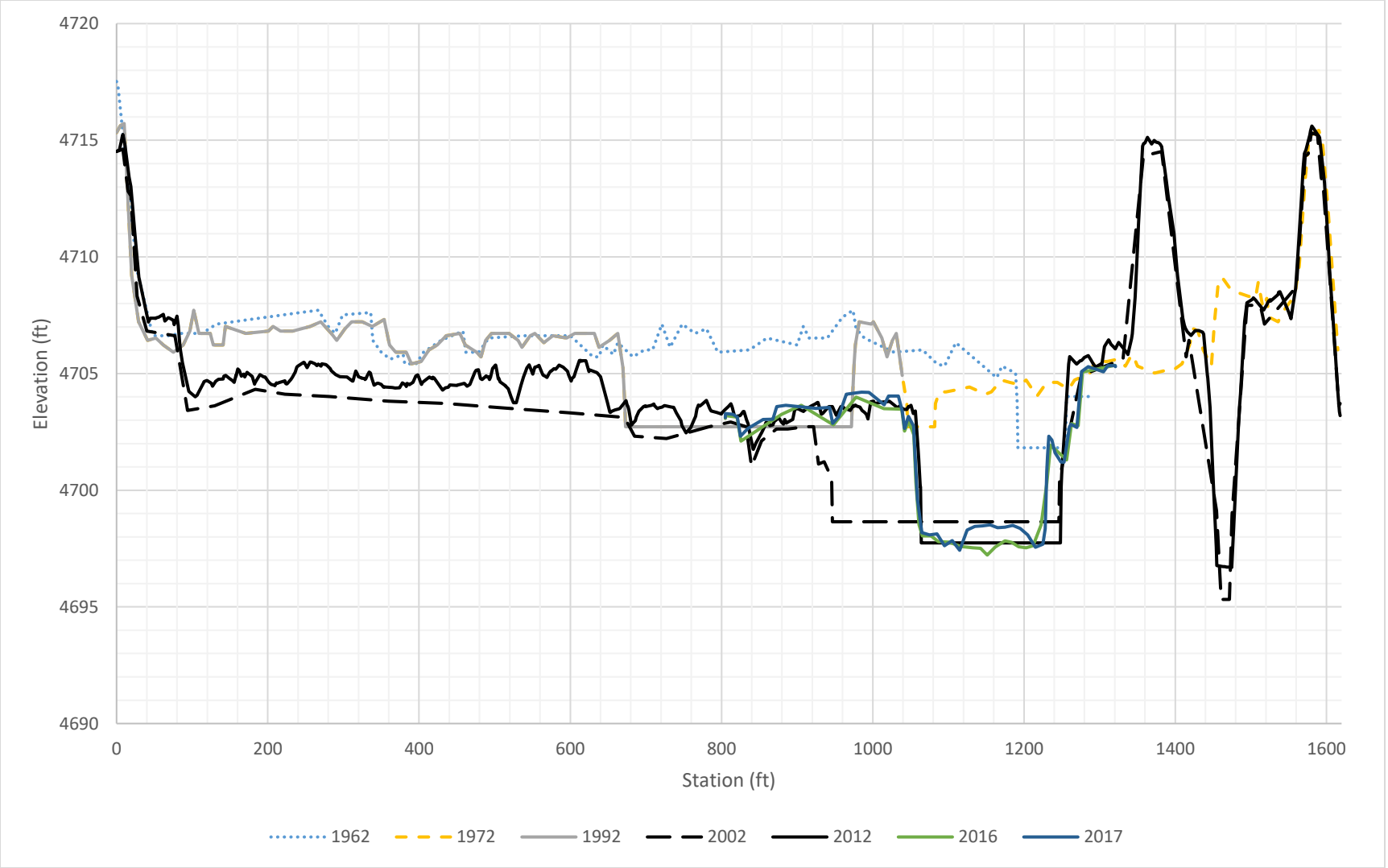

Figure 39: Comparison of cross-section 1190 from 1962-2016. Each stage classified by USBR is in a box and has an arrow pointing to the cross-section that it describes. These cross-sections are not compared after station 2600 because it is far away from the main channel. Also, there is very little variation in that area from year to year

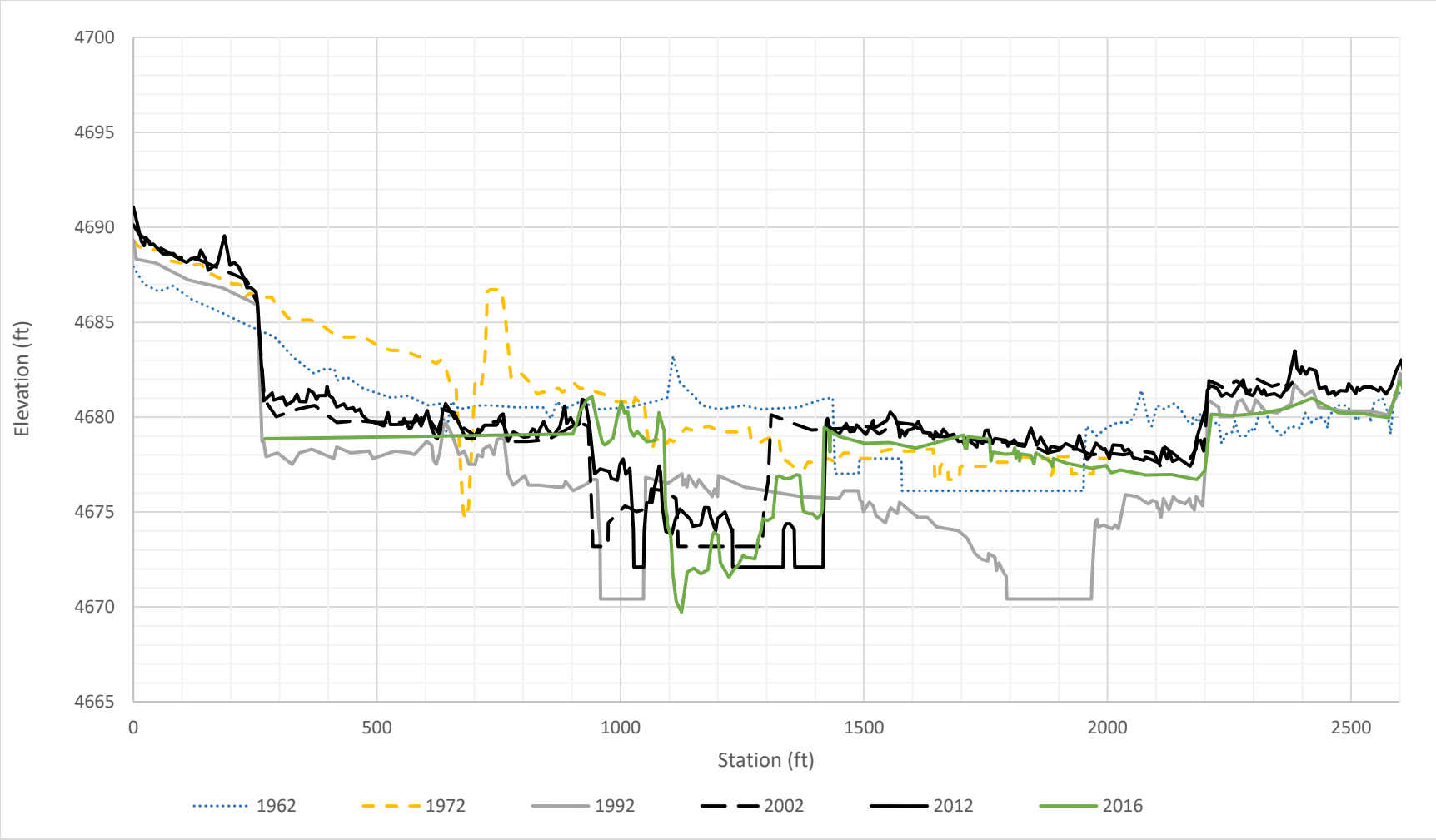

Figure 40: Comparison of cross-section 1190 from 1962-2016. Each stage classified by USBR is in a box and has an arrow pointing to the cross-section that it describes. These cross-sections are not compared after station 2600 because it is far away from the main channel. Also, there is very little variation in that area from year to year.

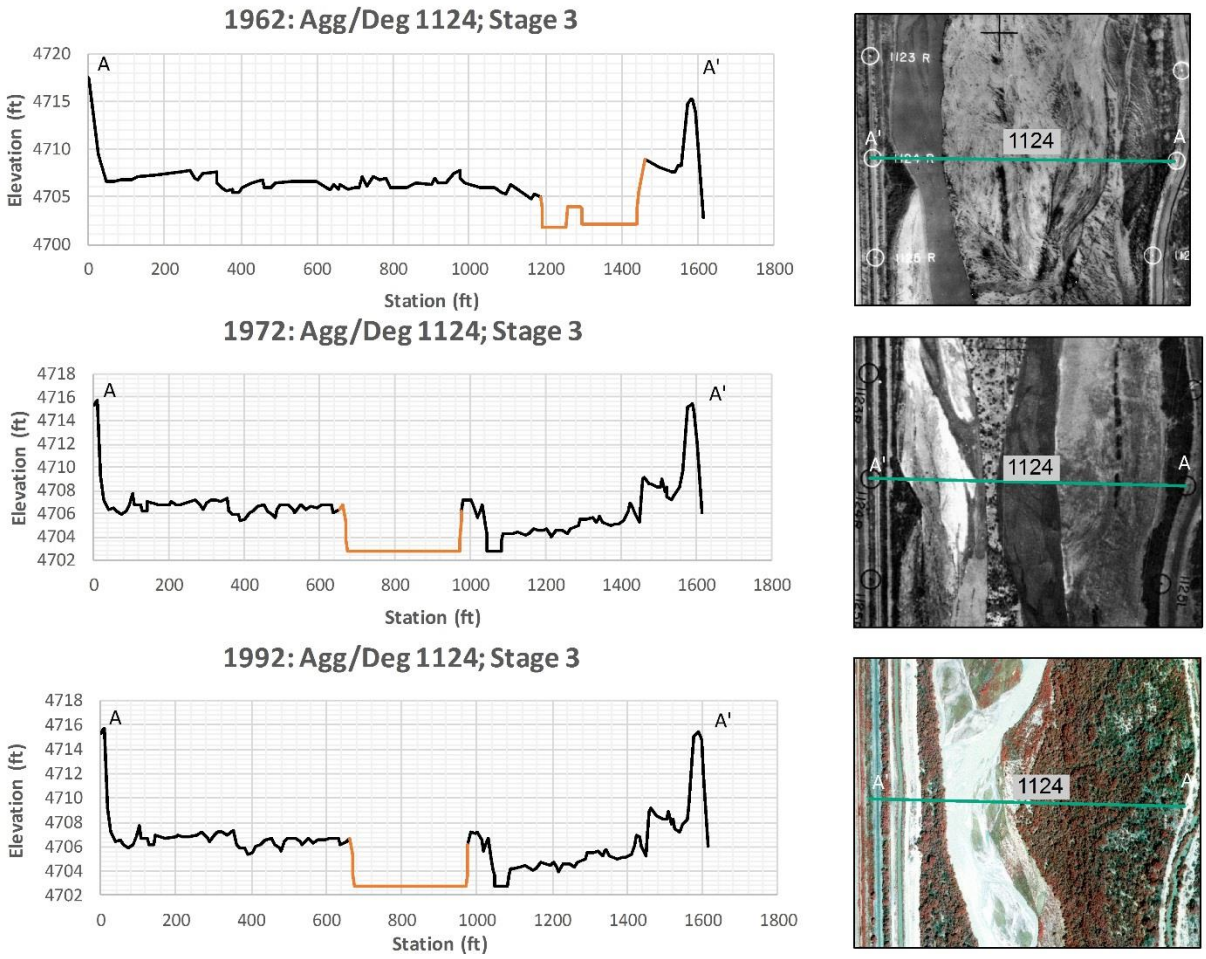

Figure 41: 1962, 1972 and 1992 cross-section 1124 and planform views (planform to the right of each corresponding year). A denotes the left bank and A' denotes the right bank. The active channel is in orange and the stage is denoted at the top of the graph.

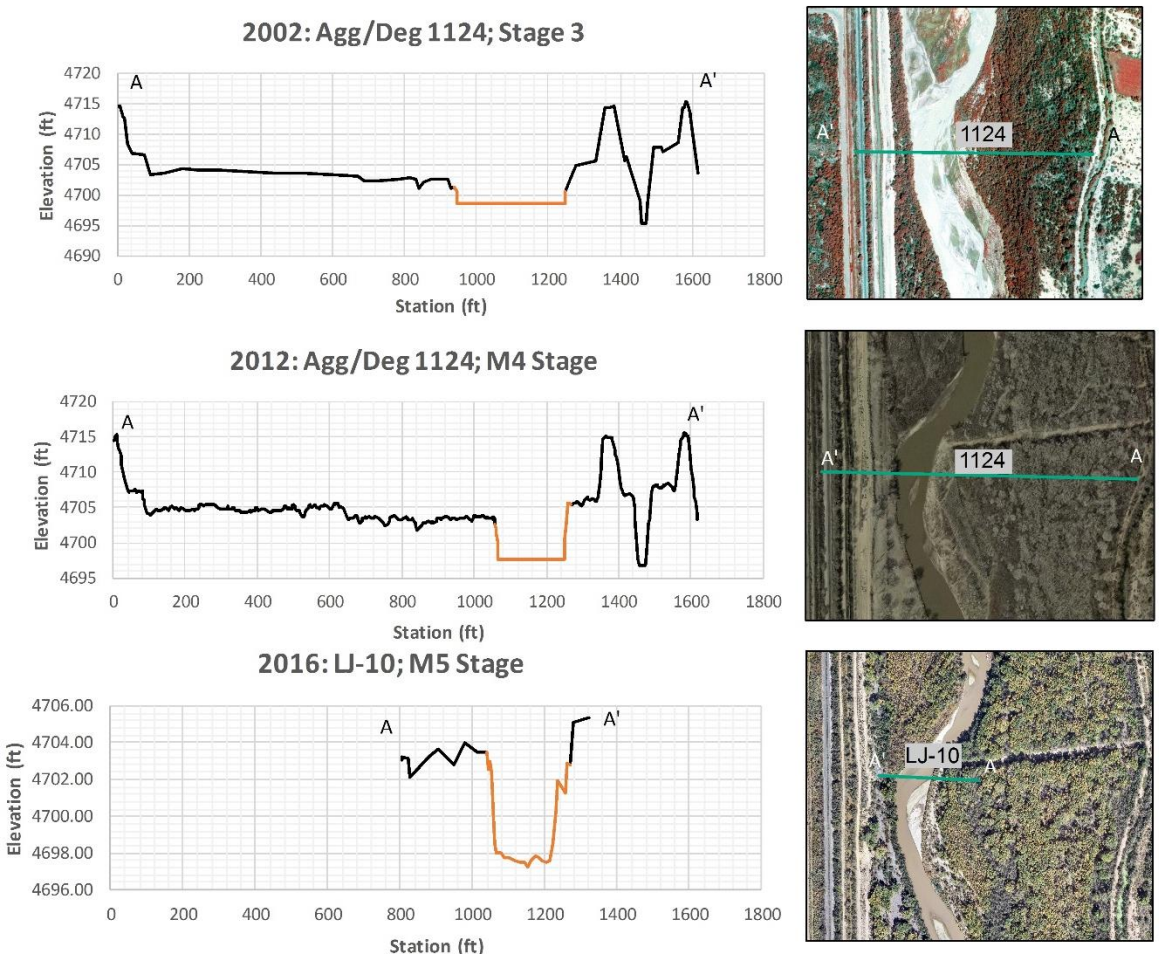

Figure 42: 2002, 2012 and 2016 cross-section 1124 and planform views (planform to the right of each corresponding year). A denotes the left bank and A' denotes the right bank. The active channel is in orange the stage is denoted at the top of the graph.

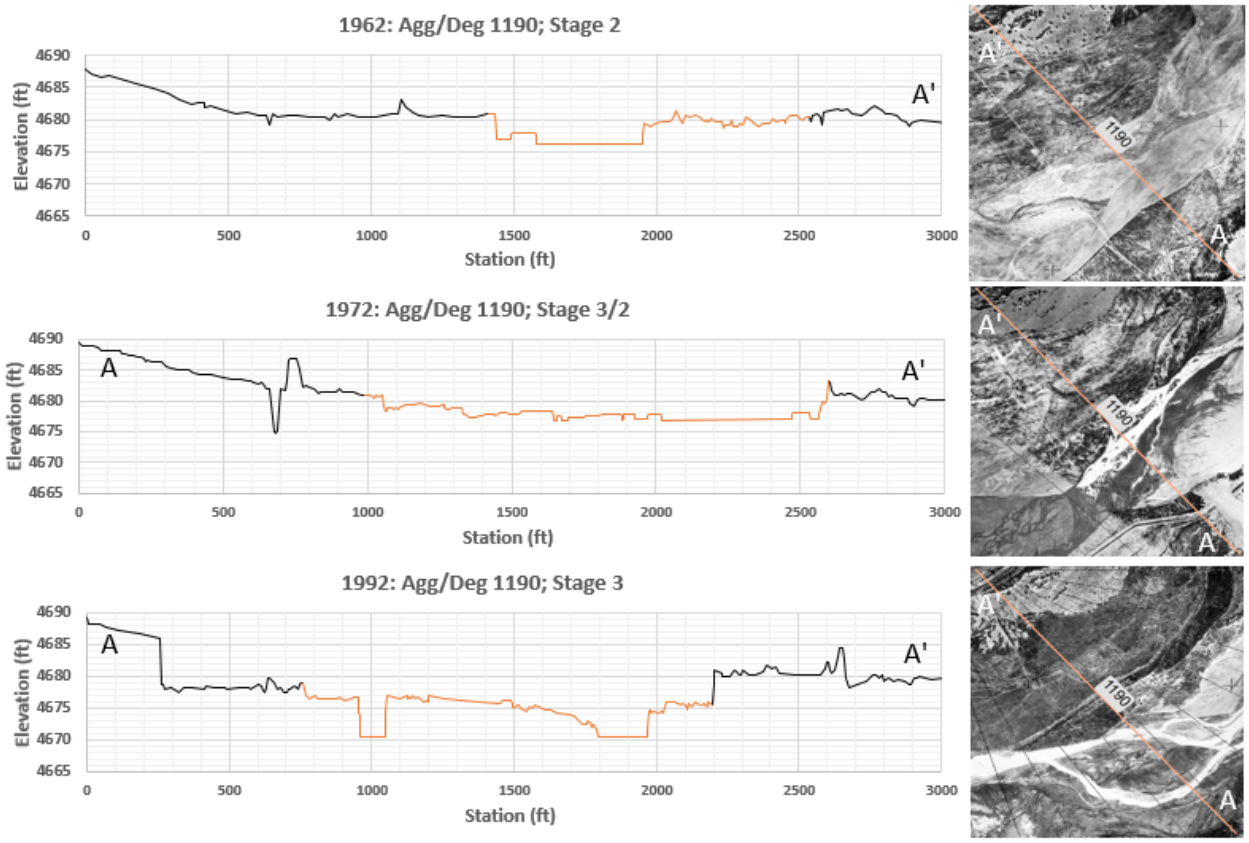

Figure 43: 1962, 1972 and 1992 cross-section 1190 and planform views (planform to the right of each corresponding year). A denotes the left bank and A' denotes the right bank. The active channel is in orange and the stage is denoted at the top of the graph.

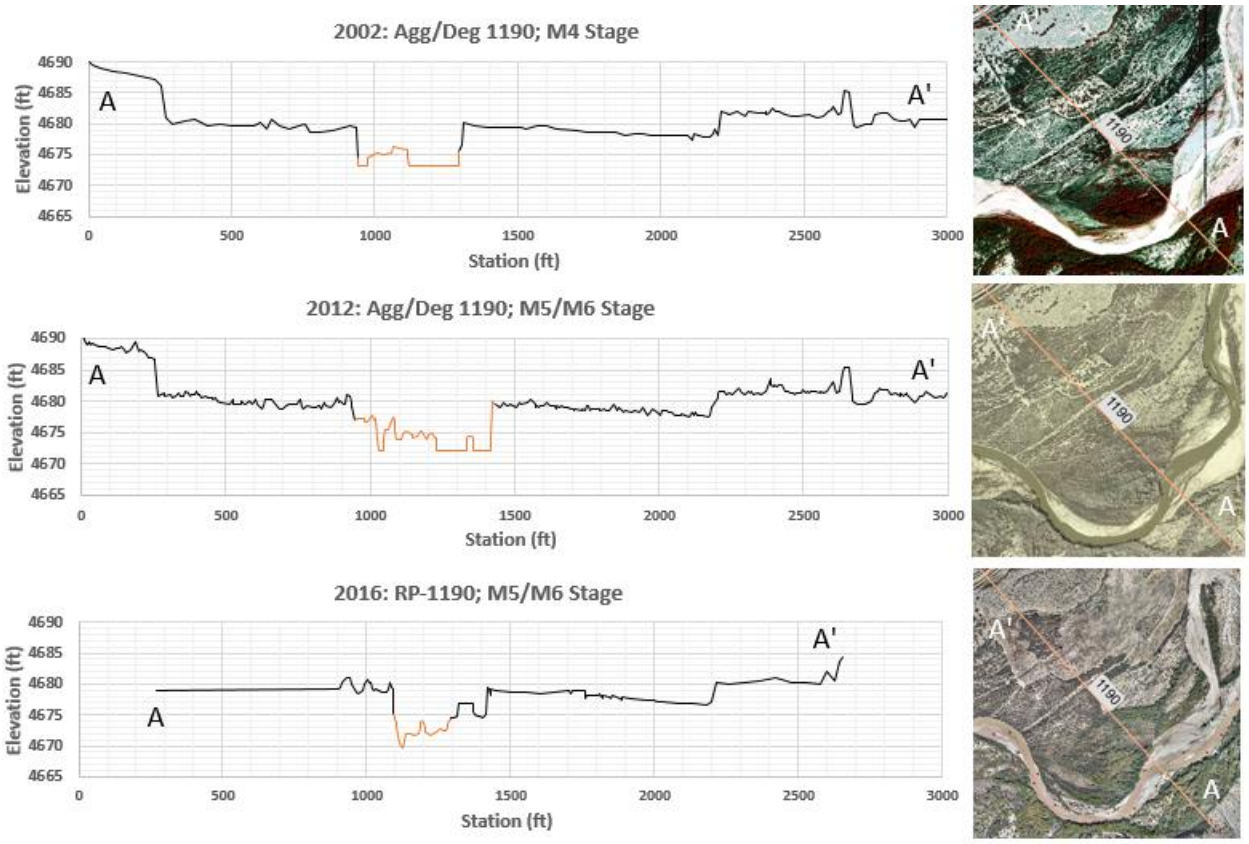

Figure 44: 2002, 2012 and 2016 cross-section 1190 and planform views (planform to the right of each corresponding year). A denotes the left bank and A' denotes the right bank. The active channel is in orange the stage is denoted at the top of the graph.

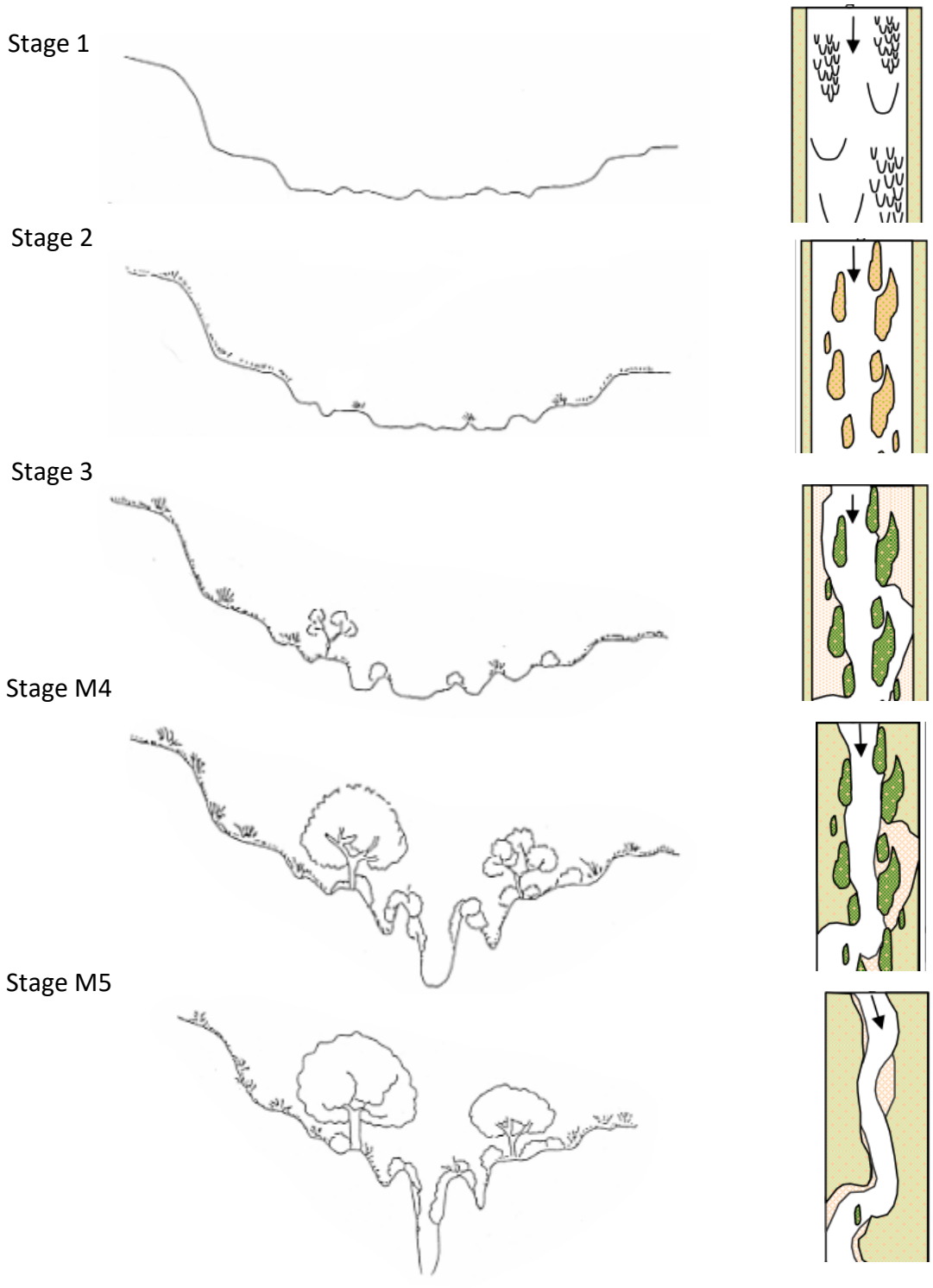

Figure 45: Cross-section view of the channel evolution model for stage 1, 2, 3, M4, and M5. (From Rozin and Schick, 1996)

4. Using HEC-RAS and GIS Analysis for Silvery Minnow Habitat

The potential for using HEC-RAS in combination with aerial photography in GIS is explored for a quantitative determination of the RGSM habitat quality. The preliminary analysis includes a set of three different discharges representing low, medium and high flow conditions, as well as three different hydraulic geometries as described from HEC-RAS files at three different decades (1992, 2002 and 2012).

4.1. Importance of the Rio Grande Silvery Minnow

Dams, levees, and channelization of the river have created an unhealthy riparian system and have led to an overall decline in ecological health of the Middle Rio Grande (U.S. Fish and Wildlife Service 2007). The silvery minnow is an indicator of the decline (Russo 2018). Silvery minnows became an endangered species in 1994 and currently, the silvery minnow occupies about only seven percent of its historic range (U.S. Fish and Wildlife Service 2010). It is believed to only occur in the Middle Rio Grande from Cochiti Dam to Elephant Butte Reservoir (Bestgen and Platania 1991; Dudley et al. 2005). The Isleta Reach falls inside of this range. Because silvery minnows are an indicator of the health of the river, great efforts are deployed to protect them.

The most important aspect of silvery minnow habitat is the connection of the main channel to the floodplain (Scurlock 1998; Cowley 2002; U.S. Fish and Wildlife Service 2010; Medley and Shirley 2013; Tetra Tech 2014; Dudley et al. 2016). Silvery minnow spawning is stimulated by peak flows in late April to early May. Ideally, these create shallow water conditions on floodplains, which are ideal nursery habitat for the silvery minnow (Mortensen et al. 2019). Peak flows that can inundate large areas of floodplains are essential to the recovery of silvery minnow populations. In-stream characteristics are also important. Silvery minnows most commonly occupy habitats with debris piles, pools and backwater. They thrive in mostly silt substrate and require low velocities and moderate depths, with slightly different requirements for juveniles and adults (Dudley and Platania 1997).

Dams, levees and diversion structures have heavily impacted the hydraulics and fluvial processes of the river. Sediment size has gone up overall, the floodplain is less connected than it has been in the past, water quality has decreased, and the river has become fragmented by dams (Osborne et al. 2012; Larsen 2007). These factors all decrease the habitat quality of silvery minnows. This is evident when looking at the decline of silvery minnow genetic diversity, densities, catch rates, and habitat range (Horner 2016). To prevent the silvery minnow from going extinct, we must study the river processes, understand how this impacts the ecological health of the system, and how to improve it. Looking at smaller scales such as reaches and subreaches may offer insight into how the rivers and minnows interact.

4.2. Relation between Flow and Population of RGSM

According to Dudley et al. (2016), the population of RGSM is "closely related to the timing, magnitude, and duration of flows in spring and summer". Figure 46 shows the relation between the population density of RGSM, spring peak discharge, annual mean discharge, and occurrence of flow higher than 2000 cfs at Albuquerque. Fish populations are positively correlated with the magnitude of the spring peak flow and the number of days with a flow exceeding 2000 cfs.

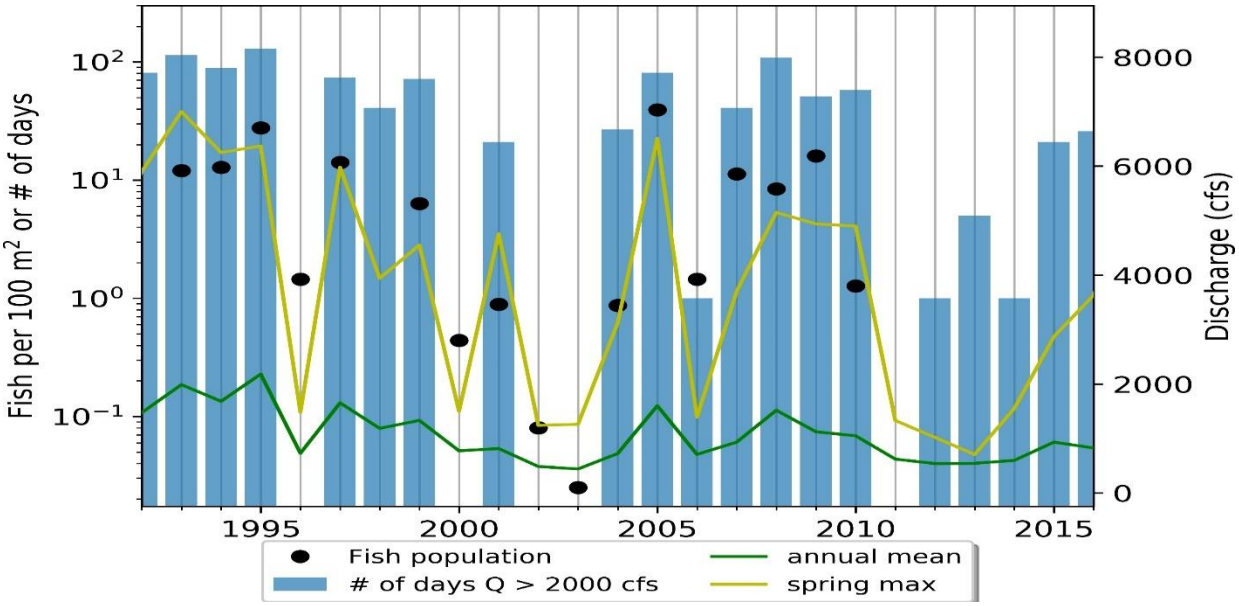

Figure 46: Population of silvery minnow vs annual mean discharge vs spring peak flow vs number of days that discharge is greater than 2000 cfs.

Figure 47 shows the scatter plots of fish population vs spring peak discharge and fish population vs number of days that discharge is higher than 2000 cfs.

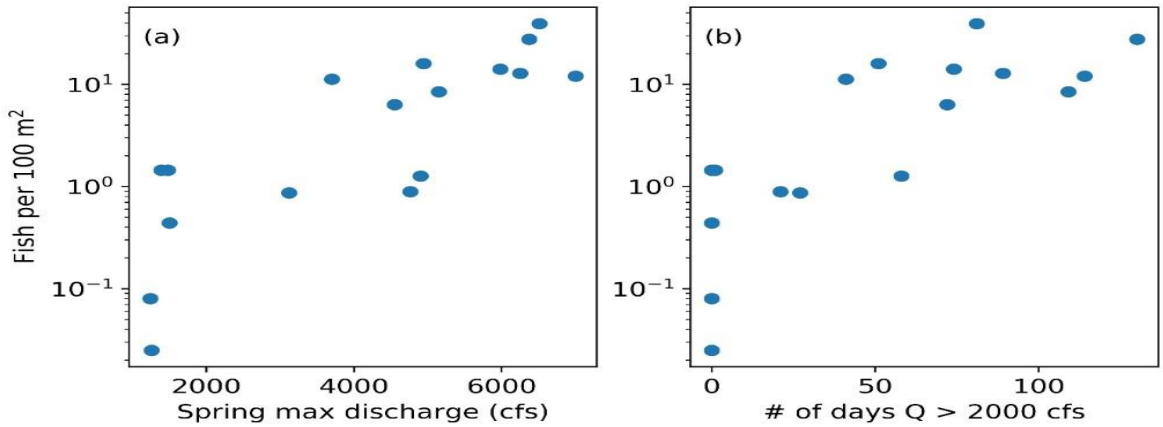

Figure 47: (a) Fish population density vs spring peak discharge, and (b) Fish population density vs number of days discharge is higher than 2000 cfs.

4.3. HEC-RAS

HEC-RAS models were set up for the Isleta reach at three different discharges (600 cfs, 1400 cfs and 3500 cfs). Certain depths and velocities are ideal for the minnows at various stages of their life cycle. A model allows one to find the percentage of area in a reach that matches these ideal flow characteristics. This can give a general estimate of the suitability of a reach for the RGSM. For more information on how this was performed, please see Appendix B and C – HEC-RAS Silvery Minnow Hydraulic Modeling.

Detailed HEC-RAS simulations are shown in Appendices B and C. For instance, Figure 48 shows that the best "spawning" and "feeding/rearing" habitats are at 3500 cfs (compared to 600 and 1400 cfs). These habitats tend to occur in subreach P2 due to better floodplain connectivity. Subreach P2 has the highest area of "good" habitat within the river at low flows of 600 cfs. However, the "good" habitat area decreases from 1992 to 2012.

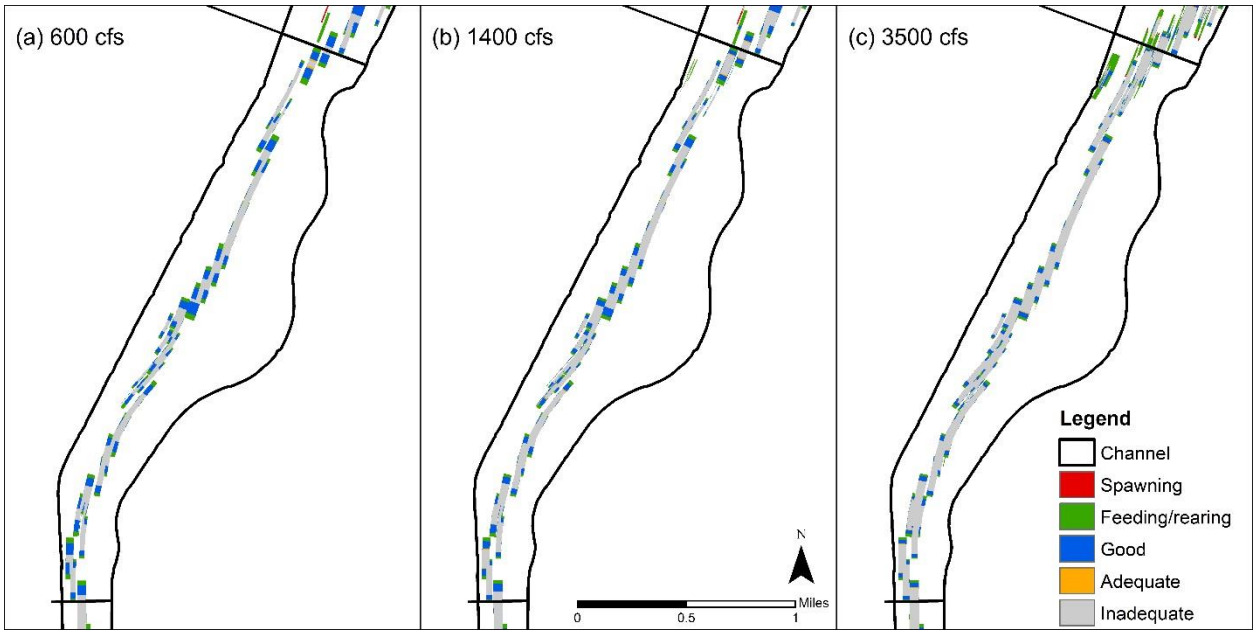

Figure 48: Hydraulic habitat at subreach P1 at flow rate 600, 1400, and 3500 in 2012

4.4. GIS (Aerial Photograph) Analysis

Aerial photographs provided by the USBR were analyzed for the RGSM habitat characteristics. Certain types of river features, such as shoreline complexity, bars, backwater, islands, and channels provide acceptable habitat for the RGSM. Each of these features can be assigned a numerical score, depending on complexity and type. By quantifying these points with in a reach and calculating their density between agg/deg lines, a measure of a reach's habitat suitability for the RGSM can be calculated. For more information on how this was performed, please see Appendix D and E – Silvery Minnow Habitat Scoring System.

For the GIS analysis in Appendices F-J, the best scores are found in earlier years or when the flow is high enough to inundate the floodplain (>3500 cfs). Subreaches P2 and P4 have the highest scores when comparing all years. By comparing the aerial photographs that were taken under similar flow conditions (~600 cfs), it shown in Figure 49 that subreaches P2 and P4 have the best habitat score. Similar results for all years are shown in Figure 50. The shoreline complexity was also analyzed with GIS. It does not have a consistent pattern over the years, but the highest score was found in 2005 with the flow just under 6000 cfs.

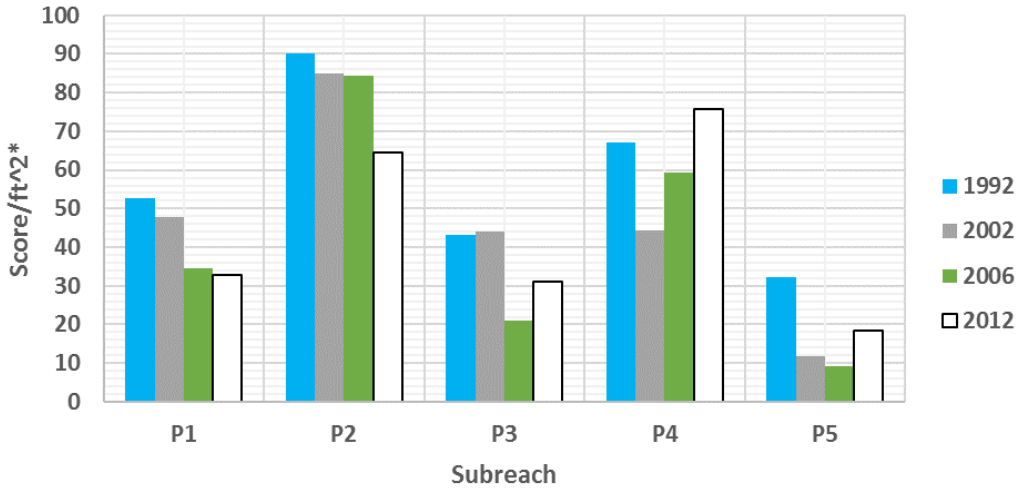

Figure 49: The column graph shows the overall habitat scores in each of the four comparable years in each subreach.

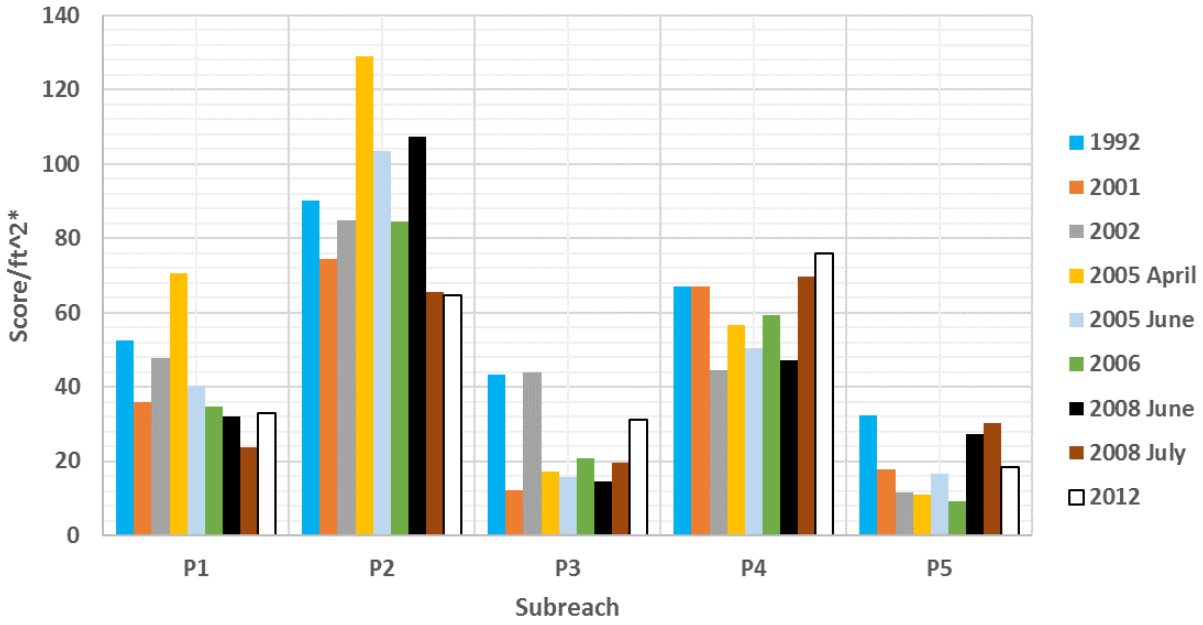

*Figure 50: The column graph shows the overall score in every year in each subreach. * Score/ft^2 is the score weighted for area of the subreach.*

A summary of all the habitat scores is presented in Table 10. It shows that the total habitat score is not always the highest at high flows, although the lowest score is at the lowest discharge. Also, under similar discharge, the score between different categories can change significantly.

Table 10: Summary of total habitat score, flows, and number of habitat types for each year. The comparable years are highlighted in blue.

				Shoreline Complexity			Main Channel Complexity		Side Channels					Backwater		Bars			Islands							Confluences	
Year	Month	Total Habitat Score	Flow (cfs)	1a	1b	1c	2a	2b	3a	3b	3c	3d	3f	4a	4b	5a	5b	5c	6a	6b	6c	6d	6e	6f	7a	7b
1992	February	596	650^{SA}	9	2	1	10	10	0	6	6	18	18	1	0	18	20	20	0	7	0	2	14	18	0	9
2001	February	422	687^{A}	5	3	0	14	9	2	8	0	5	5	0	0	12	13	19	4	3	8	0	15	7	2	6
2002	February	481	600^{SA}	3	1	0	14	7	0	2	0	21	13	0	0	7	23	11	5	0	7	2	20	0	0	0
2005	April	623	4500^{I}	15	5	1	13	11	0	0	0	21	14	9	0	20	9	4	1	2	2	2	26	7	4	3
2005	June	479	5980^{I}	3	3	2	0	3	0	1	0	13	10	0	0	43	3	1	0	0	1	7	22	5	2	4
2006	January	415	580^{SA}	4	15	0	4	12	1	9	4	13	4	1	0	0	32	15	0	3	2	1	17	8	1	5
2008	June	488	4990^{I}	14	1	0	7	3	0	4	0	20	5	3	1	27	9	1	2	5	0	6	16	6	0	6
2008	July	415	1630^{I}	5	9	3	6	4	0	4	5	21	10	2	3	5	9	2	1	14	5	7	12	4	0	7
2012	January	429	740^{SA}	8	8	0	2	6	1	22	5	16	4	1	0	5	14	20	2	5	10	3	7	16	1	4
2016	October	2430	40^{SA}	59	54	49	82	80	2	74	17	30	54	16	12	14	47	140	12	54	19	37	17	12	0	2

Note: Flows at different gages are given the follow subcripts: ^{I} Isleta gage daily average discharge, ^{SA} San Acacia gage daily average discharge, ^{A} Albuquerque gage daily average discharge

4.5. Combined HEC-RAS and Aerial Photograph Analysis

Ultimately, HEC-RAS and visual observations of aerial photographs with GIS were used to assess the habitat conditions in 1992, 2002, and 2012. All the results are shown in Appendices K and L and are briefly summarized here. It is found that subreach P2 have the best habitat and the overall habitat quality declines from 1992 to 2012. The decrease in habitat quality is likely due to: (1) a reduction in the frequency and magnitude of peak discharges; and (2) the channel narrowing and incising causing a loss of connectivity to the floodplain. For example, The summary of the combined analysis for Subreach P2 is shown in Figure 51.

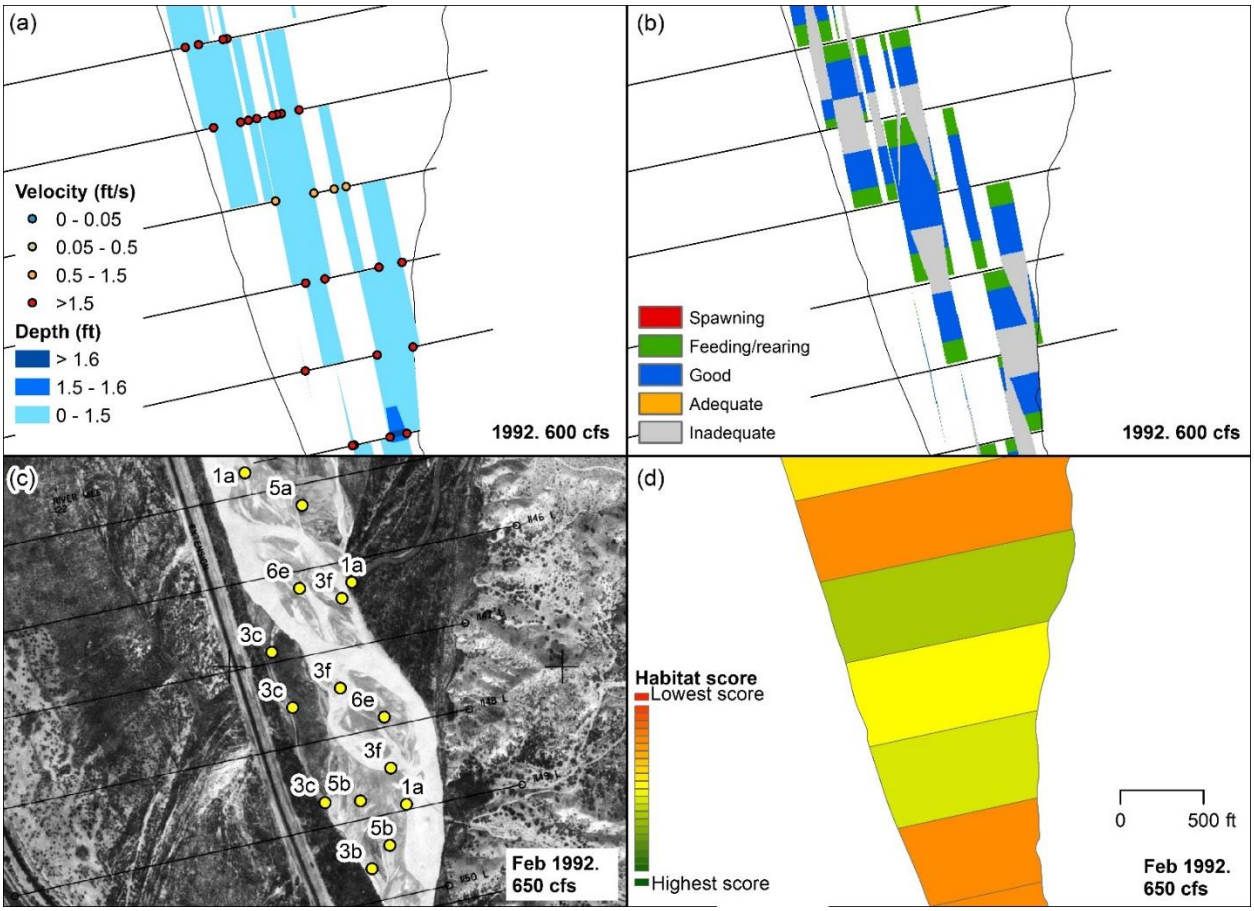

Figure 51: Summary of HEC-RAS and GIS habitat at subreach P2, agg-deg 1145 to 1150. (a) Velocity and depth of the simulation. (b) Habitat criteria mapped based on velocity and depth. (c) Habitat features mapped out by points and letters. (d) Habitat color scheme based on habitat features.

5. Conclusions

The Puerco reach was analyzed for hydrologic, hydraulic and geomorphic trends between 1918 and 2017. This reach covers about 11 miles from the Rio Puerco to the San Acacia Diversion Dam and has many tributaries.

Hydrologic and hydraulic trends were based on past reports (recently compiled by Klein et al. in 2018), but our analysis has been extended from 2014 til 2017 whenever data were available. HEC-RAS and GIS were used to find the geomorphic and river characteristics such as sinuosity, width, multiple channels, bed elevation, volume change, and other hydraulic parameters. These analyses were broken into six subreaches which enabled detailed results on a smaller scale. A conceptual geomorphic analysis was used to try to understand how the river may change in the future.

The major findings are:

- The annual water volume has been reduced recently (since the 2000s). Peak discharges have become less frequent, shorter and have decreased in the past few decades.
- The annual suspended sediment discharge in the Rio Grande and Rio Puerco have decreased since the 1970s, although the average suspended sediment concentration increased after 1993.
- The predominant sediment size moving through the reach is sand, and finer material such silts and clay make up less of the total sediment load.
- The measured sediment load exceeds 80% of the total sediment load when the flow depth is larger than 5 ft.
- In most subreaches the flow depth, velocity, grain size and sinuosity increased. The wetted perimeter, energy slope and bed slope also decreased.
- A conceptual geomorphic model shows the channel is becoming more incised and less connected to its floodplain.

A summary of a combined HEC-RAS and aerial photography analysis is presented here with ample details in Appendices B to L. Preliminary results on a HEC-RAS simulation for three different geometries and three different discharges characterize the RGSM habitat. Conditions favorable to “spawning”, “feeding/rearing”, or “good” habitat were identified. A GIS analysis of aerial photography was used to map habitat types and quality over different decades and over a range of discharges from 40 to 5980 cfs. This work deserves further consideration as it shows considerable potential for use in a later process linkage report.

References

Baird, D. (2014). Historical Rio Grande Channel Width Design Literature Review Summary, U.S. Department of the Interior, Bureau of Reclamation, Technical Services Center, Sedimentation and River Hydraulics Group. Denver, CO, 42 p.

Baird, D. C. (2016). *Rio Grande silvery minnow habitat restoration design review*, Department of the Interior, Bureau of Reclamation, Technical Services Center, Sedimentation and River Hydraulics Group. Denver, CO.

Bauer, T.R. (2000). *Morphology of the Middle Rio Grande from Bernalillo Bridge to San Acacia Diversion Dam, New Mexico*, Colorado State University, Fort Collins, CO.

Bauer, T.R. (2009). *Sediment Evolution on the Middle Rio Grande, New Mexico*, U.S. Department of the Interior, Bureau of Reclamation, Technical Services Center, Sedimentation and River Hydraulics Group. Denver, CO. 36 p.

Bauer, T.R. and Hilldale, R. (2006). *Sediment Model for the Middle Rio Grande – Phase 2: Isleta Diversion Dam to San Acacia Diversion Dam*. U.S. Department of the Interior, Bureau of Reclamation, Technical Services Center, Sedimentation and River Hydraulics Group. Denver, CO. 295 pp.

BEMP Data. (2017). BEMP Database: Precipitation 1997-2017. From Bosque Ecosystem Monitoring Program. BEMP, University of New Mexico, Albuquerque, NM. Online: http://bemp.org/data-sets/ Accessed on March 19, 2019.

Berry, K. L. and Lewis, K. (1997). *Historical Documentation of Middle Rio Grande Flood Protection Projects, Corrales to San Marcial*. Office of Contract Archeology, University of New Mexico, Albuquerque, NM.

Bestgen, K. R., Mefford, B., Bundy, J., Walford, C., Compton B., Seal S., and Sorensen T. (2003). *Swimming performance of Rio Grande silvery minnow. Final Report to U.S. Bureau of Reclamation, Albuquerque Area Office, New Mexico*. Colorado State University, Larval Fish Laboratory Contribution 132, 70 p.

Bestgen, K.R., and Platania S.P. (1991). “Status and Conservation of the Rio Grande Silvery Minnow, Hybognathus amarus.” The Southwestern Naturalist. 36 (2), 225-232

Bovee, K.D., Waddle, T.J., and Spears, J.M. (2008). “Streamflow and endangered species habitat in the lower Isleta reach of the middle Rio Grande.” *U.S. Geological Survey Open-File Report 2008-1323*.

Cluer, B., and Thorne, C. (2014). “A stream evolution model integrating habitat and ecosystem benefits.” *River Research and Applications*, 30(2), 135–154.

Cowley, D.E. (2002). “Water Requirements for Endangered Species- Rio Grande Silvery Minnow (Hybognathus Amarus).” New Mexico Water Resources Research Institute. 97-107

Crawford, C. S., Cully, A. C., Leutheuser, R., Sifuentes, M. S., White, L. H., and Wilber, J. P. (1993). *Middle Rio Grande ecosystem: Bosque biological management plan*, Middle Rio Grande Biological Interagency team, Albuquerque, NM, 320p.

Culbertson, J. K., and Dawdy, D. R. (1964). "A study of fluvial characteristics and hydraulic variables, Middle Rio Grande, New Mexico." *U.S. Geological Survey, Professional Paper 1498-F*, Washington, D.C., 82 p.

Dudley, R. K., and Platania, S. P. (1997). *Habitat use of Rio Grande silvery minnow*. Division of Fishes, Museum of Southwestern Biology, Department of Biology, University of New Mexico.

Dudley, R.K., Platania, S.P., and Gottlieb, S.J. (2005). *Rio Grande Silvery Minnow Population Monitoring Program Results from 2004*. American Southwest Ichthyological Research Foundation, Albuquerque, NM, 184 p.

Dudley, R. K., Platania, S. P., and White, G. C. (2016). *Rio Grande Silvery Minnow population monitoring results from February to December 2015*, American Southwest Ichthyological Researchers, LLC, Albuquerque, New Mexico.

Easterling Consultants LLC, and Tetra Tech Inc. (2015). *Geomorphic and Hydraulic Assessment of the Rio Grande from the Rio Puerco to San Acacia Diversion Dam 1998 to 2015*, Middle Rio Grande Project Hydrographic Data Collection, U.S. Bureau of Reclamation, Albuquerque, New Mexico.

Happ, S.C. (1948). "Sedimentation in the Middle Rio Grande Valley, New Mexico." Bulletin of the Geological Society of America. 59, 1191 – 1216

Holmes, R., and Hayes, J., (2011). "Broad-scale Trout Habitat Mapping for Streams (Using Aerial Photography and GIS)." *Cwathron Report, No. 1979*, Nelson, New Zealand, 40 p.

Holmquist-Johnson, C., Raff, D. A., and Russell, K. (2009). "Bureau of Reclamation Automated Modified Einstein Procedure (BORAMEP) program for computing total sediment discharge." User's Manual, Denver, CO

Horner, C. (2016). *Middle Rio Grande Habitat Suitability Criteria*, Colorado State University, Fort Collins, CO.

Klein, M., Herrington, C., AuBuchon, J., and Lampert, T. (2018a). *Isleta to San Acacia Geomorphic Analysis*, U.S. Bureau of Reclamation, Reclamation River Analysis Group, Albuquerque, New Mexico.

Klein, M., Herrington, C., AuBuchon, J., and Lampert, T. (2018b). *Isleta to San Acacia Hydraulic Modeling Report*, U.S. Bureau of Reclamation, Reclamation River Analysis Group, Albuquerque, New Mexico.

Julien, P.Y. (2002). *River Mechanics,* Cambridge University Press, New York

Julien, P. Y., and Wargadalam, J. (1995). "Alluvial channel geometry: theory and applications." *Journal of Hydraulic Engineering*, American Society of Civil Engineers, 121(4), 312–325.

Larsen, A. (2007). *Hydraulic Modeling Analysis of the Middle Rio Grande – Escondida Reach, New Mexico*, Colorado State University, Fort Collins, CO.

Makar, P. (2010). *Channel Characteristics of the Middle Rio Grande, New Mexico*. U.S. Department of the Interior, Bureau of Reclamation, Technical Service Center, Denver, CO, 48 p.

Makar, P. and AuBuchon, J. (2012). *Channel Conditions and Dynamics of the Middle Rio Grande*, U.S. Department of the Interior, Bureau of Reclamation, Upper Colorado Region, Albuquerque, NM, 108 p.

Marshall, M. (2015). "Earth - What is the point of saving endangered species?" *BBC News, BBC*, <http://www.bbc.com/earth/story/20150715-why-save-an-endangered-species> (Jul. 4, 2018).

Massong, T., Paula, M., and Bauer, T. (2010). "Planform Evolution Model for the Middle Rio Grande, NM." *2nd Joint Federal Interagency Conference, Las Vegas, NV, June 27 - July 1, 2010*.

Medley, C. N., and Shirey, P. D. (2013). "Review and reinterpretation of Rio Grande silvery minnow reproductive ecology using egg biology, life history, hydrology, and geomorphology information" *U.S. National Park Service Publications and Papers.* 133.

MEI. (2002). *Geomorphic and Sedimentologic Investigations of the Middle Rio Grande between Cochiti Dam and Elephant Butte Reservoir*, Mussetter Engineering, Inc., Fort Collins, CO, 220 p.

MEI. (2006). "Evaluation of Bar Morphology, Distribution and Dynamics as Indices of Fluvial Processes in the Middle Rio Grande, New Mexico." Report prepared for the New Mexico Interstate Stream Commission and the Middle Rio Grande Endangered Species Act Collaborative Program.

Mortensen, J.G., Dudley, R.K., Platania, S.P., and Turner, T.F. (2019). Draft report. *Rio Grande Silvery Minnow Habitat Synthesis,* University of New Mexico with American Southwest Ichthyological Researchers, Albuquerque, NM.

Osborne, M. J., Carson, E. W., and Turner, T. F. (2012). "Genetic monitoring and complex population dynamics: insights from a 12-year study of the Rio Grande silvery minnow." *Evolutionary Applications*, 5(6), 553–574.

Parametrix. (2008). *Restoration analysis and recommendations for the Isleta Reach of the Middle Rio Grande, NM*, Parametrix, Inc. Albuquerque, NM, 292 p.

Perschbacher, J. (2011). *The Use of Aerial Imagery to Map In-Stream Physical Habitat Related to Summer Distribution of Juvenile Salmonids in a Southcentral Alaskan Stream*, University of Alaska Fairbanks, Fairbanks, AK.

Posner, A. J. (2017). Draft report. *Channel conditions and dynamics of the Middle Rio Grande River,* U.S. Bureau of Reclamation, Albuquerque, New Mexico.

Richard, G. A. (2001). *Quantification and prediction of lateral channel adjustments downstream from Cochiti Dam, Rio Grande*, NM, Colorado State University, Fort Collins, CO.

Rozin, U. and Schick, A.P. (1996). *Land use change, conservation measures and stream channel response in the Mediterranean/semiarid transition zone: Nahal Hoga, southern Coastal Plain, Israel,* Erosion and Sediment Yield: Global and Regional Perspectives, Proc. Exeter Symposium, IAHS Pub. # 236, 1996.

Russo, B. (2018). "An Endangered Fish Out of Water." *Earth Island Journal. News of the World Environment*, < http://www.earthisland.org/journal/index.php/elist/eListRead/an_endangered_fish_out_of_water/> (July. 4, 2018)

Scurlock, D. (1998). "From the Rio to the Sierra: an environmental history of the Middle Rio Grande Basin." *General Technical Report RMRS-GTR-5. Fort Collins, CO: US Department of Agriculture, Forest Service, Rocky Mountain Research Station*, *440 p.*

Shah-Fairbank, S. C., Julien, P. Y., and Baird, D. C. (2011). "Total sediment load from SEMEP using depth-integrated concentration measurements." Journal of Hydraulic Engineering, 137(12), 1606–1614.

Swanson, B., Meyer, G., and Coonrod, J. (2010). *Coupling of Hydrologic/Hydraulic Models and Aerial Photographs through Time, Rio Grande near Albuquerque, New Mexico: Report Documentary 2007 Work*. U.S. Army Engineer Research and Development Center, Vicksburg, MS.

Tashjian, P. and Massong, T. (2006). "The Implications of Recent Floodplain Evolution on Habitat within the Middle Rio Grande, NM." *2006 Federal interagency Sedimentation Conference*, 9 p.

Tetra Tech. (2002). *Development of the Middle Rio Grande FLO-2D Flood Routing Model Cochiti Dam to Elephant Butte Reservoir.* Tetra Tech, Inc. 48 p.

Tetra Tech. (2014). *Ecohydrological Relationships along the Middle Rio Grande of New Mexico for the Endangered Rio Grande Silvery Minnow*. US Army Corps of Engineers, Albuquerque district, Albuquerque, New Mexico, 109 p.

Torres, L.T. (2007). *Habitat Availability for Rio Grande Silvery Minnow (Hybognathus amarus) Pena Blanca, Rio Grande, New Mexico*, University of New Mexico, Albuquerque, New Mexico.

U.S. Bureau of Reclamation. (n.d.). "PROJECTS & FACILITIES." Central Valley Project - Mid-Pacific Region | Bureau of Reclamation, <https://www.usbr.gov/projects/index.php?id=130> (accessed Feb 1, 2019).

U.S. Bureau of Reclamation. (2012). "Middle Rio Grande River Maintenance Program - Comprehensive Plan and Guide." Albuquerque Area Office, Albuquerque, New Mexico, 202p.

U.S. Fish and Wildlife Service. (2007). "Rio Grande Silvery Minnow (Hybognathus amarus)." Draft Revised Recovery Plan, Albuquerque, New Mexico, 174 p.

U.S. Fish and Wildlife Service. (2010). “Rio Grande Silvery Minnow Recovery Plan, First Revision” Southwest Region U.S. Fish and Wildlife Service Albuquerque, New Mexico, 210 p.

Varyu, D. (2013). *Aggradation / Degradation Volume Calculations: 2002-2012*. U.S. Department of the Interior, Bureau of Reclamation, Technical Services Center, Sedimentation and River Hydraulics Group. Denver, CO.

Varyu, D. (2016). *SRH-1D Numerical Model for the Middle Rio Grande: Isleta Diversion Dam to San Acacia Diversion Dam*. U.S. Department of the Interior, Bureau of Reclamation, Technical Services Center, Sedimentation and River Hydraulics Group. Denver, CO.

Yang, C.Y. (2019). *The Sediment Yield of South Korean Rivers*, Colorado State University, Fort Collins, CO.

Yang, C.Y. and Julien, P.Y. (2019). “The ratio of measured to total sediment discharge.” *International Journal of Sediment Research*, 34(3), pp.262-269.

APPENDIX A

Subreach Delineation

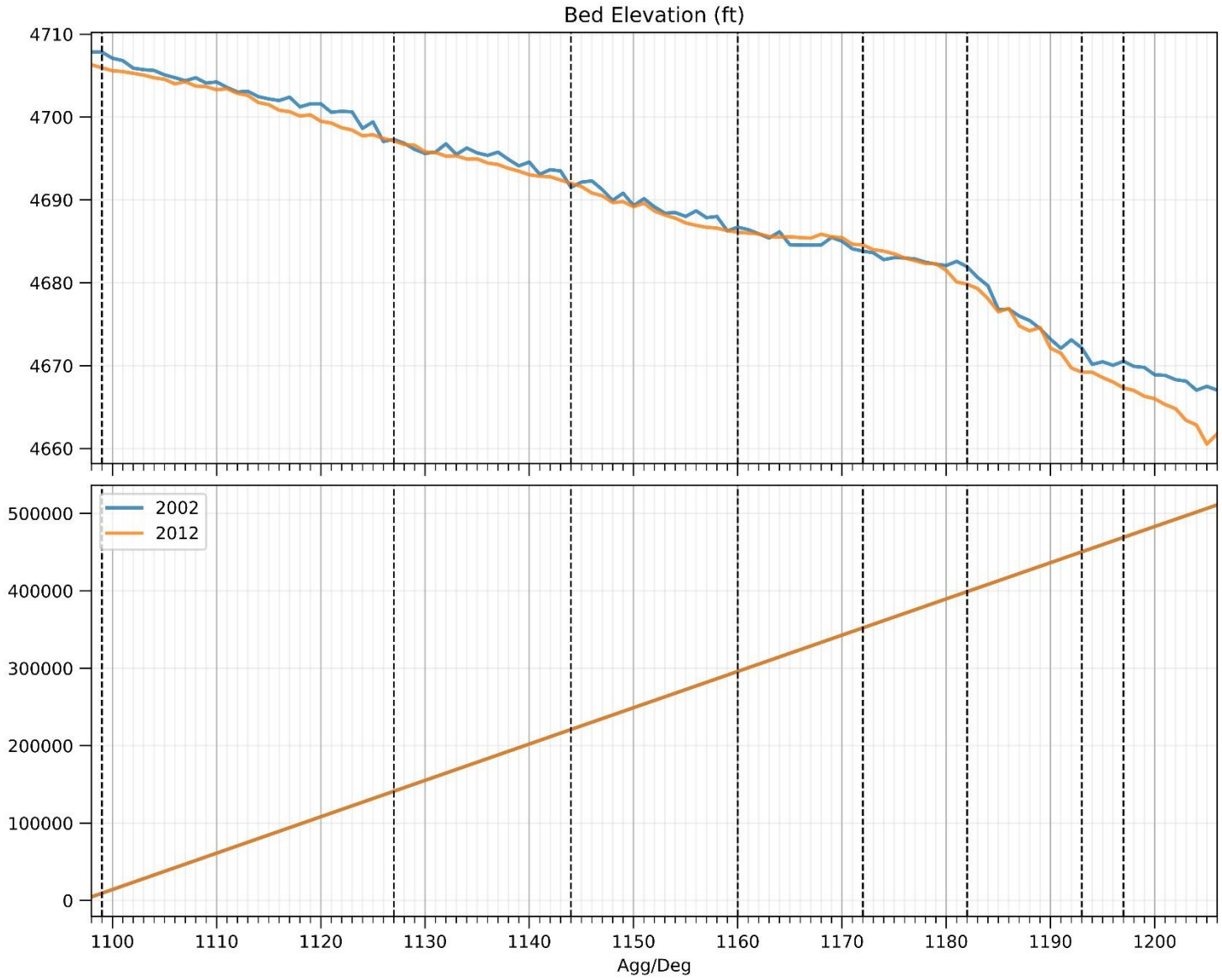
Bed Elevation (ft)
4710
4700
4690
4680
4670
4660
2002
2012
500000
400000
300000
200000
100000
0
1100
1110
1120
1130
1140
1150
1160
1170
1180
1190
1200
Agg/Deg

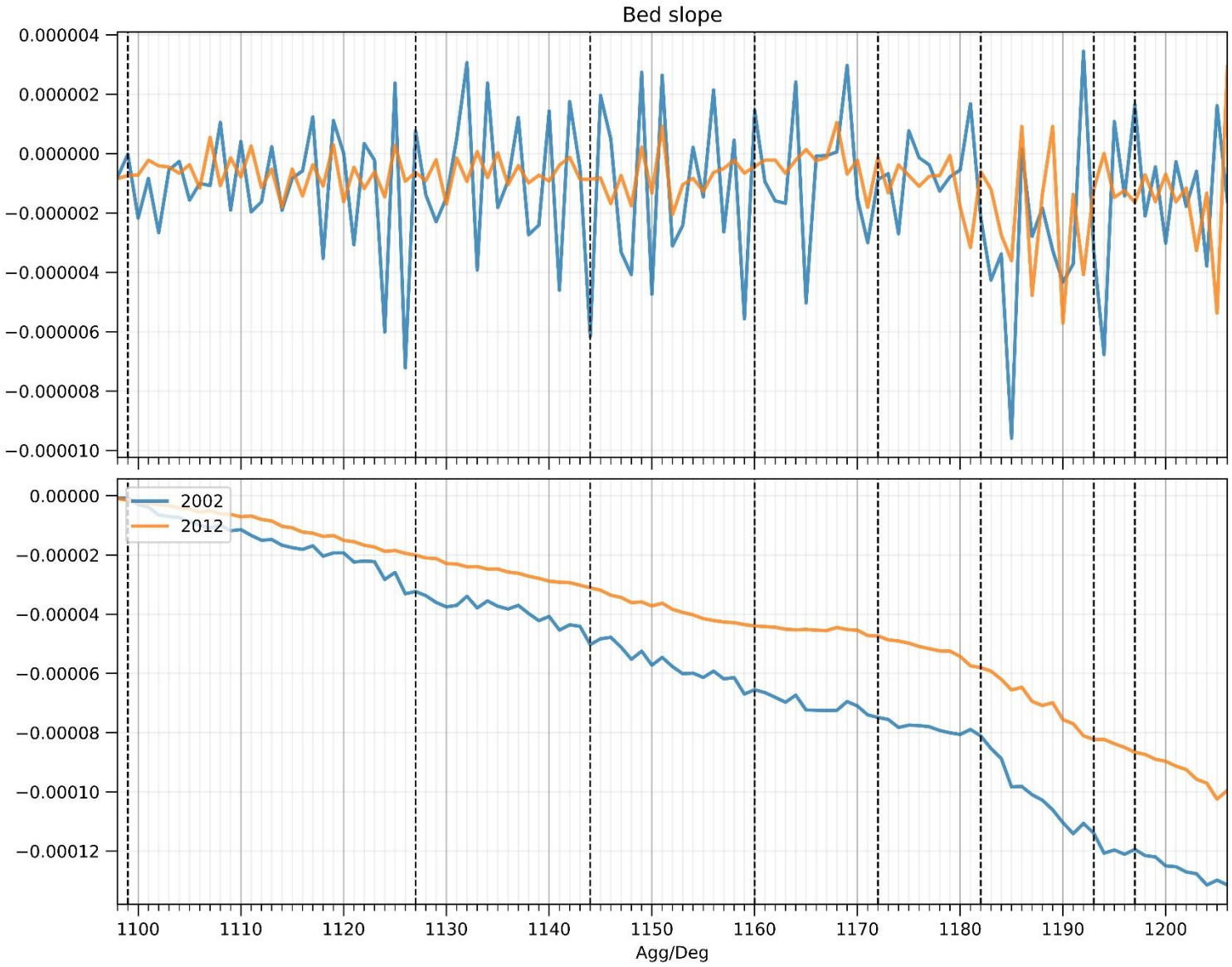
Bed slope
0.000004
0.000002
0.000000
−0.000002
−0.000004
−0.000006
−0.000008
−0.000010
0.00000
−0.00002
−0.00004
−0.00006
−0.00008
−0.00010
−0.00012
2002
2012
1100
1110
1120
1130
1140
1150
1160
1170
1180
1190
1200
Agg/Deg

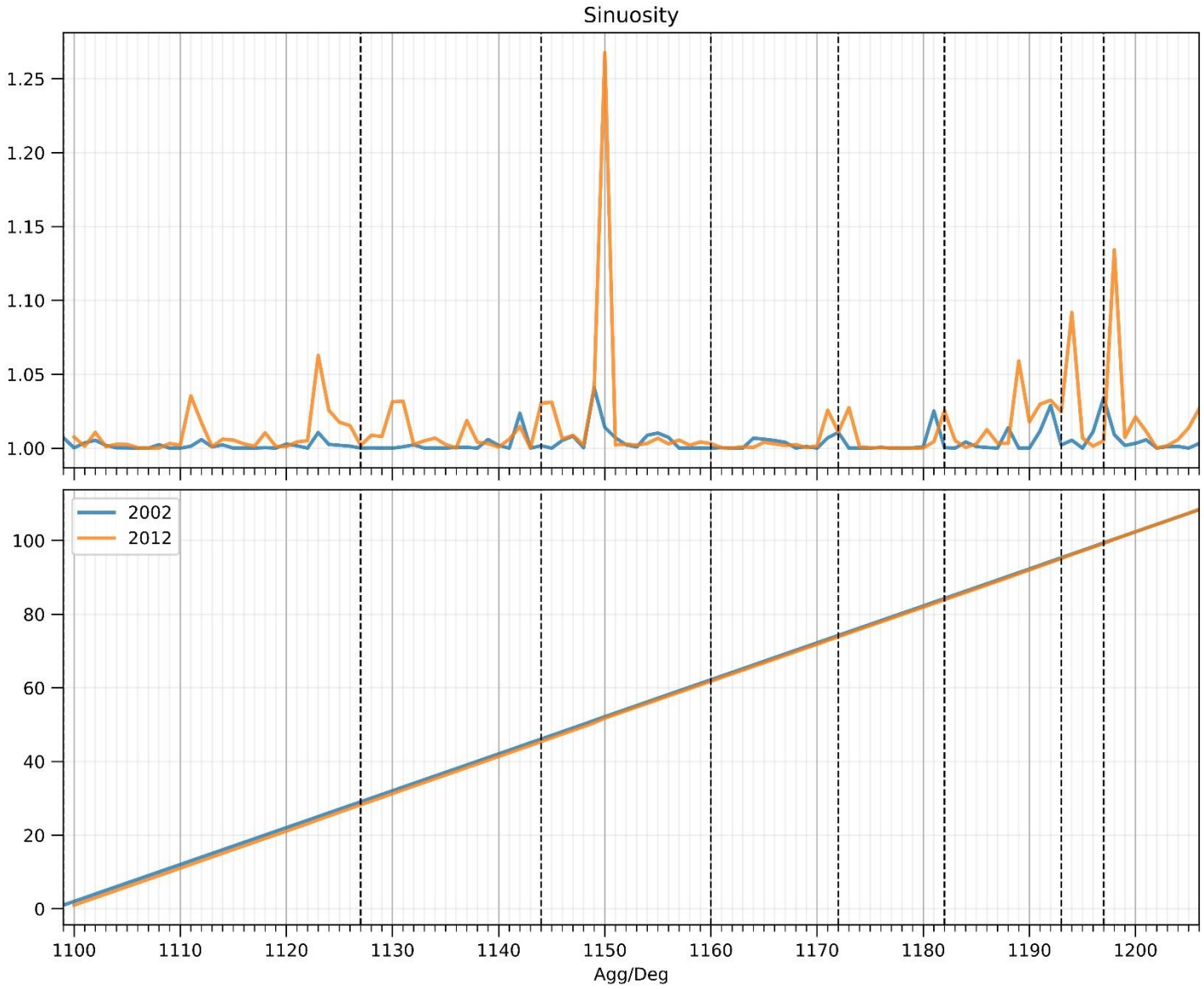
Sinuosity
1.25
1.20
1.15
1.10
1.05
1.00
2002
2012
100
80
60
40
20
0
1100
1110
1120
1130
1140
1150
1160
1170
1180
1190
1200
Agg/Deg

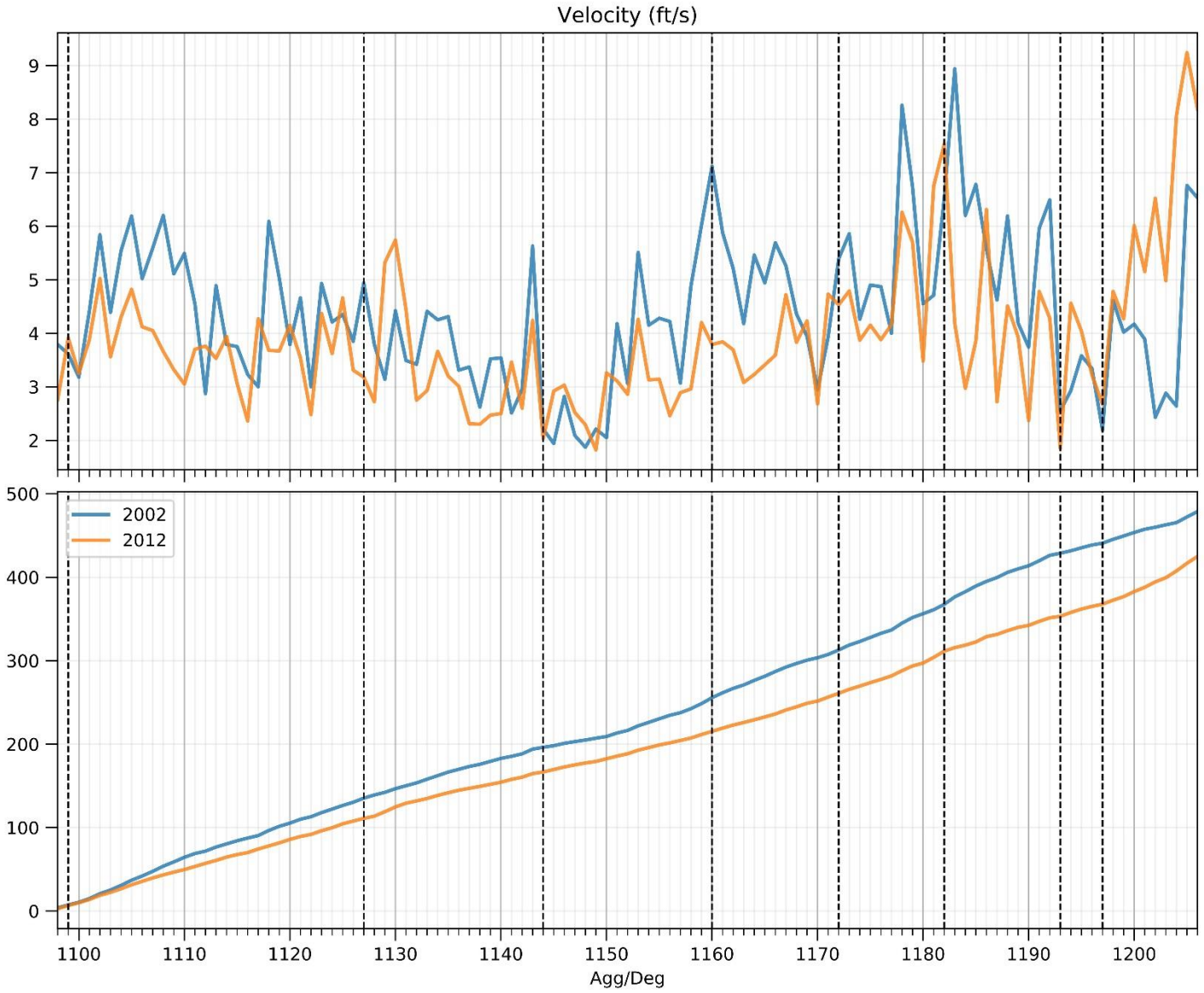
Velocity (ft/s)
9
8
7
6
5
4
3
2
500
400
300
200
100
0
2002
2012
1100
1110
1120
1130
1140
1150
1160
1170
1180
1190
1200
Agg/Deg

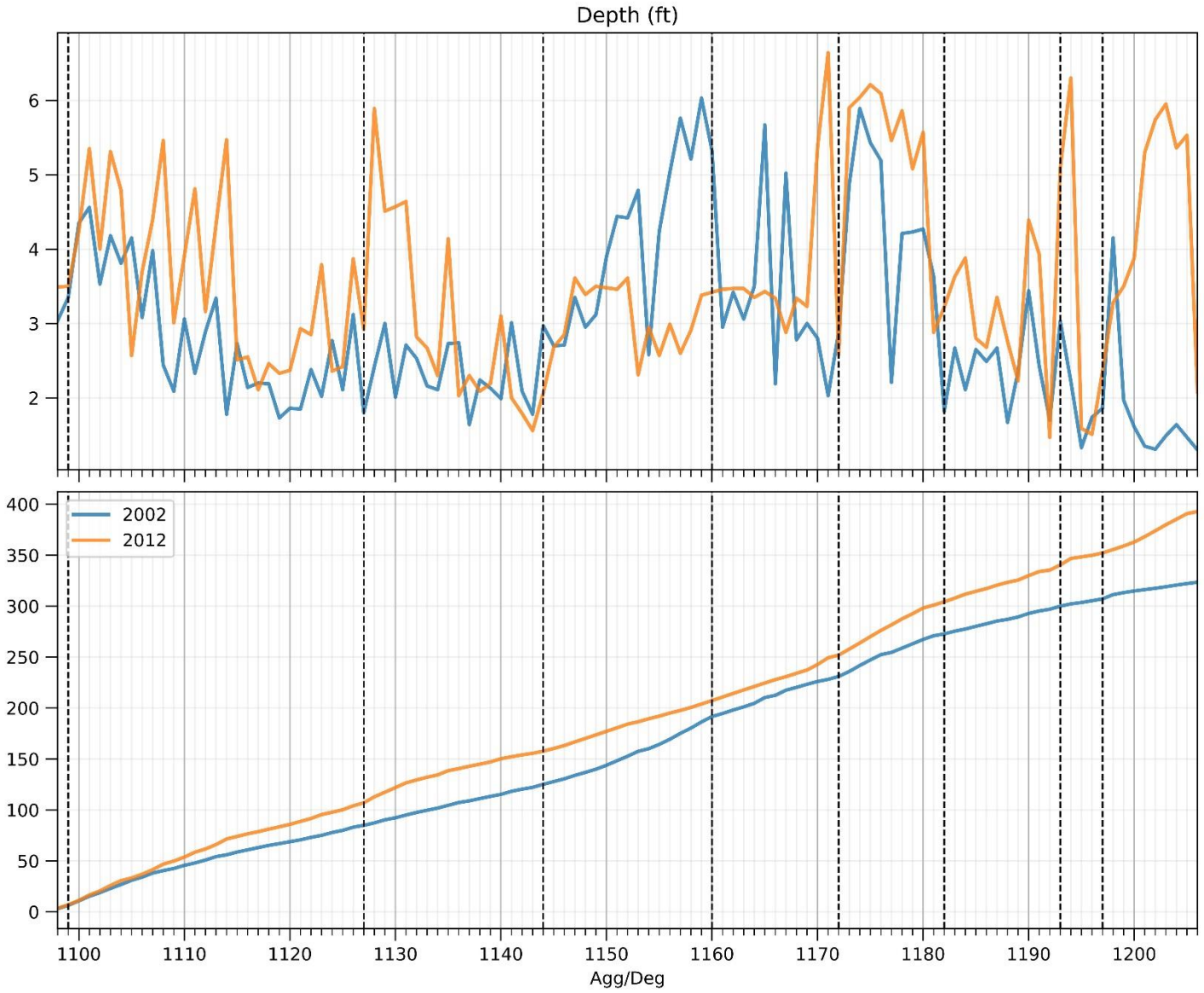
Depth (ft)
6
5
4
3
2
400
350
300
250
200
150
100
50
0
2002
2012
1100
1110
1120
1130
1140
1150
1160
1170
1180
1190
1200
Agg/Deg

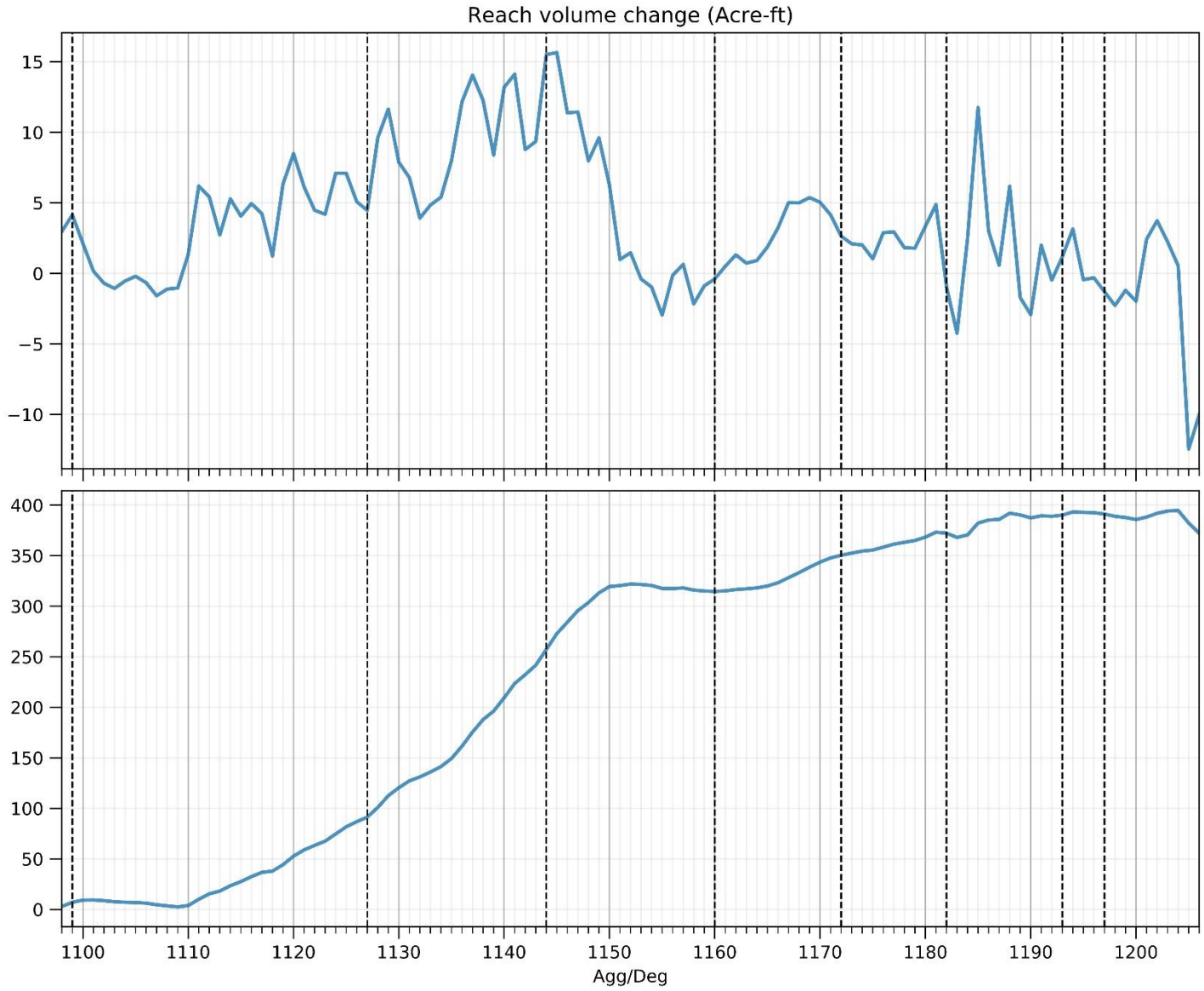
Reach volume change (Acre-ft)
15
10
5
0
−5
−10
400
350
300
250
200
150
100
50
0
1100
1110
1120
1130
1140
1150
1160
1170
1180
1190
1200
Agg/Deg

APPENDIX B

HEC-RAS Silvery Minnow Hydraulic Modeling

Flow depth and velocity can help determine the quality of habitat of RGSM. In this study, HEC-RAS 5.0.3 is used to analyze hydraulic conditions at different flow discharges in 1992, 2002, and 2012. The depth and velocity from the HEC-RAS model were used to quantify the location and area of high quality habitat.

Habitat Criteria

To understand the quality of silvery minnow habitat and how it is changing, it was useful to classify the habitats into different types. These types of habitats indicate how good the habitat is and what it is used for. For instance, feeding, rearing and spawning habitats are necessary for silvery minnows to propagate. Feeding habitats for silvery minnows include benthic food sources, which includes organic detritus, algae, diatoms, and small invertebrates. For "feeding/rearing" habitat to form, it requires low velocity flow so that the river bed is stable (< 0.5 ft/s) and sufficient sunlight so the algae can grow. Also, spawning habitat is better if it is warm and has a low velocity so eggs don't drift downstream. The warm water triggers spawning and provides the energy for algae to grow and therefore ensures food supply for larval development. "Spawning" is a rare habitat that has a velocity less than 0.05 ft/s and a depth less than 1.5 ft which ensures survival of eggs and larvae. This is why inundated floodplains are the perfect habitat for spawning. Other categories include "good", "adequate", and "inadequate". Studies have shown that the silvery minnow is most commonly collected from water less than 1.6 ft (USFWS 2010 from Tetra Tech 2014), so this would be classified as "good" habitat. Because "good" habitat is habitable, but does not provide prime areas for feeding, rearing, or spawning it is best for the adult life stage of the minnows. "Inadequate" meets none of the ideal habitat criteria and "adequate" meets some of the criteria. The category between 1.5 ft and 1.6 ft exists based on the Tetra Tech report, and is somewhat negligible because it has a very small range. The classification of habitat for silvery minnow used in this section is based on criteria and descriptions of habitat from Tetra Tech (2014).

These descriptions of habitats are translated into numerical ranges that fit certain depths and velocities based off of Tetra Tech's report from 2014. Flow depth is divided into four groups: 0 – 1.5 ft, 1.5 ft – 1.6 ft, and > 1.6 ft. Velocity is broken down into four tiers, 0 – 0.05 ft/s, 0.05 – 0.5 ft/s, 0.5 – 1.5 ft/s, and > 1.5 ft/s. Also, the ideal habitat for RGSM should have flow depth between 0.16 ft (5 cm) and 1.5 ft (45 cm) and flow velocity less than 1.5 ft/s (Baird 2016). A summary of the depth and velocities and which habitats they represent is described in Table B-1.

Table B-1: Habitat Classification based on flow depth and velocity.

Depth (ft)	Velocity (ft/s)			
	0 – 0.05	0.05 – 0.5	0.5 – 1.5	> 1.5
0 – 1.5	Spawning	Feeding/rearing	Good	Inadequate
1.5 – 1.6	Adequate	Adequate	Adequate	Inadequate
>1.6	Inadequate	Inadequate	Inadequate	Inadequate

Method

The amount of “Inadequate”, “Adequate”, “Good”, “Feeding/rearing”, and “Spawning” habitat and where it is can be visualized and analyzed from the process outlined in this section. By looking at the simulated velocities and depths of the range of flows, we can have insight into silvery minnow habitat and how it changes with different flow regimes, spatially, and temporally.

HEC-RAS was employed to analyze the hydraulic condition at different flow conditions. The flows used in HEC-RAS were based on past analyses and practicality. For instance, the 25-day exceedance spring runoff peak flow for dry, mean, and wet year were identified by MEI (2006) to be 1400, 3500, and 5600 cfs, respectively. Spring runoff for the last decade has been lower than the past runoffs, so flow of 600, 1400 and 3500 cfs were used for the fish habitat analysis. Spring flow was targeted because the population of RGSM is highly correlated to the connectivity to floodplain in spring. 600 cfs was chosen because several years of aerial photographs were taken with the flow discharge around this value (1992 at 650 cfs, 2002 at 600 cfs, 2006 at 580 cfs and 2012 at 740 cfs). This allows the comparison of HEC-RAS results with aerial photograph.

Three years (1992, 2002, and 2012) were chosen run the various flows to compare the data temporally. These years were chosen because they are around when fish population started being collected and aerial photography is available during these years. The HEC-RAS geometry cross sections used for the analysis were developed by USBR. An example of a cross-section from 2002 is shown in Figure B-1. The 1992 and 2002 are derived by using photogrammetry and the 2012 geometry was derived from LiDAR. The reach from Isleta Diversion Dam to San Acacia was extracted from the entire Middle Rio Grande HEC-RAS file with additional 10 cross sections adjacent to upstream and downstream ends. Modifications were made to the main channel designation and levee stations to more accurately reflect the flood extent in the aerial photographs (Figure). Aerial photographs from April of 2005 (4500 cfs), 2006 January (580 cfs), and 2008 July (1630 cfs), and a digitized flood map of 2005 June (5980 cfs) were used to identified the location of levees. Manning n was set as 0.019 for the main channel and 0.1 for the floodplain according to Klein et al. (2018b). The simulation was run under uniform steady condition.

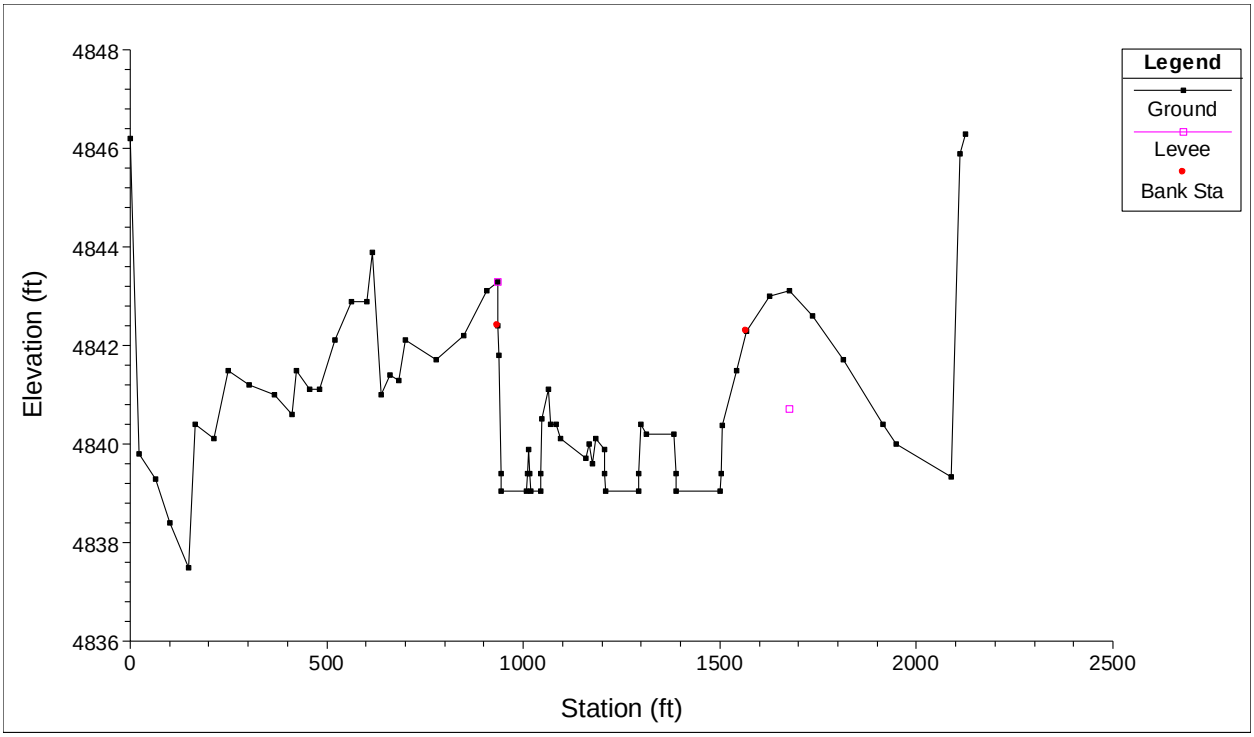

Figure B-1: Example of modified levee station: agg/deg 764 (river station 1177) in 2002. The 2005 flood map shows that the flow only overtopped at the right bank. Furthermore, the right bank side channel is found inundated in April of 2005 but not in the aerial photos in January of 2006, so the levee on the right bank is placed between side channel and main channel and at the elevation with flow between 1500 cfs and 3150 cfs. The levee on the left bank is placed at the top of the main channel banks.

Flow depth and velocity for each station are exported to ArcGIS to analyze the habitat spatially. The habitat quality was broken up into subreaches and compared. Because the HEC-RAS geometries were not geo-referenced, a program was developed to compute the coordinate for every station. A point polygon with flow depth, flow velocity, and xy-coordinate for a given flow condition was generated. The point feature was used to create a TIN to generate surface features for depth and velocity. Lastly, depth and velocity were classified and combined based on Table B-1. The classes of “Spawning”, “Feeding/Rearing”, “Good”, and “Adequate” were analyzed spatially through the subreaches.

Results & Discussion

Figures B-2 and B-3 illustrate the simulation results of flow depth and velocity at subreach P1 when the discharge is 600, 1400, and 3500 cfs in 2012. As shown in Figure B-4, we can identify the location with the flow depth and velocity that is suitable for silvery minnows according to . Maps for the rest of the reach can be found in Appendix C.

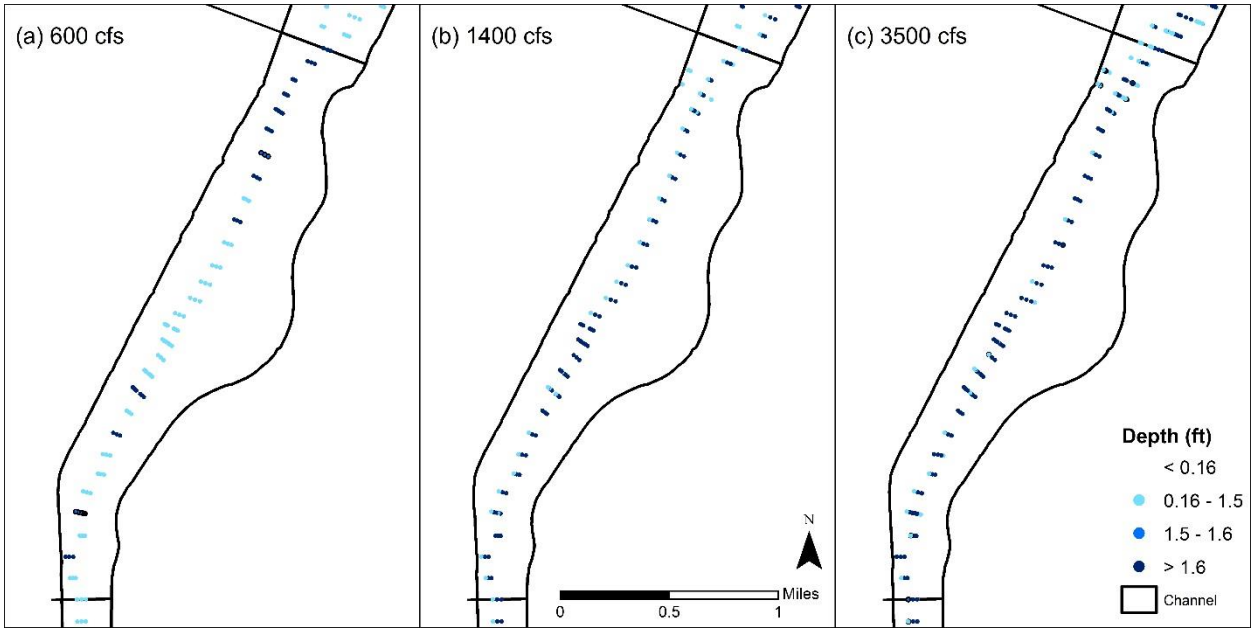

Figure B-2: Simulated depth at subreach I1 at flow rate 600, 1400, and 3500 cfs in 2012.

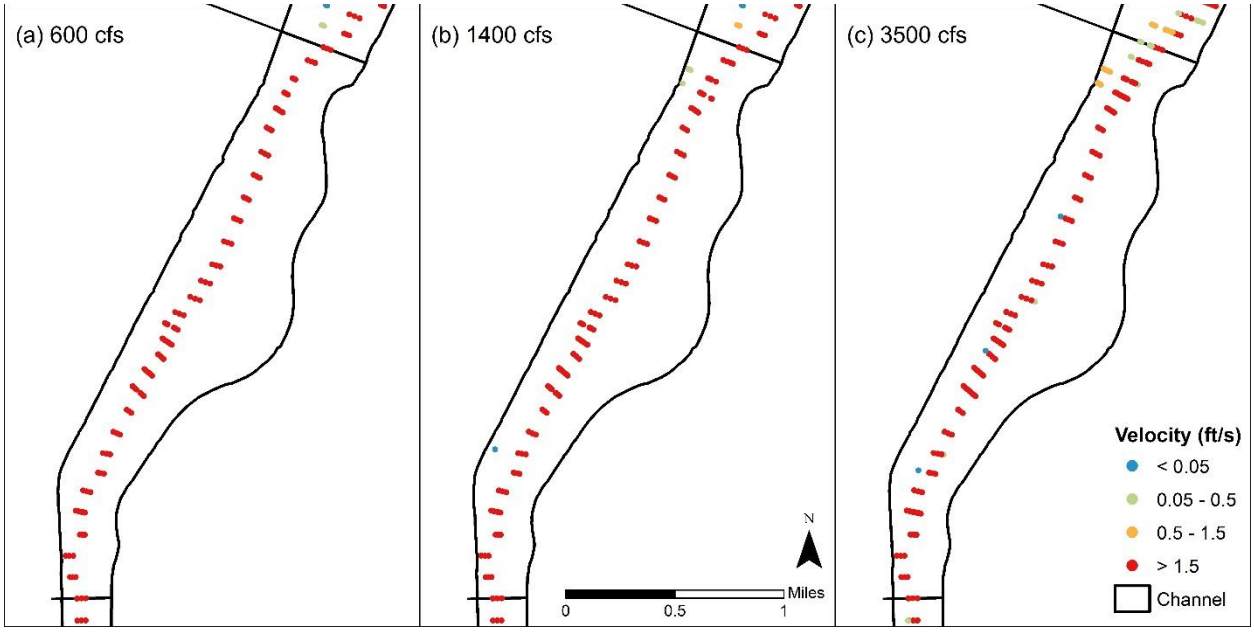

Figure B-3: Simulated velocity at subreach I1 at flow rate 600, 1400, and 3500 cfs in 2012.

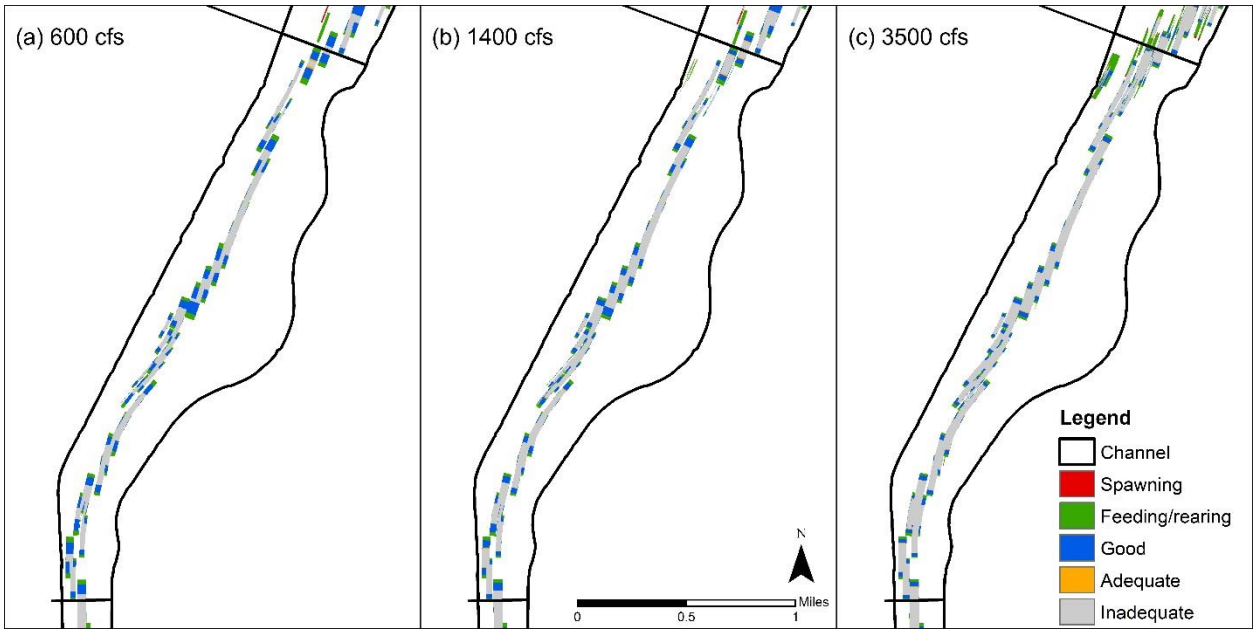

Figure B-4: Simulated habitat at subreach P1 at flow rate 600, 1400, and 3500 in 2012.

The results show the area for silvery minnows is limited in the main channel and not much overbank inundation occurs in this reach. The relationship between discharge and area are not consistent for "spawning" and "feeding/rearing" area across different subreaches as shown in Figures B-5 and B-6. The habitat density depicted in (b) in these figures gives a more meaningful representation of the habitat quality because it is weighted by subreach area.

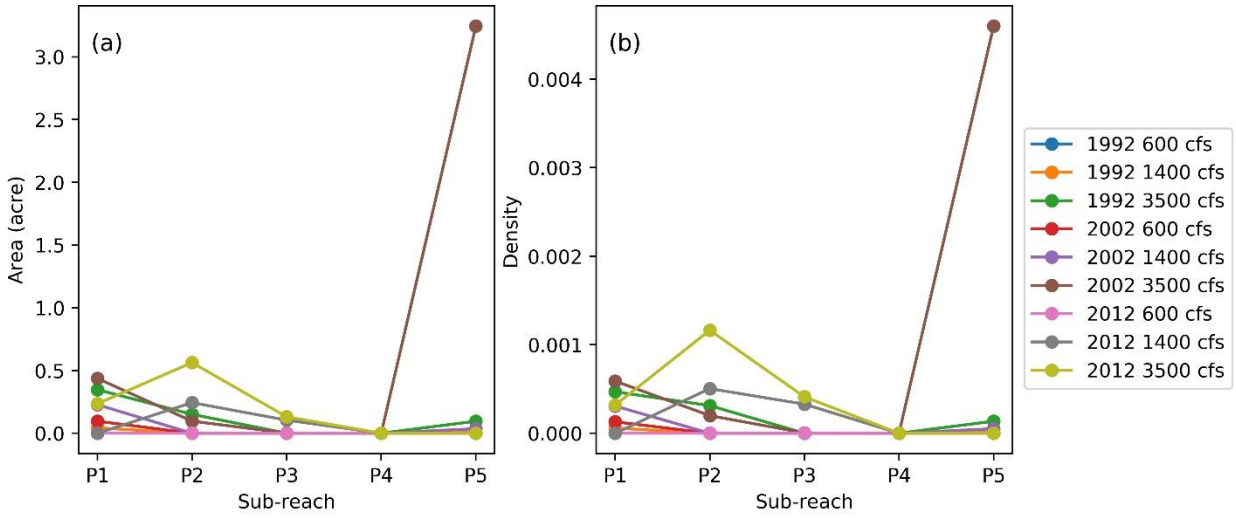

Figure B-5: "Spawning" habitat: (a) area, (b) density (area of habitat divided by area of subreach).

It can be seen in Figure B-5 that the amount of "spawning" area is only high in 2002 in subreach P5. The means the habitat quality is high, which is correlated with floodplain inundation that starts at 3500 cfs in this reach (Tetra Tech 2014). This may indicate that the floodplain does not

inundate at 3500 cfs except at subreach P5 in 2002. Also, there is not an obvious trend of habitat areas between years.

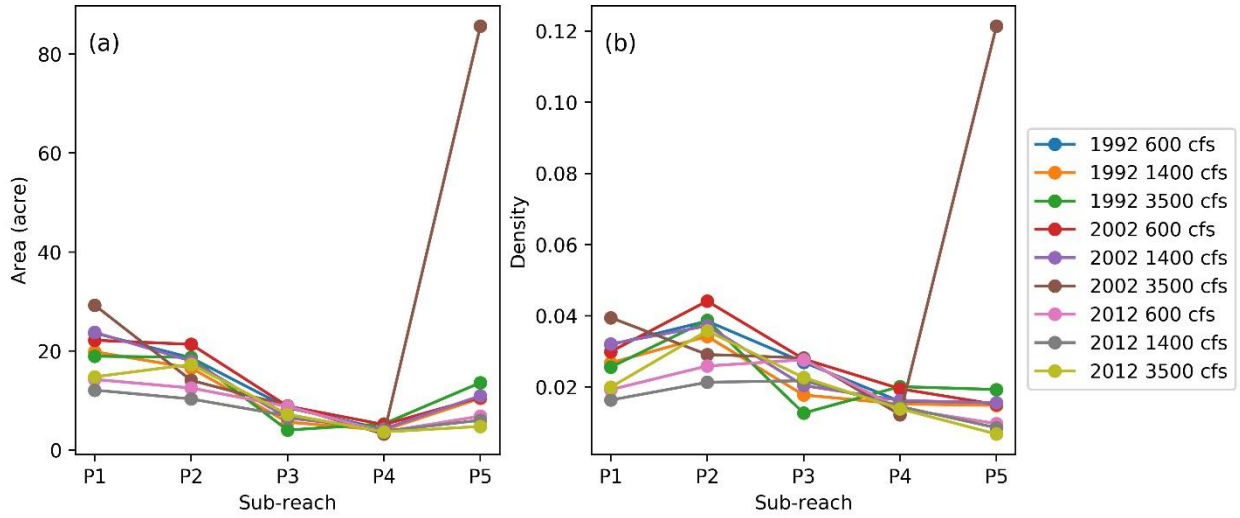

Figure B-6: "Feeding/rearing" habitat: (a) area, (b) density (area of habitat divided by area of subreach).

2012 has the lowest scores at all three flows for "feeding/rearing" habitat as shown in Figure B-6. Like "spawning" habitat the 3500 cfs flow in 2002 for P5 has the highest area. Other than that P2 has the greatest density of habitat for all flows.

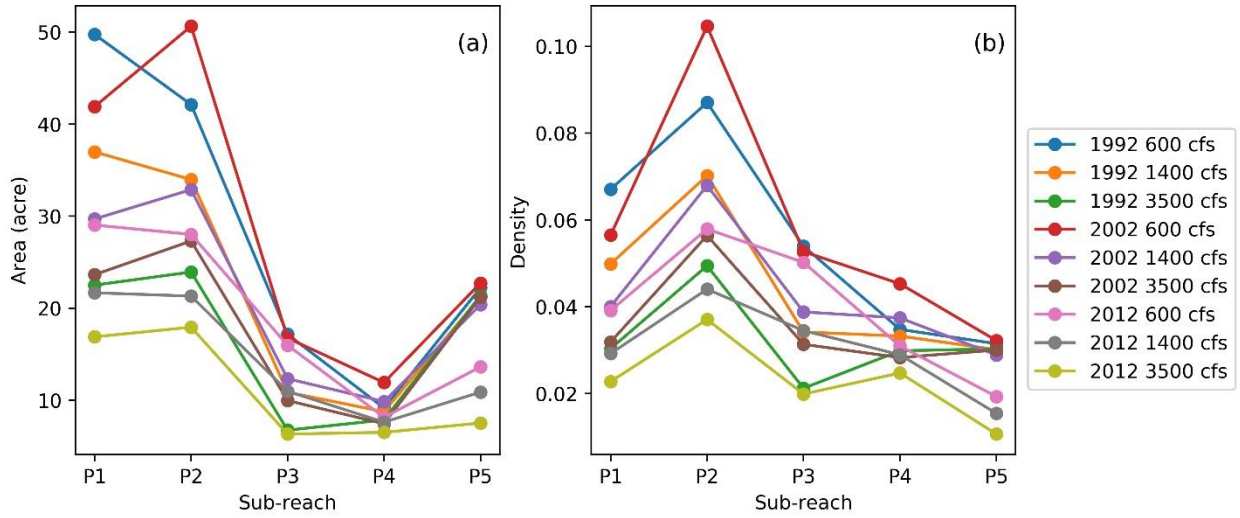

Figure B-7: "Good" habitat: (a) area, (b) density (area of habitat divided by area of subreach).

For the "good" habitat, the area is negatively related to discharge (Figure B-7). Therefore, the highest density of "good" habitat is at the lowest flow of 600 cfs for all years. This could be due to more accessible channels in the main channel, and shallower areas at low flow providing better habitat. Also, subreach P2 appears to have the majority of "good" habitat.

When the discharge increases, the area of low velocity in the channel decreases and therefore the area of “good” habitat decreases until floodplain inundation occurs. It would be expected that the “good” habitat would be lowest at 1400 cfs and higher at 3500 cfs when the floodplain becomes inundated (Bovee et al. 2008; Tetra Tech 2014), yet this does not occur. The “good” habitat is lowest at 3500 cfs. This is most likely because a very small amount of inundation occurs starting at 3500 cfs (Tetra Tech 2014), so that area become all “feeding/rearing” and “spawning” habitat. When significant inundation begins at flows such as at 5000 cfs, greater amounts of “good” habitat would be expected.

Over time, the “good” habitat has decreased which is consistent with the knowledge of what is happening in the Middle Rio Grande over time (Scurlock 1998; Bovee et al. 2008; Tetra Tech 2014). The reach channelizing and narrowing causes this loss of slow and shallow areas at low flow. When looking at the weighted results, P5 is best for spawning and “feeding/rearing” whereas P2 has the majority of “good” habitat. This may be because P2 is the most braided or tends to be less sinuous than the other reaches. P5 might have better floodplain connectivity but why that occurs is unknown. It is also important to note that even though the simulation shows 3500 cfs has the best habitat quality for P5, the actual flow is not usually that high. For instance, the peak flow in 2002 was only 1920 cfs and peak flows are greatly correlated with silvery minnow population (Dudley et al. 2016).

Overall habitat quality has decreased over time and P2 has the best habitat quality at low flows. The middle flow level of 1400 cfs never has the highest habitat area, and usually has the least amount of quality habitat. The highest “spawning” and “feeding/rearing” habitat is at 3500 cfs. The majority of “good” habitat occurs at 600 cfs.

APPENDIX C

All Results from HEC-RAS RGSM Modeling

(a) 1992

P1

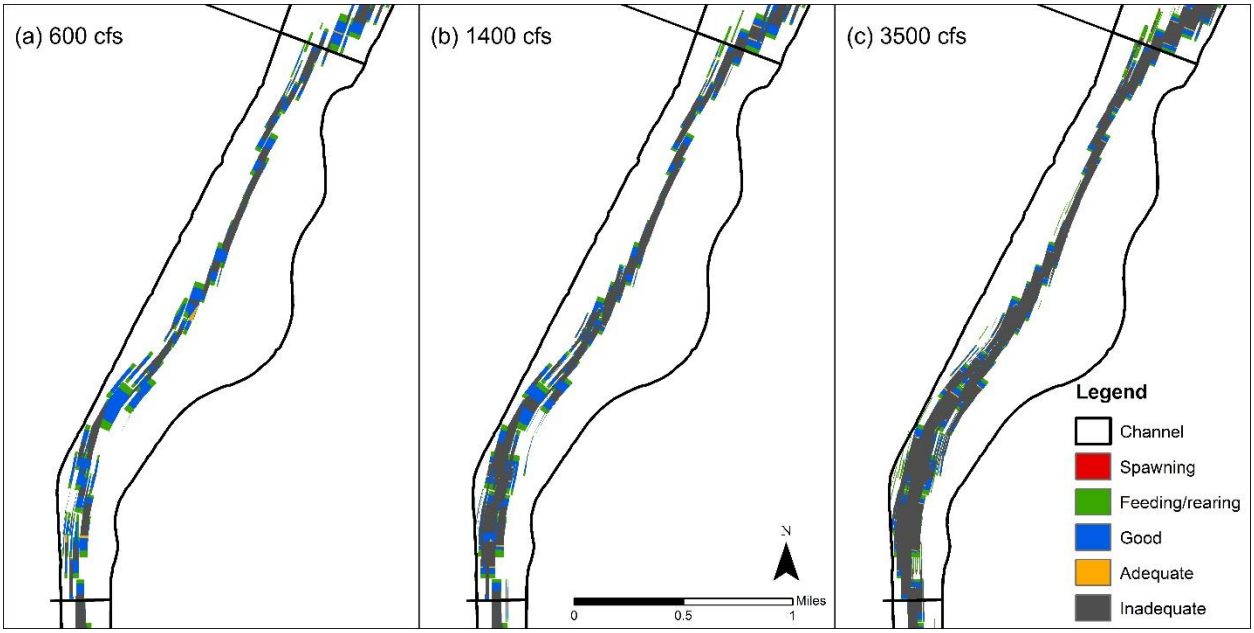
(a) 600 cfs
(b) 1400 cfs
(c) 3500 cfs
N
0
0.5
1
Miles
Legend
Channel
Spawning
Feeding/rearing
Good
Adequate
Inadequate

P2

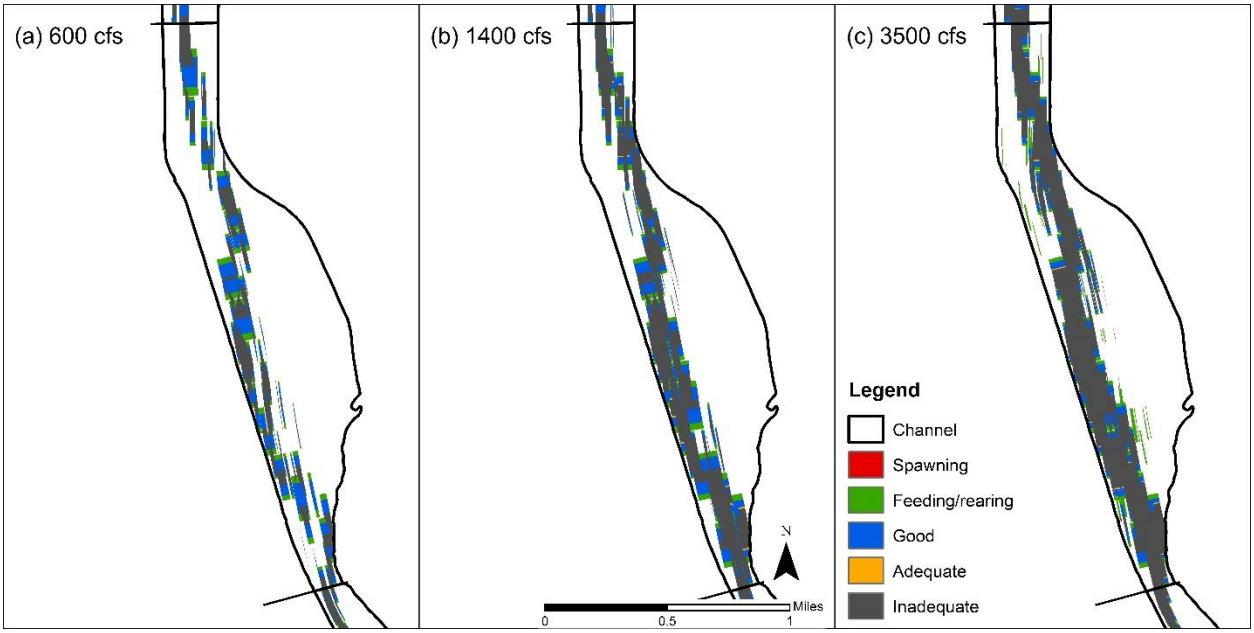
(a) 600 cfs
(b) 1400 cfs
(c) 3500 cfs
N
0
0.5
1
Miles
Legend
Channel
Spawning
Feeding/rearing
Good
Adequate
Inadequate

P3

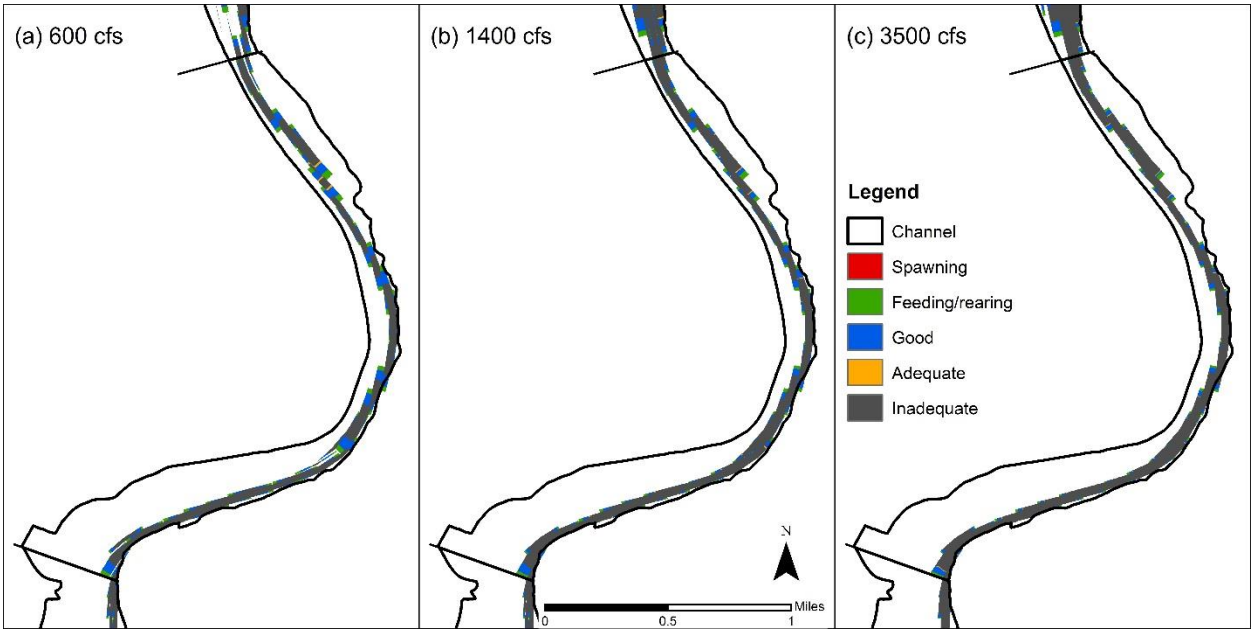
(a) 600 cfs
(b) 1400 cfs
(c) 3500 cfs
Legend
Channel
Spawning
Feeding/rearing
Good
Adequate
Inadequate
N
0
0.5
1
Miles

P4

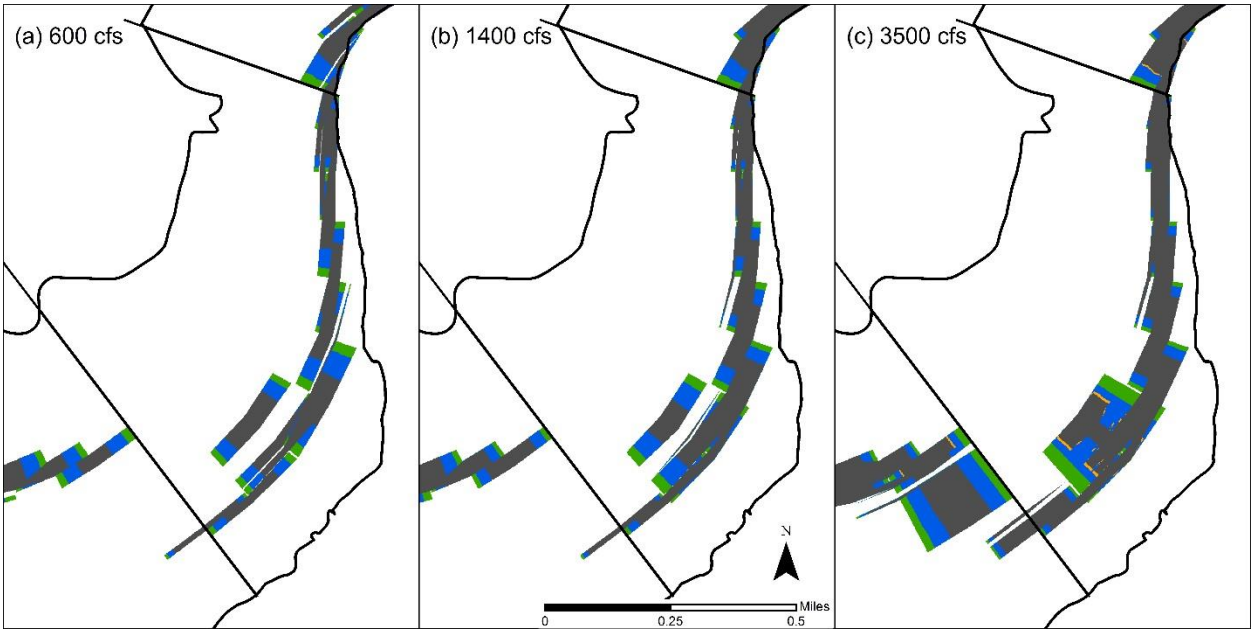
(a) 600 cfs
(b) 1400 cfs
(c) 3500 cfs
N
0
0.25
0.5
Miles

P5

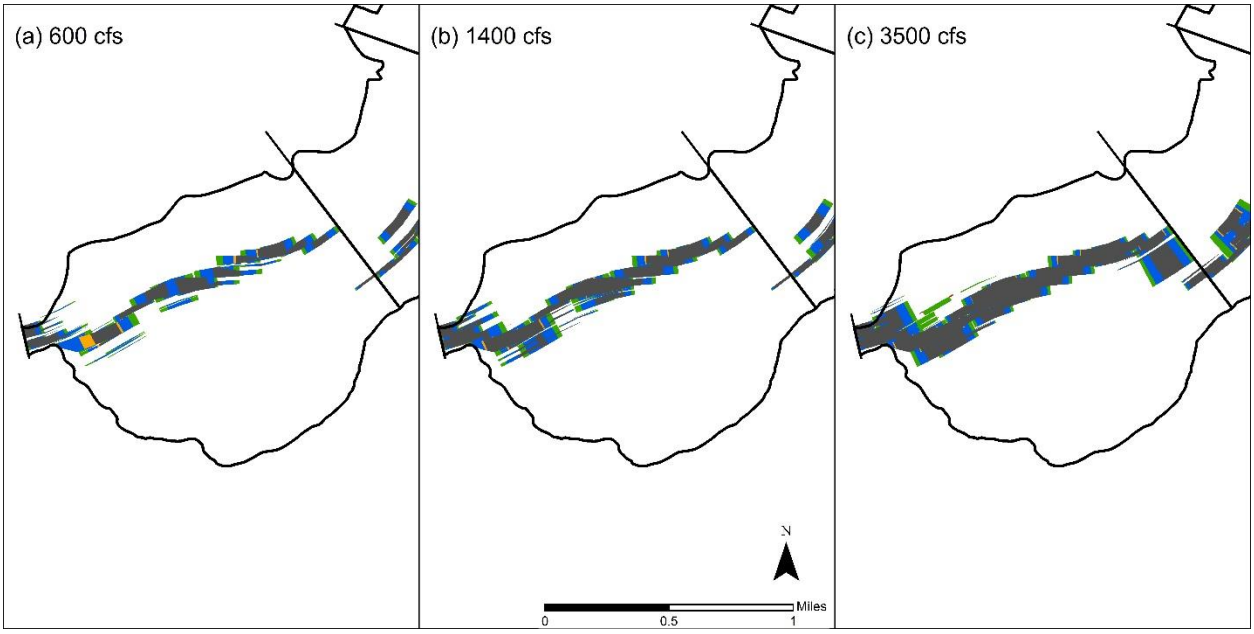
(a) 600 cfs
(b) 1400 cfs
(c) 3500 cfs
N
Miles
0
0.5
1

(b) 2002

P1

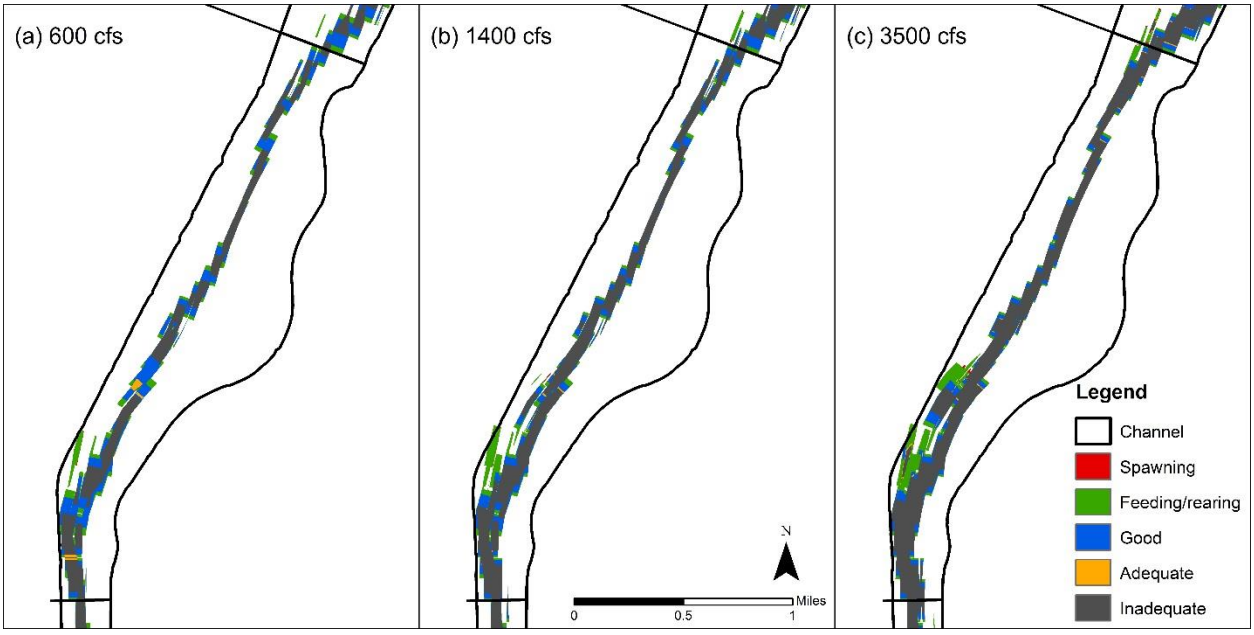
(a) 600 cfs
(b) 1400 cfs
(c) 3500 cfs
N
Miles
0
0.5
1
Legend
Channel
Spawning
Feeding/rearing
Good
Adequate
Inadequate

P2

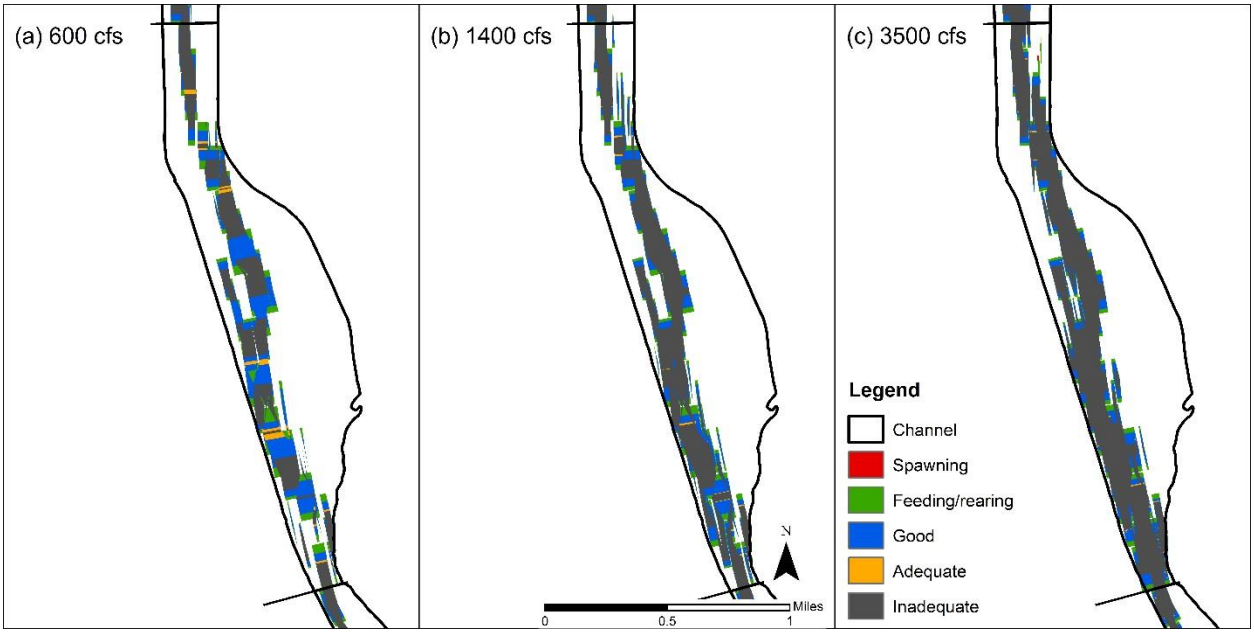
(a) 600 cfs
(b) 1400 cfs
(c) 3500 cfs
Legend
Channel
Spawning
Feeding/rearing
Good
Adequate
Inadequate
N
0
0.5
1
Miles

P3

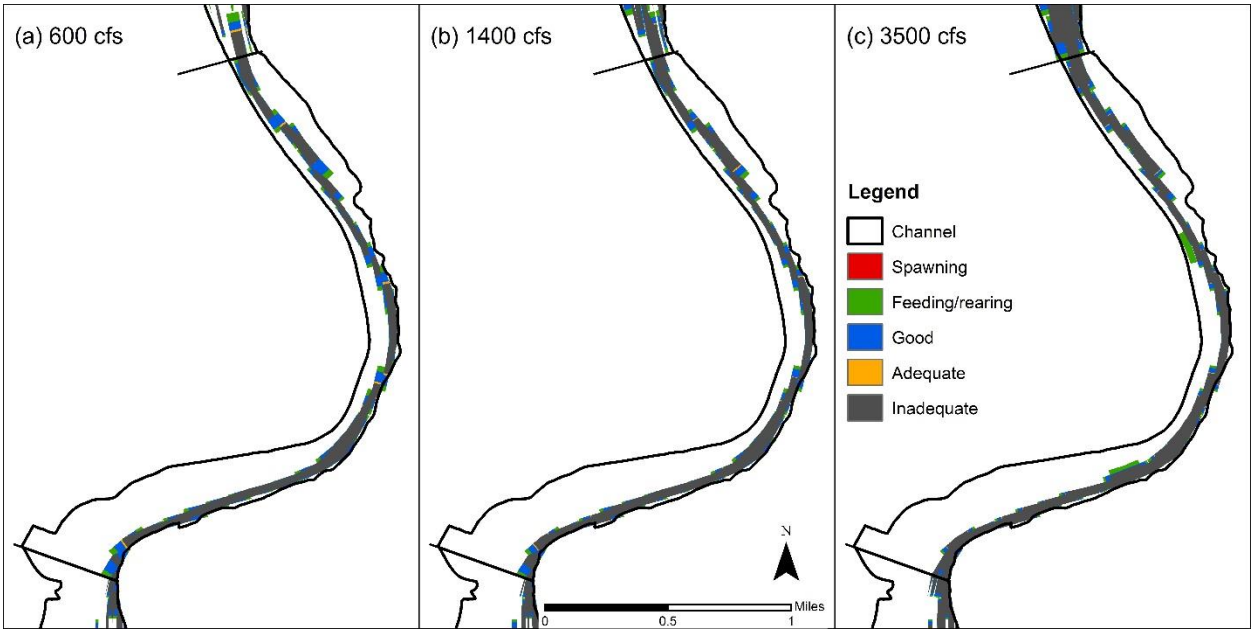
(a) 600 cfs
(b) 1400 cfs
(c) 3500 cfs
Legend
Channel
Spawning
Feeding/rearing
Good
Adequate
Inadequate
N
0
0.5
1
Miles

P4

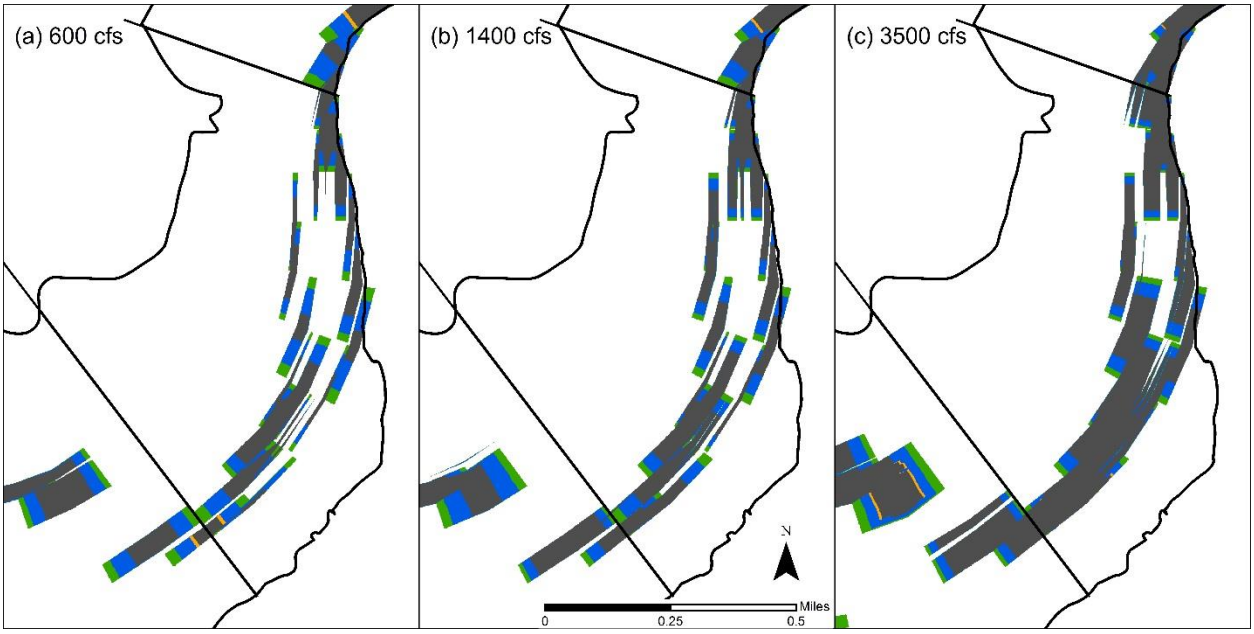
(a) 600 cfs
(b) 1400 cfs
(c) 3500 cfs
N
Miles
0
0.25
0.5

P5

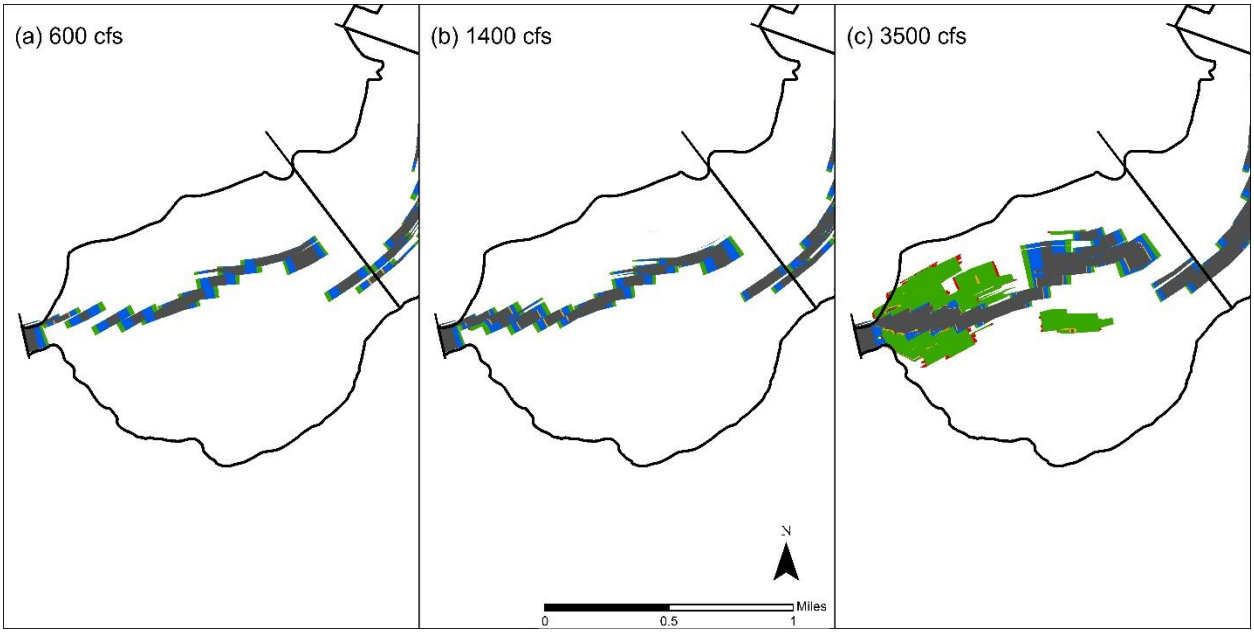
(a) 600 cfs
(b) 1400 cfs
(c) 3500 cfs
N
Miles
0
0.5
1

(c) 2012

P1

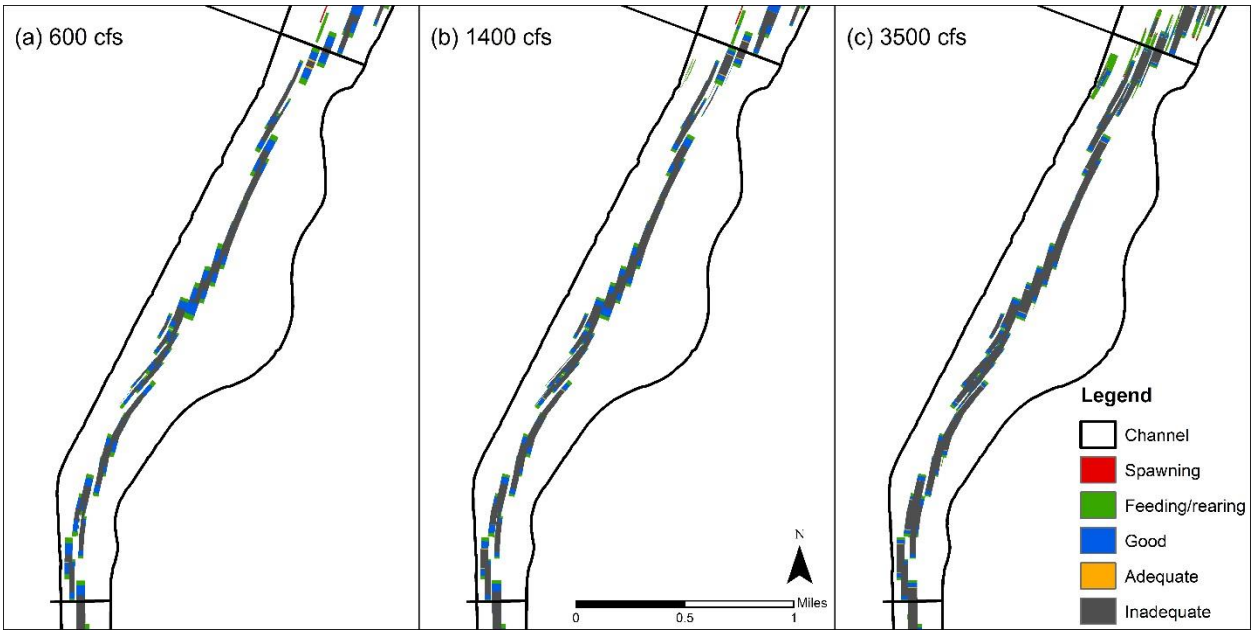
(a) 600 cfs
(b) 1400 cfs
(c) 3500 cfs
N
Miles
0
0.5
1
Legend
Channel
Spawning
Feeding/rearing
Good
Adequate
Inadequate

P2

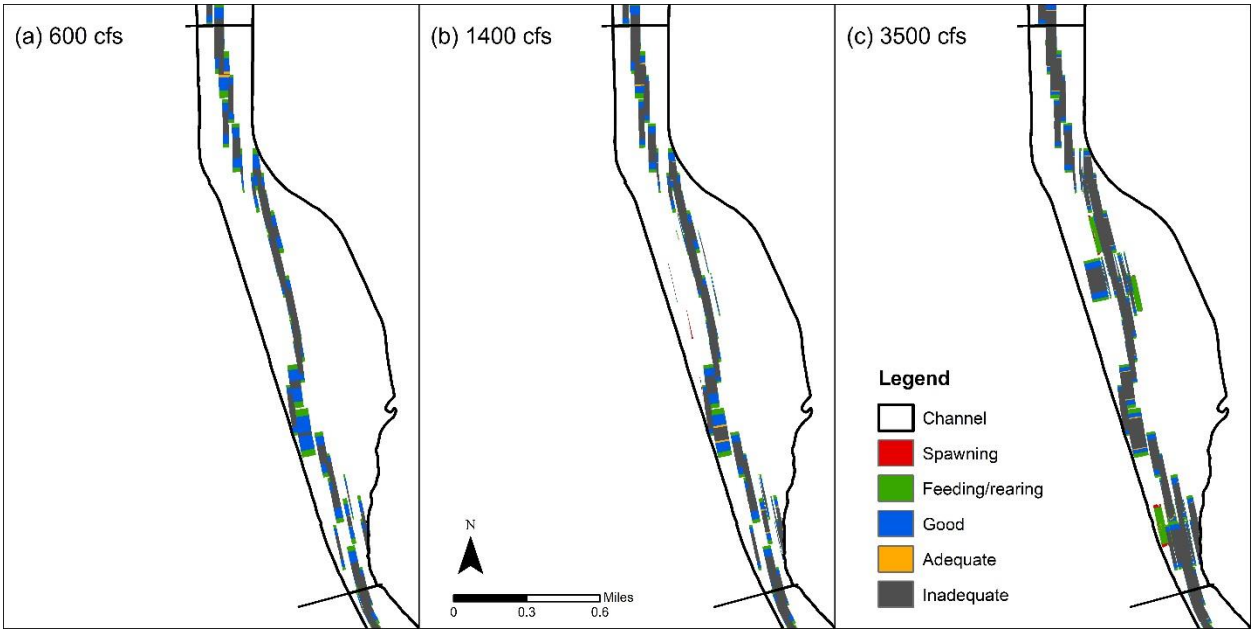
(a) 600 cfs
(b) 1400 cfs
(c) 3500 cfs
N
Miles
0
0.3
0.6
Legend
Channel
Spawning
Feeding/rearing
Good
Adequate
Inadequate

P3

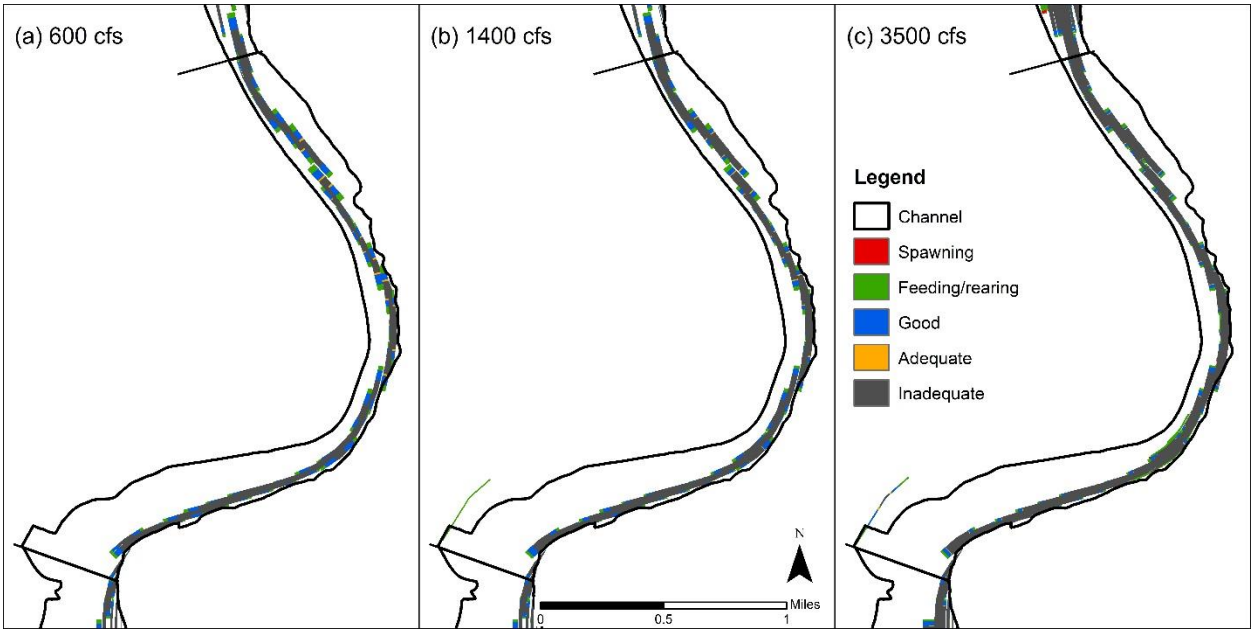
(a) 600 cfs
(b) 1400 cfs
(c) 3500 cfs
Legend
Channel
Spawning
Feeding/rearing
Good
Adequate
Inadequate
N
Miles
0
0.5
1

P4

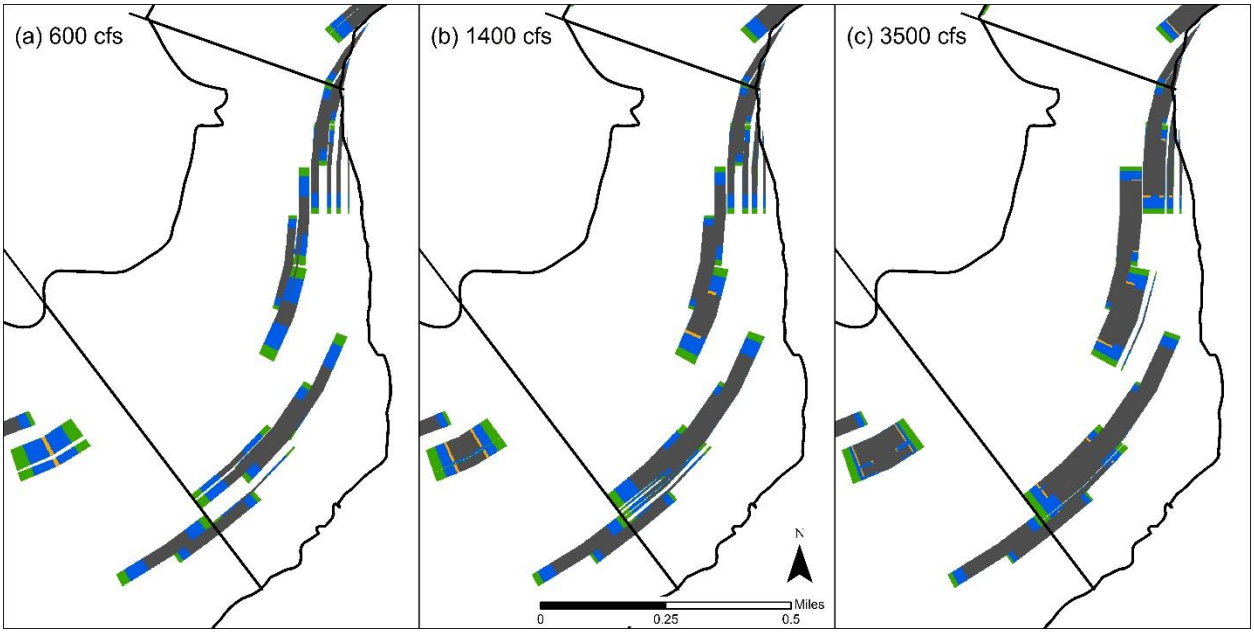
(a) 600 cfs
(b) 1400 cfs
(c) 3500 cfs
N
Miles
0
0.25
0.5

P5

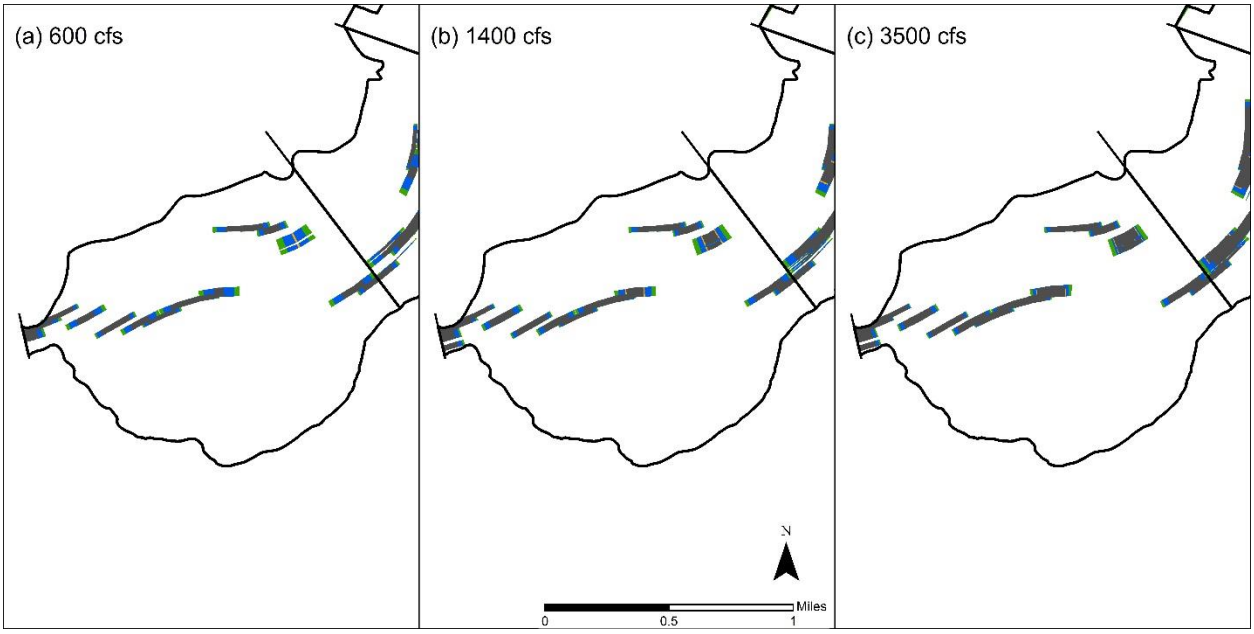

APPENDIX D

Silvery Minnow Habitat Scoring System

Introduction

This section outlines how silvery minnow habitat can be analyzed with GIS from aerial photography. It covers the methods, results and discussion of the findings. The analysis is based on finding what habitat features silvery minnows thrive in, identifying those features in the same reach over different years, and seeing how the habitat changes spatially and temporally. A future goal is to link this analysis to how fish population densities have changed with the habitat.

Methods

Data Use/Aerial Photography

Analyzing orthographic aerial photography over many years can show how silvery minnow habitat has changed over time. Once we know how the habitat is changing and how this is related to fish population, habitat suitability can be improved. A link between habitat and population trends can be determined by looking at population data from population monitoring reports by Dudley and Platania (1997). They have been collecting data on the fish population throughout the Middle Rio Grande since 1993. The aerial photographs listed in Table D-1were used to analyze habitat quality (1992 is also analyzed because it is the closest year to 1993 of aerial photography available):

Table D-1. The year, month and flow corresponding aerial photographs used for this study. Data from Klein et al., 2018a, Swanson et al., 2010 and GIS metadata provided by USBR.

Year	Month	Flow (cfs):
2016	October	40[SA]
2012	January	740[SA]
2008	July	1630[I]
2008	June	4990[I]
2006	January	580[SA]
2005	June	5980[I]
2005	April	4500[I]
2002	February	600[SA]
2001	February	687[A]
1992	February	650[SA]
[I] Isleta gage daily average discharge		
[SA] San Acacia gage daily average discharge		
[A] Albuquerque gage daily average discharge		

The years analyzed are based on availability of data from USBR starting with 1992, so there is not a consistent spacing of years. The uncertainty created by varying image quality is also a limitation of analyzing the photographs. This is a known limitation based on many other studies using aerial photography to map fish habitat quality (Holmes and Hayes 2011; Perschbacher 2011). Other limitations include the flow being variable within the reach and between years, limited amounts of data, the analysis being subjective, limited data aids such as LiDAR and

thermal imagery, and ability to ground truth the data (Holmes and Hayes, 2011; Perschbacher 2011).

An effort can be made to address these limitations. For instance, picking only years that have the same flow can allow the habitat analysis to be compared. 1992, 2001, 2002, 2006, and 2012 all have flows around 650 cfs so these ones are chosen to compare to each other. To keep it as consistent as possible, 2001 is not used because it uses flow data from a different gage than the rest.

Though it would be useful to analyze habitat that meet the needs of different life history stages of silvery minnows, it is not plausible to do a thorough analysis of this with the given set of aerial photography. High flows around the same value across many years would be necessary to see how much the floodplain inundates and how the habitat quality changes over time. Aerial photography analyzed during low and peak flows can still be analyzed because this can give insight into habitat quality spatially and across different flow regimes. Still, the focus must be on analyzing adult silvery minnow habitat in the main channel because that is the available habitat for the comparable photographs at 650 cfs. Though there are a limited amount of photographs to work with, analyzing this low flow of 650 cfs may be very useful because the Middle Rio Grande has experienced lower and less peak flows than it has in the past. This trend is expected to continue, so focusing on lower discharges that don't lead to floodplain inundation may be more a more realistic focus for improving silvery minnow habitat (Drew Baird, personal communication, June 19th, 2018).

To make the analysis as objective as possible, a detailed description of discernable habitat features will be given. This is still a challenge because distinctions between features such as islands, bars, bedforms and shoreline complexity are not always clear. Also, if more LiDAR or thermal imagery data were available that would help as well. Lastly, ground truthing to test the analysis with actually field surveys can be done in the future.

Even with limitations, there are advantages of using remote sensing for habitat analysis. The amount of habitat that can be mapped in a short amount of time can be very useful (Holmes and Hayes 2011; Perschbacher 2011). For this study, it took less than a day to map 50 miles of river habitat. This mapping technique allows a researcher to take a cursory look at a large area and find large-scale trends. Also, this exact type of habitat analysis for this exact reach has not been done before. Therefore, this analysis may yield interesting results (Torres 2007; Klein et al. 2018a).

Criteria Development

The criteria developed is based on literature that discusses physical features of silvery minnow habitat. That criteria from research is then simplified and shortened based on ability to analyze it based quality of aerial photography and practicality. Physical features determined to be important based on literature include: bankline complexity, main channel complexity, side channels, backwater, bars, islands, confluences, and pools. Limited suspended sediment, suitable amounts of vegetation, and a correct range of temperatures are all important aspects

of the functioning ecosystem as well. Lastly, connection to the floodplain is paramount. These components of the river are important because they are representative of suitable silvery minnow habitat that requires low velocities, shallow depths, diverse habitat, silt and sand substrate, and good water quality (Tetra Tech 2014; Cluer and Thorne 2014; Bovee et al. 2008; Bestgen et al. 2003; Dudley and Platania 1997).

Even though all these features are important, only a handful of these can be accurately measured from aerial photography using GIS. These include bankline complexity, main channel complexity, side channels, backwaters, bars, islands, and confluences. Therefore, the habitat requirements that can be physically depicted from aerial are narrowed down to low velocities, shallow depths, and habitat diversity (In this criterion diverse habitat is defined as anything that adds to complexity and diversity of the physical habitat topographically or with features such as debris piles).

There are a few reasons why certain features are not included. For instance, suspended sediment can sometimes be analyzed by looking at the color of the water, yet the aerial photographs vary so much spatially and temporally, it is impossible to analyze visually. Substrate is too hard to analyze because aerial photography from most years is not detailed enough. Also, temperature is something that cannot be seen on the imagery. Isolated pools can be seen from aerial imagery, but it is hard to determine how connected the pools are to the main channel, so they are removed as well. Floodplain connectivity is also almost impossible to determine and quantify just by looking at features from aerial photography. This is mostly due to inundated areas being hard to identify at high flows. There is also not enough aerial photography capturing high flows to compare over time. There are only three data sets of photography that show signs of inundation. When there is inundation, it is identified as shoreline complexity, so floodplain connectivity can be roughly compared in these years.

Vegetation is not included in this list because vegetation is incorporated indirectly through certain habitat features. For instance, vegetation indicates complexity on bars, shorelines, or islands which affects habitat scores. It also affects how wide side channels are, which impacts the habitat area, and the likelihood that a channel gets inundated during high flows. It further adds complexity because vegetation provides shade to regulate temperatures and produces leaf litter. Leaf litter provides nutrients to feed algae and diatoms that in turn feed silvery minnows. Temperature regulation is also very important for the minnow (Tetra Tech 2014; Bovee et al. 2008; Bestgen et al. 2003; Dudley and Platania 1997). Therefore, vegetation density in the active channel is incorporated through other habitat features.

Also, though runs and pools would be useful to identify (Dudley et al. 2016), they are unable to be identified from the set of aerial photography given. Identifying runs and pools have been a focus of other studies identifying habitat features with remote sensing. They were able to do this by using ground truthing to identify where the pools and runs were and use that information to identify the features in aerial photography (Holmes and Hayes 2011;

Perschbacher 2011). Ground truthing was not an option for this study. Using agg/deg cross-sectional data from HEC-RAS to identify pools and runs could be an option as well, but these lines are far apart so the data would not be as accurate.

The following schematic in Figure D-1 shows the main features that were considered for the criteria.

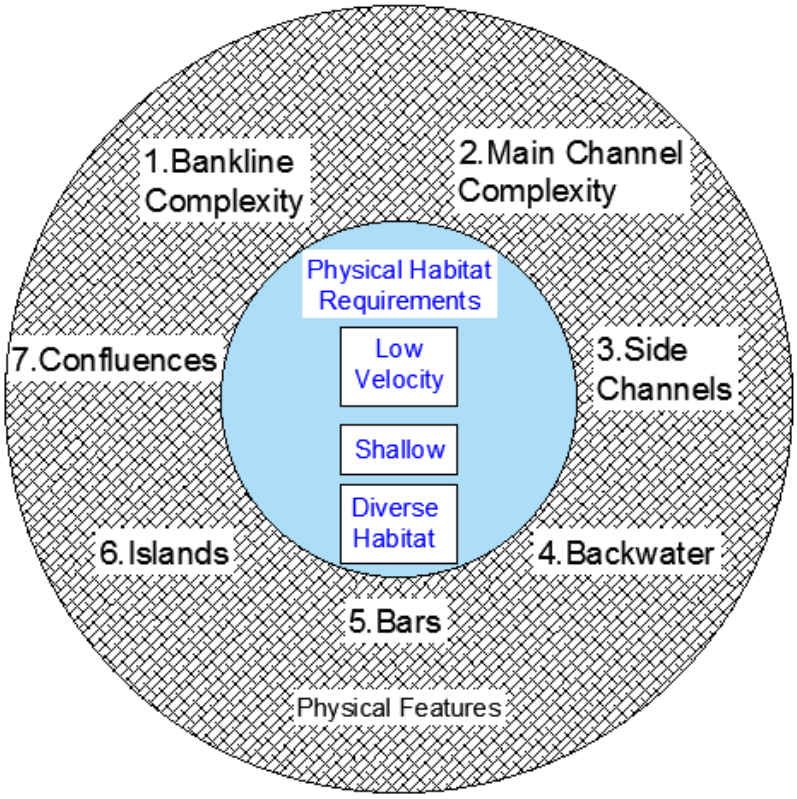

Figure D-1. Physical habitat requirements are listed in the blue inner circle. Physical features that meet these requirements and can be seen from aerial photography are in the outer circle.

Overall, certain physical features that may indicate good quality silvery minnow habitat can be analyzed with GIS from aerial photography. These include features such as backwaters, secondary channels, and debris piles. These components of the river create low velocities, shallow depths and diverse habitats that are crucial for silvery minnow survival. By identifying features in the river, giving those features a score based on habitat suitability, and comparing the scores spatially and across time we can see how the physical habitat is changing.

General guidelines for Scoring and Mapping

Each habitat feature is identified with a point using GIS and identified with a criteria that has a number and letter. The criteria is correlated with a habitat feature (number), subdivided into the quality of that feature (letter), and given a score based on the quality of the habitat. The score is determined from literature review and is outlined in Appendix B. Table D-2 to D-4 outline and briefly describe the criteria, what type of habitat it is and the score it receives. The entire outline of features which pictures and a description of what they are is given in Appendix E.

Table D-2: Habitat type, criteria and scores. Scores range from 1-5 and are further explained in Table.

	Shoreline Complexity			**Main Channel Complexity**		**Side Channels**					**Backwater**		**Bars**			**Islands**						**Confluences**	
Criteria:	1a	1b	1c	2a	2b	3a	3b	3c	3d	3f	4a	4b	5a	5b	5c	6a	6b	6c	6d	6e	6f	7a	7b
Score:	4	3	2	4	3	4	3	2	3	5	5	4	5	2	1	3	2	1	1	4	3	4	3

Table D-3: Brief description of habitat types and scores.

Habitat Description	**Criteria**	**Score**
Complex Shoreline	1a	4
Less Complex Shoreline	1b	3
Less Complex, Less Accessible Shoreline	1c	2
Main Channel Complexity (Large)	2a	4
Main Channel Complexity (Small)	2b	3
Large, Easily Accessible Dry Side Channel	3a	4
Medium, Easily Accessible Dry Side Channel	3b	3
Small, Less Accessible Dry Side Channel	3c	2
Non- Complex Wetted Side Channel	3d	3
Complex Wetted Side Channel	3f	5
Large Backwater	4a	5
Small Backwater	4b	4
Complex Bar	5a	5
Less Complex Bar	5b	2
Simple Unvegetated Bar	5c	1
Large Unvegetated Island	6a	3
Small Unvegetated Island	6c	2
Large Vegetated Island	6b	1
Small Unvegetated Island	6d	1
Large Complex Island	6f	4
Small Complex Island	6e	3
Active Confluence	7a	4
Inactive Confluence	7b	3

Table D-4: Score Criteria. Each category depicts habitat that is beneficial to silvery minnows. 5 provides the most optimum habitat and 1 provides the least amount of benefits.

Score	***Habitat Description***
1	Low chance of becoming inundated, in main channel, small features, and low complexity of topography.
2	Low chance of becoming inundated, in main channel or could be in margins, bigger features than 1 or smaller than 3, and low complexity of topography.
3	Medium chance of becoming inundated, in main channel or near shoreline, bigger features than 2 or smaller than 4, and medium complexity of topography.
4	High likelihood of becoming inundated on side channel, or inundated but not very complex in main channel. Bigger features than 3 or smaller than 5.
5	Areas that are currently inundated with water and form complex flow with shallow areas and low velocities. Tend to be isolated from the main channel. Large features with high topographic complexity.

The amount of points given for a feature is based on agg/deg polygons (area between each line). For instance, if an island spans over two agg/deg polygons it is given two points. The same is done for every feature including side channels. The longer the side channel, the more points it gets because it provides more silvery minnow habitat. Figure D-2a. depicts scoring with islands and channels across agg/deg lines.

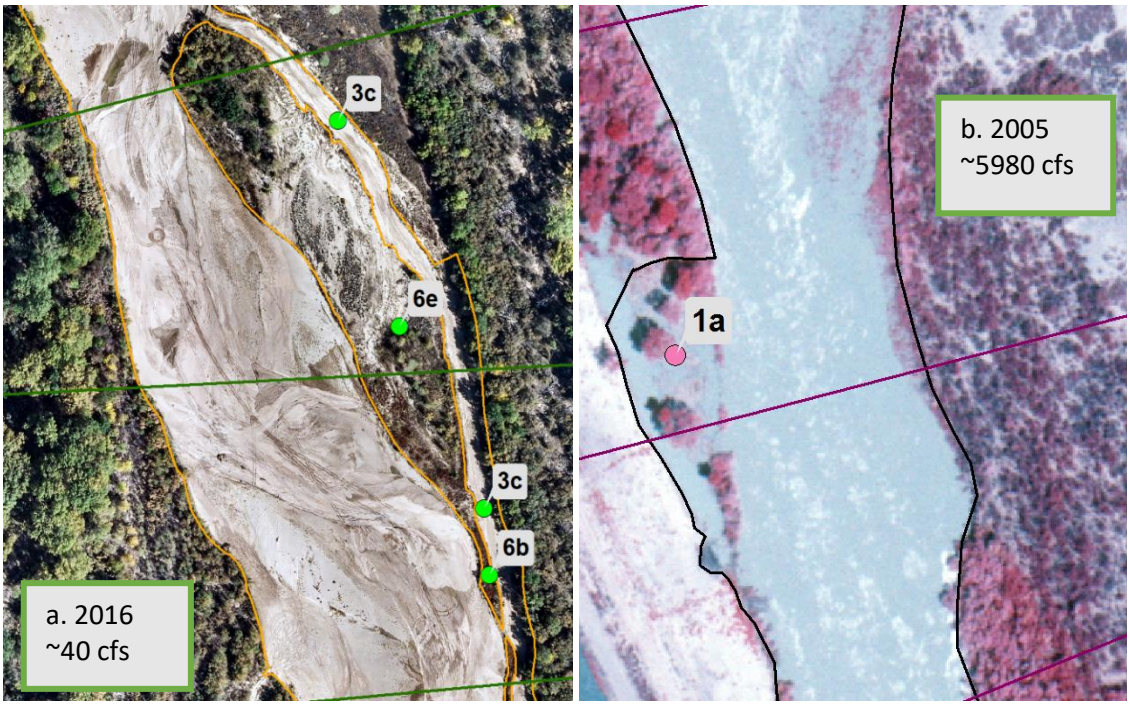

Figure D-2: a. A dry side channel (3c) and islands (6b and 6e) are depicted above in an aerial photograph from 2016. Agg/Deg lines are shown in green lines perpendicular to the main channel. The active channel is outlined in orange. b. 1a depicts shoreline complexity in an aerial photograph from June of 2005. Agg/Deg lines are shown in purple perpendicular to the main channel. The active channel is outlined in black. The flow is going to the bottom of the page for both images.

In Figure D-2a., the channel and the island span over two polygon lengths so they are each given a point in each polygon. The criteria is not exact, but instead an estimate of how many features there are. The criteria is not meant to be exact and map feature areas, but instead depict the amount of features that offer suitable habitat to get a general idea of how change is occurring. In Figure D-2b. 1a is counted once instead of twice in this example. Even though the channel complexity spans over two agg/deg polygons, it only occupies the length of one agg/deg polygon so it is counted once.

For each year, the points are mapped and the scores are assigned. The results are compiled and compared in a few different ways shown in the following sections.

Analysis

Overall Habitat Score

An overall score for each year was calculated as well as a count for how many of each habitat types there were in the Rio Puerco reach. An overall score was calculated by subreach as well.

Subreach Delineation

Each year with available photographs is analyzed. The points are broken up and grouped into subreaches using ArcGIS. Scores given to different habitat types are added up within each subreach and compared across years. Because the subreaches have different areas, the scores are weighted by area by computing the score per ft^2.The score is divided by the area and multiplied by a multiple of 10 that makes the data easy to work with. Below is a sample calculation:

$$Raw\ score\ for\ P1\ in\ 1992: 170$$

$$Area\ for\ P1: 32{,}305{,}506\ ft^2$$

$$Multiple\ of\ 10: 10{,}000{,}000$$

$$Weighted\ score: \frac{170}{32{,}305{,}506 ft^2} * 10{,}000{,}000 = 52.6$$

Also, the number of points in each subreach are counted and grouped into categories such as shoreline complexity, side channels, backwater etc. These scores are weighted as well. The following habitat features are grouped into the associated categories in Table D-5. This is done to reduce the amount of graphs needed to compare how the habitat changes over time. When the habitat types are quite similar and mainly vary by size instead of quality, they were grouped.

Table D-5: Habitat types grouped into broader categories.

Complex Shoreline	1a, 1b, 1c
Main Channel Complexity	2a, 2b
Easily Accessible Dry Side Channels	3a, 3b
Less Accessible Dry Side Channels	3c
Non-Complex Wetted Side Channel	3d
Complex Wetted Side Channel	3f
Backwater	4a, 4b
Complex Bars	5a
Simple Bars	5b, 5c
Unvegetated Islands	6a, 6c
Vegetated Islands	6b, 6d
Complex Islands	6f, 6e
Active Confluence	7a
Inactive Confluence	7b

Agg/Deg Line Delineation

Using ArcGIS, the points were broken up and grouped into agg/deg polygons divided by each agg/deg line. Each polygon was given one value. This value is the summation of the criteria score given to the points based on the type of habitat outlined in the precious section. The polygon was given a color based on its value. The colors in agg/deg polygons were visualized in the six subreaches using ArcGIS.

Results

Overall Habitat Score

Table D-6 below summarizes the analysis. Overall, 2016 had the highest score and 2006 and July of 2008 had the lowest score. The rest of the scores only vary by a couple hundred points so the differences are somewhat negligible. Out of the comparable years, 1992 has the highest score by over 100 points and 2002 is the next highest. 2002, 2006 and 2012 still all have very similar scores.

2016 has the highest amount of all types of habitat features with a few exceptions. June of 2005 has the most complex bars, April of 2005 has the most complex islands, and 1992 has the most confluences.

Table D-6: Summary of total habitat score, flows, and number of habitat types for each year. The comparable years are highlighted in blue.

				Shoreline Complexity			Main Channel Complexity		Side Channels					Backwater		Bars			Islands						Confluences	
Year	Month	Total Habitat Score	Flow (cfs)	1a	1b	1c	2a	2b	3a	3b	3c	3d	3f	4a	4b	5a	5b	5c	6a	6b	6c	6d	6e	6f	7a	7b
1992	February	596	650[SA]	9	2	1	10	10	0	6	6	18	18	1	0	18	20	20	0	7	0	2	14	18	0	9
2001	February	422	687[A]	5	3	0	14	9	2	8	0	5	5	0	0	12	13	19	4	3	8	0	15	7	2	6
2002	February	481	600[SA]	3	1	0	14	7	0	2	0	21	13	0	0	7	23	11	5	0	7	2	20	0	0	0
2005	April	623	4500[I]	15	5	1	13	11	0	0	0	21	14	9	0	20	9	4	1	2	2	2	26	7	4	3
2005	June	479	5980[I]	3	3	2	0	3	0	1	0	13	10	0	0	43	3	1	0	0	1	7	22	5	2	4
2006	January	415	580[SA]	4	15	0	4	12	1	9	4	13	4	1	0	0	32	15	0	3	2	1	17	8	1	5
2008	June	488	4990[I]	14	1	0	7	3	0	4	0	20	5	3	1	27	9	1	2	5	0	6	16	6	0	6
2008	July	415	1630[I]	5	9	3	6	4	0	4	5	21	10	2	3	5	9	2	1	14	5	7	12	4	0	7
2012	January	429	740[SA]	8	8	0	2	6	1	22	5	16	4	1	0	5	14	20	2	5	10	3	7	16	1	4
2016	October	2430	40[SA]	59	54	49	82	80	2	74	17	30	54	16	12	14	47	140	12	54	19	37	17	12	0	2

Note: Flows at different gages are given the follow subcripts: [I] Isleta gage daily average discharge, [SA] San Acacia gage daily average discharge, [A] Albuquerque gage daily average discharge

Subreach Delineation

Table D-7 shows that P4 has the highest score followed by P2. P5 has the lowest score. The total scores for the four years with photographs taken around 650 cfs are compared in Figure D-3.

Table D-7: Total weighted score by subreach. Summation of all years combined.

Subreach	Score
P1	421
P2	938
P3	831
P4	1209
P5	294

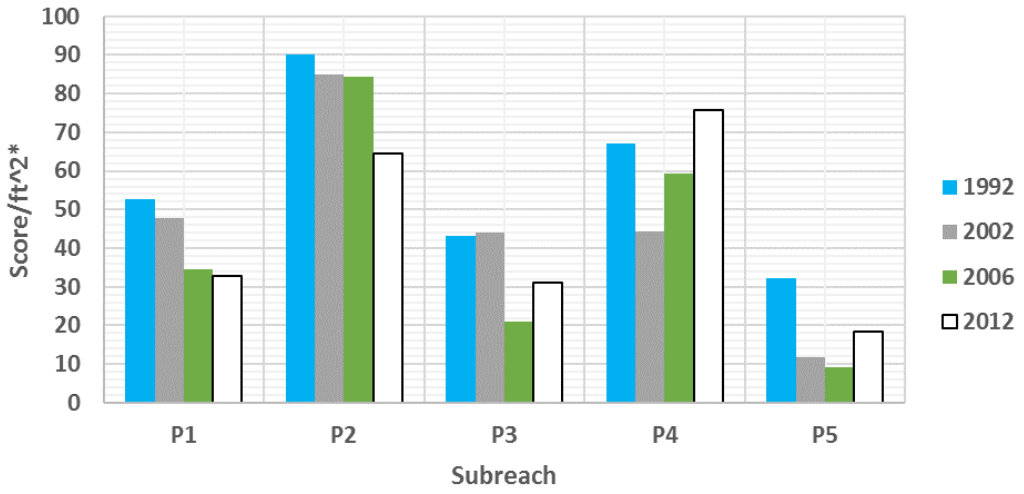

Figure D-3: The column graph shows the overall habitat scores in each of the four comparable years in each subreach.

Subreach P2 has overall highest scores for 1992, 2002, and 2006 and P4 has the highest score in 2012. P5 contains the lowest scores of each of the years. The scores in 2006 and 2012 generally tend to be lower than those in 1992 and 2002, but there is not a dramatic change over the years. 1992 has the top score in P1, P2 and P5 and second top score in P3 and P4.

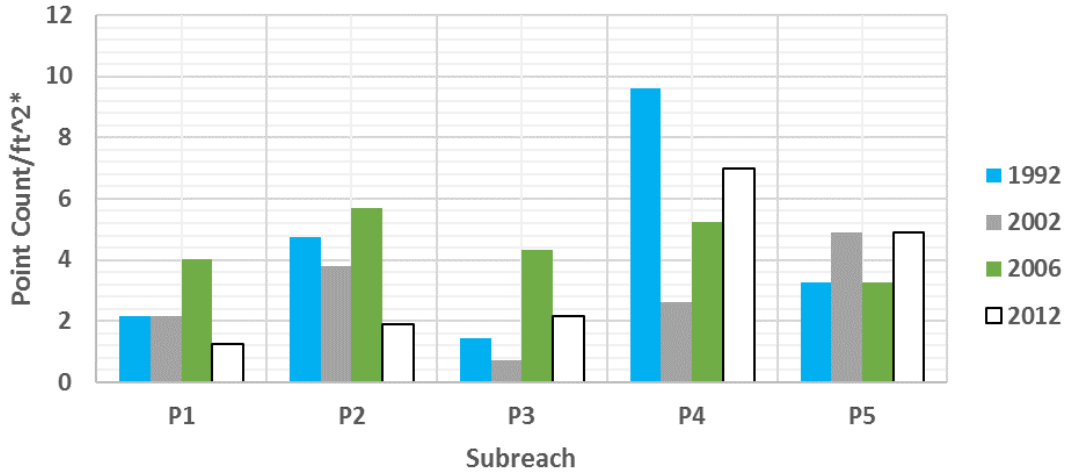

Figure D-4: The column graph shows the amount of simple bars in each of the four comparable years in each subreach.

Over time, the simple bars do not show a trend favoring any year's score. From P1-P3 2006 has the highest score, then in P4 1992 is highest, and in P5 2002 and 2015 are tied for the highest score. Looking at similar graphs like this one that are listed in Appendix E, there are other trends that can be analyzed. For instance, complex islands and complex bars have generally decreased over time. Easily accessible dry side channels and less accessible dry channel have increased over time. The rest of the parameters don't show consistent enough patterns to draw conclusions from.

The overall scores comparing all years are shown in Figure D-5.

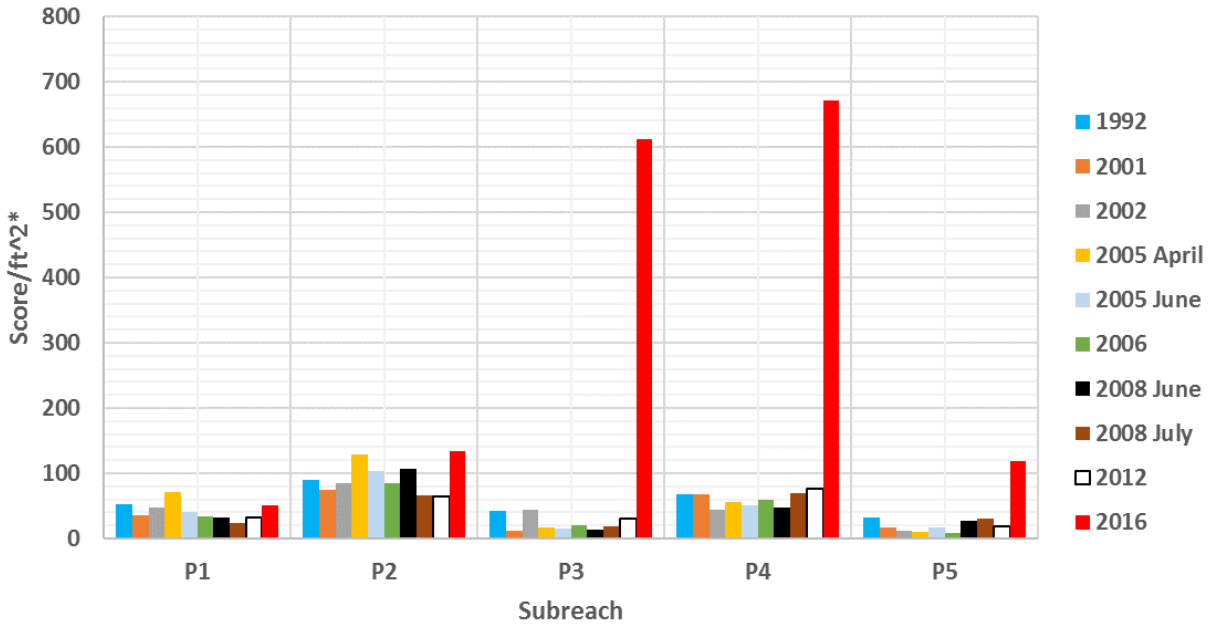

*Figure D-5: The column graph shows the overall score in each of the four comparable years in each subreach. *Score/ft^2 is the score weighted for area of the subreach as discussed in section 0.*

Year 2016 has major peaks in P3-P5 subreaches. These are areas have adequate flow because of the Rio Puerco confluence. Just upstream of the Rio Puerco reach the flow is closer to zero. The 40 cfs is based off of the San Acacia dam just downstream of this reach.

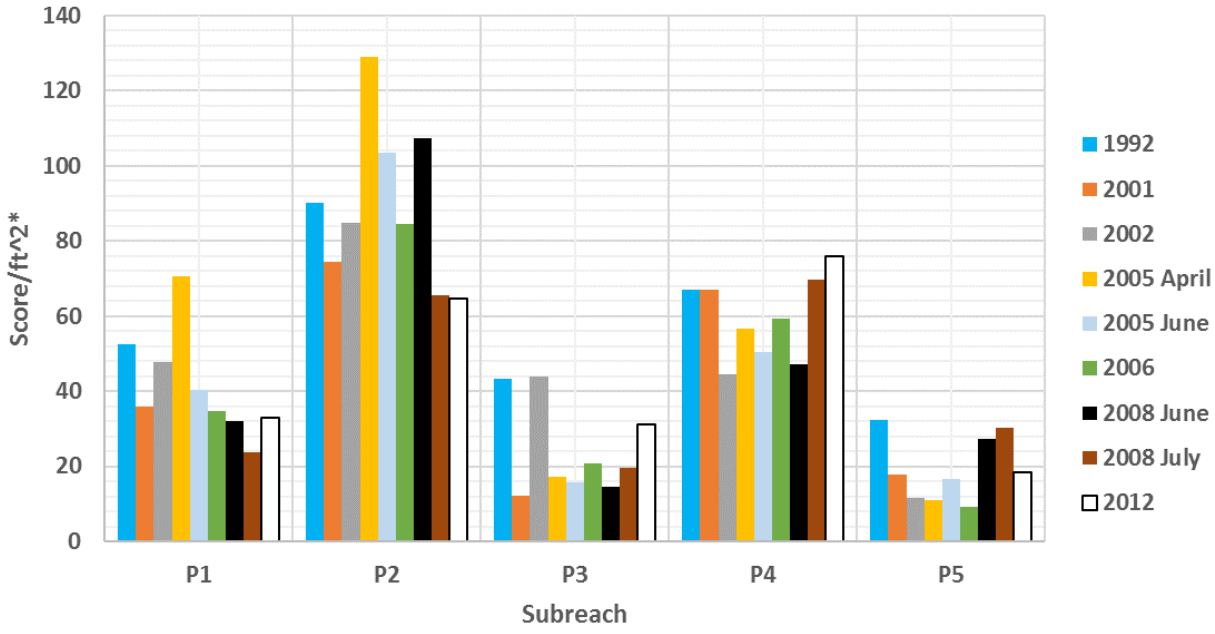

Figure D-6: The column graph shows the overall score without 2016 in every year in each subreach.

When taking 2016 out of the graph it is easier to compare the other years. The highest scores in the subreaches in Figure tend to occur most consistently in 1992. April of 2005 and June of 2008 have some high peaks, but are not consistently high. All other years and flows vary and are middle of the range of high and low point counts/ft^2. Comparing the different habitat types of all years does not prove very useful, because there are too many variables to find any trends.

Agg/Deg Line Delineation

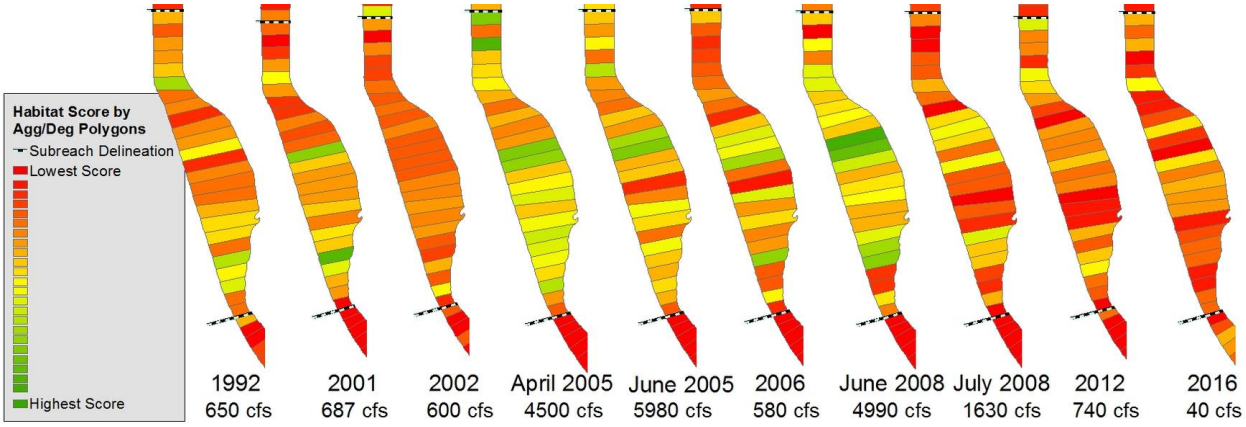

Figure D-7: Subreach P2 summation of habitat scores indicated by the color scheme in the legend and separated by agg/deg lines. Green represents the highest scores, red is the lowest score, and yellow falls in the middle range of scores in the spectrum.

In Figure D-7, green represents the highest scores, red is the lowest score, and yellow falls in the middle range of scores on the spectrum as shown in Figure D-7. The years with the highest scores are in June of 2008 and April 2005 in subreach P2 based on color of the bands. They have the highest proportion of green polygons and the darkest green polygons. 2016, 2012, July of 2008 and 2002 have the lowest scores overall with the highest proportion of red, orange and yellow bands. The rest of the subreaches for the Isleta reach are in Appendix E.

The lowest scored subreach is P3 because all years had the most amount of red polygons. There is not a noticeable difference between all the other subreaches. The rest of the subreaches vary in habitat quality over the years. For instance, 2002, 2006, July of 2008, and 2012 have higher proportions of red polygons. Also, 1992, April and June of 2005, June of 2008, and 2016 tend to have more green polygons in their subreaches.

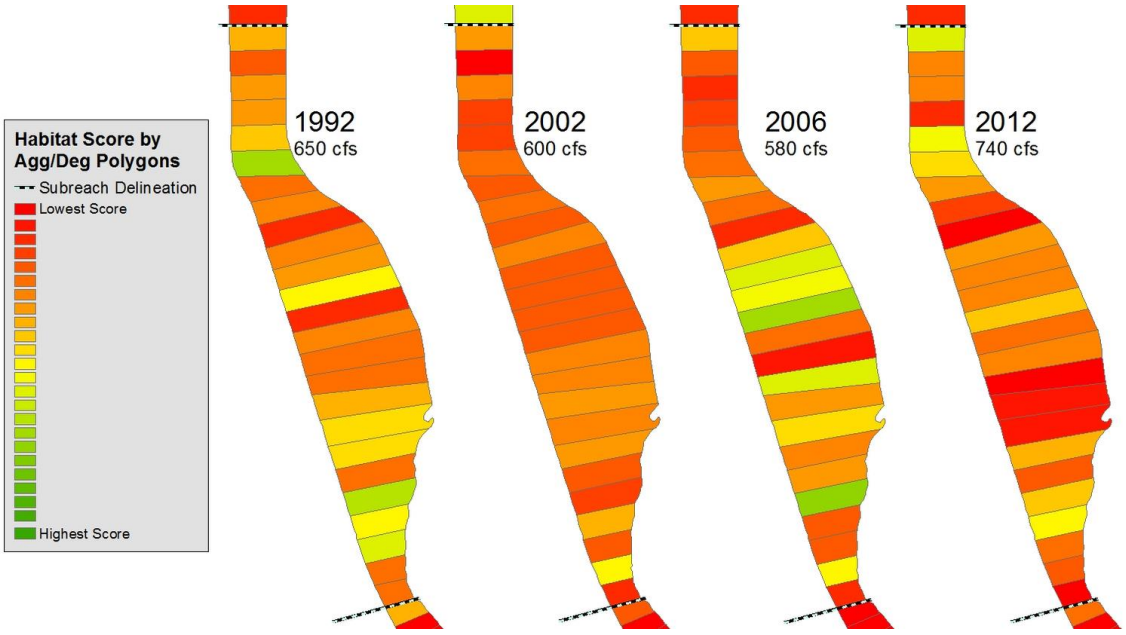

Figure D-8: Subreach P2 summation of habitat scores indicated by the color scheme in the legend and separated by agg/deg lines. Only years around 650 cfs are shown. 2001 is excluded because location of the gage is far away from this study site, so this information is not as accurate.

In Figure D-8, looking at just the four comparable years, 1992 and 2006 appear to have higher scores in this subreach compared to 2002 and 2012. Subreaches P1 and P3-P5 are in appendix F. There is not a consistent trend when comparing these four years over the whole reach. By taking a cursory look at how many green polygons appear in each subreach in each year, the order of higher to lower quality habitat can be estimated. 1992 has the most amount of green polygons, then 2006 and 2012 are very similar and 2002 has the lowest scores. Again, P3 is consistently populated by just red polygons throughout the years.

Discussion

The overall habitat score, subreach delineation scores, and agg/deg line delineation figures generally share the same results. Looking at the comparable years, 1992 and 2002 have better habitat than 2006 and 2012. This makes sense because habitat quality for silvery minnows in the Middle Rio Grande has been decreasing over time (Scurlock 1998; Bovee et al. 2008; Tetra Tech 2014). For subreaches, P2 has the best in-channel habitat when comparing these years. P2 may have the highest score because it is more braided and less sinuous than other subreaches, or it may be due to local changes in that subreach that were not analyzed in this report.

When comparing all the years, 2016 consistently has the highest scores. June and April of 2005, June of 2008, and 1992 also have high scores. 2006, July of 2008 and 2012 generally have the lowest scores.

June of 2005 has a couple of the highest peaks mostly likely because of its high flow. By looking at the aerial photography, it is evident that the floodplain is inundated. This is further

supported by the fact that significant floodplain inundation begins at 5000 cfs in the Rio Puerco reach (Tetra Tech 2014) and the aerial photographs in this year are taken when the flow was 5980 cfs. Floodplain inundation is extremely important for the survival of silvery minnows, especially during their spawning stages (Dudley and Platantia 1997; Bovee et al. 2008; Tetra Tech 2014; Klein et al. 2018a). Also, it has been shown that "prolonged high flows during spring were most predictive of increased density" (Dudley et al. 2016). It is also interesting to note that there are no other photographs that captured a flow above 5000 cfs which may be why the other scores are not as high as June in 2005. April of 2005 also has a flow that causes a small amount of inundation which would explain why it has higher habitat scores.

The scores may be low in July of 2008 due to the flow of 1630 cfs. This flow is suboptimum for silvery minnow as suggested by a study done on silvery minnow by Bovee et al. (2008). The study was done in 2008 in a few small reaches (1-2 km each) downstream of the Rio Puerco and upstream of the San Acacia Diversion dam. They mapped out adult and juvenile hydraulic habitat in the study areas at flows up to 1000 cfs. Looking at connectivity, woody debris, depths and velocities, they found that habitat areas were reduced when flows exceeded 150 cfs mainly because of flow depth and velocity as shown in Figure. In stream habitat such as connectivity and woody debris decreased over time as well for flows exceeding 150 cfs (Bovee et al. 2008).

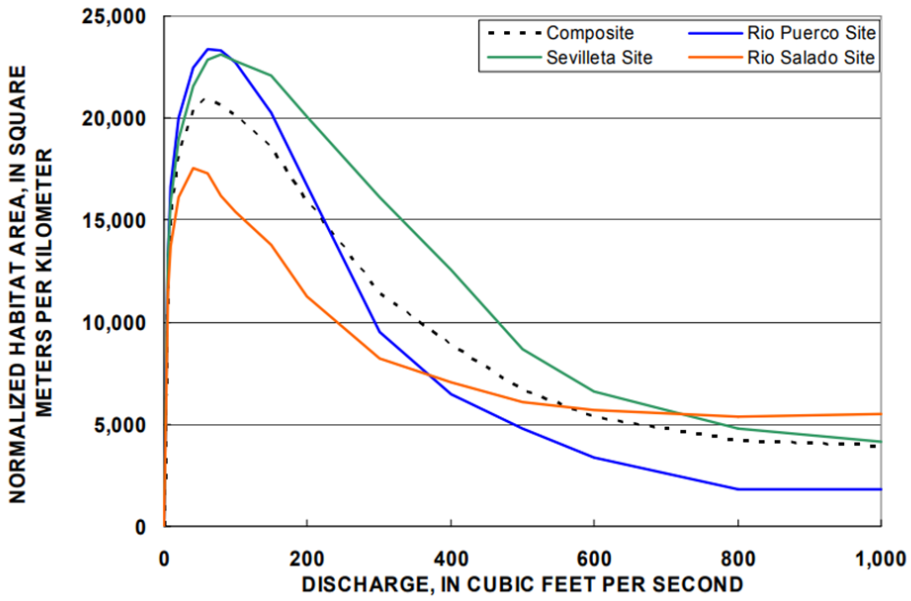

Figure D-9: Habitat area for silvery minnows (H. amarus) from Bovee et al. (2008).

This study also suggests why the 2016 score is so high for this reach. Figure D-9 shows that the habitat is very high at lower flows. In 2016, the flow is at 40 cfs, so the habitat area should be high based on Bovee et al. (2008). The habitat score developed for this report may be high because the flow uncovers many features cause them to appear very complex, thus giving it a

high score. It uncovers bars, islands, bedforms, debris piles and increased the shoreline complexity with such a low flow. Though the low flows create adequate complexity, velocities and depths for silvery minnow spawning and rearing in theory, low flow conditions do not create the appropriate spawning environment. Unless spawning is triggered by high flows that connect to the floodplain, silvery minnows' eggs and juveniles do not tend to survive. Exactly how spawning is trigged and what exactly allow eggs and juveniles to survive is still unknown (Rob Dudley and Steven Platania, personal communication, September 13th, 2018).

Though low flows provide habitat that fits numerically into spawning, rearing and feeding, they are not likely to be areas where silvery minnows will spawn and feed. This may be because these areas are not continuous like floodplains and they could likely get swept away from drifting into close-by faster waters. Low flows can also be correlated with very turbid water, which limits primary productivity so silvery minnow have less to feed on. Also, if food does form, and a higher flow occurs in the main channel, it has a higher propensity of the food being washed downstream than if the food were in the floodplain. Still the minimum flow to stimulate a spawning event remains unknown, although it is probably greater than 1500 cfs. In-channel spawning does occur, but it does not provide an area for egg/larval retention that the floodplain can (Tetra Tech 2014).

By overall years, subreach P4 has the highest score and P5 has the lowest. This may be due to locations relative to the San Acacia Dam and how that affects the hydraulic parameters. P5 is closer to the dam, which has a higher the velocity, energy slope, bed slope, and depth. Also, the wetted perimeter and width decrease as shown in Figure 37. These parameters don't create a high quality habitat for silvery minnows. P4 on the other hand is just downstream of the Rio Salado, which could impact the habitat quality because of the sediment supply. Also, confluences tend to be hotspots for biodiversity (Cluer and Thorne 2013).

Complex islands and bars decreasing could mean that overall, the channel is becoming less braided. Dry side channels are also becoming more abundant, meaning the main channel is becoming more incised and the side channels could be less accessible.

APPENDIX E

In Depth Habitat Criteria

Bankline complexity:

Bankline complexity criteria

1a. Bankline juts out greatly, forms a small inlet, is rocky or has diverse substrate (vegetated islands, sandy banks and water inundating some parts of the bank). Provides a great amount of habitat, potentially causes eddies.	
1b. Bankline juts out or caves in slightly and is somewhat diverse. Provides some amount of habitat.	
1c. Possible access to more complex shoreline during higher flows (outside of active channel so it is less accessible)	

Bankline complexity scores

	Shoreline Complexity		
Criteria	1a	1b	1c
Score	4	3	2

Complex margins, or shorelines, are very important for silvery minnow habitat because they cause lower velocities, eddies, and shallower waters (Bovee et al. 2008). 1a has the most complex shoreline with inlets, channels that cause eddies, lower velocities, and diverse water levels. This is not classified as backwater because backwater has a more definite channel away from the main flow. Backwater is also more isolated from the main channel, so it would have

lower velocities and would score higher than 1a. 1b offers a refuge, yet it is a simple inlet and the area of complexity is not as large as 1a, so it counts for less habitat points than 1a. 1c is even less diverse and gets the lowest score for bankline complexity. It has the potential to become inundated and provide habitat, but is less accessible than bankline in the active channel. Most banklines analyzed have an active channel outline (provided by USBR) that matches with the water surface. In 2016 though, the water surface is much lower than the active channel so channel complexity is based on the active channel outline instead of the water surface.

Main Channel Complexity:

The clarity and quality of aerial photographs varies across years, within the reaches, and between different flow conditions. This makes it hard to analyze small features of the habitat criteria across the years of photographs provided. For instance, debris piles and bedforms can only be distinguished in highest quality photographs from 2016. The figure below shows the difference in quality of the photographs.

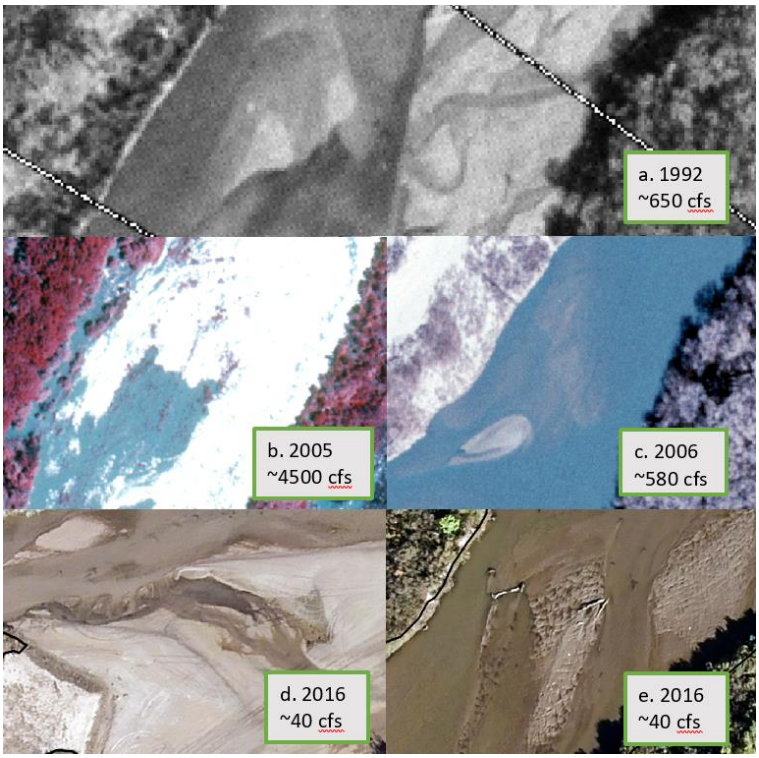

A set of aerial photography that shows the differences in close up quality. The zoom in each picture is as follows: a. 1:1000, b. 1:1500, c. 1:800, d. 1:600, e. 1:500). 1992 zoomed away by twice as much as 2016 gives a much more pixilated image than in 2016. 2016 has much better resolution even compared to 2006 (and 2008 which is not depicted here). 2005 has areas where light is reflecting off the water that makes it difficult to see what is happening in the channel. It also depicts the variability of flows and how that affects what is seen.

Therefore, lumping together features that require close up analysis that create main channel complexity is necessary. These features include bedforms, low flow complexity, substrate or formations causing shallow waters, and debris piles.

All of these images vary by a great amount, but they all depict low flow features that are diverse so they could all be identified as the same criteria (2a). Counting these smaller features together does not change the overall score very much because they all serve similar purposes of creating complex flow, eddies, and shallower waters. For example, in 2016 (2d.) more of the river is exposed, so it appears much more complex at a low flow. 2e. is in a higher flow area, yet has debris piles and beforms that cause ripples which could be suitable as well. In the bottom left corner of 2b. and center of 2c. images, bedforms or low geologic features could be the result of what is seen. These look like shallow and physically diverse areas, so they receive a high suitability score as well. In 1992, the complexity is hard to see at a small scale, but shallow areas with various geomorphic features can still be identified.

Main channel complexity criteria

2a. Large debris piles/low-flow complexity in the main channel (possibly braided). Large substrate/ formations create shallow depths	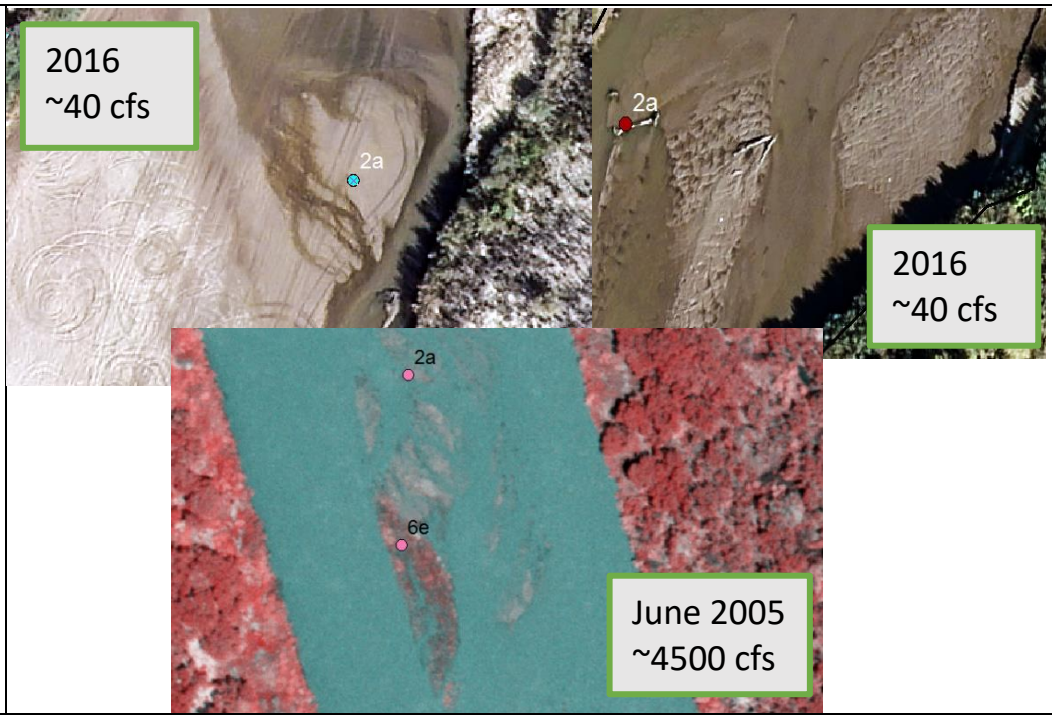

2b. Small to Medium sized debris piles/low-flow complexity in main channel. Medium substrate/ formations create shallow depths	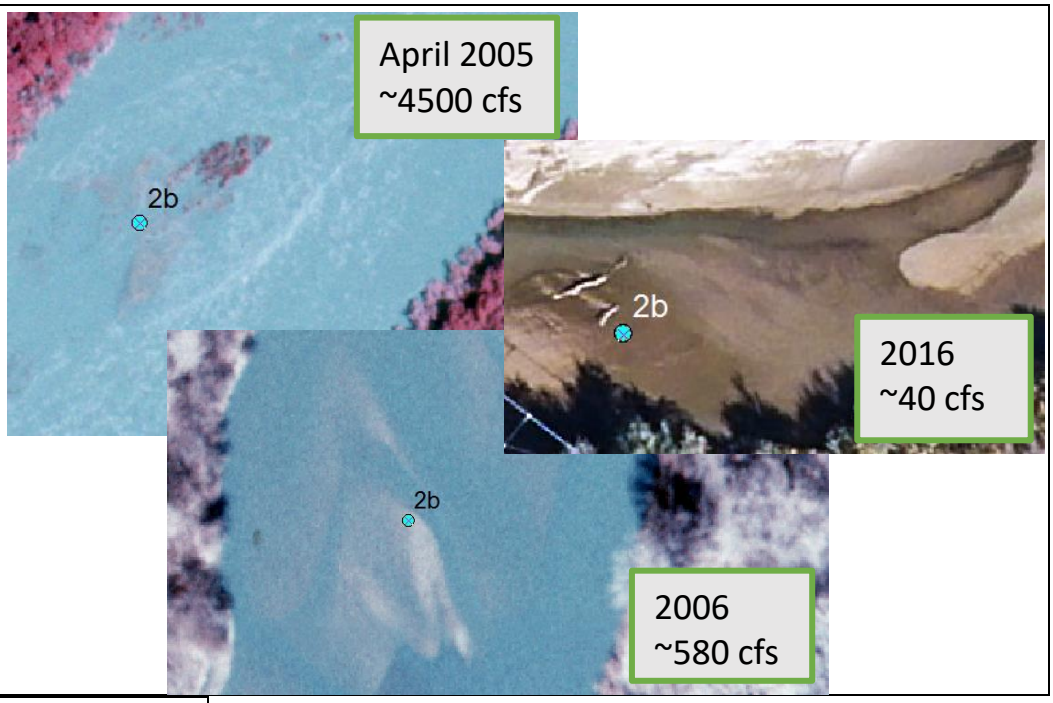

	Main Channel Complexity	
Criteria	2a	2b
Score	4	3

Main channel complexity scores

In-channel complexity, extensive debris piles, bedforms and formations are depicted in above. Bedforms, channel complexity and debris piles all offer suitable habitat for fish (Bovee et al., 2008, Cluer, Thorne 2013, Tetra Tech, 2014). Therefore, main-channel complexity scores are relatively height. In 2b, there are images of debris piles and substrate formations that are less extensive as those depicted in 2a figures. Because both 2a and 2b are in the main channel that experiences higher velocities, the scores are not as high as backwater or complex side channels. They are still high because they offer refuge to silvery minnows when side channels or backwaters are not accessible at high flows. 2a is given one more point that 2b because it is bigger and generally more complex than 2b.

*Note: 2a is differentiated from an island or mid channel bar based on level of inundation. If the island is underwater so much that it is broken up into too many formations to count, or there is not an obvious continuous stretch of land, it is counted as substrate/formations.

Side channels:

Side channels criteria

3a. Dry bed- 3+ parallel side channels are in active channel. Channels appear accessible and wide	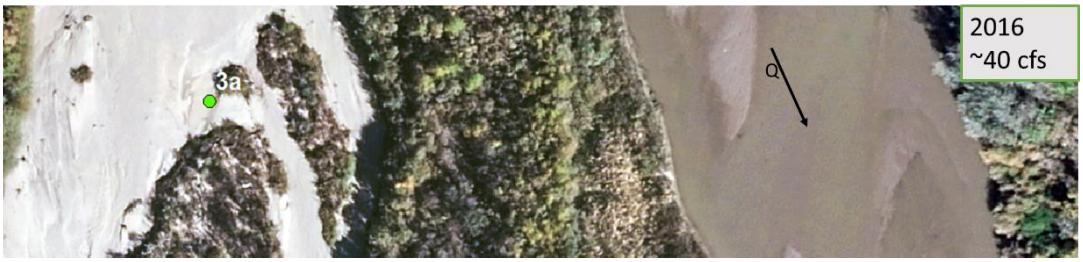
3b. Dry bed- 1-2 side channels are in active channel and appear accessible- wide (50 + feet)	
3c. Dry bed- 1-2 side channels are in active channel and appear accessible- narrow or not as accessible	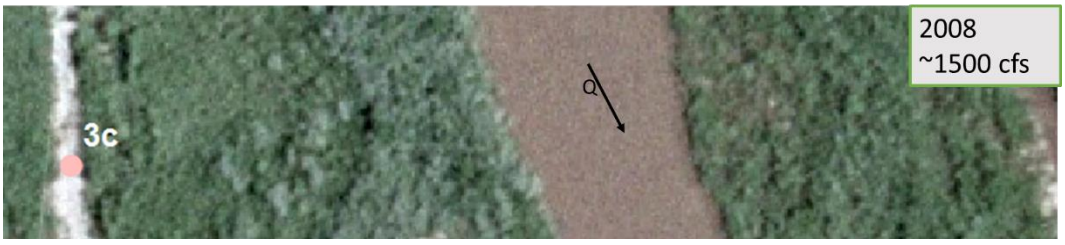

3d. Wet channel- simple and generally not braided- single threaded channel	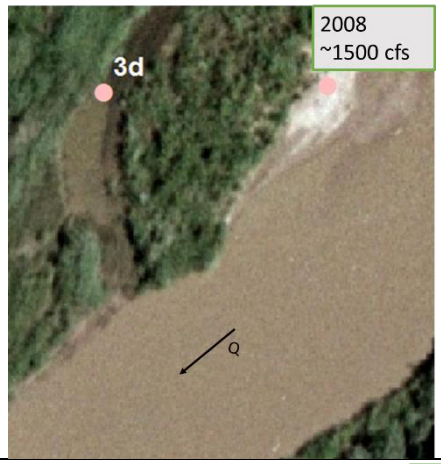
3f. Wet channel- Side channels are complex and winding (may cause eddies and slower flows). 2+ channels- braided	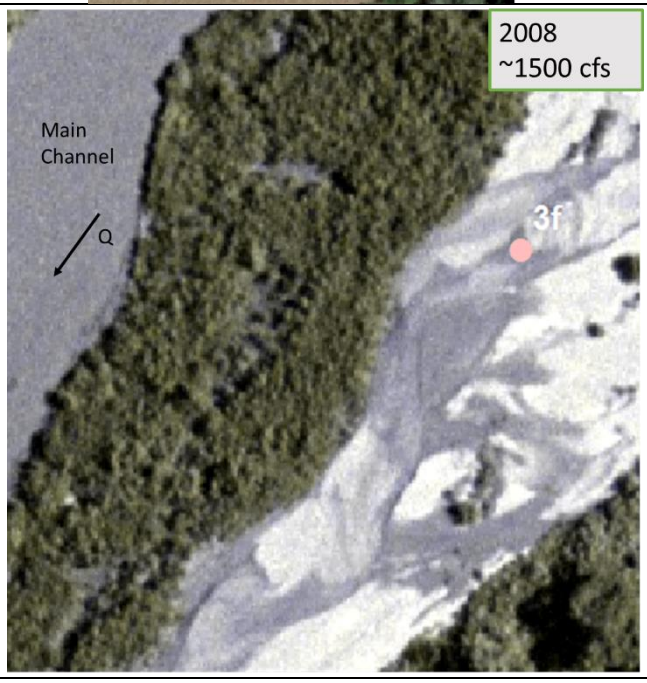

Side channels score

	Side Channels				
Criteria	3a	3b	3c	3d	3f
Score	4	3	2	3	5

A report by Tetra Tech found that complex, braided and anastomosing channels provide the best habitat suitability for silvery minnows (Tetra Tech 2014). Therefore, the more complex and accessible the side channel is, the greater the habitat score. For instance, 3f has the highest score because it has braided features that create eddies and low velocity flows. 3f is also underwater, so it is proven to be accessible. The next highest ranked is 3a because it is the most complex of the dry channels. If the river gets a large flow, this area could become inundated

and create shallow, low velocity complex channels for silvery minnows to occupy (3a-3d and 3f are within the active channel delineated by USBR). Next, 3b and 3d are all ranked the same. 3b provides habitat during higher flows, but is less complex and accessible than 3a channels. 3d is ranked similarly because while it is more accessible, there are higher velocities and deeper depths at higher flows. Finally, 3c offers the least suitable habitat because the channels are narrower than 3b channels. The more narrow the less habitat area. Also, 3c is narrower because there is a higher density of vegetation, which indicates that this area is less likely to become inundated and provide habitat. Overall, side channels are given relatively high scores because they are essential for high flow situations when the silvery minnow needs to be connected to more diverse areas with slower velocities.

Areas that can become inundated at very high flows are disregarded because they are too hard to analyze the areas beyond the active channel from year to year. The dry channels are identified by being within the active channel. Areas that could become inundated beyond the active channel are too subjective to analyze. For instance, the density of vegetation and previous years of flow areas give an idea of what channels could potentially become inundated. Using LiDAR data also helps with the analysis, but there is only LiDAR available for 2012. This makes analyzing areas that could be inundated in other years inconsistent. Even though potential channels for inundation are highly important for the life cycle of silvery minnows, there is not enough data to effectively analyze them. If there were aerial photographs compared across years that had the same high flow that inundate the floodplain, temporal trends in habitat could be analyzed.

As Middle Rio Grande has become more and more incised over time and peak flows are reducing, the availability of the floodplain habitat is greatly decreasing over the years (Tetra Tech 2014). Because the analysis is focused on the main channel for adult silvery minnows (all that can be analyzed across years at about 650 cfs), channels accessible during a large flood are not considered. This channel would be called 3e, but was removed from the analysis.

*Note: 3f could be confused with 1a because it is near the shoreline. They are differentiated because 3f is generally a complete, yet braided, channel with many offshoots. 1a does not have continuous flow through that section and does not take the form of a channel. 3f is generally more extensive than 1a.

Hydraulic backwater:

Hydraulic backwater criteria

4a. Backwater extending back > 100 ft, wide and appear accessible	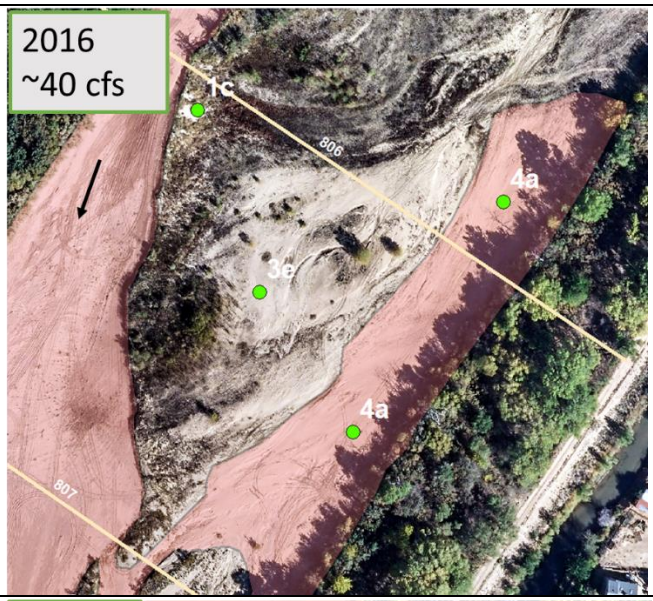
4b. Backwater extending back < 100 ft, not as accessible or wide	

Hydraulic backwater scores

	Backwater	
Criteria	4a	4b
Score	5	4

The backwater is determined by the active channel outline provided by USBR. In the figures depicting 4a and 4b, the water does not actually flow in these channels, yet it has been delineated as a place where water would normally flow. Backwaters are an essential component of silvery minnow habitat because they provide very low velocities that are near zero. The backwaters are especially important for larvae and juvenile silvery minnows when

they first hatch and grow (Bovee et al. 2008). 4a is much larger than 4b so it provides more suitable habitat, and therefore receives a higher score.

Bank-attached bars:

Bank-attached bars criteria

5a. Bar is large and provides shallow channels and complex habitat	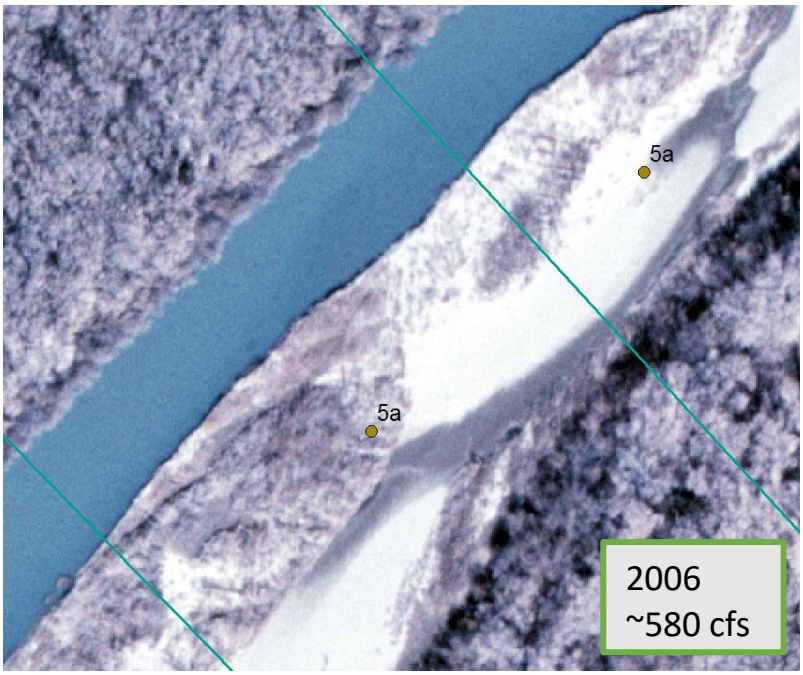
5b. Bar is small and provides some silvery minnow habitat (some vegetation)	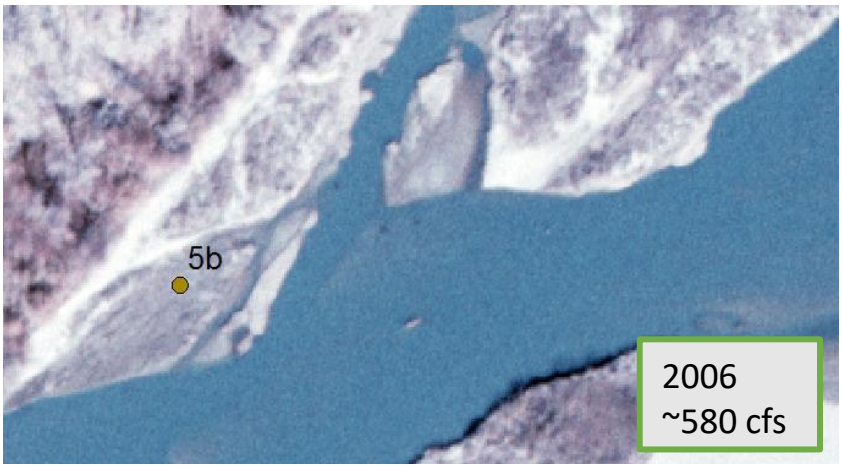

5c. Non-vegetated bar with little geomorphic variability	

Bank-attached bars scores

	Bars		
Criteria	5a	5b	5c
Score	4	2	1

Bars provide some habitat during high flows, yet they do not provide extensive spawning areas for silvery minnows. Because bank-attached bars are not very complex in their topography, only the most complex and extensive structural features provide in-channel habitat. Even when their complexity is evident and may provide some in channel habitat for adults, this does not always translate into optimum spawning habitat (Tetra Tech 2014). Bars still provide important habitat features during higher flows because they offer shallower habitat than the main channel if they become inundated so they are given a relatively high score. The more complex the bar, the more suitable the habitat is for silvery minnows. For instance, 5a is generally characterized by having more complex geomorphic features, small side channels or vegetation that would provide lower velocity areas and shelter from predators (Cluer and Thorne 2014). 5a is similar to 1a (shoreline complexity), so they must be differentiated. 5a is identified as being much larger and wider than 1a. 5b has less of these features, and 5c does provide overall shallower habitat at higher flows, yet it adds little topographic complexity to the habitat.

Islands/Mid-channel Bars:

Islands/mid-channel bar criteria

6a. Large and non-vegetated 6c. Small and non-vegetated	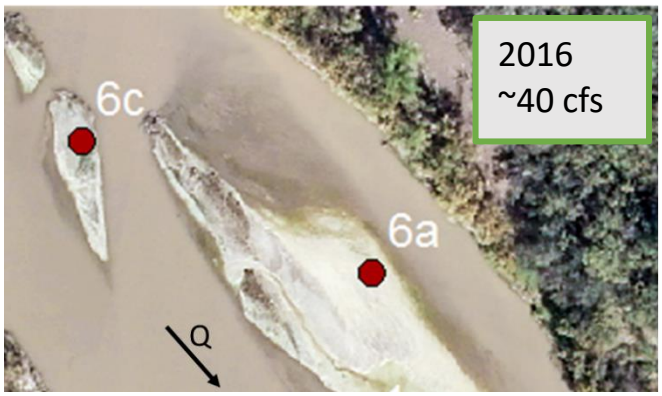
6b. Large and vegetated 6d. Small and vegetated	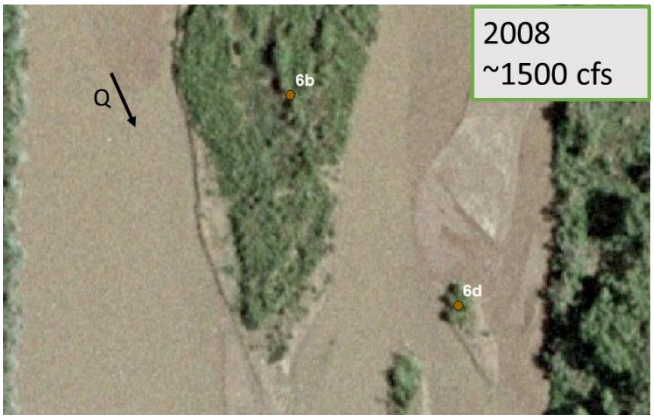
6e. Large- Some vegetation and some bare ground (Around 50% uniform veg cover over whole island). Could also have shoreline complexity or braided features within island. 6f. Small- Some vegetation and some bare ground (Around 50% uniform veg cover over whole island). Could also have shoreline complexity or braided features within island.	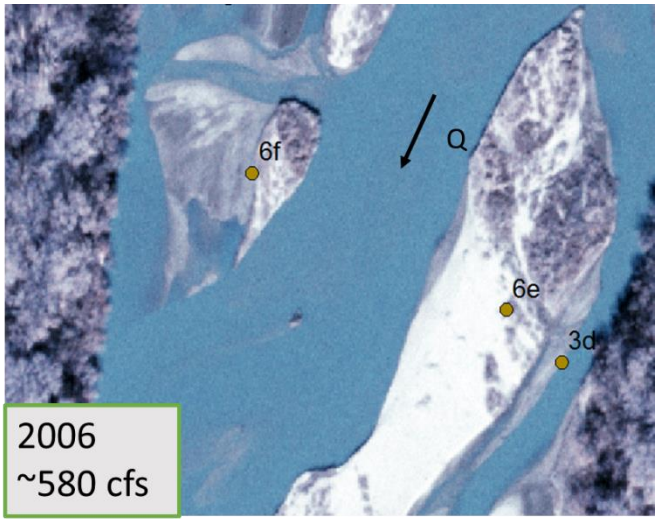

Islands/mid-channel bar scores

	Islands					
Criteria	6a	6b	6c	6d	6e	6f
Score	3	2	1	1	4	3

Islands in this section area defined as not being attached to the bank and are also referred to as mid-channel bars. An island or mid-channel bar is differentiated from a bank-attached bar based on what it is surrounded by. If there is an obvious, continuous separation from the bar and the shoreline, it is considered an island/mid-channel bar. It can be surrounded by water on both sides, a dry channel on both sides, or water on one side and dry channel on the other. A bank-attached bar has no major side-channels going through it that cause obvious and continuous separation from the bank.

Islands provide habitat to silvery minnows in a similar manner to bank-attached bars. During higher flows, the islands could become partially or fully inundated which helps in-channel habitat, yet is not necessarily most suitable for spawning (Tetra Tech 2014). 6e gets the highest score because it generally has some vegetation, small channels or backwaters within the island providing complex topography and habitat. 6f is a smaller version of 6e so it gets a lower score by one. 6a has no vegetation which indicates it is more accessible at higher flows, and 6b is less accessible because it is densely vegetation. Therefore, 6a has a slightly higher score than 6b. Small islands that are not complex have little to no impact on habitat suitability (Tetra Tech 2014) so these are given the lowest score (6b and 6c). A large island (6a,6b,6e) is considered to reach across one agg/deg polygon, and a small island (6c,6d,6f) spans across half or less of the polygon. Exceptions to this rule may occur when an island is very skinny so it may be considered small instead of large even if it spans across the entire polygon.

Confluences:

Confluences criteria

7a. Active confluence- wet	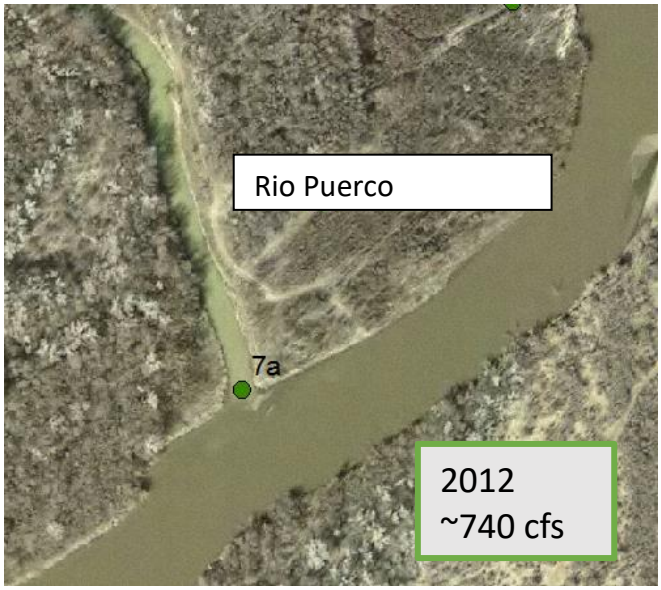
7b. Active confluence- dry	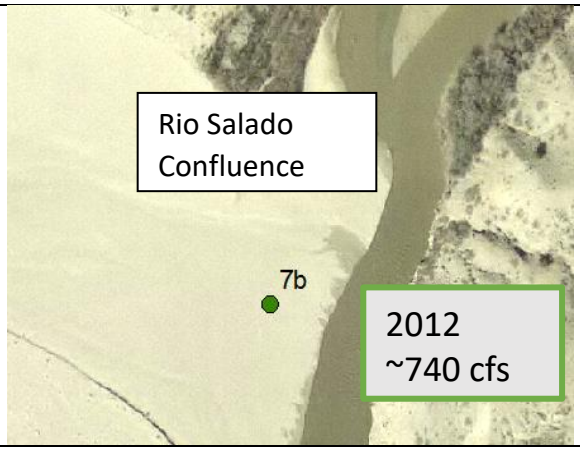

Confluence scores

	Wet Confluence	Dry Confluence
Criteria	7a	7b
Score	4	3

Confluences are spots where eddies, accelerating and decelerating velocities, sediment deposits, and large wood tend to accumulate. These factors create ecological hotspots (Cluer and Thorne 2014). Confluences are given a relatively high score because of this. If the confluence does not appear to be active or is disconnected from the Rio Grande, it is not included in the analysis. Also, spots where irrigation canals are not counted as confluences

because their flow is variable and cannot be compared across years. While these aren't counted as confluences, they are designated as shoreline complexity or backwater depending on how the "irrigation confluence" interacts with the main channel. Wet, active confluences are given a higher score than dry ones because they provide habitat instead of just channel margin complexity.

APPENDIX F

Habitat Counts (Years with flows around 650 cfs)

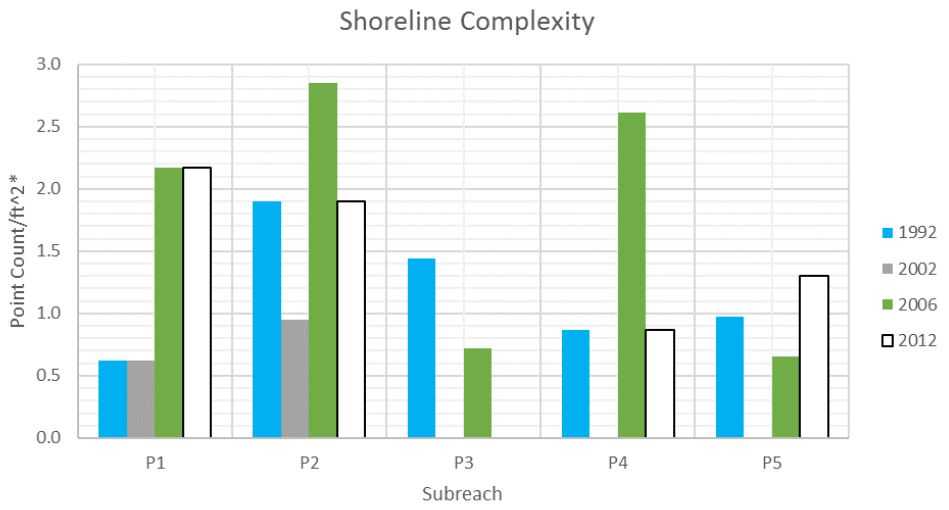
Shoreline Complexity
Point Count/ft^2*
3.0
2.5
2.0
1.5
1.0
0.5
0.0
P1
P2
P3
P4
P5
Subreach
1992
2002
2006
2012

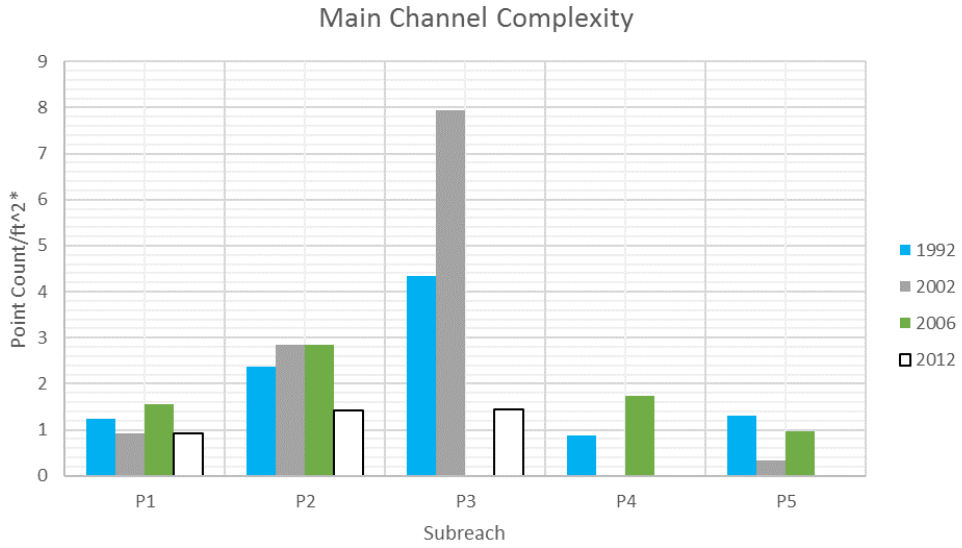
Main Channel Complexity
Point Count/ft^2*
9
8
7
6
5
4
3
2
1
0
P1
P2
P3
P4
P5
Subreach
1992
2002
2006
2012

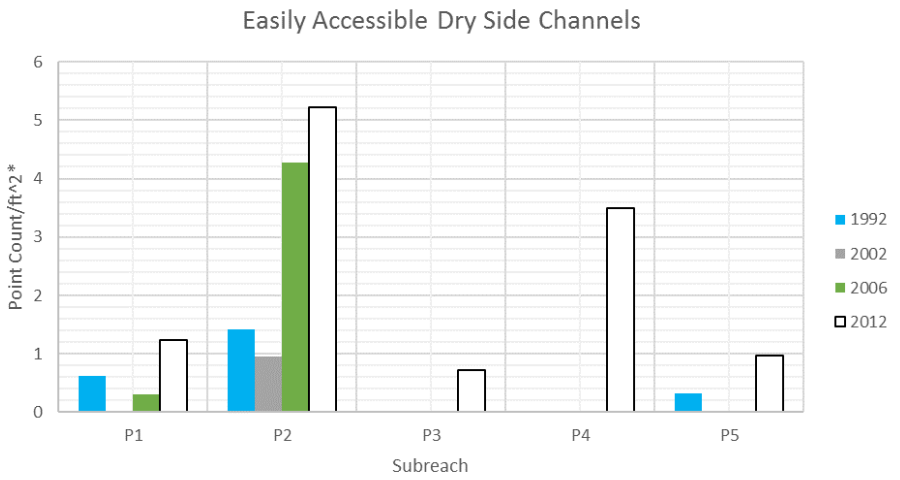
Easily Accessible Dry Side Channels
Point Count/ft^2*
0
1
2
3
4
5
6
P1
P2
P3
P4
P5
Subreach
1992
2002
2006
2012

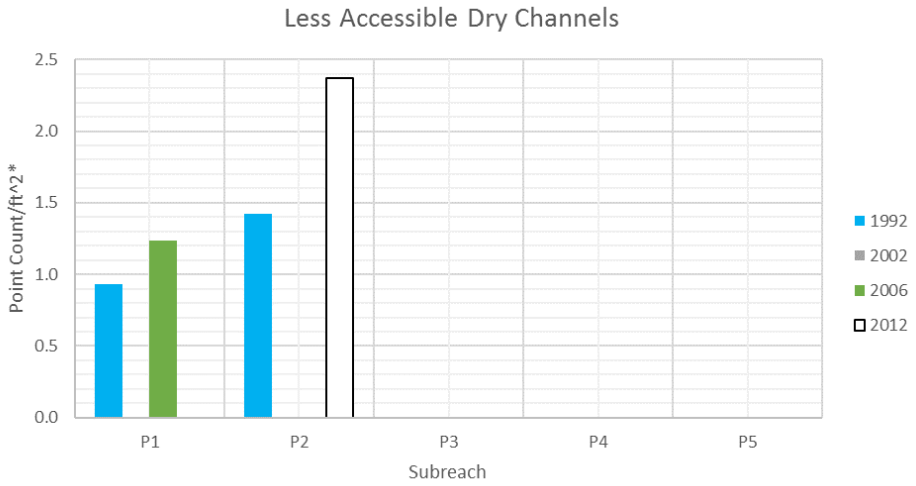
Less Accessible Dry Channels
Point Count/ft^2*
0.0
0.5
1.0
1.5
2.0
2.5
P1
P2
P3
P4
P5
Subreach
1992
2002
2006
2012

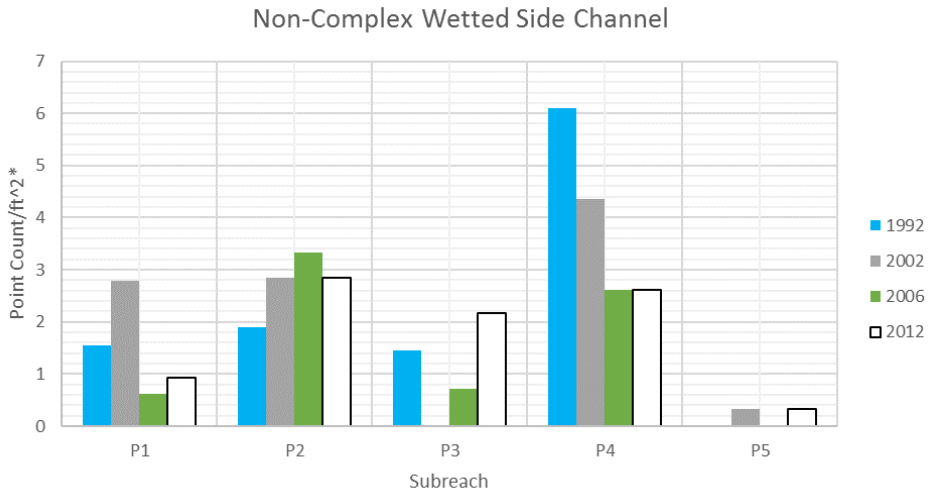
Non-Complex Wetted Side Channel
Point Count/ft^2*
0
1
2
3
4
5
6
7
P1
P2
P3
P4
P5
Subreach
1992
2002
2006
2012

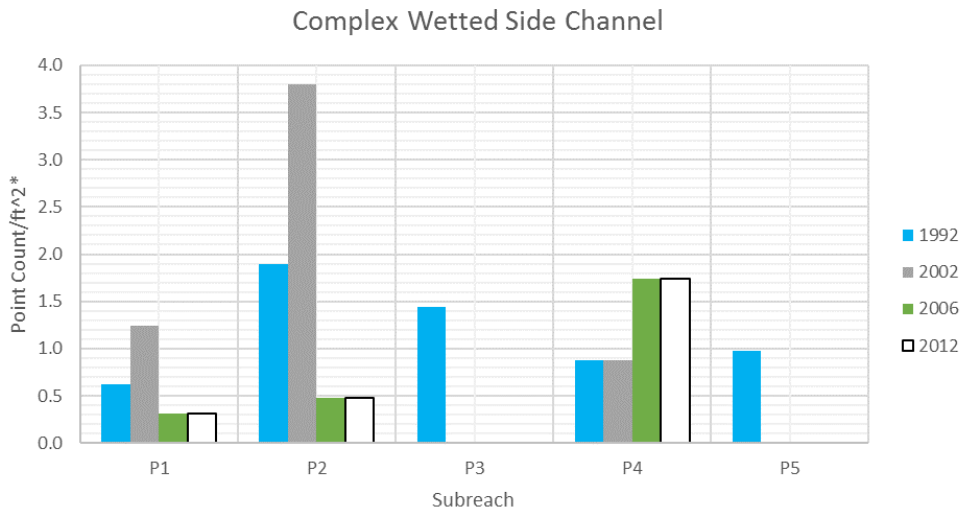
Complex Wetted Side Channel
Point Count/ft^2*
4.0
3.5
3.0
2.5
2.0
1.5
1.0
0.5
0.0
P1
P2
P3
P4
P5
Subreach
1992
2002
2006
2012

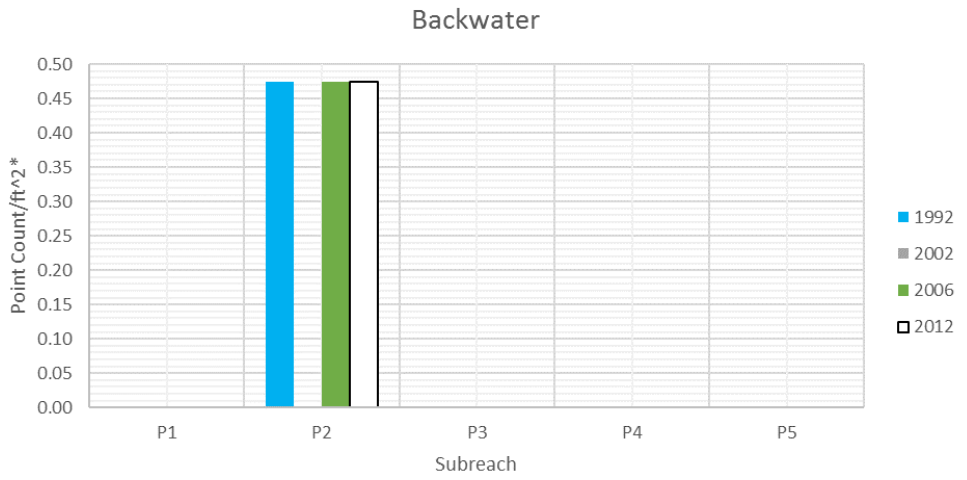
Backwater
Point Count/ft^2*
0.50
0.45
0.40
0.35
0.30
0.25
0.20
0.15
0.10
0.05
0.00
P1
P2
P3
P4
P5
Subreach
1992
2002
2006
2012

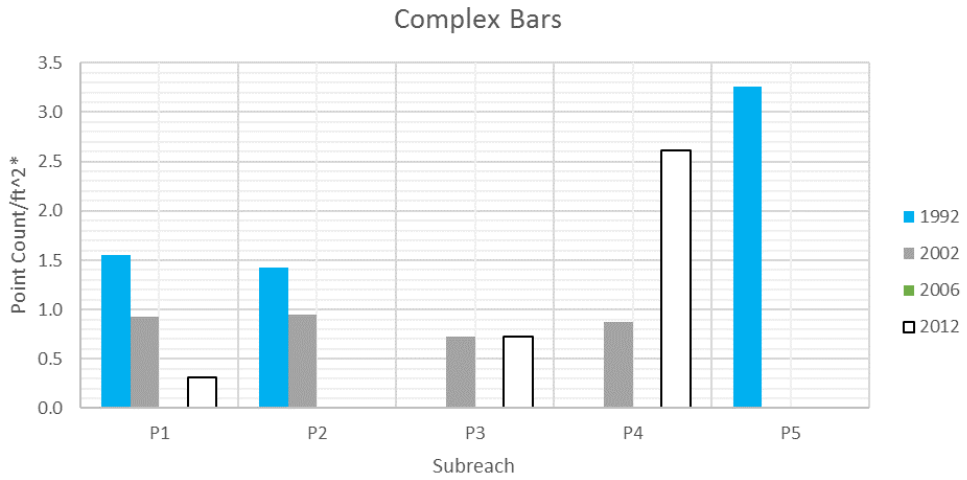
Complex Bars
Point Count/ft^2*
3.5
3.0
2.5
2.0
1.5
1.0
0.5
0.0
P1
P2
P3
P4
P5
Subreach
1992
2002
2006
2012

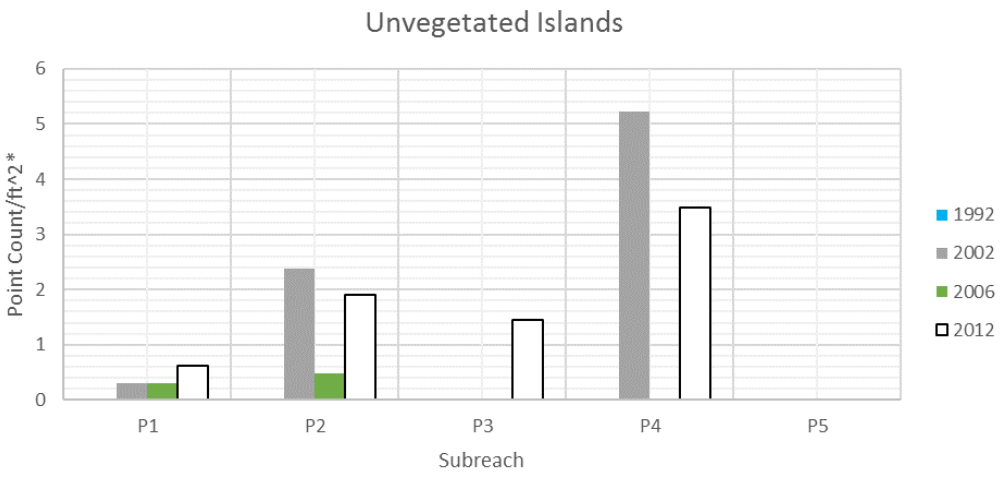
Unvegetated Islands
Point Count/ft^2*
0
1
2
3
4
5
6
P1
P2
P3
P4
P5
Subreach
1992
2002
2006
2012

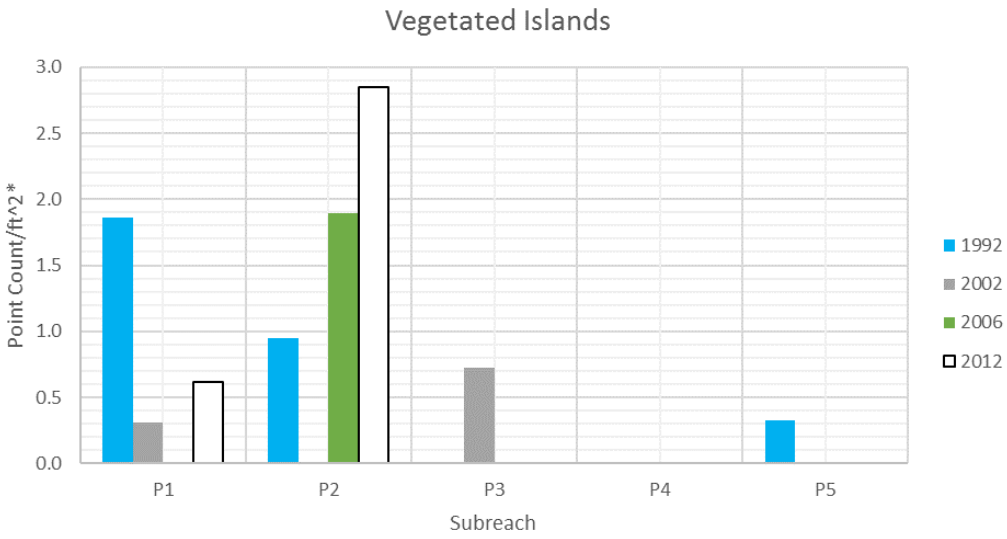
Vegetated Islands
Point Count/ft^2*
0.0
0.5
1.0
1.5
2.0
2.5
3.0
P1
P2
P3
P4
P5
Subreach
1992
2002
2006
2012

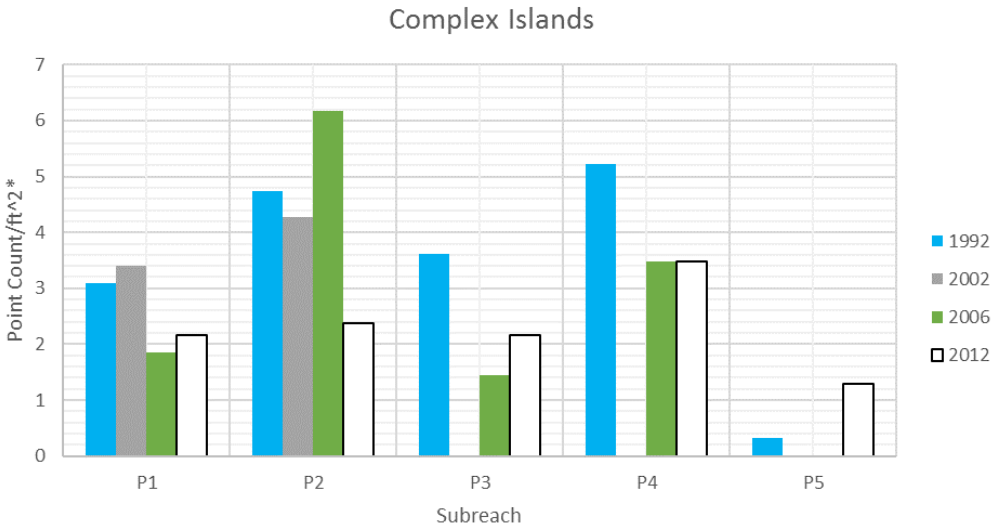
Complex Islands
Point Count/ft^2*
0
1
2
3
4
5
6
7
P1
P2
P3
P4
P5
Subreach
1992
2002
2006
2012

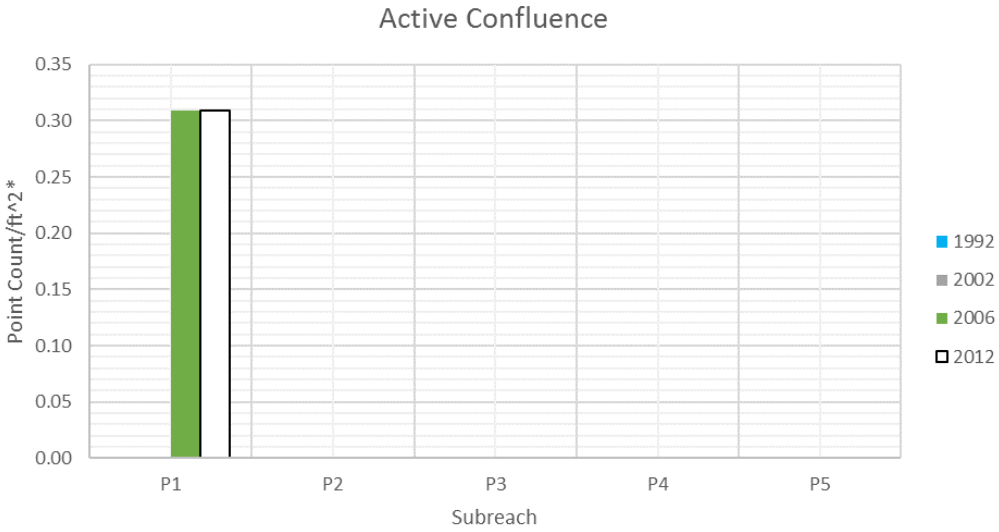
Active Confluence
Point Count/ft^2*
0.00
0.05
0.10
0.15
0.20
0.25
0.30
0.35
P1
P2
P3
P4
P5
Subreach
1992
2002
2006
2012

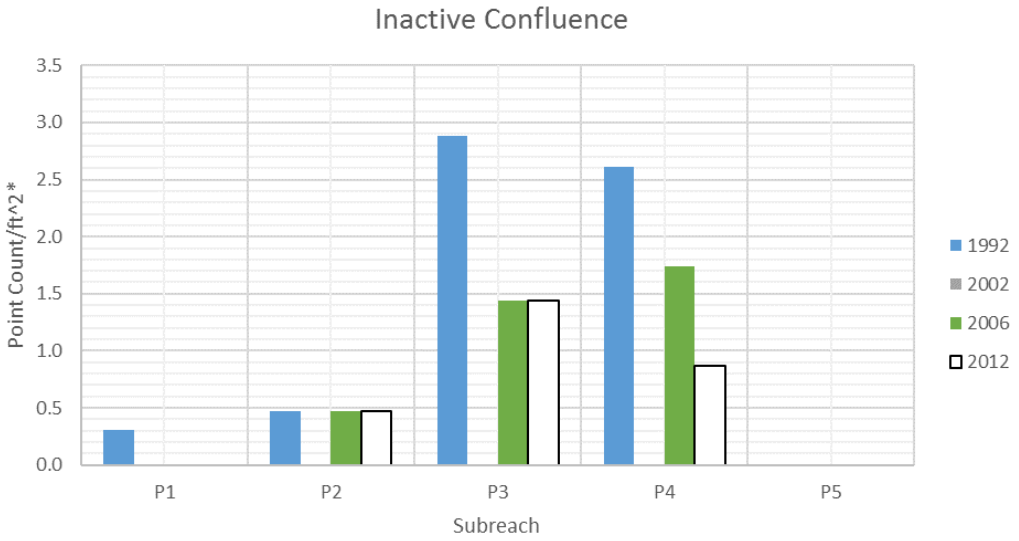
Inactive Confluence
Point Count/ft^2*
3.5
3.0
2.5
2.0
1.5
1.0
0.5
0.0
P1
P2
P3
P4
P5
Subreach
1992
2002
2006
2012

APPENDIX G

Shoreline Complexity

Shoreline complexity incorporates some silvery minnow habitat criteria, yet also incorporates geomorphic parameters for its analysis. Because it combines aspects from section 0 and geomorphic characteristics that could fit into section 4, shoreline complexity stands alone as its own section.

Methods

Two aspects of the shoreline were analyzed: the length of the shoreline and habitat features that indicate complex shoreline. The set of data used to analyze these aspects is shown in Table G-1.

Table G-1: Years of the photographs used for analyzing the shoreline complexity.

1992	February
2001	February
2002	February
2005	June
2006	January
2008	July
2012	January
2016	October

These are the years with planforms supplied by the USBR available. Data before 1992 is not used for the same reason it is not used in the habitat criteria analysis. Records of fish population before 1993 is not available, so it would be impossible to relate fish population to geomorphic trends before the early 1990's. April of 2005 and June of 2008 are excluded because planforms were not drawn for these photographs. It is unknown how each year's planform was drawn and how they differed, so there may be inconsistencies that affect the lengths.

Features including complex shoreline (1a, 1b, and 1c), bank attached bars (5a, 5b, and 5c), backwater (4a, 4b), and confluences (7a,7b) were considered to impact shoreline complexity. These points and their scores were used to find a habitat shoreline complexity score. Whatever points fall into each subreach were multiplied by their corresponding score and added up to get an overall score for each subreach in each year. These scores were weighted by area by using the same method as outlined in Appendix D.

The length of the shoreline is also an indicator of complexity. It was measured using ArcGIS by breaking up the active channel outline provided by USBR into subreaches as shown in Figure G-1. The rest of the planform drawings are shown in Appendix D. The cumulative length of the right and left bank was used to compare each subreach in each year. To account for different sizes of the subreaches, the length was weighted. This was accomplished by drawing a straight line between each subsequent subreach delineation line perpendicular to the river. Then the cumulative shoreline lengths were divided by the straight line and multiplied by 10 to get a weighted length index.

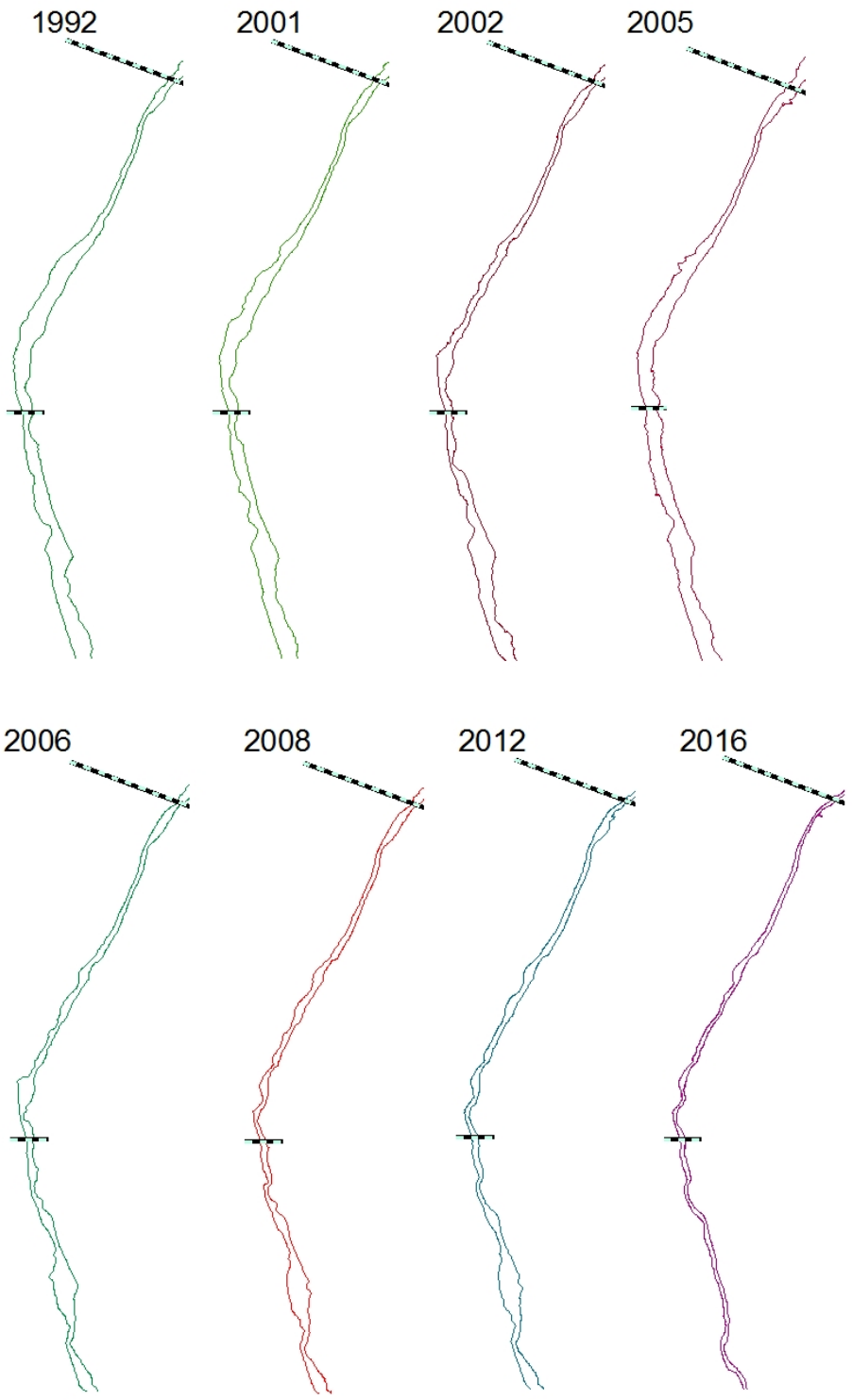

Figure G-1: Subreach P1 shoreline length shown with the planform drawing from USBR for each year. The subreach is within the bounds of the perpendicular lines to the planform.

The weight length index and the weighted habitat score were then added together to get an overall shoreline complexity score. They were weighted to be on the same order of magnitude

so they when they were added up, each would equally impact the overall score. These overall scores were compared across all years and across the comparable years at 650 cfs. The length of each subreach was also compared across every year and in the comparable years with 650 cfs. The individual parameters were also compared to the overall scores for each year and subreach.

Results

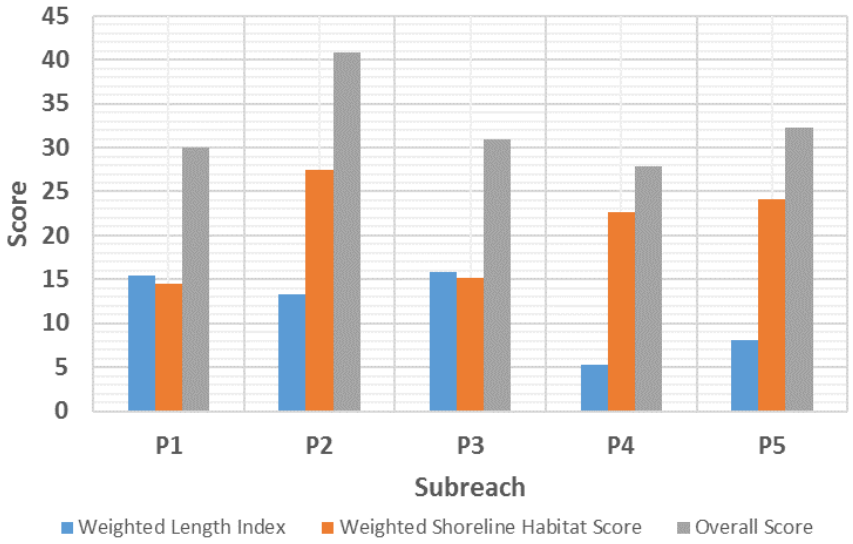

Figure G-2: Two parameters for analyzing shoreline complexity are compared and added up to show the overall score in 1992.

In Figure G-2, the overall complexity scores show that P2 is the most complex in 1992. The rest of the scores in the subreaches are lower and similar to each other. There is not consistent trend in the other years as shown in Appendix H. The shoreline complexity habitat score and the length of the shoreline do not seem to be correlated.

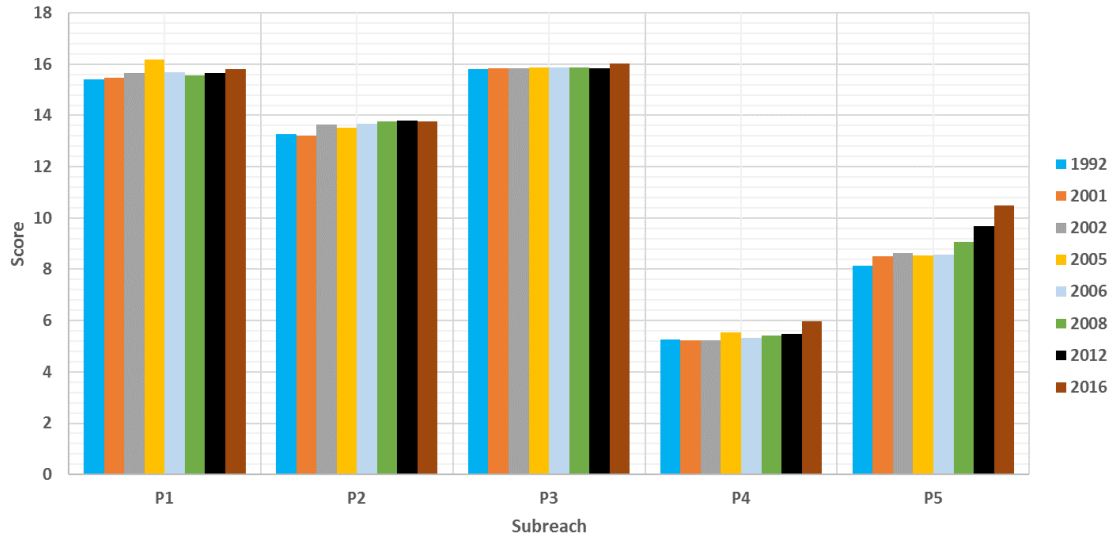

Figure G-3: The weighted length of the shoreline is compared over every subreach and every year.

In Figure G-3, when comparing the lengths only across years, there is a slight increase in length as time goes on.

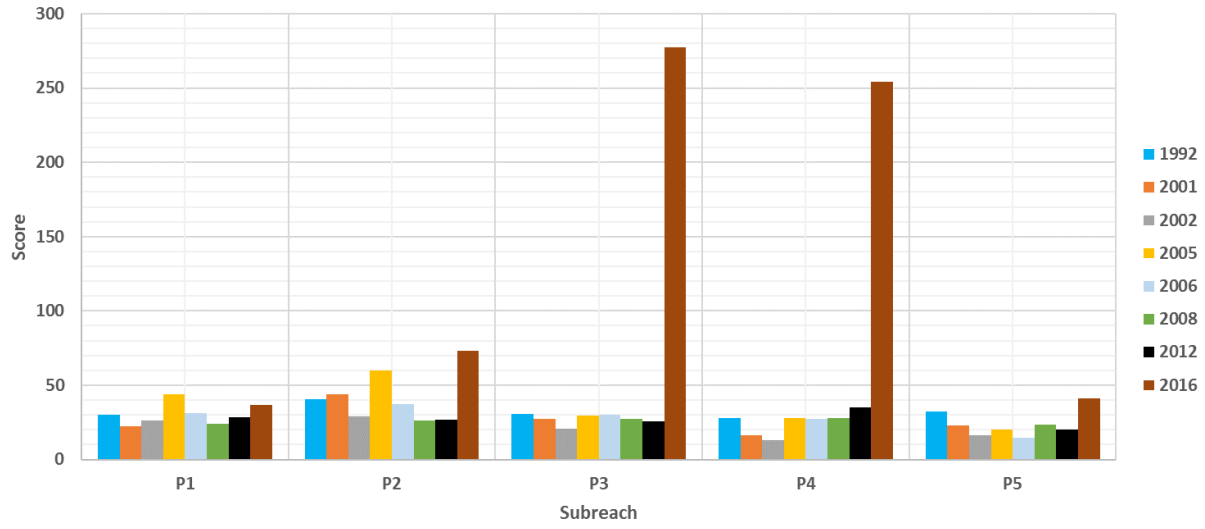

Figure G-4: The overall score for shoreline complexity is compared over every subreach and every year.

In Figure G-4, the overall score has more variation among the years, and 2016 still has the highest scores in each subreach except in P1.

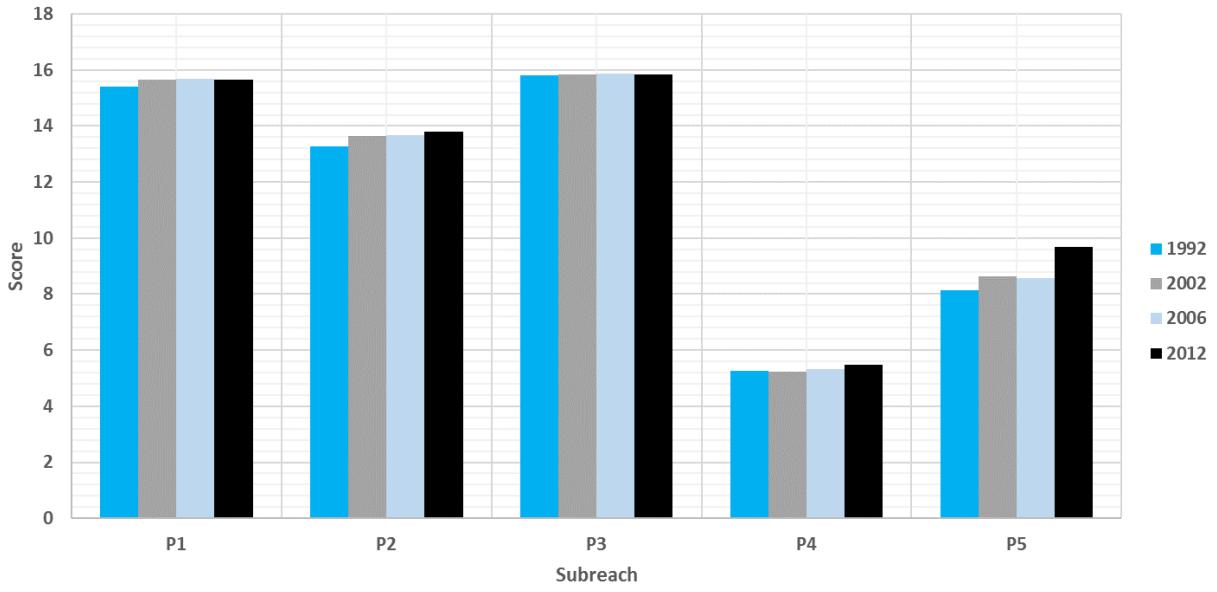

Figure G-5: The weighted length of the shoreline is compared over every subreach during years with a flow around 650 cfs when the aerial photograph was taken.

In Figure G-5, there is not much change in any of the subreaches over the years, but in some subreaches the complexity goes up slightly.

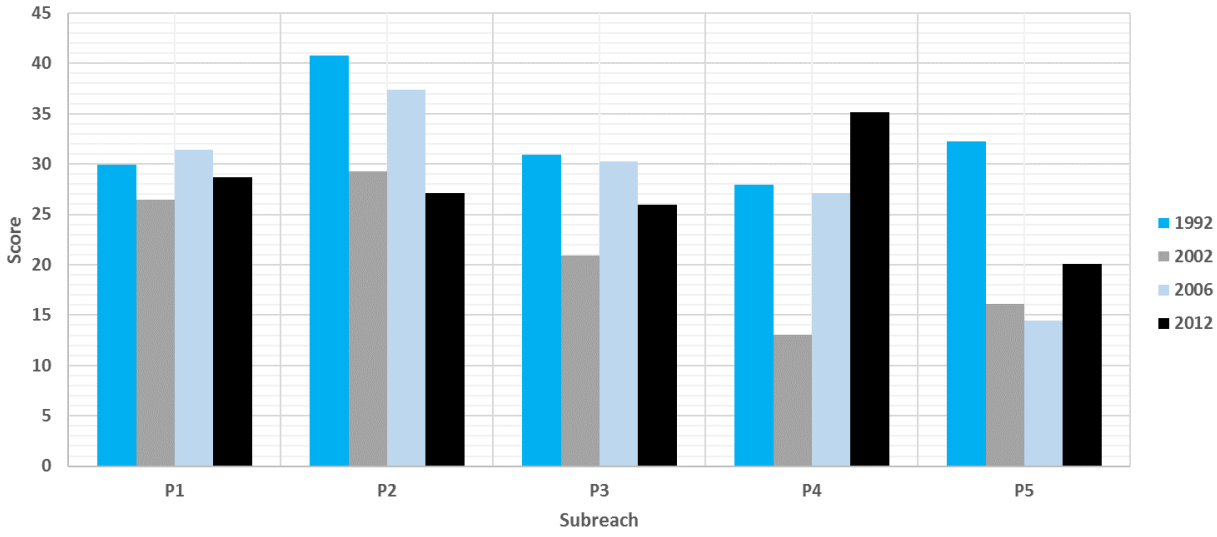

Figure G-6: The overall score for shoreline complexity is compared over every subreach during years with a flow around 650 cfs when the aerial photograph was taken.

In Figure G-6. throughout these years, each subreach has a different trend. There is not much consistency for the overall score.

In each of these figures where the years and only lengths are compared, the overall trend is the same. P1-P3 are the most complex and P4 and P5 are less so. When looking at the overall score, there is not an obvious trend.

Discussion

P1-P3 may be have a longer shoreline than P4 and P5 because P4 and P5 are closest to the San Acacia Diversion Dam. The closer the position to the dam, the higher the velocity, energy slope, bed slope, and depth. Also, the wetted perimeter and width decrease as shown in Figure 37. These occurrences indicate that the channel is straighter in P3-P5, which is consistent with decreasing shoreline complexity. There are not any other consistent trends, especially when looking at the overall scores. Year 2016 may be more complex because the flow is so low that the channel is more sinuous as mentioned in the discussion in Section 3. Near the downstream end of the reach, there are "basalt-capped mesas on both sides of the river" that creates a natural geological constriction of the width (Easterling Consultants LLC 2015). This may also be impacting the channel complexity in certain subreaches as well.

The complexity increasing over time since the 1990's may be due to sinuosity slightly increasing, braiding decreasing and width decreased. Because islands and side channels are not factored into the channel length and complexity, the results are not reflective of braiding decreasing, but instead just sinuosity increasing. This may be why it appears like the complexity is increasing over time.

APPENDIX H

Complete Shoreline Complexity Results

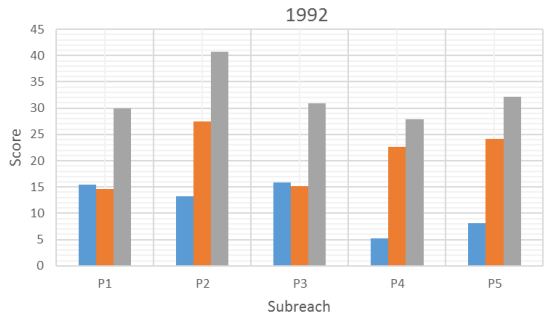
1992
Score
Subreach
P1
P2
P3
P4
P5

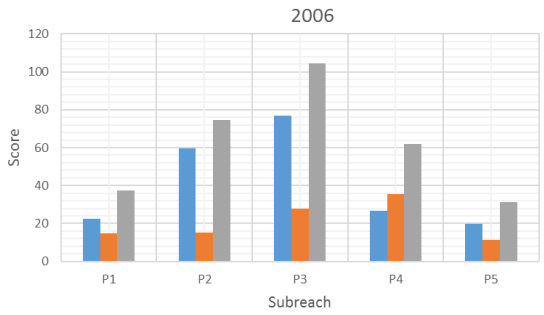
2006
Score
Subreach
P1
P2
P3
P4
P5

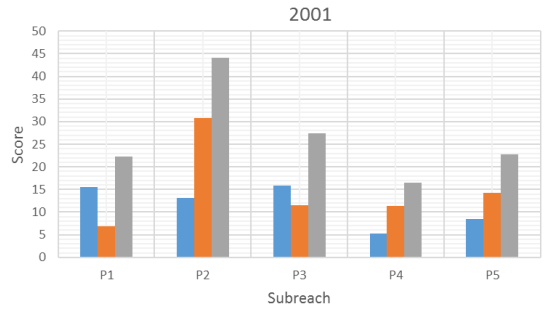
2001
Score
Subreach
P1
P2
P3
P4
P5

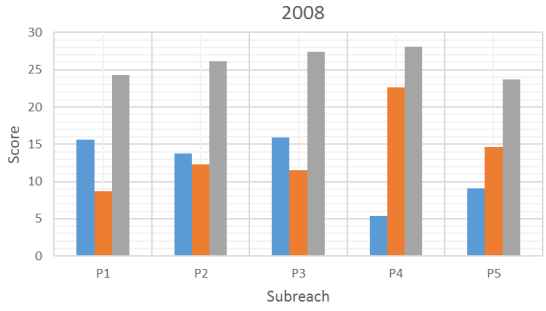
2008
Score
Subreach
P1
P2
P3
P4
P5

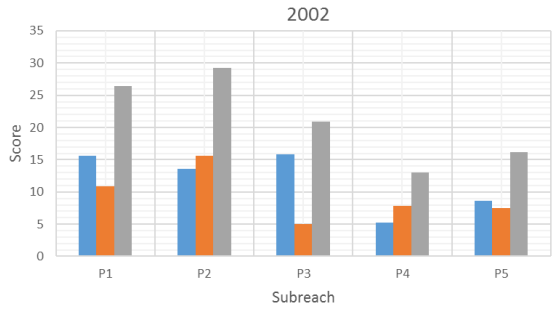
2002
Score
Subreach
P1
P2
P3
P4
P5

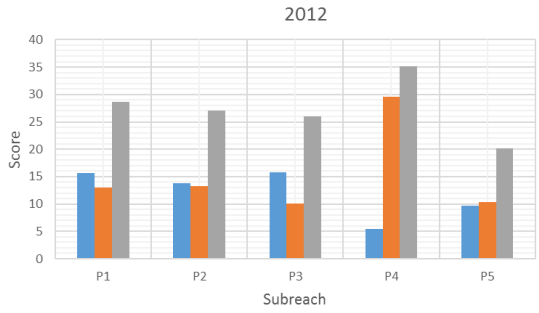
2012
Score
Subreach
P1
P2
P3
P4
P5

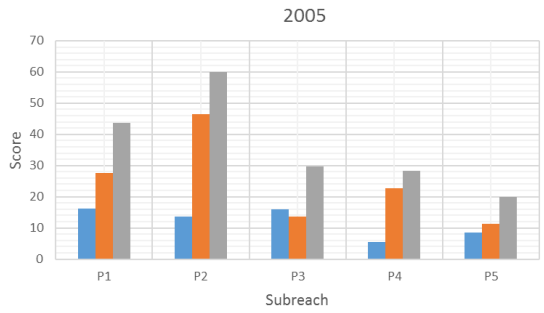
2005
Score
Subreach
P1
P2
P3
P4
P5

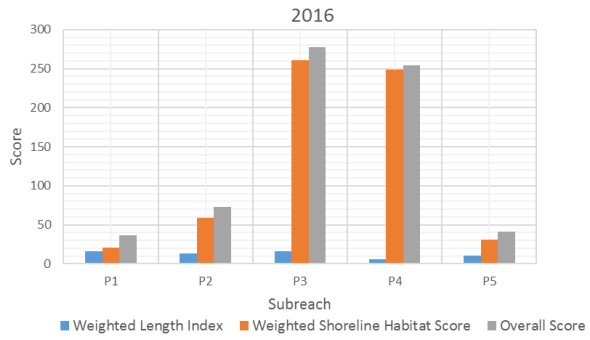
2016
Score
Subreach
P1
P2
P3
P4
P5
Weighted Length Index
Weighted Shoreline Habitat Score
Overall Score

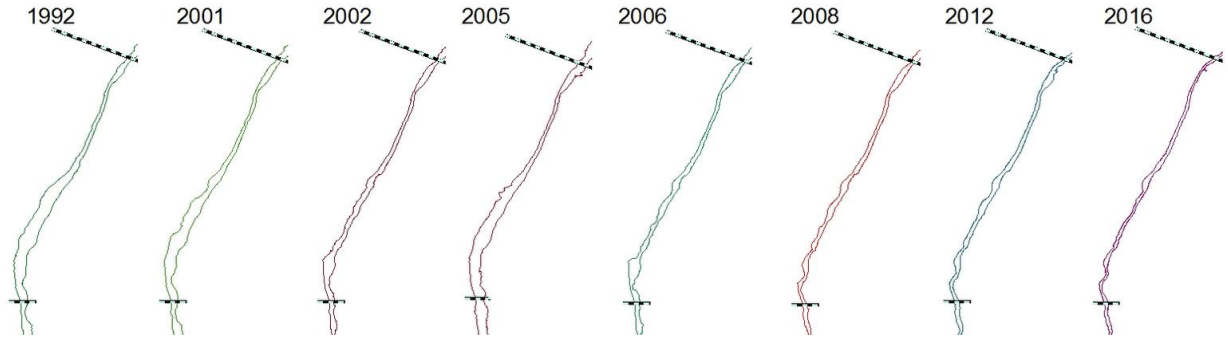
1992
2001
2002
2005
2006
2008
2012
2016

P1

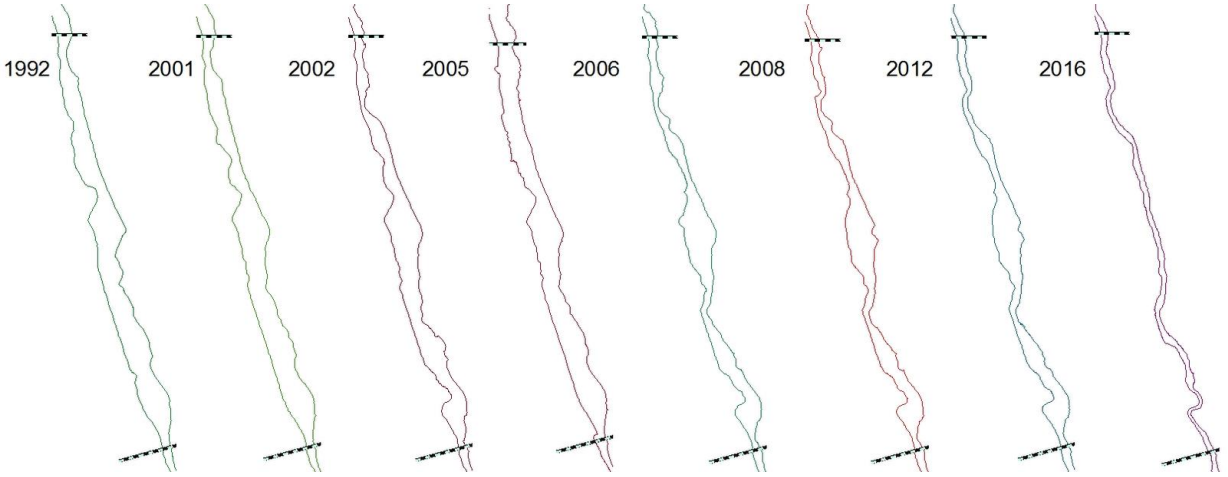
1992
2001
2002
2005
2006
2008
2012
2016

P2


1992
2001
2002
2005
2006
2008
2012
2016

P3

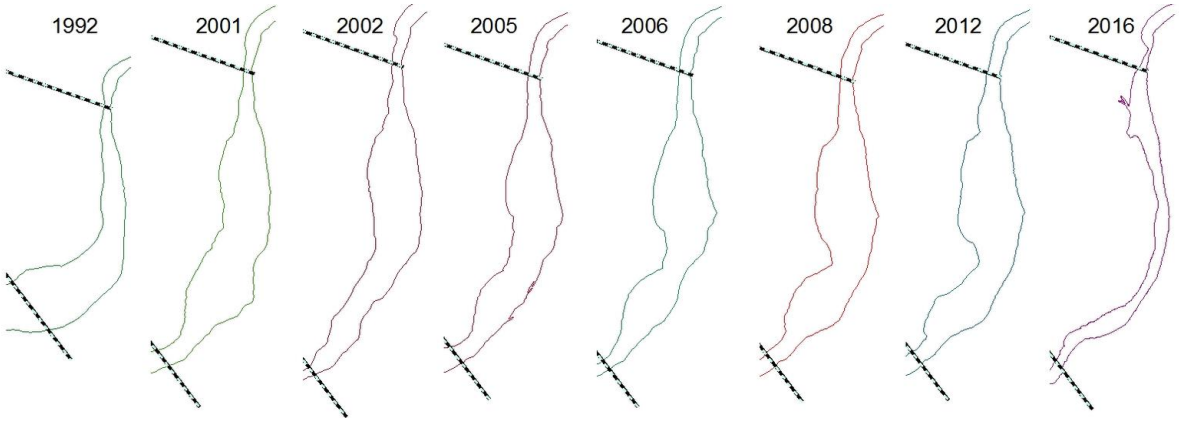
1992
2001
2002
2005
2006
2008
2012
2016

P4


1992
2001
2002
2005
2006
2008
2012
2016

P5

APPENDIX I

Habitat Score by Subreach (All Years)

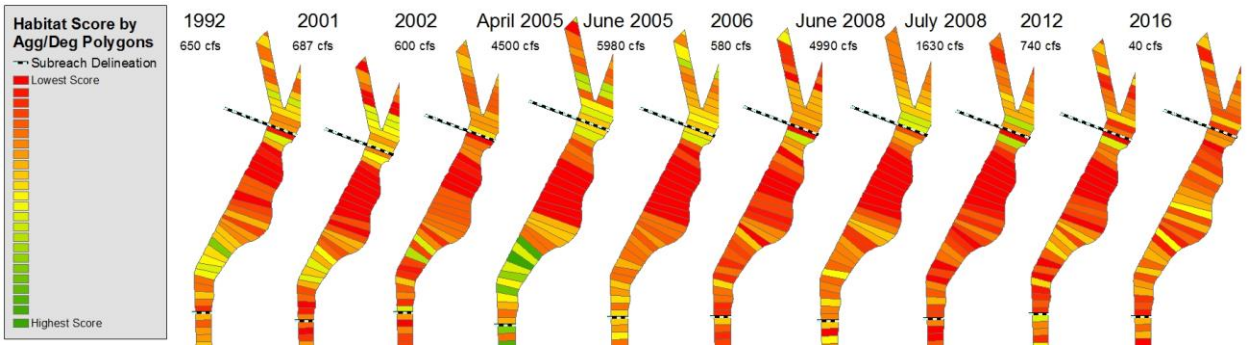
Habitat Score by Agg/Deg Polygons
Subreach Delineation
Lowest Score
Highest Score
1992
650 cfs
2001
687 cfs
2002
600 cfs
April 2005
4500 cfs
June 2005
5980 cfs
2006
580 cfs
June 2008
4990 cfs
July 2008
1630 cfs
2012
740 cfs
2016
40 cfs

P1

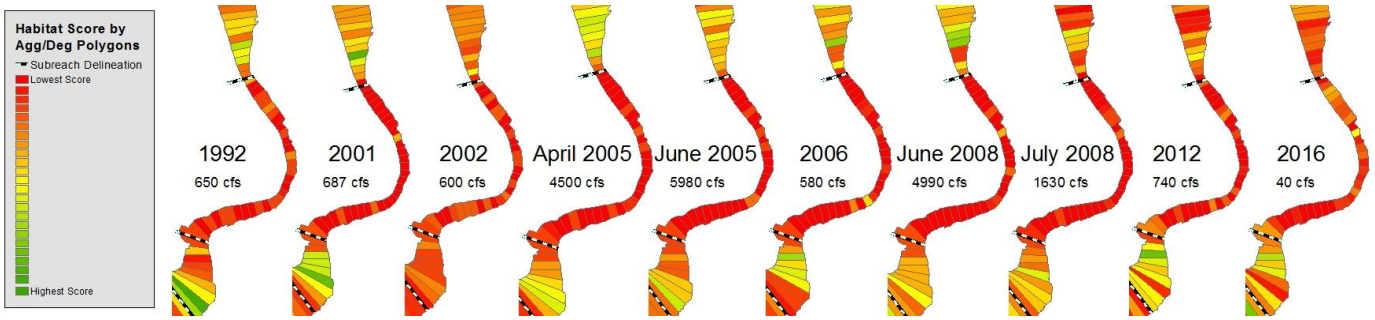
Habitat Score by Agg/Deg Polygons
Subreach Delineation
Lowest Score
Highest Score
1992
650 cfs
2001
687 cfs
2002
600 cfs
April 2005
4500 cfs
June 2005
5980 cfs
2006
580 cfs
June 2008
4990 cfs
July 2008
1630 cfs
2012
740 cfs
2016
40 cfs

P3

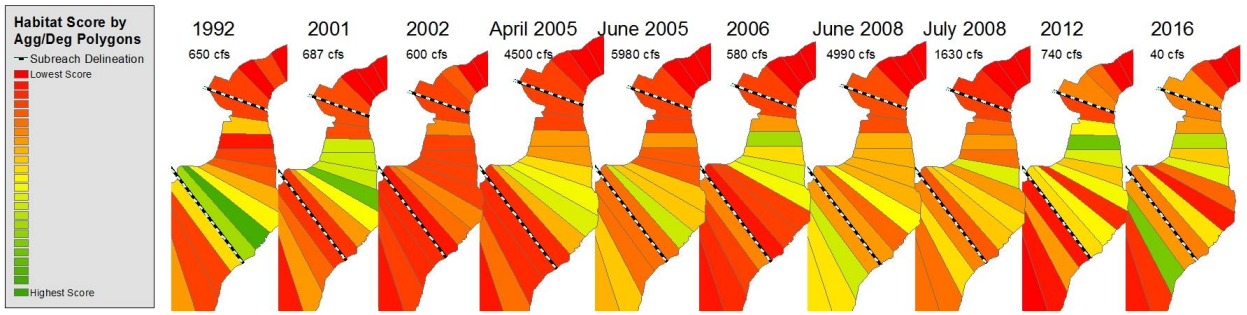
Habitat Score by Agg/Deg Polygons
Subreach Delineation
Lowest Score
Highest Score
1992
650 cfs
2001
687 cfs
2002
600 cfs
April 2005
4500 cfs
June 2005
5980 cfs
2006
580 cfs
June 2008
4990 cfs
July 2008
1630 cfs
2012
740 cfs
2016
40 cfs

P4

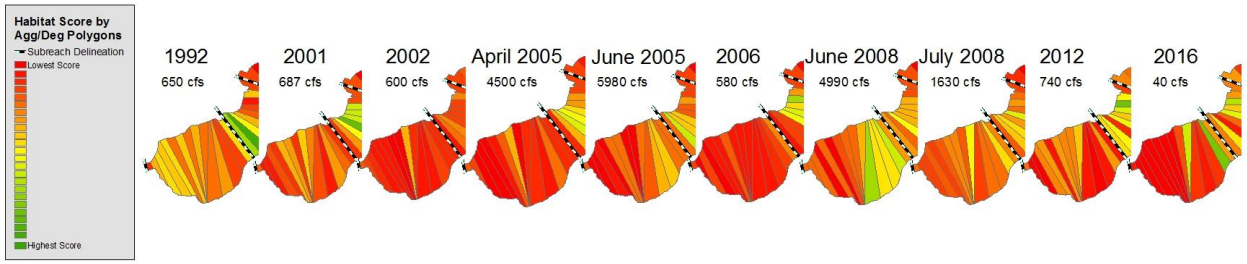
Habitat Score by Agg/Deg Polygons
Subreach Delineation
Lowest Score
Highest Score
1992
650 cfs
2001
687 cfs
2002
600 cfs
April 2005
4500 cfs
June 2005
5980 cfs
2006
580 cfs
June 2008
4990 cfs
July 2008
1630 cfs
2012
740 cfs
2016
40 cfs

P5

APPENDIX J

Habitat Score by Subreach (Years with flows around 650 cfs)

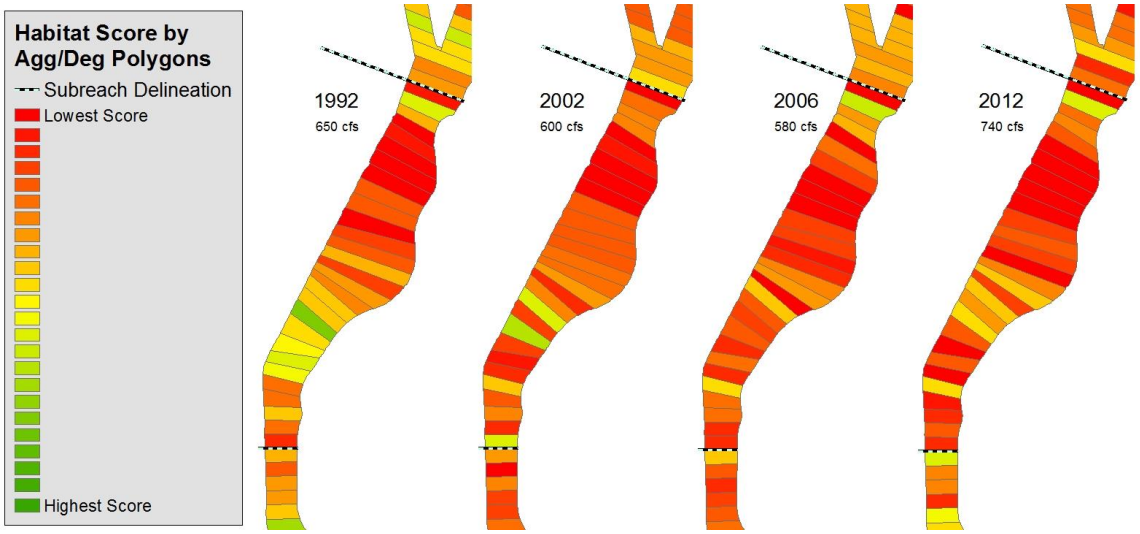
Habitat Score by Agg/Deg Polygons
Subreach Delineation
Lowest Score
Highest Score
1992
650 cfs
2002
600 cfs
2006
580 cfs
2012
740 cfs

P1

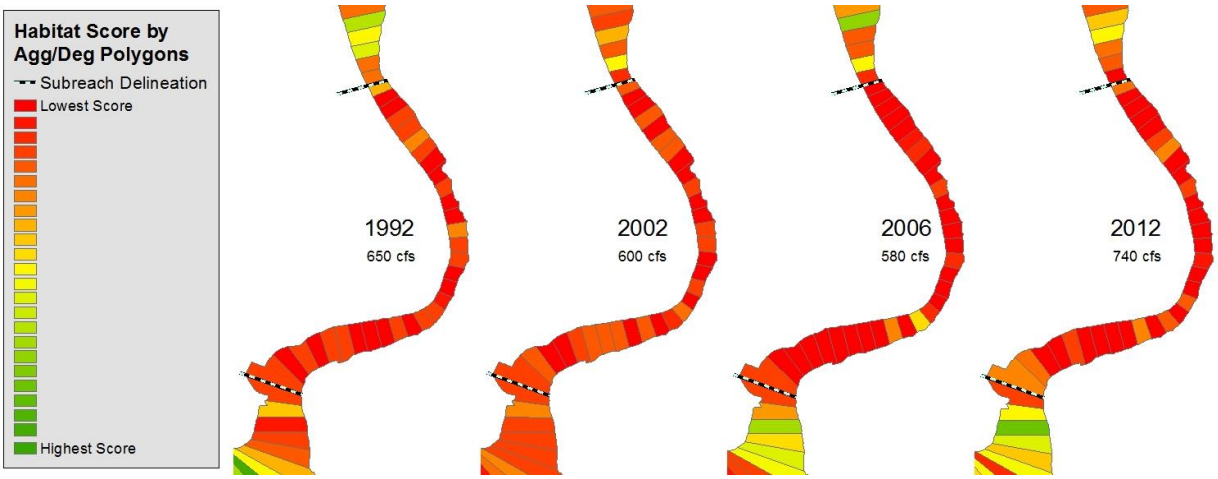
Habitat Score by Agg/Deg Polygons
Subreach Delineation
Lowest Score
Highest Score
1992
650 cfs
2002
600 cfs
2006
580 cfs
2012
740 cfs

P3

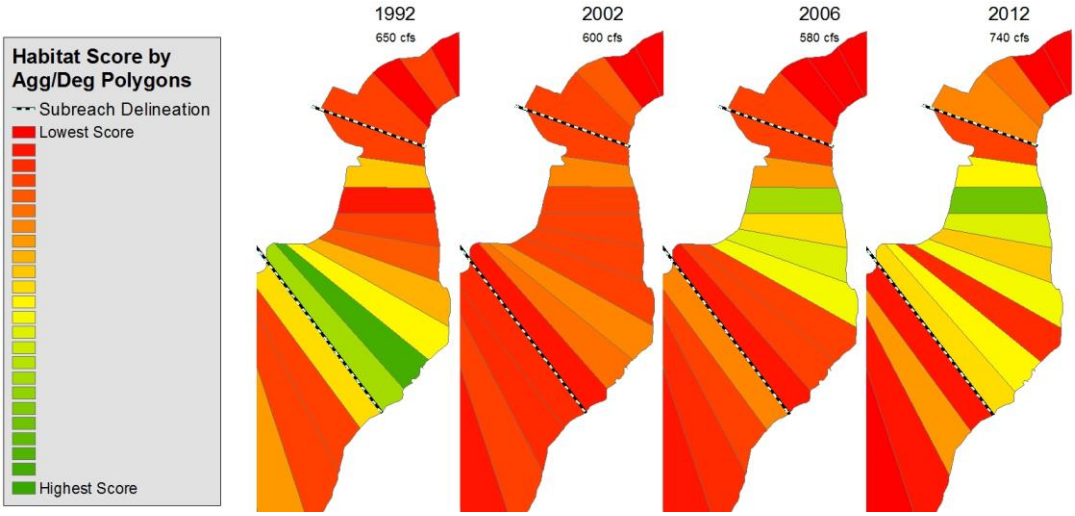
Habitat Score by Agg/Deg Polygons
Subreach Delineation
Lowest Score
Highest Score
1992
650 cfs
2002
600 cfs
2006
580 cfs
2012
740 cfs

P4

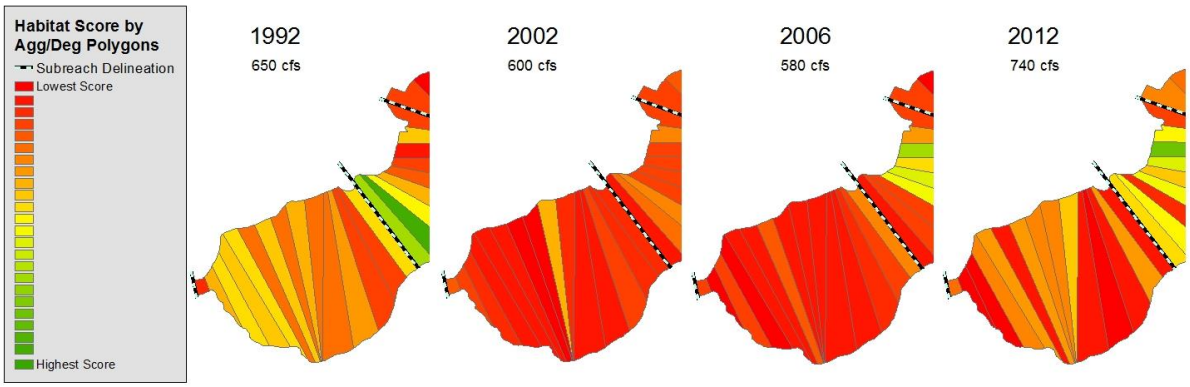
Habitat Score by
Agg/Deg Polygons
Subreach Delineation
Lowest Score
Highest Score
1992
650 cfs
2002
600 cfs
2006
580 cfs
2012
740 cfs

P5

APPENDIX K

Summary of HEC-RAS and GIS Habitat Analysis

To showcase the methods used for habitat analysis, figures representing one subreach at two flow conditions are presented. The rest of the subreaches at these flow conditions are in the appendix.

Subreach P2 is depicted in Figure K-1 and K2 because it is the subreach that provides the best habitat. There is also a great amount of habitat variability in this subreach. This allows us to analyze how the habitats are different and what that looks like. Only a portion of the subreach is shown so the points and figures are decipherable.

The two different flow conditions are at a low and high flow. The low flow analyzed is in 1992 at 650 cfs in GIS and 600 cfs in HEC-RAS shown in Figure K-1. The high flow is analyzed at 4500 cfs in GIS in 2005 and 3500 cfs in HEC-RAS in 2002 shown in Figure K-2. The difference in years and flows and the high flow analysis come from limitations in available data. The HEC-RAS simulation includes low, medium and high flows from 1992, 2002, and 2012. The only high flow data from aerial photographs analyzed is in 2005. The closest match for year and flow data to 3500 cfs from 2002 in HEC-RAS is aerial photography from April of 2005 at 4500 cfs. Therefore, the high flow results are not perfectly comparable because there is a difference in time and flow.

The top half of Figure K-1 and K-2 (a) and (b) are from HEC-RAS and the bottom half (c and d) are from GIS. They both depict a portion of subreach P2. The results show that the HEC-RAS and GIS analyses are somewhat comparable. Where there is a large area of good quality habitat from HEC-RAS there tends to be more habitat features mapped in GIS as seen in Figure K-2. The trend does not always occur such as in Figure K-1 which shows little correlation between the two analyses. These figures are mainly presented to get a visual idea of what the habitat and results look like.

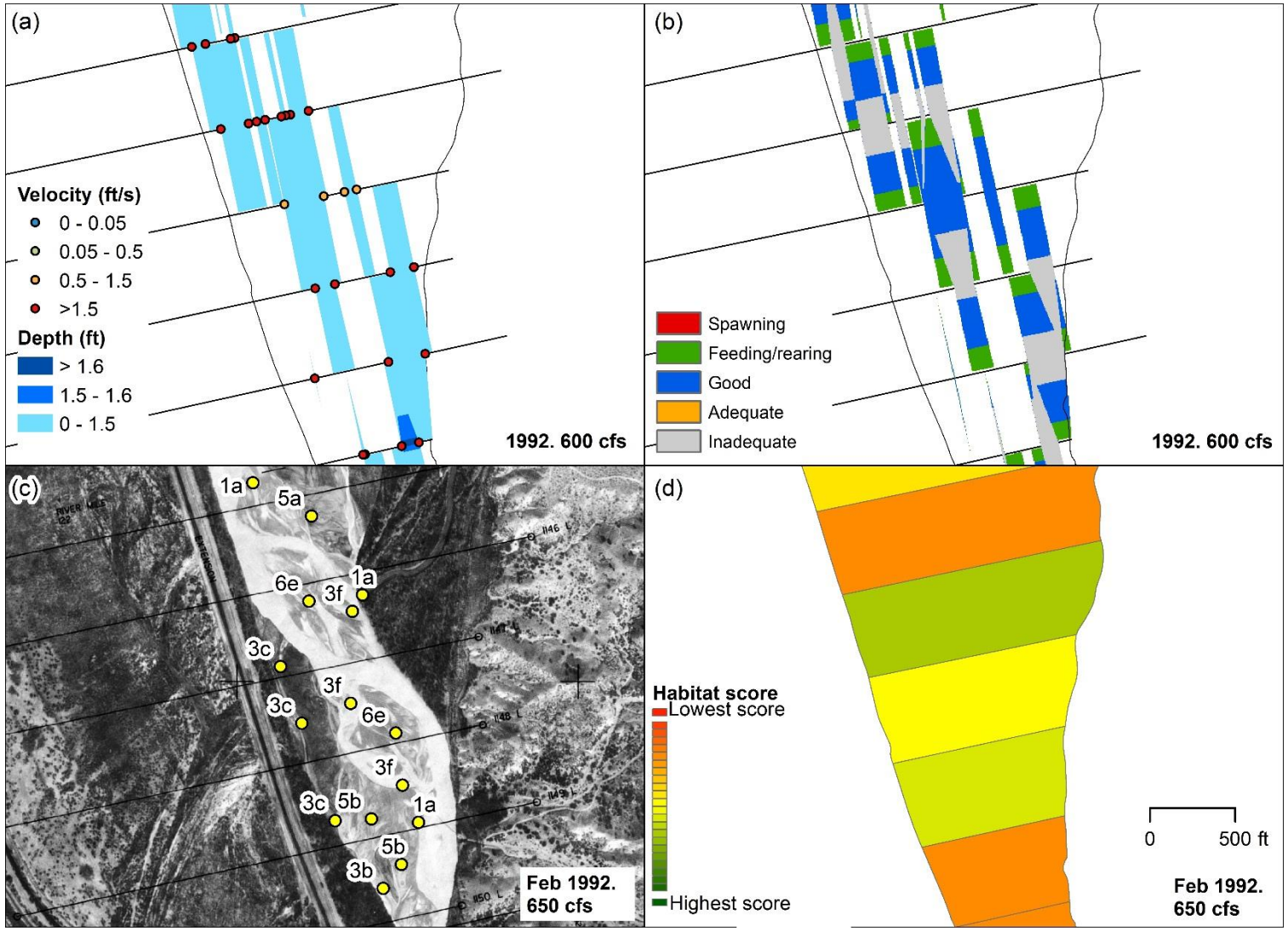

Figure K-1: Summary of HEC-RAS and GIS habitat at subreach P2, aggdeg 1145 to 1150. (a) Velocity and depth of the simulation. (b) Habitat criteria mapped based on velocity and depth. (c) Habitat features mapped out by points and letters. The description of these points is given in 0 and section 0. (d) Habitat color scheme based on habitat features.

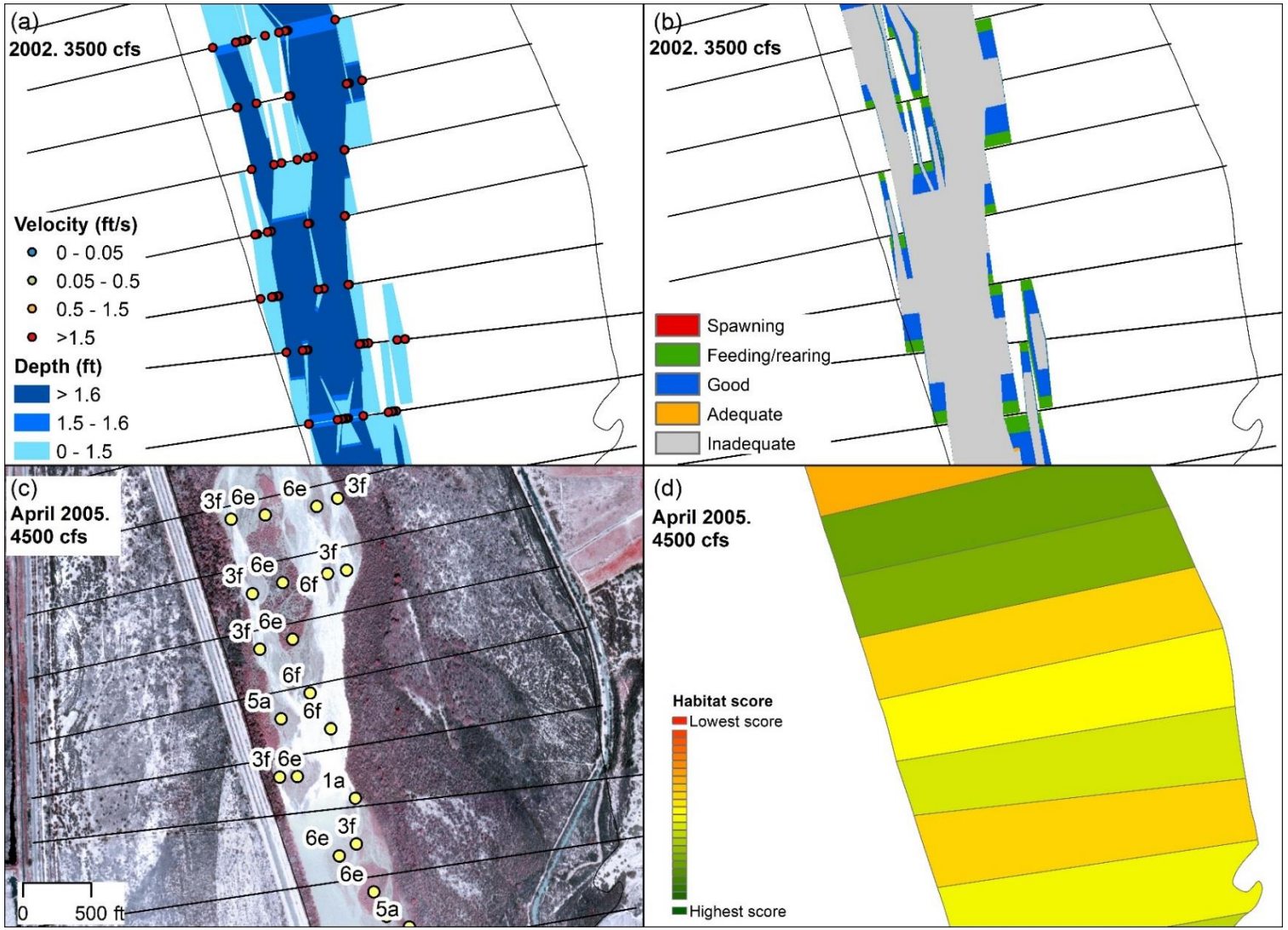

Figure K-2: Summary of HEC-RAS and GIS habitat at subreach P2, aggdeg 1137 to 1143. (a) Velocity and depth of the simulation. (b) Habitat criteria mapped based on velocity and depth. (c) Habitat features mapped out by points and letters. The description of these points is given in 0and section 0. (d) Habitat color scheme based on habitat features.

APPENDIX L

All Comparisons of HEC-RAS and GIS Habitat Analysis

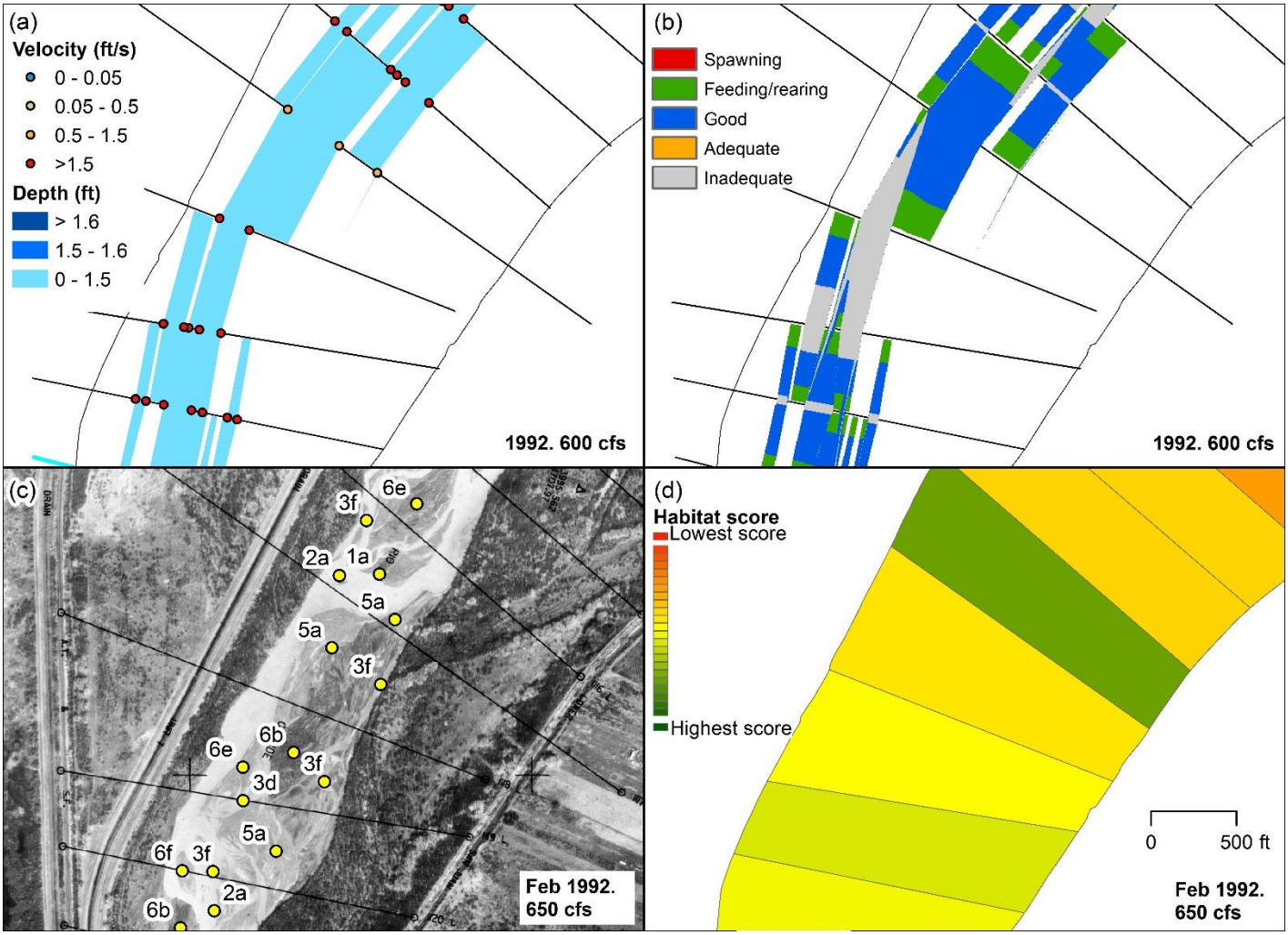

Summary of HEC-RAS and GIS habitat at subreach P1, aggdeg 1115 to 1121. (a) Velocity and depth of the simulation. (b) Habitat criteria mapped based on velocity and depth. (c) Habitat features mapped out by points and letters. (d) Habitat color scheme based on habitat features.

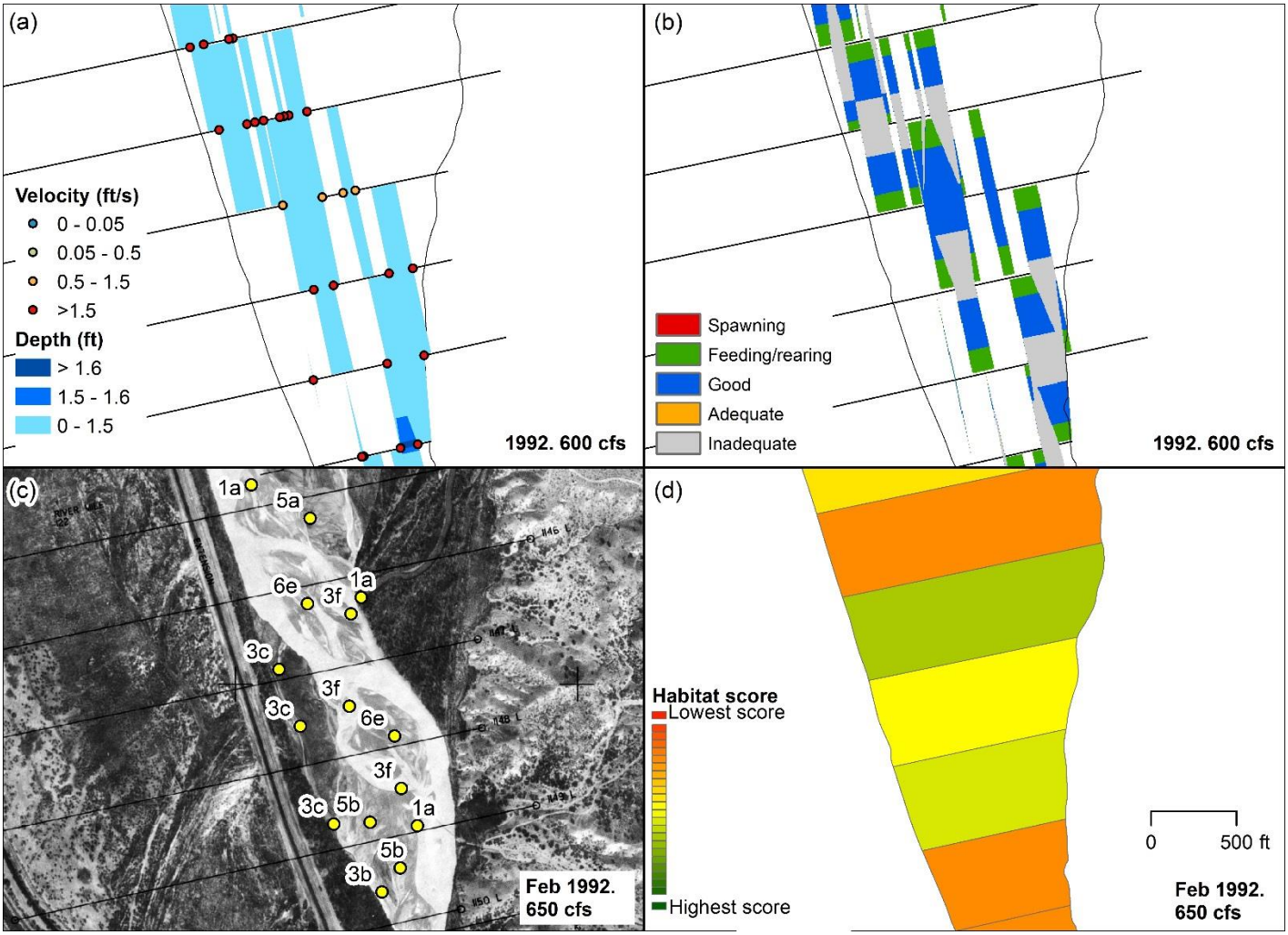

Summary of HEC-RAS and GIS habitat at subreach P2, aggdeg 1145 to 1150. (a) Velocity and depth of the simulation. (b) Habitat criteria mapped based on velocity and depth. (c) Habitat features mapped out by points and letters. (d) Habitat color scheme based on habitat features.

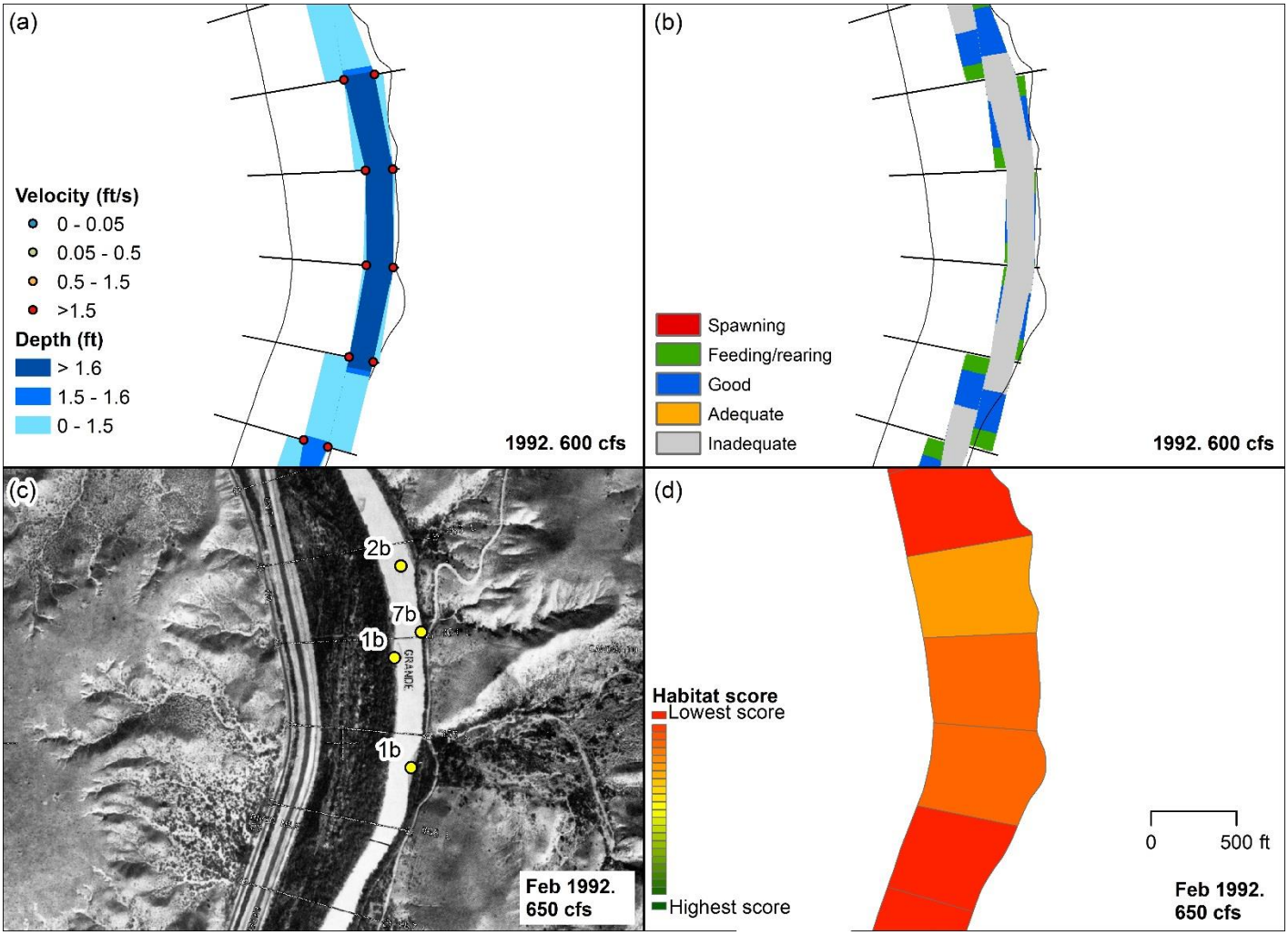

Summary of HEC-RAS and GIS habitat at subreach P3, aggdeg 1162 to 1167. (a) Velocity and depth of the simulation. (b) Habitat criteria mapped based on velocity and depth. (c) Habitat features mapped out by points and letters. (d) Habitat color scheme based on habitat features.

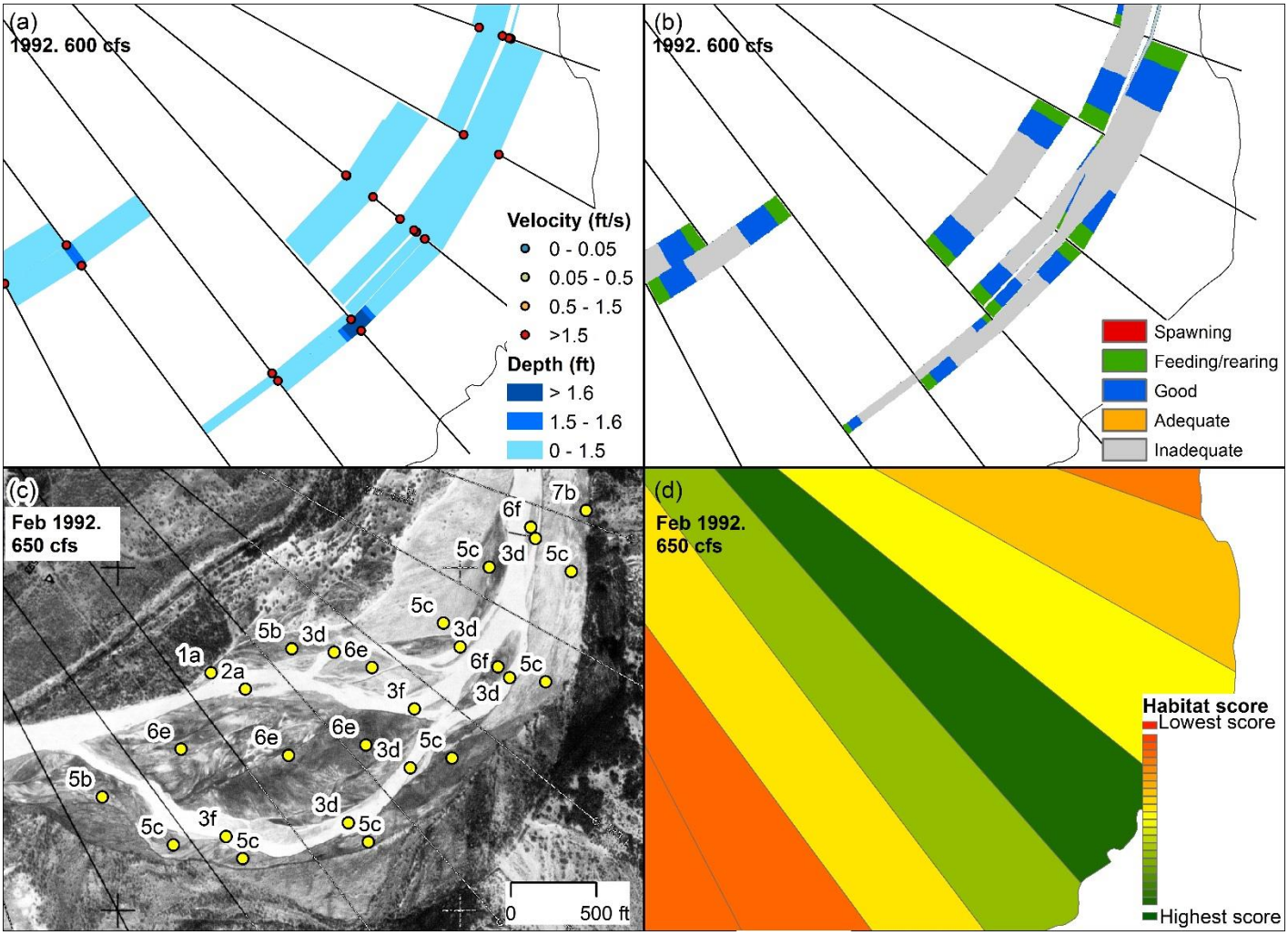

Summary of HEC-RAS and GIS habitat at subreach P4, aggdeg 1187 to 1193. (a) Velocity and depth of the simulation. (b) Habitat criteria mapped based on velocity and depth. (c) Habitat features mapped out by points and letters. (d) Habitat color scheme based on habitat features.

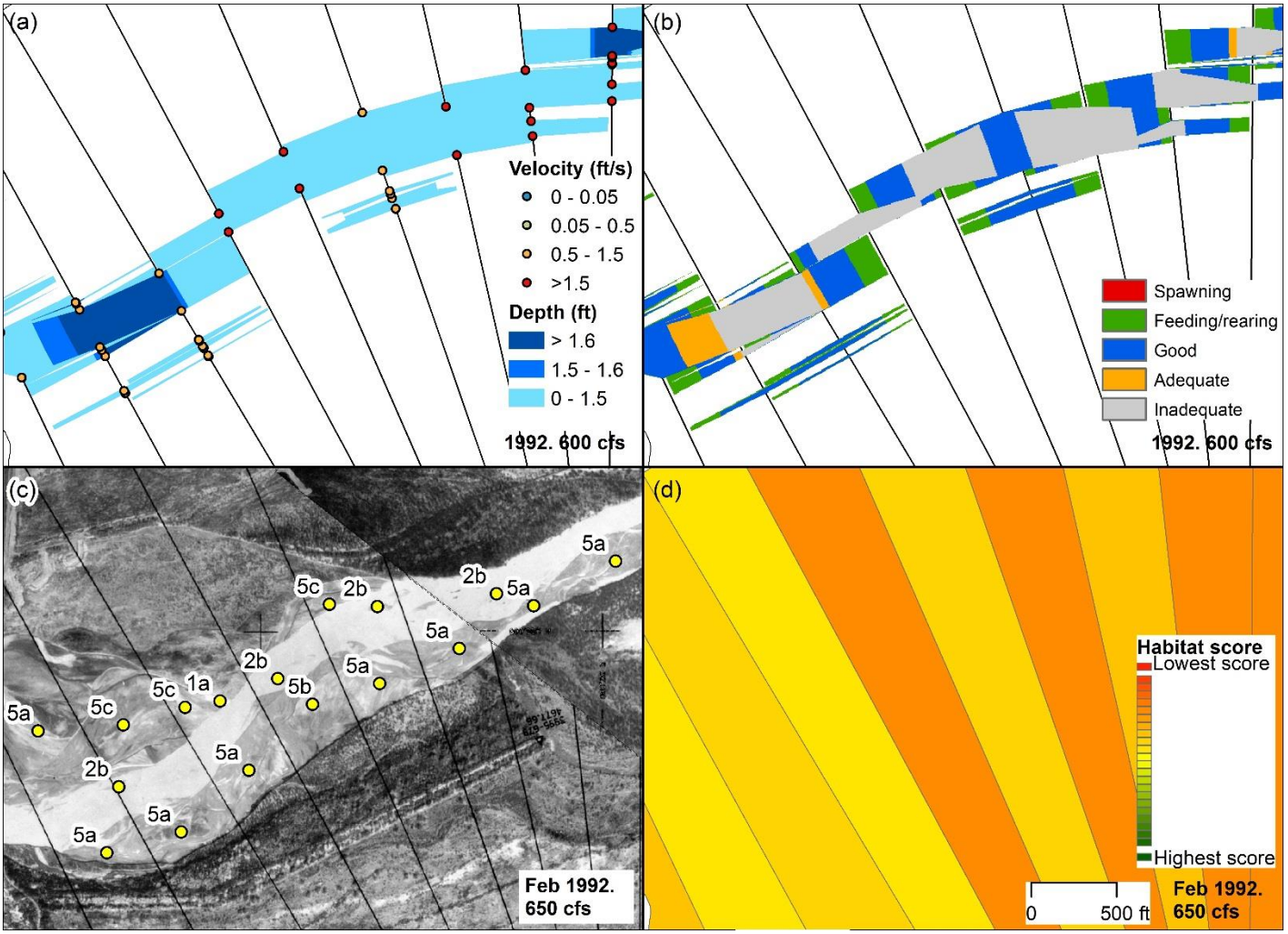

Summary of HEC-RAS and GIS habitat at subreach P5, aggdeg 1196 to 1204. (a) Velocity and depth of the simulation. (b) Habitat criteria mapped based on velocity and depth. (c) Habitat features mapped out by points and letters. (d) Habitat color scheme based on habitat features.